Aus dem Institut für Molekulare Medizin

Direktor: Univ. Prof. Dr. rer. nat. Klaus Schulze-Osthoff

Habilitationsschrift

Regulationsebenen der Apoptose: Vom DNA-Schaden zur Proteinspaltung

zur Erlangung der Venia Legendi
für das Fach Molekulare Medizin

vorgelegt der Medizinischen Fakultät
der Heinrich-Heine-Universität Düsseldorf

von
Dr. rer. nat. Frank Eßmann
aus Waltrop

Dekan: Herr Univ. Prof. Dr. rer. nat. Dr. med. Bernd Nürnberg

Eingereicht am 20.12.2006

DANKSAGUNG

Ich möchte mich sehr herzlich bei allen Kollegen und Freunden bedanken, die mich auf meinem Weg bis hierher begleitet haben!
Mein besonderer Dank gilt Prof. Klaus Schulze-Osthoff, PD Dr. Reiner U. Jänicke, Prof. Peter T. Daniel, Prof. Brigitte Wittmann-Liebold, Prof. Johann Salnikow und Dr. Bernd Gillissen. Weiterhin und keineswegs zuletzt möchte ich Vilma Graupner und meinen Eltern danken!

Index

Danksagung **1**
Index **3**
Abkürzungen **4**
1 Einleitung **5**
1.1 Formen des Zelltodes 5
1.2 Organisationsebenen der Apoptose 6
1.3 Caspasen: Schlüsselenzyme der Apoptose 8
1.4 Extrinsische Apoptose-Induktion: Todesrezeptoren 10
1.5 Intrinsisch vermittelte Apoptose 12
1.5.1 Die Bcl-2-Proteinfamilie 12
1.5.2 Das Apoptosom 15
1.6 Verknüpfung der Apoptose-Signalwege 16
1.7 Das Tumorsuppressorprotein p53 in der Apoptose 17
1.7.1 Die Rolle von p53 auf transkriptioneller Ebene 19
1.7.2 Die Rolle von p53 auf nicht-transkriptioneller Ebene 20
2 Zusammenfassung ausgewählter eigener Publikationen **22**
2.1 D4-GDI wird bei Zytostatika-induzierter Apoptose durch Caspase-3 gespalten 22
2.2 Caspase-8 als Substrat von Effektorcaspasen 24
2.3 Die Rolle von Caspase-8 in der mitochondrial vermittelten Apoptose 25
2.4 Alpha-Toxin induziert Nekrose mit Apoptose-Charakteristika 28
2.5 Die Apoptose-Induktion durch das BH3-only-Protein Nbk/Bik ist Bax-abhängig 30
2.6 Die Rolle von p53 bei Resistenzmechanismen gegenüber γ-Bestrahlung 31
2.7 Die Rolle von mitochondrial lokalisiertem p53 bei der Apoptose 33
3 Fazit **36**
4 Bibliographie **38**
5 Curriculum Vitae **48**
6 Publikationsliste **49**

ABKÜRZUNGEN

Arf	*alternative reading frame, p14Arf*
ATM	*ataxia teleangiectasia mutated*
ATP	Adenosintriphosphat
ATR	*ataxia telangiectasia and Rad3-related protein*
Bad	*Bcl-2 antagonist of cell death*
Bak	*Bcl-2 homologous antagonist/killer*
Bax	*Bcl-2-associated X protein*
Bcl-2	*B-cell leukemia/lymphoma 2*
BH	Bcl-2 Homologie
Bid	*BH3-interacting domain death agonist*
Bik	*Bcl-2-interacting killer*
Bim	*Bcl-2-interacting modulator of cell death*
Bok	*Bcl-2-related ovarian killer protein*
CAD	*caspase-activated DNase*
CARD	*caspase recruitment domain*
CED	*cell death protein*
Chk	*check point kinase*
DD	*death domain*
DED	*death effector domain*
DISC	*death-inducing signalling complex*
DNA	*desoxyribonucleic acid*
EGL-1	*egg-laying defective protein 1*
FADD	*Fas-associated protein with death domain*
Fas	*fibroblast-associated antigen*
FLICE	*FADD-like ICE*
FLIP	*FLICE-inhibitory protein*
MDM2	*mouse double minute 2 protein*
HMG1	*high mobility group protein B1*
IAP	*inhibitor of apoptosis protein*
ICAD	Inhibitor von CAD
ICE	*interleukin-1ß-converting enzyme*
Nbk	*natural born killer*
P53	Tumorsuppressorprotein p53
Puma	*p53 upregulated modulator of apoptosis*
TNF	Tumor-Nekrose-Faktor
TRAIL	*TNF-related apoptosis-inducing ligand*

Für L-Aminosäuren wurde der 1-Buchstabencode verwendet.

1 EINLEITUNG

Schon während der Embryogenese sind der gezielte Abbau überflüssig gewordener Strukturen und die Generierung neuer Gewebe durch Proliferation und Differenzierung wichtig. Dies gilt auch für die Metamorphose bei Amphibien und Insekten. Zur Aufrechterhaltung der Gewebshomöostase und Funktion des Immunsystems ist ein Gleichgewicht zwischen Zellteilung und Zelltod erforderlich (Vaux und Korsmeyer, 1999). Proliferation und Zelltod sind daher eng miteinander verknüpft. Versagt die Regulation eines dieser beiden Mechanismen, so kann es zu malignen Erkrankungen wie Tumoren oder zu Autoimmunerkrankungen kommen (Bakhshi *et al.*, 1985; Fisher *et al.*, 1995). Die Deregulation der zugrunde liegenden Mechanismen spielt auch bei vielen neurodegenerativen Erkrankungen und AIDS eine zentrale Rolle (Mattson, 2000; Rathmell und Thompson, 2002). Defekte in Zelltodsignalwegen können aber nicht nur zur Entstehung von Tumoren, sondern auch zur Entwicklung von Resistenzphänomenen gegenüber therapeutischer Behandlung führen (Guner *et al.*, 2003). Das Studium der zum Zelltod führenden Signalwege bildet daher die Grundlage für Therapieansätze bei verschiedensten Erkrankungen (Fischer und Schulze-Osthoff, 2005a; Fischer und Schulze-Osthoff, 2005b). Ein detailliertes Verständnis der beteiligten Mechanismen ist somit eine Voraussetzung für die gezielte Entwicklung neuer und wirkungsvoller Behandlungsstrategien von Erkrankungen, denen eine erhöhte oder verminderte Apoptoserate zugrunde liegt.

1.1 Formen des Zelltodes

Die Begriffe Apoptose, Nekrose und Autophagie bezeichnen morphologisch unterschiedliche Formen des Zelltodes. Das aus dem Griechischen entlehnte Wort Apoptose (*αποπτωσις*: das Abfallen, der Niedergang) definiert einen feinregulierten Selbstmordprozess, der im Genom aller Metazoen kodiert ist. Schon 1890 beschrieb William Councilman vakuolisierte, azidophile Körperchen im Lebergewebe von Gelbfieberpatienten (Councilman, 1890). Trotz dieser frühen phänomenologischen Beschreibung wurde erst im Jahr 1972 von Kerr und Kollegen der Begriff Apoptose geprägt, die mit Hilfe der Elektronenmikroskopie morphologische Veränderungen von sterbenden Zellen systematisch erfassten. Charakteristische Merkmale der Apoptose sind die Zellschrumpfung, die Ausstülpung der Zellmembran, die Kondensation des Chromatins sowie eine Fragmentierung des Zellkerns (Kerr *et al.*, 1972). Apoptose ist ein aktiver, energieverbrauchender Prozess, der mit der Generierung sogenannter apoptotischer Körperchen endet. In diesen Vesikeln sind die zellulären Bestandteile und Organellen von der Plasmamembran umgeben, die jedoch ihre asymmetrische Lipidverteilung verloren hat. Schon in frühen Phasen der Apoptose gelangt

Phosphatidylserin, das sich normalerweise auf der Innenseite der Zellmembran befindet, an die Außenseite, wo es als Erkennungssignal für phagozytierende Zellen dient (Li *et al.*, 2003).

Im Gegensatz zum physiologischen und aktiven Prozess der Apoptose erfolgt der nekrotische Zelltod passiv. Nekrose ist morphologisch durch ein Anschwellen der Zelle und die unregulierte Freisetzung intrazellulärer Bestandteile charakterisiert. Dies kann zu Entzündungserscheinungen im umliegenden Gewebe führen. Daneben wurde ein dritter Mechanismus, die Autophagie, beschrieben, bei der zelluläre Bestandteile in zytoplasmatischen Vakuolen, den sog. Autophagosomen, degradiert werden. Die Autophagie ist ebenfalls ein aktiver und feinregulierter Prozess, der zum Zelltod führen kann. Obwohl sich das Absterben einer Zelle durch die Autophagie nicht nur hinsichtlich morphologischer, sondern auch biochemischer Kriterien eindeutig von der Apoptose unterscheidet, wurde eine gemeinsame Beteiligung verschiedener Proteine an beiden Prozessen beschrieben (Hetz *et al.*, 2005; Levine und Yuan, 2005; Pattingre *et al.*, 2005). Während aber die Rolle der Apoptose in Entwicklungs- und Differenzierungsprozessen eindeutig etabliert ist, ist die Funktion des autophagischen Zelltodes noch weitgehend unklar.

1.2 Organisationsebenen der Apoptose

Die zentralen molekularen Komponenten der Apoptose wurden erstmalig durch genetische Studien in dem Spulwurm *Caenorhabditis elegans* identifiziert. In *C. elegans* sterben während der Entwicklung zum adulten Organismus exakt 131 der 1090 somatischen Zellen durch Apoptose (Sulston *et al.*, 1992). Hierfür sind im wesentlichen drei Genprodukte, CED-3, CED-4 und CED-9, notwendig (Banda *et al.*, 1992; Ellis *et al.*, 1991; Laurent-Crawford *et al.*, 1991). CED-3 ist ein Effektorprotein der Apoptose, dessen Aktivität in vitalen Zellen durch den Zelltod-Inhibitor CED-9 unterdrückt wird (Abbildung 1). Das Protein CED-4 ist ein aktivierender Adapter, der im Signalweg zwischen dem Effektor CED-3 und dem Inhibitor CED-9 angesiedelt ist. In vitalen Zellen des Wurms bilden die Proteine CED-3, CED-4 und CED-9 einen Komplex, in dem die Aktivierung des Effektors CED-3 durch CED-4 konstitutiv von CED-9 inhibiert wird. Zur Aktivierung des Apoptoseprogramms ist die Expression von EGL-1 (Conradt und Horvitz, 1998) erforderlich. Der Aktivator EGL-1 dissoziiert den Inhibitor CED-9 aus dem Komplex, wodurch CED-3 aktiviert wird und die Apoptose einleitet (Chinnaiyan *et al.*, 1997; Conradt und Horvitz, 1998; Hengartner und Horvitz, 1994).

Weitere Untersuchungen zur Regulation der Apoptose zeigten, dass die Schlüsselproteine in der Evolution außerordentlich konserviert sind und sowohl in *Drosophila* als auch in Primaten über ähnliche Signalkaskaden reguliert werden (Bergmann *et al.*, 1998).

In allen Organismen erfolgt die Regulation der Apoptose durch Inhibitoren und Aktivatoren am oberen Ende der Kaskade. Ihnen sind vermittelnde Adaptoren nachgeschaltet, die für die Aktivierung der Effektoren notwendig sind (Abbildung 1).

Im Gegensatz zu *C. elegans* unterscheidet man in Säugern jedoch zwei zentrale Signalwege: den extrinsischen und den intrinsischen Apoptose-Signalweg. Der intrinsische Signalweg wird durch zellulären Stress unterschiedlicher Natur (z.B. DNA-Schaden) eingeleitet und entscheidend von Mitochondrien kontrolliert. In Säugerzellen entsprechen die regulatorischen Genprodukte CED-9 und EGL-1 den anti-apoptotisch wirkendem Bcl-2- bzw. den pro-apoptotischen Bax-ähnlichen Proteinen. Unterhalb dieser regulatorischen Proteine ist das zu CED-4 homologe Adaptermolekül Apaf-1 angesiedelt. Dieses ist zur Aktivierung von Caspase-9, dem Homolog des Effektors CED-3, notwendig (Abbildung 1).

Der extrinsische Signalweg bildet in höheren Organismen den zweiten gut verstandenen Mechanismus der Apoptose-Induktion und wird durch sogenannte Todesrezeptoren auf der Zellmembran kontrolliert. Hierbei wird nach spezifischer Rezeptor-Ligand-Interaktion der Zelltodprozess in Gang gesetzt, in dem das Adapterprotein FADD an den Rezeptor rekrutiert wird und anschließend die Caspase-8 aktiviert (Abbildung 1). Alle Signalwege münden also in der Aktivierung von Caspasen, die am Ende des Signalweges zahlreiche Substrate proteolytisch spalten. Dies führt schließlich zum Absterben der Zelle und zur Ausbildung des charakteristischen apoptotischen Phänotyps.

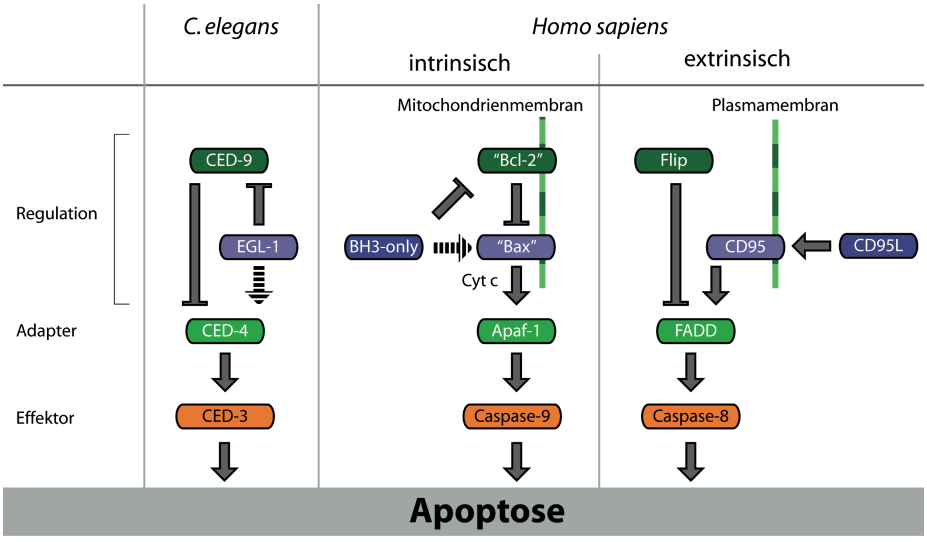

Abbildung 1: Ebenen der Apoptose-Regulation. Sowohl die extrinsisch wie auch die intrinsisch vermittelte Apoptose gliedert sich analog zum Modellorganismus *C. elegans* in drei Ebenen: die regulatorische Ebene wird von Inhibitoren und Aktivatoren gebildet, ihnen nachgeschaltet sind Adaptoren, an denen die Effektoren aktiviert werden. Ein unterbrochener Pfeil symbolisiert eine indirekte Wirkung.

1.3 Caspasen: Schlüsselenzyme der Apoptose

Alle charakteristischen Veränderungen der Apoptose werden durch intrazelluläre Proteasen der Caspase-Familie vermittelt, die eine Vielzahl von Substraten spalten und somit zum apoptotischen Zelltod beitragen. Der Name Caspase ist ein Akronym, das die Aminosäure Cystein im aktiven Zentrum und die Substratspezifität (Spaltung nach Aspartat) widerspiegelt und diese Proteasen daher als Cysteinyl-Aspartasen klassifiziert (Alnemri *et al.*, 1996). Die Proteinfamilie der Caspasen umfasst neben den in der Apoptose involvierten Mitgliedern auch Vertreter, die bei inflammatorischen Prozessen von Bedeutung sind (Abbildung 2). Alle Caspasen verfügen über eine große und eine kleine Untereinheit sowie eine charakteristische Prodomäne (Fuentes-Prior und Salvesen, 2004). Im Rahmen der Apoptose unterscheidet man die apikalen Initiatorcaspasen von den distalen Effektorcaspasen. Initiatorcaspasen verfügen über eine lange N-terminale Prodomäne, welche mittels charakteristischer Protein-Interaktionsmotive die Assoziation mit einer hochmolekularen Aktivierungsplattform erlaubt. Diese lange Prodomäne fehlt den Effektorcaspasen, die nur über eine kurze Prodomäne verfügen (Abbildung 2). Die Assoziation der Initiatorcaspasen mit dem jeweiligen Adaptermolekül in einer Aktivierungsplattform führt zu ihrer Dimerisierung (Boatright *et al.*, 2003; Pop *et al.*, 2006). Durch die Dimerisierung erfolgt eine Konformationsänderung, wodurch die Initiatorcaspasen aktiviert werden und ihre proteolytische Aktivität entfalten (Debatin und Krammer, 2004; Jiang und Wang, 2004).

Im Gegensatz zu Initiatorcaspasen, die als inaktive Monomere existieren, liegen Effektorcaspasen in der Zelle als dimere Zymogene vor (Renatus *et al.*, 2001; Riedl *et al.*, 2001). Zur Aktivierung der Effektorcaspasen ist ihre proteolytische Prozessierung zwingend notwenig. Diese erfolgt durch Initiatorcaspasen, welche die Effektorcaspasen in der Linkerregion zwischen großer und kleiner Untereinheit spalten und hierdurch aktivieren. Im Verlauf dieser Aktivierung wird weiterhin die kurze Prodomäne abgespalten, so dass aktive Effektorcaspasen aus einem Heterotetramer gebildet werden, das sich aus zwei großen und zwei kleinen Untereinheiten zusammensetzt (Fuentes-Prior und Salvesen, 2004).

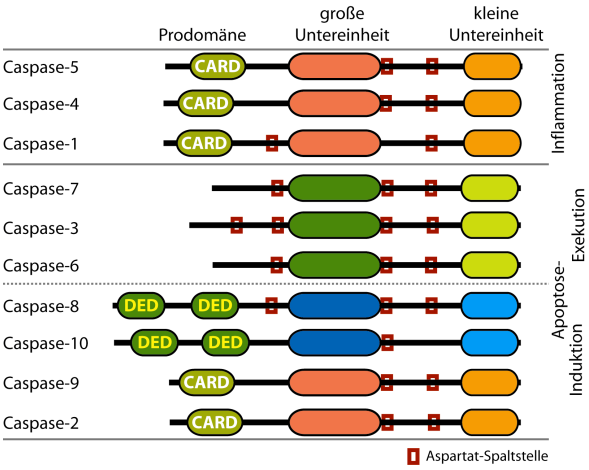

Abbildung 2: Einteilung der Familie der Caspasen (human). Caspase-1, -4 und –5 sind an inflammatorischen Prozessen beteiligt. Caspase-2, -8, -9 und –10 fungieren als pro-apoptotische Initiatorcaspasen, welche die Effektorcaspase-3, -6 und –7 durch spezifische Spaltung nach einem Aspartatrest aktivieren (Fuentes-Prior und Salvesen, 2004). Allen Caspasen ist eine große und kleine Untereinheit gemein. Initiatorcaspasen verfügen zudem über eine lange Prodomäne mit Interaktionsmotiven, die als DED *(death effector domain)* bzw. CARD *(caspase recruitment domain)* bezeichnet werden.

Ähnlich dem Gerinnungssystem wird folglich die proteolytische Aktivität der Caspasen in einer Kaskade reguliert, indem eine apikale Initiatorcaspase die distalen Effektorcaspasen spaltet und aktiviert. Für die im intrinsischen Signalweg essentielle Caspase-9 wurde die in Abbildung 3 dargestellte proteolytische Kaskade durch Experimente *in vitro* untersucht (Slee *et al.*, 1999). Hierbei stellte sich heraus, dass Caspase-9 nicht nur Effektorcaspasen aktiviert, sondern dass auch umgekehrt eine proteolytische Spaltung von Initiatorcaspasen durch Effektorcaspasen erfolgen kann.

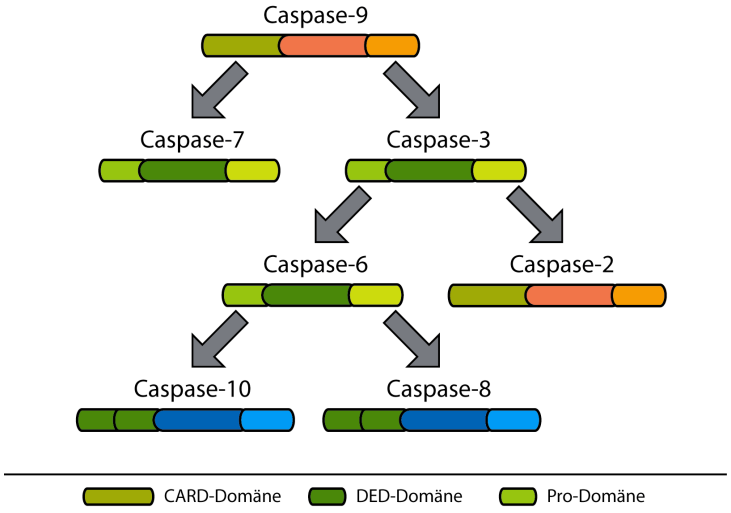

Abbildung 3: Die Caspase-Kaskade. Nach Aktivierung der Initiatorcaspase-9 spaltet und aktiviert diese die Effektorcaspasen 3 und 7. Caspase-3 kann wiederum Caspase-7 aktivieren. *In vitro* erfolgt zudem eine Spaltung der Initiatorcaspasen 8 und 10 durch Caspase-6 (Slee *et al.*, 1999).

Neben ihren Aktivierungsmechanismen unterscheiden sich Caspasen auch hinsichtlich ihrer Substratspezifität. Das allgemeine Erkennungsmotiv der Caspasen ist durch ein Tetrapeptid charakterisiert (P4-P3-P2-P1), an dessen P1-Position ein Aspartat Voraussetzung ist (Thornberry *et al.*, 2000; Thornberry *et al.*, 1997). Die an Position P4 bis P2 bevorzugten Aminosäuren sind durch die Primärstruktur der Caspasen und den damit

einhergehenden molekularen Wechselwirkungen begründet. Aktive Caspasen spalten eine Vielzahl von intrazellulären Substraten und führen hierdurch zur Ausprägung des apoptotischen Phänotyps (Fischer *et al.*, 2003; Martin und Green, 1995; Stroh und Schulze-Osthoff, 1998). Die Spaltung zahlreicher Strukturproteine ist für die Reorganisation der Zellarchitektur während der Apoptose verantwortlich. Die typische DNA-Fragmentierung ist eine Folge der Aktivierung der Endonuklease CAD *(caspase-activated DNase),* die über die Degradation der inhibitorischen Untereinheit ICAD *(inhibitor of CAD)* eingeleitet wird (Enari *et al.*, 1998; Liu *et al.*, 1997; Sakahira *et al.*, 1998).

1.4 Extrinsische Apoptose-Induktion: Todesrezeptoren

Ein relativ gut verstandener Mechanismus der Apoptose-Induktion wird im extrinsischen Signalweg über Todesrezeptoren gesteuert, welche in der Zellmembran verankert sind und zur TNF-Rezeptor-Superfamilie gehören. Todesrezeptoren verfügen über zwei bis vier extrazelluläre cysteinreiche Domänen und im Falle der funktionellen Mitglieder über eine intrazelluläre, etwa 80 Aminosäuren große Todesdomäne (*death domain*; Abbildung 4). Die Signaltransduktion der durch Todesrezeptoren vermittelten Apoptose ist am besten am Rezeptor CD95 untersucht worden. Die Stimulation von CD95 durch löslichen oder membrangebundenen CD95-Liganden führt zur Trimerisierung des Rezeptors und leitet damit die Bildung des Todessignal-Komplexes (DISC, *death-inducing signaling complex*) ein (Kischkel *et al.*, 1995). In diesem Komplex bindet zunächst das Adapterprotein FADD *(Fas-associating protein with death domain)* an den CD95-Rezeptor. Ermöglicht wird diese Bindung durch die homophile Interaktion der Todesdomäne von FADD mit der intrazellulären Todesdomäne von CD95. FADD seinerseits verfügt über eine weitere Interaktionsdomäne, die sogenannte Todeseffektordomäne (DED, *death effector domain*), die nun ihrerseits die Todeseffektordomäne der Initiatorcapase-8 und -10 bindet (Boldin *et al.*, 1996; Muzio *et al.*, 1996). Die räumliche Bindung im DISC erzeugt eine Konformationsänderung in den Initiatorcaspasen, durch die das aktive Zentrum zugänglich und die Protease aktiv wird (Ashkenazi und Dixit, 1998; Salvesen und Dixit, 1999). Im Falle des TNF-R1 wird ein leicht abgewandeltes Modell postuliert, in dem der aktive Caspase-8-Komplex nicht an der Zellmembran, sondern erst nach Internalisierung des Rezeptors im Zytoplasma gebildet wird (Micheau und Tschopp, 2003).

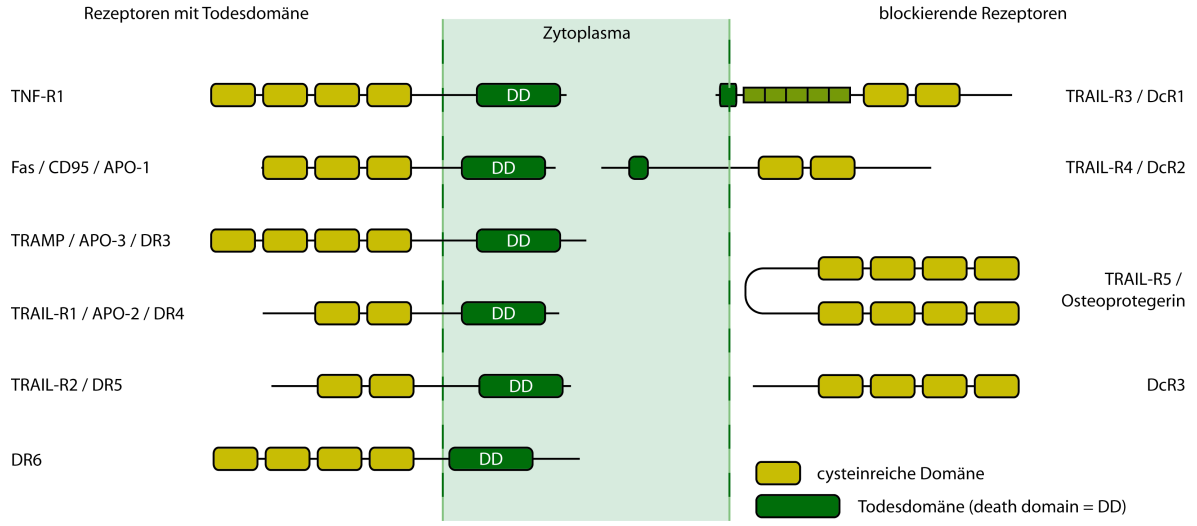

Abbildung 4: Exemplarische Darstellung von Vertretern der Familie der Todesrezeptoren. TNF = Tumor-Nekrose-Faktor; TRAIL = *TNF related apoptosis-inducing ligand; DR = death receptor; DcR = decoy receptor*.

Das Apoptosesignal der Todesrezeptoren kann auf der Ebene des DISC durch inhibitorische Proteine wie FLIP (*FLICE-inhibitory protein*, FLICE = Synonym für Caspase-8) reguliert werden (Irmler *et al.*, 1997; Scaffidi *et al.*, 1999a; Scaffidi *et al.*, 1999b). Im Gegensatz zu den anti-apoptotisch wirkenden Isoformen $FLIP_S$ und $FLIP_R$ (Golks *et al.*, 2005), die lediglich über die Todeseffektor-Domäne verfügen (Thome *et al.*, 1997) und Bindungsstellen für Procaspase-8 am DISC blockieren, ist für das längere Homolog $FLIP_L$ sowohl eine inhibierende Funktion bei hoher Proteinmenge (Irmler *et al.*, 1997; Srinivasula *et al.*, 1997) als auch eine aktivierende Wirkung bei geringen $FLIP_L$-Konzentrationen (Boatright *et al.*, 2003; Goltsev *et al.*, 1997; Inohara *et al.*, 1997) beschrieben (Abbildung 5).

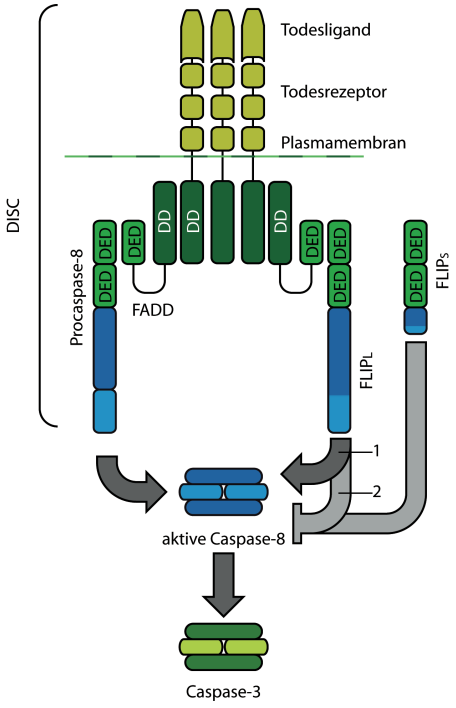

Abbildung 5: Der todesinduzierende Signalkomplex (DISC). Der DISC wird aus Ligand, Rezeptor, dem Adaptermolekül FADD und der Initiatorcaspase-8 gebildet (nach Lavrik *et al.*, 2005). $FLIP_S$ sowie hohe Konzentrationen von $FLIP_L$ (2) wirken inhibierend. Geringe Konzentrationen von $FLIP_L$ (1) können pro-apoptotisch wirken. Caspase-8 spaltet aktivierend die Effektorcaspase-3.

Die Todesrezeptoren können neben pro-apoptotischen auch anti-apoptotische Signale vermitteln. Dies ist insbesondere für den TNF-R1 vielfach belegt, bei dessen Stimulation es zur Aktivierung des klassischen NF-κB-Signalwegs kommt, der die Expression anti-apoptotischer Proteine wie z.B. FLIP und Bcl-2 induziert (Hsu *et al.*, 1996b). Ein wichtiger Regulator ist hierbei das Adaptermolekül TRADD *(TNF-receptor-associated protein with death domain),* welches einerseits FADD rekrutieren und so die Ausbildung des DISC initiieren kann, aber auch andererseits über die Kinase RIP-1 den Transkriptionsfaktor NF-κB aktiviert (Ashkenazi und Dixit, 1998; Hsu *et al.*, 1996a; Kelliher *et al.*, 1998).

1.5 Intrinsisch vermittelte Apoptose

1.5.1 Die Bcl-2-Proteinfamilie

Die Proteine der Bcl-2-Familie sind von essentieller Bedeutung für die Regulation der intrinsischen, mitochondrial vermittelten Apoptose. Charakteristisch für Proteine der Bcl-2-Familie ist das Vorhandensein sogenannter BH-Domänen (Bcl-2 Homologiedomäne). Man unterscheidet die anti-apoptotischen Bcl-2-Mitglieder von den pro-apoptotisch wirkenden Vertretern, die wiederum in die Unterfamilien der Multitdomänenproteine und die sogenannten BH3-only-Proteine unterteilt werden (Abbildung 6).

Die meisten anti-apoptotischen Familienmitglieder (z.B. Bcl-2 oder Bcl-xL) verfügen über alle vier BH-Domänen (BH1-4) und inhibieren über noch relativ unverstandene Mechanismen die pro-apoptotischen Multidomänenproteine (Adams und Cory, 1998). Sicher ist, dass die pro-apoptotischen Multidomänenproteine Bax (OItvai *et al.*, 1993), Bak (Chittenden *et al.*, 1995; Farrow *et al.*, 1995) und Bok (Hsu *et al.*, 1997), welche über eine BH1-, BH2- und BH3-Domäne verfügen, die Apoptose-assoziierte Aktivierung der Mitochondrien induzieren. Ein wichtiger Schritt ist hierbei die Exposition ihres N-Terminus, die im Falle von Bax mit der Translokation zu den Mitochondrien einhergeht (Nechushtan *et al.*, 1999; Wei *et al.*, 2000).

Die Konformationsänderung der pro-apoptotischen Multidomänenproteine wird entscheidend von den BH3-only-Proteinen kontrolliert, die als primäre Sensoren für verschiedene Todesstimuli fungieren. Sie weisen ausschließlich in der BH3-Domäne eine Homologie zu den übrigen Familienmitgliedern auf. BH3-only-Proteine können mittels ihrer BH3-Domäne mit anti-apoptotischen Familienmitgliedern, wie z.B. Bcl-2 oder Bcl-xL, durch Bindung an eine hydrophobe Spalte interagieren, die von den BH1-3 Domänen gebildet wird. Diese Interaktion von BH3-only-Proteinen mit den anti-apoptotischen Bcl-2-Proteinen

resultiert schließlich in der Freisetzung und Aktivierung der pro-apoptotischen Multidomänenproteine Bax oder Bak aus einem inaktiven Komplex (Liu *et al.*, 2003).

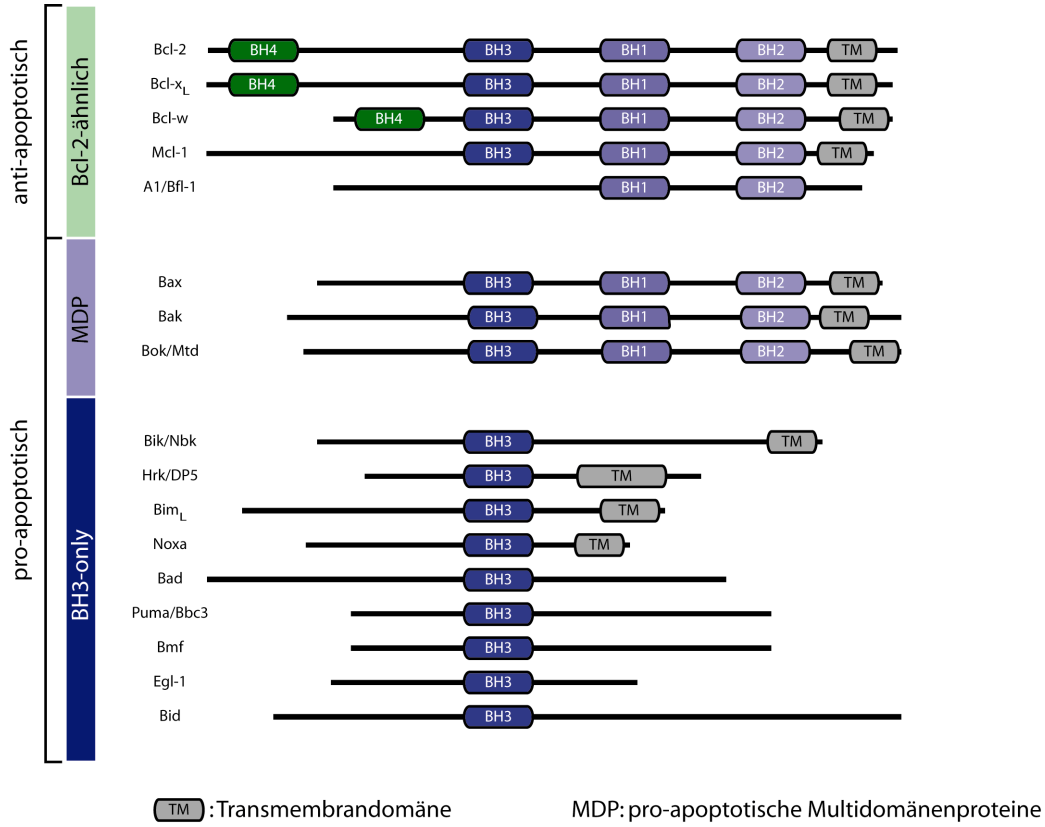

Abbildung 6: Vertreter der Bcl-2-Proteinfamilie und ihre Unterteilung in die drei Untergruppen. Die Bcl-2-ähnlichen Proteine wirken anti-apoptotisch. Bei den pro-apoptotischen Familienmitgliedern unterscheidet man Multidomänenproteine (MDPs) und BH3-only-Proteine.

BH3-only-Proteine zeigen innerhalb der Bcl-2-Proteinfamilie die größte Variabilität hinsichtlich ihrer Regulation. Diese erfolgt transkriptionell oder durch posttranslationale Modifikationen wie Phosphorylierung oder Spaltung und beruht vielfach auf der Änderung der subzellulären Lokalisation. Das BH3-only-Protein Puma *(p53 upregulated modulator of apoptosis)* z.B. ist aufgrund seiner Wechselwirkung mit vielen anti-apoptotischen Bcl-2-Proteinen ein sehr potenter Induktor der Apoptose und wird transkriptionell über p53 und p73 reguliert (Melino *et al.*, 2004; Nakano und Vousden, 2001). Ebenso ist Noxa ein transkriptionelles Zielgen von p53 (Oda *et al.*, 2000a); aufgrund seiner spezifischen Wechselwirkung mit dem anti-apoptotischen Mcl-1 zeigt es allerdings geringere Effizienz bei der Apoptose-Induktion. Nbk/Bik (*natural born killer/Bcl-2 interacting killer*), ein weiteres BH3-only-Protein, wird spezifisch in bestimmten Epithelgeweben und aktivierten B-Zellen exprimiert (Daniel *et al.*, 1999) und kann durch Phosphorylierung aktiviert werden (Verma *et al.*, 2001). Das BH3-only-Protein Bim (*Bcl-2-interacting modulator of cell death*), das in

verschiedenen Spleißformen exprimiert wird (Marani *et al.*, 2002; O'Connor *et al.*, 1998), ist an den Mikrotubuli lokalisiert und wird als Antwort auf verschiedene Apoptosestimuli freigesetzt. Die Aktivität von Bad (*Bcl-2 antagonist of cell death*), einem weiteren Vertreter derselben Untergruppe, wird ebenfalls durch Phosphorylierung reguliert (Datta *et al.*, 1997; Harada *et al.*, 1999; Zha *et al.*, 1996). Schließlich spielt das BH3-only-Protein Bid (*BH3-interacting domain death agonist*) eine wichtige Rolle bei der Verknüpfung des extrinsischen und des intrinsischen Apoptose-Signalweges (Gross *et al.*, 1999; Li *et al.*, 1998; Luo *et al.*, 1998). Bid kann von verschiedenen Caspasen gespalten werden, wodurch seine Aktivität als BH3-only-Protein freigesetzt wird. Diese aktivierende Spaltung von Bid wird wiederum durch spezifische Phosphorylierung negativ beeinflusst (Degli Esposti *et al.*, 2003; Desagher *et al.*, 2001).

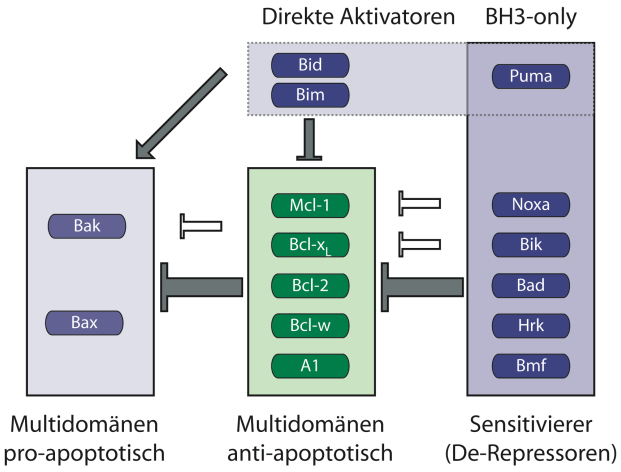

Abbildung 7: Wechselwirkungen der Bcl-2-Proteinfamilie. Die anti-apoptotischen Multidomänenproteine wirken inhibierend auf ihre pro-apoptotischen Gegenspieler. Für BH3-only-Proteine wird eine Unterteilung in aktivierende und sensitivierende Vertreter diskutiert. Die spezifische Wechselwirkung von Noxa mit Mcl-1 sowie Bik/Nbk mit Bcl-xL ist ebenso angedeutet wie die Wechselwirkung von Mcl-1 und Bcl-xL mit Bak. Puma wirkt inhibierend auf alle Bcl-2-ähnlichen Vertreter, aber auch eine aktivierende Funktion wird aktuell diskutiert.

Da die BH3-only-Proteine als Zelltodsensoren funktionieren, wurde die spezifische Interaktion ihrer BH3-Domänen mit anti-apoptotischen Vertretern der Bcl-2-Proteinfamilie detailliert untersucht und unterschiedliche Affinitäten gefunden (Chen et al., 2005). Auch wird aktuell eine Unterteilung der BH3-only-Proteine in De-Repressoren und Aktivatoren diskutiert (Abbildung 7). De-reprimierende BH3-only-Proteine binden an anti-apoptotische Bcl-2-Proteine und setzen so pro-apoptotische Multidomänen-Proteine aus ihrer Bindung an anti-apoptotische Proteine frei. Durch die De-Repression der Multidomänen-Proteine wird die Zelle für die Apoptose prädisponiert. Zur Induktion des Apoptose-Signalwegs ist zusätzlich ein Aktivator (z.B. Bid oder Puma) notwendig. Die aktivierenden BH3-only-Proteine interagieren transient mit den pro-apoptotischen Multidomänen-Proteinen und induzieren hierdurch eine aktivierende Konformationsänderung (Vousden, 2005).

Obzwar die Aktivität der zahlreichen BH3-only-Proteine differentiell reguliert wird, so ist doch das Schlüsselereignis des intrinsischen Apoptose-Signalweges in allen Fällen

identisch: Cytochrom c wird aus dem mitochondrialen Intermembranraum freigesetzt. Dies erfolgt nach Aktivierung des pro-apoptotischen Potentials der Multidomänen-Proteine, die hierauf multimere Komplexe in der äußeren Mitochondrienmembran ausbilden (Kroemer und Reed, 2000; Martinou und Green, 2001). Oligomere von Bax und Bak bilden Poren in der äußeren Mitochondrienmembran, durch die Cytochrom c und andere pro-apoptotische Faktoren freigesetzt werden (Puthalakath und Strasser, 2002).

1.5.2 Das Apoptosom

Ähnlich dem Rezeptor-vermittelten Signalweg, in dem Caspase-8 durch Rekrutierung an den DISC aktiviert wird, erfolgt bei der intrinsisch vermittelten Apoptose die Aktivierung der Initiatorcaspase-9 ebenfalls an einem hochmolekularen Multiproteinkomplex, dem Apoptosom. Nach Aktivierung durch Bax oder Bak setzen die Mitochondrien Cytochrom c aus dem Intermembranraum frei (Abbildung 8). Die Freisetzung von Cytochrom c ins Zytosol ist Voraussetzung für die Bildung des Aktivierungskomplexes im intrinsischen Apoptose-Signalweg und geht mit dem Verlust des mitochondrialen Membranpotentials einher. Cytochrom c bindet an die WD40-Domäne des Adapterproteins Apaf-1. Die Bindung von Cytochrom c führt zur Exposition der CARD *(caspase recruitment domain)* von Apaf-1, dessen Konformationsänderung zusätzlich durch ATP-Hydrolyse stabilisiert wird. Die Exposition der CARD erlaubt sowohl eine Komplexbildung von heptameren Apaf-1 als auch die Rekrutierung von Procaspase-9 über dessen CARD (Acehan *et al.*, 2002; Riedl *et al.*, 2005). Der Komplex aus Cytochrom c, Apaf-1 und Caspase-9 bildet das funktionelle Apoptosom. In Caspase-9 wird durch die Dimerisierung am Apoptosom eine Konformationsänderung induziert, wodurch diese aktiviert wird (Pop *et al.*, 2006). Die Ausbildung des Apoptosoms und Aktivierung von Caspase-9 bilden somit den Schlüsselschritt der intrinsisch vermittelten Apoptose (Jiang und Wang, 2004).

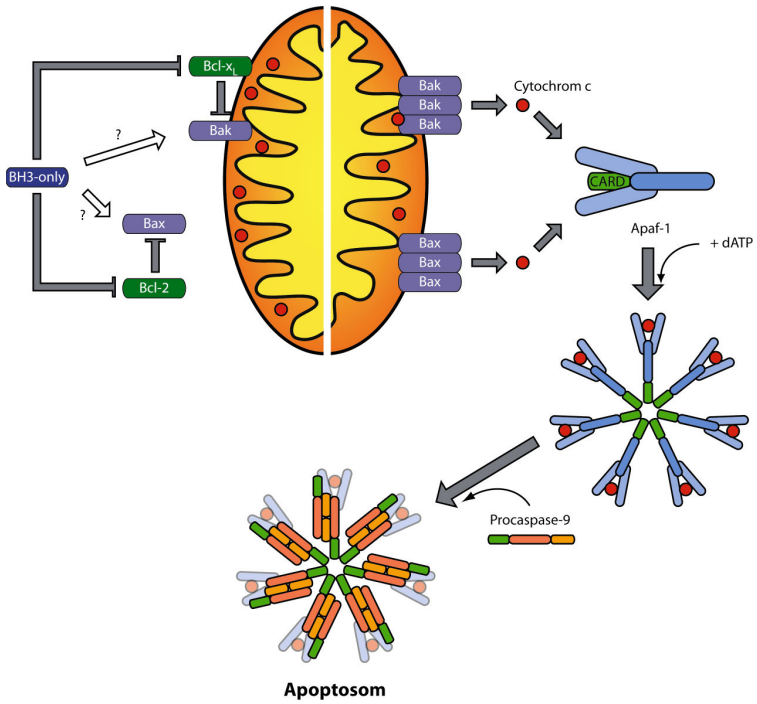

Abbildung 8: Schematische Darstellung der intrinsisch vermittelten Apoptose-Signalkaskade. Die Freisetzung von Cytochrom c und Bindung an Apaf-1 führt zur Ausbildung des proteolytisch aktiven Multiproteinkomplexes aus Apaf-1/Cytochrom c/Caspase-9, dem Apoptosom. Die Regulation erfolgt durch Proteine der Bcl-2-Familie. Durch BH3-only-Proteine werden anti-apoptotische Bcl-2-Proteine blockiert und/oder pro-apoptotische Multidomänenproteine aktiviert. Dies bewirkt die Oligomerisierung von Bax und Bak und hierdurch die Freisetzung von Cytochrom c.

Neben Cytochrom c werden nach dem Verlust der mitochondrialen Integrität auch andere pro-apoptotische Faktoren ins Zytosol freigesetzt, so z.B. AIF *(apoptosis-inducing factor)* und Smac/Diablo *(second mitochondria-derived activator of caspases / direct IAP binding protein with low pI)* (Du *et al.*, 2000). Während AIF die Fragmentierung zellulärer DNA induziert, wirkt Smac/Diablo der Inhibition von Caspasen durch IAPs *(inhibitor of apoptosis proteins)* entgegen (Chai *et al.*, 2000; Liu *et al.*, 2000; Srinivasula *et al.*, 2000). Die mitochondriale Freisetzung dieser pro-apoptotischen Proteine kann daher den intrinsischen Apoptose-Signalweg zusätzlich verstärken.

1.6 Verknüpfung der Apoptose-Signalwege

Schon bald nach der Identifizierung des CD95-DISC zeigte sich, dass nicht alle Zellen eine identische Signalleitung unterhalb der Todesrezeptoren aufweisen, sondern dass unterschiedliche Zelltypen in zwei Gruppen aufgeteilt werden können (Scaffidi *et al.*, 1998). So werden Typ I- und Typ II-Zellen aufgrund der Intensität der DISC-Bildung unterschieden. In Typ I-Zellen führt eine massive DISC-Bildung zu großen Mengen aktiver Caspase-8

und -10, der eine rasche Aktivierung der Caspase-3 folgt. Im Gegensatz dazu ist in Typ II-Zellen trotz ähnlicher Rezeptorexpression nur eine schwache DISC-Bildung nachzuweisen, die nicht ausreicht, um die Caspase-Kaskade zu aktivieren. In Typ II-Zellen muss das am Rezeptor generierte Signal über die Mitochondrien verstärkt werden, um effektiv Apoptose zu induzieren. Dies geschieht über die von Caspase-8/-10 vermittelte Spaltung des BH3-only-Proteins Bid zur aktiven Form tBid *(truncated Bid).* Das aktive tBid induziert durch Aktivierung von Bax oder Bak die beschriebene Freisetzung von Cytochrom c und Ausbildung des Apoptosoms (Gross *et al.*, 1999; Li *et al.*, 1998; Luo *et al.*, 1998).

Eine inverse Aktivierungsfolge wurde ebenso beschrieben, in der aktive Caspase-3 die Procaspase-8 spalten und so die proteolytische Kaskade verstärken kann (Engels *et al.*, 2000; Wieder *et al.*, 2001). In Übereinstimmung mit diesen Befunden kann bei der intrinsisch vermittelten Apoptose Caspase-8 in einer verstärkenden, rezeptorunabhängigen Rückkopplungsschleife aktiviert werden (Sohn *et al.*, 2005; von Haefen *et al.*, 2003).

1.7 Das Tumorsuppressorprotein p53 in der Apoptose

Wegen seiner herausragenden Rolle beim Schutz gegenüber der Tumorgenese wird das Protein p53 auch häufig als Wächter des Genoms bezeichnet. Es ist ein zentraler Knotenpunkt bei der Integration verschiedener zellulärer Prozesse und vermittelt Antworten, die von DNA-Reparatur über Zellzyklusarrest bis hin zu Seneszenz und Apoptose reichen (Jin und Levine, 2001). Inaktivierende Mutationen im p53-Gen treten in etwa 50 v.Hd. der Tumorerkrankungen auf (Hollstein *et al.*, 1991; Vousden und Prives, 2005), und der Verlust von p53 prädisponiert für die Entstehung kanzerogener Erkrankungen (Malkin *et al.*, 1990). Unter normalen Bedingungen liegt p53 in geringen Mengen in der Zelle vor und wird bei zellulärem Stress stabilisiert und aktiviert (Balint *et al.*, 1999; Wahl und Carr, 2001). Mutationen beeinflussen die Proteinstabilität von p53 nur zu einem geringen Ausmaß. Ein zentraler Regulator der p53-Stabilität ist vielmehr hMDM2, das humane Homolog von MDM2 *(mouse double minute 2 protein)* (Midgley und Lane, 1997). Die Regulation der p53-Stabilität erfolgt in einer autoregulatorischen Schleife. MDM2 ist eine E3 Ubiquitin-Ligase und markiert p53 durch Ubiquitinierung für den proteasomalen Abbau. MDM2 wird selbst transkriptionell von p53 reguliert (Barak *et al.*, 1994; Prives und Hall, 1999). Die Ubiquitinierung von p53 durch MDM2 bewirkt nicht nur die Markierung für den proteasomalen Abbau, sondern auch den Export von p53 aus dem Kern (Ashcroft und Vousden, 1999; Gu *et al.*, 2001). MDM2 wird seinerseits von Arf (*alternative reading frame*, alternativer Leserahmen des INK4a/Arf Genlokus) negativ reguliert (Pomerantz *et al.*, 1998; Sherr, 2006; Stott *et al.*, 1998), das hierdurch indirekt eine Stabilisierung von p53 bewirkt. Weiterhin wird die Expression von Arf

einerseits durch p53 negativ und andererseits über Onkogene wie E2F-1 positiv reguliert (Bates *et al.*, 1998), so dass sich ein komplexer Regelmechanismus ergibt (Abbildung 9).

DNA-Schäden werden von den Kinasen ATM *(ataxia teleangiectasia mutated)* und ATR *(ataxia telangiectasia and Rad3-related protein)* detektiert, die sowohl direkt als auch indirekt über die „Checkpoint"-Kinase-1 und –2 die Phosphorylierung und Aktivierung von p53 bewirken (Nakanishi *et al.*, 2006; Niida und Nakanishi, 2006; Sherr, 2006). Die zur p53-Aktivierung führenden Stresssignale können intrinsischer oder extrinsischer Natur sein. Zu den aktivierenden Signalen gehört insbesondere die Schädigung genomischer DNA, die durch γ-Strahlung (Doppelstrangbrüche) (Khanna und Jackson, 2001) oder UV-Strahlung (Smith *et al.*, 1995), Alkylierung, Depurinierung oder Oxidation hervorgerufen werden kann.

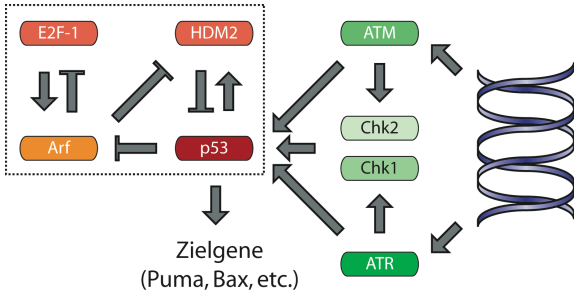

Abbildung 9: Zentrale Regulation des p53-Signalweges. Die Autoregulation von p53 durch MDM2 sowie durch Arf und Onkogene wie E2F-1 ist in der Box dargestellt. Nach DNA-Schädigung vermitteln ATM- und ATR-Kinasen die Phosphorylierung von p53 direkt oder über „Checkpoint"-Kinasen Chk2 und Chk1.

Die aktivierten Reparaturenzyme kommunizieren den DNA-Schaden über spezifische enzymatische Aktivitäten an p53. Dies geschieht durch vielfältige posttranslationale Modifikationen wie Phosphorylierung, Azetylierung, Methylierung, Ubiquitinierung oder Sumoylierung von p53 (Appella und Anderson, 2001). Phosphorylierungen treten vermehrt im N-terminalen Bereich in der Transaktivierungsdomäne von p53 auf. Azetylierung, Ubiquitinierung und Sumoylierung sind auf den C-terminalen Bereich beschränkt, der die Tetramerisierung und die Lokalisation von p53 beeinflusst (Abbildung 10). Die Kombination der verschiedenen Modifikationen ist vielfach spezifisch für den Typ des Stresssignals. Die durch verschiedenartige genotoxische Stimuli induzierten Signale werden also durch die Modifikationsereignisse in p53 integriert (Colman *et al.*, 2000). Hierdurch werden die unterschiedlichen Aktivitäten und Spezifitäten von p53 in noch nicht vollständig verstandener Weise gesteuert. Die durch p53 induzierte Apoptose wird über die Mitochondrien vermittelt (Vousden und Lu, 2002) und setzt daher einen intakten intrinsischen Apoptose-Signalweg voraus.

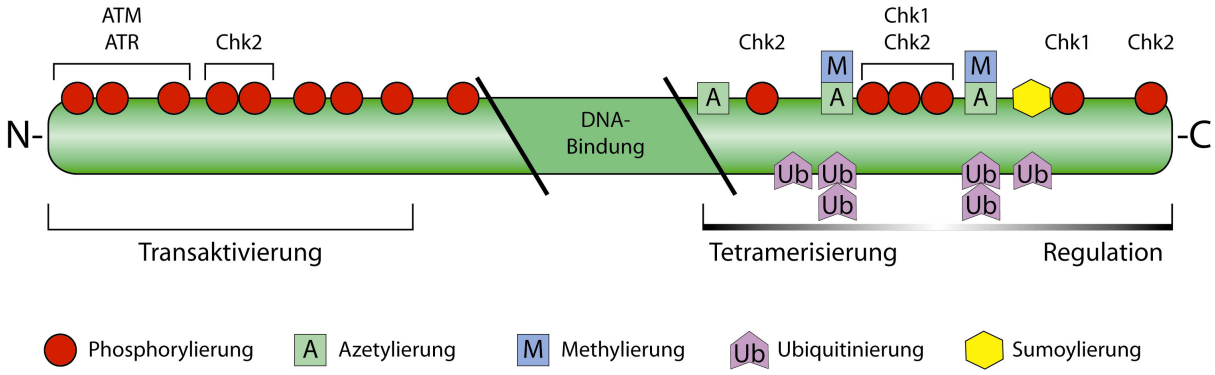

Abbildung 10: Bekannte Modifikationen des Tumorsuppressorproteins p53. Die unterschiedlichen Modifikationen von p53, Phosphorylierung, Azetylierung, Methylierung sowie Ubiquitinierung und Sumoylierung beeinflussen die Lokalisation, Aktivität und Stabilität von p53. Als Antwort auf Schädigung der DNA erfolgen verschiedene Phosphorylierungen durch ATM- oder ATR-Kinasen sowie durch die „Checkpoint"-Kinasen Chk1 und Chk2 (Lavin und Gueven, 2006).

1.7.1 Die Rolle von p53 auf transkriptioneller Ebene

Für das Tumorsuppressorprotein p53 sind zahlreiche Funktionen sowohl im Zellzyklus als auch in der Apoptose beschrieben (Chen *et al.*, 1996; Ko und Prives, 1996; Levine, 1997). Als Antwort auf genotoxischen Stress beeinflusst p53 die Progression durch den Zellzyklus und arretiert die betroffene Zelle in der späten G_1-Phase oder in der G_2-Phase (Di Leonardo *et al.*, 1994). Die Aktivierung von p53 nach DNA-Schädigung durch γ-Bestrahlung wird, wie beschrieben, über die Serin-Proteinkinase ATM (Banin *et al.*, 1998; Canman *et al.*, 1998) vermittelt, wohingegen durch UV-Strahlung hervorgerufene DNA-Schäden eine Antwort über ATR hervorrufen (Tibbetts *et al.*, 1999). Die „Ckeckpoint"-Kinasen Chk1 und Chk2 agieren unterhalb von ATR und ATM und bewirken ebenfalls die Phosphorylierung von p53, die dessen transkriptionelle Aktivität stimuliert (Chehab *et al.*, 2000; Shieh *et al.*, 2000). Von den über 150 beschriebenen Zielgenen von p53 ist in diesem Zusammenhang insbesondere der Cdk *(cyclin-dependent kinase)* Inhibitor p21 von Bedeutung, der den Zellzyklusarrest induziert und so die Zelle indirekt vor der Apoptose schützt (Xiong *et al.*, 1993). Als Apoptose-relevantes Zielgen von p53 wurden ebenso der CD95-Rezeptor und sein Ligand beschrieben. Auch das Bcl-2-Familienmitglied Bax wird in seiner Expression stark von p53 reguliert (Miyashita und Reed, 1995). Darüber hinaus scheint für die p53-abhängige Induktion der Apoptose die transkriptionelle Aktivierung der BH3-only-Proteine Puma (Miyashita und Reed, 1995; Nakano und Vousden, 2001; Yu *et al.*, 2001) und Noxa (Oda *et al.*, 2000a) sowie p53AIP (Oda *et al.*, 2000b) eine wichtige Rolle zu spielen.

1.7.2 Die Rolle von p53 auf nicht-transkriptioneller Ebene

Neben seiner anerkannten Funktion als Transkriptionsfaktor deutet eine zunehmende Zahl von Studien darauf hin, dass p53 auch eine transkriptionsunabhängige Rolle in der Apoptose spielt (Abbildung 11). In zellfreien Extrakten kann p53 nämlich in Gegenwart von Bax direkt die Freisetzung von Cytochrom c aus den Mitochondrien induzieren (Schuler *et al.*, 2000). Es wurde auch beschrieben, dass p53-Mutationen, die zum Verlust der transkriptionellen Aktivität führen, die p53-induzierte Apoptose nicht verhindern (Chipuk *et al.*, 2003; Dumont *et al.*, 2003). Jüngere Arbeiten lassen in der Tat vermuten, dass p53 direkt mit der mitochondrialen Apoptose-Maschinerie interagiert und möglicherweise eine den BH-3-only-Proteinen verwandte pro-apoptotische Aktivität besitzt (Marchenko *et al.*, 2000; Sansome *et al.*, 2001). So wurde gezeigt, dass p53 an die Mitochondrien transloziert und direkt an Bcl-xL und Bcl-2 bindet (Erster und Moll, 2004; Mihara *et al.*, 2003; Tomita *et al.*, 2006). In diesem Modell fungiert p53 ähnlich wie BH3-only-Proteine als De-Repressor und trägt so zur Freisetzung von Bak oder Bax bei. Ein anderes Modell bezieht das p53-Targetgen Puma in die transkriptionsunabhängigen Effekte von p53 ein. Demnach soll PUMA p53 aus seinem Komplex mit Bcl-2 verdrängen, wonach das freigesetzte p53 direkt an Bax binden und dessen pro-apoptotische Aktivität induzieren soll (Chipuk *et al.,* 2005). Es wurde auch eine direkte Interaktion von p53 mit Bak beschrieben, welche dessen Bindung an Mcl-1 aufhebt (Leu *et al.*, 2004).

Obwohl augenblicklich unklar ist, ob p53 als Aktivator oder De-Repressor von Bcl-2 Proteinen wirkt, beeinflusst zytosolisches p53 unzweifelhaft die Apoptose-Induktion. Das Ausmaß der transkriptionsunabhängigen pro-apoptotischen Wirkung von p53 wird nicht nur durch dessen Proteinmenge beeinflusst (Speidel *et al.*, 2006), sondern möglicherweise auch durch posttranslationale Modifizierung der anti-apoptotischen Bcl-2-Proteine (Deng *et al.*, 2006). Obwohl die Funktion von p53 als BH3-only-ähnlicher Aktivator ein attraktives Modell darstellt, bleiben jedoch Zweifel an dieser Funktion. So ist die p53-induzierte Apoptose in Puma-defizienten Fibroblasten blockiert (Yu *et al.*, 2003). Puma kann auch unabhängig von p53 direkt die Bindung von Bax an Bcl-xL aufheben (Ming *et al.*, 2006). Welche Relevanz einer transkriptionsunabhängigen Wirkung von p53 demnach für die Apoptose-Induktion zukommt, bedarf sicherlich weiterer Untersuchungen.

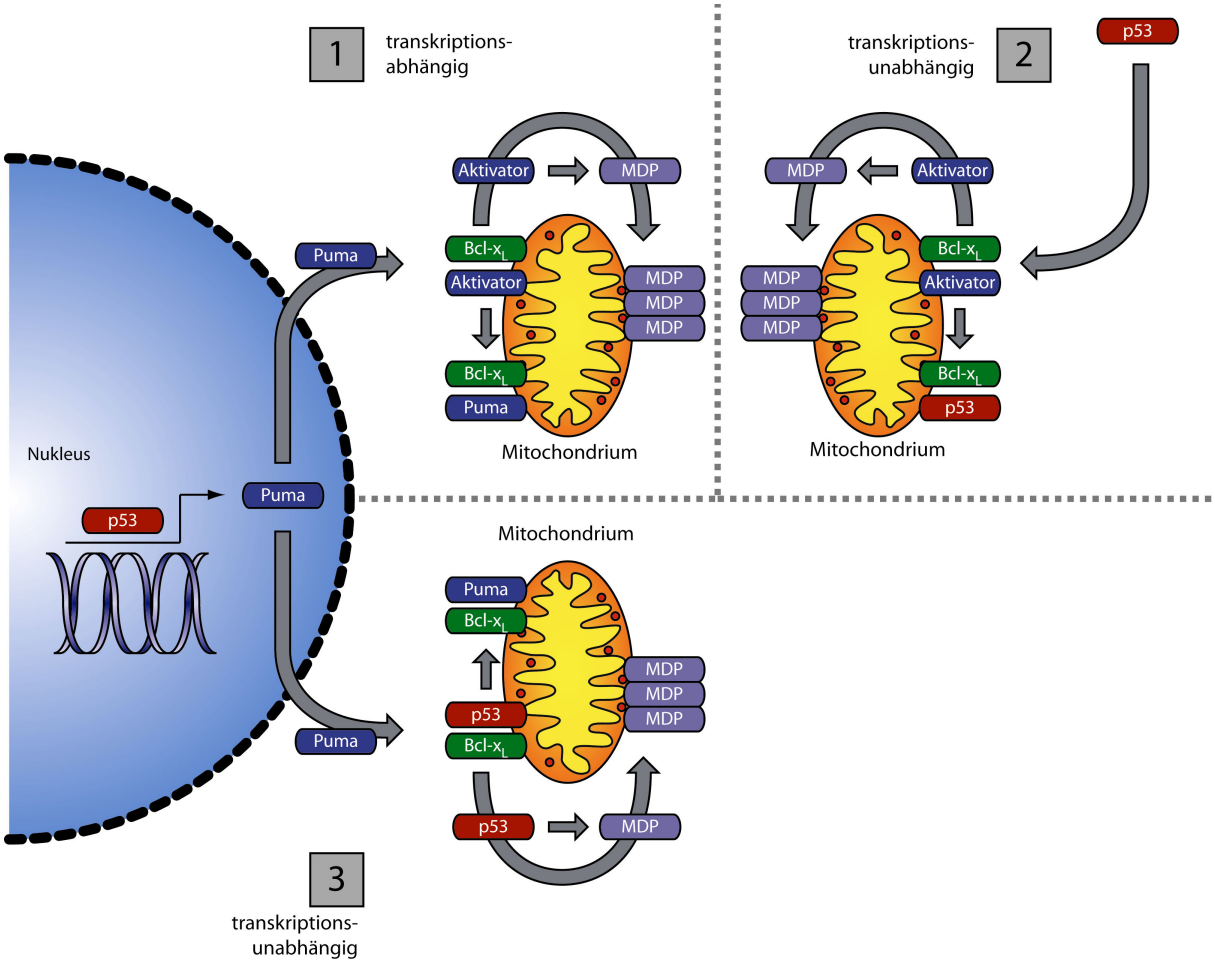

Abbildung 11: Aktuell diskutierte Mechanismen der pro-apoptotischen Wirkung von p53. (1) Das Protein p53 wirkt durch transkriptionelle Regulation des De-Repressors Puma. (2) Das Protein p53 kann selbst als De-Repressor an anti-apoptotische Bcl-2-Proteine binden und einen Aktivator freisetzen oder (3) p53 wird selbst durch Puma aus seiner Bindung an Bcl-xL freigesetzt und wirkt als Aktivator von Bax oder Bak (Vousden, 2005).

2 ZUSAMMENFASSUNG AUSGEWÄHLTER EIGENER PUBLIKATIONEN

2.1 D4-GDI wird bei Zytostatika-induzierter Apoptose durch Caspase-3 gespalten

Essmann, F., Wieder, T., Otto, A., Müller, E.C., Dörken, B. und Daniel, P.T. (2000). GDP dissociation inhibitor D4-GDI (Rho-GDI 2), but not the homologous rho-GDI 1, is cleaved by caspase-3 during drug-induced apoptosis. *Biochem J,* **346**: 777-783

In der Exekutionsphase der Apoptose werden zahlreiche zelluläre Substrate durch Caspasen proteolytisch gespalten. Die Spaltung einiger Proteine ist an der Ausbildung der apoptotischen Morphologie beteiligt, wohingegen die Spaltung regulatorisch wirkender Proteine direkt den Zelltodprozess beeinflussen kann. So wird beispielsweise in vielen Zellen das Strukturprotein β-Aktin im Verlauf der Apoptose gespalten, was zum Zusammenbruch des Zytoskelettes führt (Mashima *et al.*, 1997), während die Disassemblierung der nukleären Lamina mit der Caspasen-vermittelten Spaltung der Lamine A, B1 und C einhergeht (Lazebnik *et al.*, 1995; Orth *et al.*, 1996; Rao *et al.*, 1996). Zu den regulatorisch wirkenden Caspase-Substraten zählen unter anderem MDM2, dessen Spaltung zur Stabilisierung von p53 führt (Chen *et al.*, 1997; Erhardt *et al.*, 1997), die an DNA-Reparaturmechanismen beteiligte Kinase ATM (Smith *et al.*, 1999), die durch Spaltung inaktiviert wird, oder der Inhibitor der DNase CAD, dessen Spaltung zur Aktivierung der Endonuklease und zu internukleosomaler Fragmentierung genomischer DNA führt (Enari *et al.*, 1998).

Zu Beginn der Untersuchungen waren weder viele Caspase-Substrate bekannt noch die Signalwege der Chemotherapeutika-induzierten Apoptose hinlänglich charakterisiert. Daher sollte mit Hilfe der zweidimensionalen Gelelektrophorese nach neuen Zielproteinen von Caspasen gesucht werden. Im Vordergrund stand hierbei die Identifizierung von Proteinen, deren Spaltung zelluläre Signalkaskaden beeinflusst oder an der Ausbildung des apoptotischen Phänotyps beteiligt ist. Hierzu wurde in der humanen B-Zelllinie BJAB durch verschiedene Zytostatika (Taxol und Epirubicin) Apoptose induziert. Anschließend wurden durch subtraktive Analyse der zweidimensionalen Proteinmuster von apoptotischen und vitalen Zellen differenzielle Proteinspots gesucht. Diese Spots wurden massenspektrometrisch analysiert und mittels Datenbankrecherche identifiziert. Im Rahmen dieser Untersuchungen konnten wir auf diese Weise erstmalig die Caspase-3-vermittelte Spaltung des Proteins D4-GDI (D4 GDP-Dissoziationsinhibitor) bei der Zytostatika-induzierten Apoptose identifizieren und näher charakterisieren.

Das Protein D4-GDI gehört zur Familie der kleinen G-Proteine, die eine vielfältige Rolle bei der Zelldifferenzierung, der Organisation des Aktin-Zytoskeletts und bei der Kontrolle der Zellteilung spielen. Die Superfamilie der kleinen G-Proteine wird aus den Unterfamilien der Ras, Rho, Arf, Rab und Ran Proteine gebildet (Wennerberg und Der,

2004). Von diesen sind die Rho-Proteine an der Regulation der Integrin-Aktivität und der Organisation des Aktin-Zytoskeletts beteiligt (Burridge und Wennerberg, 2004; Hall, 1994; Narumiya, 1996). Die Aktivität verschiedener Rho-Proteine (z.B. RhoA, RhoB, RhoC) wird durch drei andere Proteingruppen kontrolliert: die GTP-Austauschproteine (GEF: *GDP/GTP exchange factor*), die GTPase-aktivierenden Proteine (GAP: *GTPase activating protein*) und die erwähnten GDP-Dissoziationsinhibitoren (GDIs) (Geyer und Wittinghofer, 1997). Die Untergruppe der GDIs besteht aus den drei Mitgliedern Rho-GDI-1, -2 und –3, von denen das in hämatopoetischen Zellen exprimierte Protein Rho-GDI-2 auch als D4-GDI oder Ly-GDI bezeichnet wird.

Mittels Caspase-spezifischer Peptid-Inhibitoren konnten wir nachweisen, dass die Spaltung von D4-GDI während der Zytostatika-induzierten Apoptose durch Caspase-3 vermittelt wird. Im Gegensatz zu einer früheren Arbeit, in der eine Spaltung von D4-GDI durch Caspase-1 vermutet wurde (Danley *et al.*, 1996), konnte in dem von uns verwendeten System eine Rolle von Caspase-1 ausgeschlossen werden. Auch eine Western-Blot-Analyse von *in vitro* aktivierten, zellfreien Extrakten bestätigte die Spaltung von D4-GDI durch Caspase-3. Mit Hilfe der Massenspektrometrie wurde darüber hinaus die exakte Spaltstelle in D4-GDI ermittelt. So zeigte sich, dass Caspase-3 D4-GDI an Aminosäure 19 nach der Caspasen-Erkennungssequenz DELD spaltet, wodurch ein N-terminal verkürztes Fragment entsteht (Abbildung 12). Bemerkenswert an der Spaltung von D4-GDI war ihre Spezifität. Unter identischen Bedingungen wurde nämlich das verwandte Protein Rho-GDI-1 nicht gespalten.

```
Rho-GDI-1:  MAEQEPTAEQ LAQIAAENEE     DEHSVNYKPP AQKSIQEIQE LDKDDESLRK YKEALLGRVA
D4-GDI:     MTEKAPEPHV EEDDD DELD/S   KLNYKPPPQK SLKELQEMDK DDESLIKYKK TLLGDGPVVT
            1          10          20           30          40          50          60
```

Abbildung 12: Partielle Aminosäuresequenz von Rho-GDI-1 und D4-GDI. Die identifizierte Spaltstelle von Caspase-3 (DELD$_{19}$S) und die von (Danley *et al.*, 1996) beschriebene der Caspase-1 (LLGD$_{55}$G) sind hervorgehoben. Bei Zytostatika-induzierter Apoptose erfolgt ausschließlich Spaltung an der Sequenz DELD.

Diese Daten werden gestützt durch Ergebnisse, die mit Hilfe rekombinanter Proteine die Spaltung von D4-GDI zeigen (Na *et al.,* 1996), und belegen, dass D4-GDI nicht nur bei IgM-vermittelter Apoptose (Brockstedt *et al.*, 1998; Rickers *et al.*, 1998), sondern auch bei Zytostatika-induziertem Zelltod von Caspase-3 gespalten wird. Im Unterschied zu früheren Arbeiten basieren die eigenen Ergebnisse auf der Verwendung *in vitro* aktivierter Zelllysate und der direkten Analyse apoptotischer B-lymphoider Zellen. Die Befunde aus dieser Arbeit wurden nachfolgend von mehreren Arbeitsgruppen bestätigt (Kwon *et al.*, 2002; Thiede *et al.*, 2002; Thiede *et al.*, 2005). Dies führte dazu, dass die Spaltung von D4-GDI inzwischen als anerkannter und sensitiver Marker für den Nachweis apoptotischer Prozesse in hämatopoetischen Zellen dient.

Welche physiologische Rolle die Spaltung von D4-GDI spielt, ist Gegenstand laufender Untersuchungen. In D4-GDI-defizienten Mäusen wurde gezeigt, dass die IL-2-induzierte Apoptose in T-Zellen, nicht aber die Dexamethason- oder T-Zell-Rezeptor-vermittelte Apoptose verändert ist (Yin *et al.*, 1997). Interessanterweise führte die Rekonstitution der Expression von D4-GDI in defizienten Tumorzelllinien zur Inhibition ihres metastatischen Potentials und ihrer Migration (Gildea *et al.*, 2002). Man kann daher vermuten, dass die Spaltung von D4-GDI einen Schutzmechanismus gegenüber Metastasierung darstellt.

2.2 Caspase-8 als Substrat von Effektorcaspasen

Wieder, T., Essmann, F., Prokop, A., Schmelz, K., Schulze-Osthoff, K., Beyaert, R., Dörken, B. und Daniel P.T. (2001). Activation of caspase-8 in drug-induced apoptosis of B-lymphoid cells is independent of CD95/Fas receptor-ligand interaction and occurs downstream of caspase-3. *Blood,* **97**: 1378-1387.

Bei der Behandlung maligner Tumore nimmt die auf zytostatischen oder zytotoxischen Agentien beruhende Chemotherapie eine zentrale Stellung ein. Obwohl sich die zugrunde liegenden Wirkmechanismen verschiedener Zytostatika erheblich unterscheiden, vereint sie die namensgebende anti-proliferative (zytostatische) und Apoptose-induzierende (zytotoxische) Wirkung. Diese wird häufig durch irreparable Schädigung der DNA erreicht, worauf die Zelle p53 aktiviert und entweder mit einem Arrest im Zellzyklus oder mit der Induktion von Apoptose reagiert. Von einigen Arbeitsgruppen wurde postuliert, dass die Zytostatika-induzierte Apoptose über das CD95-Rezeptor/Ligand System vermittelt wird. Diese Vermutung beruht im wesentlichen auf der Beobachtung, dass verschiedene Zytostatika die Expression des CD95-Liganden induzieren und mittels einer auto- oder parakrinen Wechselwirkung Apoptose über den Rezeptor CD95 vermitteln sollen (Friesen *et al.*, 1996; Fulda *et al.*, 2000).

Um eine Beteilung von CD95 oder anderen Todesrezeptoren an der Apoptose-Induktion durch Zytostatika zu überprüfen, wurden detaillierte Untersuchungen in humanen B-Zell Lymphomlinien durchgeführt. Sowohl Epirubicin als auch Taxol induzierten effizient Apoptose in verschiedenen lymphoiden B-Zelllinien, die mit der bereits erwähnten Spaltung des Caspase-3 Substrates D4-GDI (Essmann *et al.*, 2000) assoziiert war. Interessanterweise zeigte sich in der Tat, dass nicht nur Caspase-3, sondern auch Capase-8, die Initiatorcaspase bei Rezeptor-vermittelter Apoptose, hierbei prozessiert wurde (Boldin *et al.*, 1996; Muzio *et al.*, 1996). Es stellte sich jedoch heraus, dass die Spaltung und Aktivierung der Procaspase-8 nicht nur in CD95-sensitiven Zellen, sondern auch in Zellen zu beobachten waren, die keinen CD95-Rezeptor exprimierten. Weder die Defizienz anderer DISC-

Komponenten wie FADD noch die Überexpression einer dominant-negativ wirkenden FADD-Mutante, welche die Aktivierung der Caspase-8 am CD95-DISC blockiert, hatten einen signifikanten Einfluss auf das Ausmaß der Caspase-3- bzw. Caspase-8-Aktivierung. Demzufolge fand die Prozessierung von Caspase-8 offenbar unabhängig von CD95 oder anderen Todesrezeptoren statt. Unterstützt wurde diese Annahme durch die Beobachtung, dass ein selektiver Peptid-Inhibitor der Caspase-3 nicht nur die Spaltung des Caspase-3-Substrates D4-GDI, sondern auch die Prozessierung der Procaspase-8 blockierte. Western-Blot-Analysen und enzymatische Substratspaltungstests in einem *in vitro* Aktivierungssystem unter Verwendung zellfreier Extrakte zeigten schließlich, dass die Depletion der Caspase-3 die Spaltung von Procaspase-8 verhinderte. Die Anwesenheit aktiver Caspase-3 war also Voraussetzung für die Spaltung der Caspase-8.

Diese Ergebnisse belegen eindeutig, dass die Zytostatika-induzierte Aktivierung von Procaspase-8 unabhängig von der DISC-Bildung an CD95 oder anderen Todesrezeptoren verläuft. Es muss vielmehr gefolgert werden, dass die Prozessierung der Caspase-8 post-mitochondrial und unterhalb der Aktivierung der Effektorcaspase-3 erfolgt. Welche Relevanz diese Prozessierung im physiologischen Zusammenhang hat, wurde in der folgenden Arbeit untersucht.

2.3 Die Rolle von Caspase-8 in der mitochondrial vermittelten Apoptose

Von Haefen, C., Wieder, T., Essmann, F.*, Schulze-Osthoff, K., Dörken, B. und Daniel P.T. (2003). Paclitaxel-induced apoptosis in BJAB cells proceeds via a death receptor-independent, caspases-3/-8-driven mitochondrial amplification loop. *Oncogene,* **22**: 2236-2247.

In Typ I-Zellen ist die Rezeptor-vermittelte Aktivierung von Caspase-8 am DISC ausreichend, um die Caspase-Kaskade in Gang zu setzen und effizient Apoptose zu induzieren. Typ II-Zellen hingegen benötigen für die Apoptose-Induktion einen mitochondrialen Verstärkermechanismus, in dem Caspase-8 das BH3-only-Protein Bid zu tBid spaltet, welches anschließend eine Cytochrom c-Freisetzung bewirkt (Li *et al.*, 1998; Luo *et al.*, 1998). Während Caspase-8 bei Rezeptor-vermittelter Apoptose zweifellos von zentraler Bedeutung ist, war jedoch ihre funktionelle Rolle für die Zytostatika-induzierte Apoptose lange unbekannt. Da die vorherigen Untersuchungen eine Prozessierung und Aktivierung von Caspase-8 während der Zytostatika-induzierten Apoptose gezeigt hatten, sollte nun die Frage geklärt werden, welche physiologische Relevanz dieser Spaltung zukommt. In diesem Zusammenhang ist denkbar, dass die Aktivierung von Caspase-8, ähnlich wie in der Rezeptor-vermittelten Apoptose von Typ II-Zellen, zu einer Verstärkung der Apoptose-Kaskade führt, indem es Bid oder Effektorcaspasen spaltet und aktiviert. Andererseits könnte

es sich bei der Prozessierung der Caspase-8 aber auch um einen Nebeneffekt handeln, der keine funktionelle Relevanz für das Ausmaß der Zytostatika-induzierten Apoptose besitzt.

Zur Untersuchung dieser Fragestellung wurde in humanen B-lymphoiden BJAB-Zellen Apoptose durch das Zytostatikum Paclitaxel (Taxol) induziert und anschließend die Komponenten des intrinsischen Apoptose-Signalwegs analysiert. Ähnlich wie in der vorangegangenen Studie zeigte sich, dass eine Prozessierung von Caspase-8 nicht nur bei funktioneller Abwesenheit der DISC-Komponenten CD95 und FADD möglich war, sondern auch durch Bcl-x_L blockiert wurde und daher über einen mitochondrialen, rezeptorunabhängigen Mechanismus reguliert wurde. Das Ausmaß der Caspase-8 Prozessierung korrelierte interessanterweise auch mit der Spaltung von Bid, welche ebenso von Bcl-x_L blockiert wurde. Schließlich konnten wir zeigen, dass sowohl ein Caspase-8-selektiver Peptid-Inhibitor wie auch die Expression des Serpins CrmA, welches ebenfalls spezifisch Caspase-8 inhibiert, nicht nur die CD95-vermittelte Apoptose blockierte, sondern auch eine deutliche Inhibition der Zytostatika-induzierten Apoptose und Cytochrom c-Freisetzung bewirkte. Weiterhin führte die Inhibition von Caspase-8 nach Taxol-Behandlung auch zu einer verminderten Aktivierung von Caspase-3.

Diese Daten zeigten damit erstmalig, dass der Aktivierung von Caspase-8 auch in der Zytostatika-induzierten Apoptose eine offensichtlich wichtige funktionelle Rolle zukommt (Abbildung 13). Demzufolge kann Caspase-8 das Apoptose-Signal sowohl durch Spaltung von Effektorcaspasen wie Caspase-3 als auch durch die proteolytische Aktivierung von Bid amplifizieren. Die Aktivierung von Caspase-8 resultiert damit in einer effizienten Freisetzung von Cytochrom c nach Zytostatika-Behandlung. Diese Daten werden mittlerweile auch durch Befunde anderer Arbeitsgruppen gestützt (Cory *et al.*, 2003; Engels *et al.*, 2000; Gross *et al.*, 1999; Sohn *et al.*, 2005). Insgesamt zeigen die Ergebnisse, dass Caspase-8 nicht nur als Initiatorcaspase in der Rezeptor-vermittelten Apoptose fungiert, sondern auch als Effektorcaspase und Verstärker der Apoptose-Induktion durch Zytostatika dient.

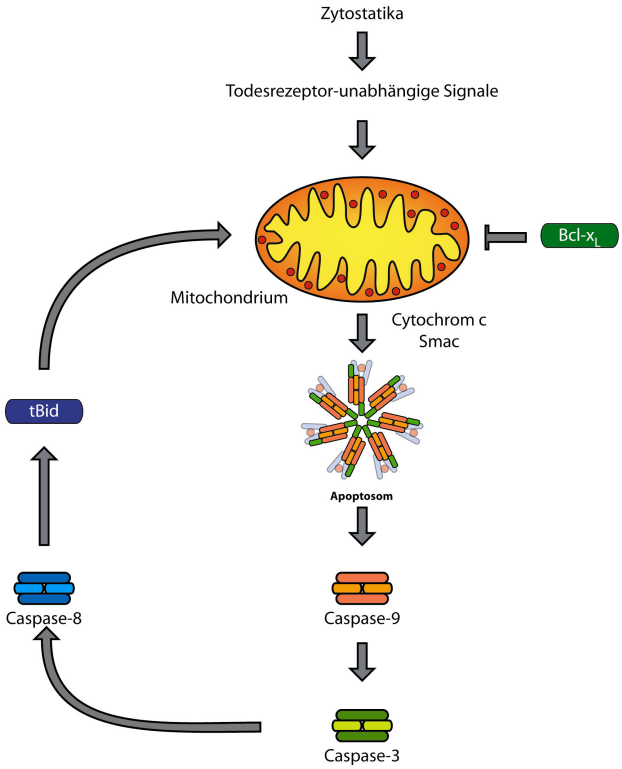

Abbildung 13: Rolle von Caspase-8 in der intrinsischen Apoptose-Signalkaskade. Durch die Spaltung von Bid durch Caspase-8 wird der Zusammenbruch des mitochondrialen Membranpotentials und die Freisetzung von Cytochrom c verstärkt. Dies resultiert in einer Amplifikationsschleife, die die mitochondriale Apoptose verstärkt.

2.4 Alpha-Toxin induziert Nekrose mit Apoptose-Charakteristika

Essmann, F., Bantel, H., Totzke, G., Engels, I.H., Sinha, B., Schulze-Osthoff, K. und Jänicke, R.U. (2003). Staphylococcus aureus alpha-toxin-induced cell death: predominant necrosis despite apoptotic caspase activation. *Cell Death Differ,* **10**: 1260-1272.

Zahlreiche pathogene Bakterien können über unterschiedliche Mechanismen den Zelltod von Wirtszellen induzieren. Vorarbeiten unserer Arbeitsgruppe hatten gezeigt, dass *Staphylococcus aureus* über den mitochondrialen Signalweg Caspasen aktiviert und hierdurch möglicherweise an der Immunsuppression bei bakterieller Sepsis beteiligt ist. Durch spezifische Antikörper und Bakterienmutanten konnte eindeutig das porenbildende Hämolysin α-Toxin als Virulenzfaktor und Mediator der *S. aureus*-vermittelten Caspase-Aktivierung identifiziert werden (Bantel *et al.*, 2001). Wie relevant die Caspase-Aktivierung jedoch für die resultierende Form des durch α-Toxin vermittelten Zelltodes (Apoptose versus Nekrose) ist, war unbekannt und wurde in der vorliegenden Arbeit untersucht.

In der Tat zeigte sich, dass geringe Konzentrationen des Hämolysins (<300 ng/mL) eine effiziente Prozessierung und Aktivierung von Caspasen induzierten, während höhere Konzentrationen eine deutlich geringere Caspase-Aktivierung bewirkten. Die Einwirkung von α-Toxin in geringen Dosen resultierte ebenso in verschiedenen Apoptose-typischen Veränderungen wie der Spaltung von Caspase-Substraten und der DNA-Fragmentierung, welches durch den Pan-Caspase-Inhibitor z-VAD-fmk blockiert wurde. Auch die Überexpression von Bcl-2 hemmte diese apoptotischen Veränderungen vollständig. Da verschiedene Bcl-2-Proteine strukturelle Ähnlichkeit mit dem porenbildenden Diphteriatoxin aufweisen (Garcia-Saez *et al.*, 2004; Muchmore *et al.*, 1996), wäre eine direkte Interaktion von α-Toxin mit Proteinen der Bcl-2-Familie denkbar. In diesem Zusammenhang wurde berichtet, dass α-Toxin auch in isolierten Mitochondrien eine Freisetzung von Cytochrom c bewirken kann (Bantel et al., 2001).

Interessanterweise zeigten weitere Analysen, dass ein Pan-Caspase-Inhibitor oder die Überexpression von Bcl-2 zwar die biochemischen Veränderungen der Apoptose blockierten, letztendlich aber keinen Einfluss auf die Zelltod-induzierende Wirkung von α-Toxin und das Überleben der behandelten Zellen besaßen. Es wurde deshalb untersucht, ob α-Toxin trotz der Aktivierung von Caspasen den Zelltod über andere, nicht-apoptotische Mechanismen wie z.B. die Nekrose hervorruft. Ein häufig verwendeter Test für die Diskriminierung von Apoptose und Nekrose ist die Doppelfärbung mit FITC (Fluorescein-Isothiocyanat)-gekoppeltem Annexin-V und Propidiumjodid (PI). Die Bindung von Annexin-V an Phosphatidylserin, das während der Apoptose an die Außenseite der Zellmembran transloziert, gilt als Zeichen von Apoptose. Die Aufnahme von PI deutet hingegen auf eine Schädigung der Plasmamembran hin, die in der Regel nur bei post-apoptotischen und

nekrotischen Zellen beobachtet wird. Es zeigte sich jedoch, dass aufgrund der porenbildenden Eigenschaften eine derartige Doppelfärbung für das Hämolysin α-Toxin nur bedingt verwendbar war und keine aussagekräftigen Resultate lieferte. Es wurden daher weitere Analysemethoden etabliert, um den α-Toxin-vermittelten Zelltod näher zu charakterisieren.

Als eine sehr brauchbare Methode hierzu erwies sich der Nachweis des *high mobility group I* Proteins (HMG1) in Kulturüberständen von α-Toxin behandelten Zellen. HMG1 wird von aktivierten Makrophagen als proinflammatorisches Signalmolekül sekretiert. Eine weitere Funktion von HMG1 ist die Bindung an Chromatin-Strukturen im Zellkern. Aufgrund einer Veränderung im Azetylierungsstatus von Chromatin setzen nekrotische Zellen HMG1 passiv aus dem Zellkern frei, was zu einer proinflammatorischen Reaktion führt (Scaffidi *et al.*, 2002). Im Gegensatz dazu bleibt HMG1 in apoptotischen Zellen an Chromatin gebunden. Somit kann die zelluläre Freisetzung von HMG1 als charakteristischer Marker für Nekrose verwendet werden. Es zeigte sich in der Tat, dass die Behandlung von Zellen mit α-Toxin, nicht jedoch eine Apoptose-Induktion über das CD95-System, zu einer deutlichen Freisetzung von HMG1 in die Kulturüberstände führte. Die Freisetzung von HMG1 wurde weder durch Expression von Bcl-2 noch durch pharmakologische Caspase-Inhibitoren verhindert. Diese Resultate weisen demnach daraufhin, dass α-Toxin einen nekrotischen Zelltod induziert.

Die Induktion der Nekrose durch α-Toxin wurde auch durch eine Freisetzung der Laktat-Dehydrogenase in das Kulturmedium bestätigt. Die Freisetzung dieses zellulären Enzyms, welches häufig als Indiz für Nekrose genutzt wird, ließ sich weder durch Inhibition von Caspasen noch durch die Überexpression von Bcl-2 verhindern. Schließlich zeigten auch elektronenmikroskopische Analysen, dass die Behandlung mit α-Toxin zu einer deutlichen Vakuolisierung der Zellen führte, während apoptotische Veränderungen, wie beispielsweise Zellschrumpfung und Kernfragmentierung, nicht ausgebildet wurden.

Insgesamt zeigten die Untersuchungen daher nicht nur, dass der durch α-Toxin von *S. aureus* induzierte Zelltod vornehmlich über nekrotische Mechanismen verläuft, sondern dass auch die Aktivierung von Caspasen nicht zwingend zur Apoptose führt. Unsere Daten belegen deshalb einen fließenden Übergang zwischen apoptotischem und nekrotischem Zelltod (vgl. Borner und Monney, 1999; Leist und Jaattela, 2001). Dieser Befund impliziert zugleich, dass zur Charakterisierung von Zelltodprozessen mehrere Analysemethoden verwendet werden sollten.

2.5 Die Apoptose-Induktion durch das BH3-only-Protein Nbk/Bik ist Bax-abhängig

Gillissen, B., Essmann, F., Graupner, V., Stärck, L., Radetzki, S., Dörken, B., Schulze-Osthoff, K. und Daniel P.T. (2003). Induction of cell death by the BH3-only Bcl-2 homolog Nbk/Bik is mediated by an entirely Bax-dependent mitochondrial pathway. *EMBO J,* **22**: 3580-3590.

Die pro- und anti-apoptotischen Mitglieder der Bcl-2-Familie sind essenziell für die Regulation der durch Mitochondrien aktivierten Signalkaskade (Cory *et al.*, 2003; Danial und Korsmeyer, 2004). Das Modell, in dem die Freisetzung von Cytochrom c aus den Mitochondrien durch die pro-apoptotischen Multidomänenproteine Bax und Bak vermittelt wird, gilt als etabliert. Auch die Funktion der BH3-only-Proteine als Sensoren für verschiedene Zelltod-Stimuli ist allgemein akzeptiert. BH3-only-Proteine leiten nach ihrer Aktivierung die Oligomerisierung der pro-apoptotischen Multidomänenproteine Bax und Bak ein (Willis und Adams, 2005). Über diese phänomenologische Beschreibung hinaus sind die Mechanismen bei der Aktivierung der BH3-only-Proteine und der Oligomerisierung von Bax und Bak aber nicht aufgeklärt.

Auch für das spezifisch in einigen Epithelgeweben und aktivierten lymphoiden B-Zellen exprimierte BH3-only-Protein Nbk/Bik (Boyd *et al.*, 1995; Han *et al.*, 1996) liegen bisher nur wenige Untersuchungen zur Funktionsweise bei der Apoptose-Induktion vor. Daher wurde die pro-apoptotische Funktion von Nbk/Bik mit Hilfe eines Tetrazyklin-regulierbaren adenoviralen Expressionssystems in humanen Zellen analysiert. Bemerkenswerterweise führte die Expression von Nbk in verschiedenen Bax-positiven, nicht aber in Bax-negativen Tumorzelllinien zum Zelltod. Diese Ergebnisse konnten in zwei spezifischen Zellsystemen verifiziert werden. So vermittelte der *Knock-out* von Bax in HCT116-Zellen eine Resistenz gegenüber Nbk-induziertem Zelltod. Komplementär hierzu führte die Rekonstitution der Bax-Expression in der Bax-defizienten Prostatakarzinomzelllinie DU145 zur Wiederherstellung der Sensitivität gegenüber Nbk/Bik-induzierter Apoptose. Wir konnten daher erstmals zeigen, dass Nbk/Bik nur in der Gegenwart von Bax effizient Apoptose induzieren kann. Wichtig ist hierbei die Tatsache, dass die Zelllinien endogen das zu Bax homologe Protein Bak exprimierten und somit Bak den Verlust von Bax nicht kompensieren kann. Nur in Bax-positiven Zellen induzierte Nbk eine Cytochrom c-Freisetzung und Caspase-9-Aktivierung. Interessanterweise konnten wir zeigen, dass während dieser Prozesse Nbk jedoch nicht zu den Mitochondrien transloziert, sondern sich am endoplasmatischen Retikulum (ER) befindet. Die durch Nbk induzierte Cytochrom c Freisetzung deutet daher auf eine Signalübermittlung zwischen ER und Mitochondrium hin und unterstreicht die in neueren Untersuchungen aufgezeigte Rolle des ER bei der Induktion von Apoptose.

Wir konnten weiterhin zeigen, dass Nbk/Bik spezifisch sowohl mit Bcl-xL als auch mit Bcl-2 interagiert, aber nicht direkt an Bax bindet. Beide Proteine wirken inhibierend auf Bax; diese Wirkung wird also wahrscheinlich durch Bindung von Nbk/Bik aufgehoben. In diesem Zusammenhang konnten wir nachweisen, dass Nbk/Bik durch die Interaktion mit Bcl-xL die Freisetzung von Bax aus der Bindung an Bcl-xL hervorruft und so die Aktivierung und Oligomerisierung von Bax induziert. Diese Befunde wurden später in Arbeiten über spezifische Interaktionen von Bcl-2-Familienproteinen verifiziert (Chen *et al.*, 2005; Willis und Adams, 2005). Hierauf beruht auch ein aktuelles Modell zur Interaktion von Proteinen der Bcl-2-Familie, in dem Bax durch Bcl-xL inhibiert wird und diese Inhibition durch Bindung von Nbk/Bik an Bcl-xL aufgehoben wird (van Delft und Huang, 2006). Zugleich zeigten unsere Daten erstmalig, dass Bak und Bax, denen häufig eine funktionelle Redundanz zugesprochen wird, vermutlich auch spezifische Funktionen in der Apoptose-Regulation besitzen.

2.6 Die Rolle von p53 bei Resistenzmechanismen gegenüber γ-Bestrahlung

Essmann, F., Engels, I.H., Totzke, G., Schulze-Osthoff, K. und Jänicke R.U. (2004). Apoptosis resistance of MCF7 breast carcinoma cells to ionizing radiation is independent of p53 and cell cycle control but caused by the lack of caspase-3 and a caffeine-inhibitable event. *Cancer Res,* **64**: 7065-7072.

Eine Resistenz gegenüber Apoptose nach DNA-Schädigung ist häufig mit dem Vorhandensein von nicht-funktionellem p53 oder dessen gänzlicher Abwesenheit assoziiert. Aufgrund der fehlenden Induktion von BH3-only-Proteinen und anderen Zielgenen von p53 kann die geschädigte Zelle dann nicht adäquat auf den DNA-Schaden reagieren. Nichtsdestotrotz zeigen verschiedene Zellsysteme eine Resistenz gegenüber der durch DNA-Schäden induzierter Apoptose, obwohl sie ein funktionelles p53-Protein exprimieren. Neben der Verwendung von zytostatisch wirkenden Substanzen können DNA-Strangbrüche auch durch hochenergetische Strahlen induziert werden. Im Falle der auch therapeutisch eingesetzten γ-Strahlen resultiert dies vorwiegend in der Erzeugung von Doppelstrangbrüchen. In einem funktionellen p53-System reagiert die Zelle hierauf mit einem Arrest im Zellzyklus (G_1- bzw. G_2-Phase), der bei entsprechender Dosis persistiert. Bestrahlung resultiert also im Verlust klonogenen Wachstums, anhaltende Proliferation wird als Bestrahlungs-Resistenz bezeichnet. Ist die Schädigung der DNA so gravierend, dass eine Reparatur unmöglich ist, wird über p53 Apoptose induziert (Levine *et al.*, 2006). Eine alternative Stressantwort ist die irreversible Induktion von zellulärer Seneszenz, bei der die Zelle zwar nicht proliferiert, jedoch metabolisch aktiv bleibt (Normand *et al.*, 2005).

Die Mammakarzinom-Zelllinie MCF7 ist resistent gegenüber Bestrahlungs-induzierter Apoptose, obwohl sie ein funktionelles p53-Protein exprimiert (Janicke *et al.*, 1998a; Janicke *et al.*, 1998b). Während die Zellen über ihren funktionellen intrinsischen Signalweg durch Zytostatika effektiv in die Apoptose getrieben werden können, induziert die γ-Bestrahlung einen Arrest in der G2-Phase des Zellzyklus (Janicke *et al.*, 2001). MCF7-Zellen exprimieren aufgrund einer partiellen Deletion des Caspase-3-Gens diese Effektorcaspase nicht, weswegen ihre Apoptose-Resistenz gegenüber γ-Strahlen mit der Abwesenheit dieses Proteins begründet wurde. Interessanterweise zeigte sich jedoch, dass γ-Bestrahlung von MCF7-Zellen auch nach Rekonstitution der Caspase-3-Expression nicht zur Induktion von Apoptose führte. Zur Aufklärung der zugrunde liegenden Mechanismen sollte daher untersucht werden, ob ein kausaler Zusammenhang zwischen der Apoptose-Resistenz und dem Zellzyklusarrest besteht. In diesem Fall sollte nach Aufhebung des G2-Arrestes p53-abhängig Apoptose induzierbar sein.

Um eine Beteiligung des p53-abhängigen Zellzyklusarrests an der Apoptose-Resistenz zu untersuchen, wurden die Inhibitoren Koffein und UCN-01 eingesetzt (Bunch und Eastman, 1996; Lau und Pardee, 1982). Koffein ist ein Inhibitor der ATM-Kinase, die nach DNA-Schädigung den p53-Signalweg aktiviert. Das Staurosporin-Analogon UCN-01 ist ebenfalls ein Kinase-Inhibitor, der allerdings selektiv auf die „Checkpoint"-Kinasen Chk1 und Chk2 wirkt (Yu *et al.*, 2002) und ebenfalls die Aktivierung von p53 inhibiert. In der Tat korrelierte die durch diese Inhibitoren erreichte Aufhebung des Bestrahlungs-induzierten Zellzyklusarrestes mit dem Zusammenbruch des mitochondrialen Membranpotentials und der Freisetzung von Cytochrom c und Smac/Diablo. Die Aktivierung der Caspase-Kaskade und apoptotischer Zelltod wurden aber selbst nach Aufhebung des G2-Arrestes nicht detektiert. Wir vermuteten deshalb, dass dies in der Abwesenheit der Effektorcaspase-3 begründet liegt. So führte nach Rekonstitution der Caspase-3-Expression die Aufhebung des Bestrahlungs-induzierten G2-Arrestes erfolgreich zur Induktion von Apoptose. Es konnte also gezeigt werden, dass Caspase-3 nicht nur für die Spaltung von Substraten, sondern auch für die vollständige Aktivierung der Initiatorcaspase-9 im Apoptosom notwendig ist.

Bemerkenswerterweise zeigte sich in Experimenten mit Caspase-3-exprimierenden MCF7-Zellen unter Verwendung des Translationsinhibitors Cycloheximid und des p53-spezifischen Inhibitors Pifithrin (Komarov *et al.*, 1999), dass die Apoptose-Induktion durch γ-Bestrahlung unabhängig von der Induktion von p53-Zielgenen ist. Durch diese Inhibitoren wird die Expression bzw. Induktion von p53-Zielgenen blockiert, wie es auch für den Zellzyklusinhibitor p21 belegt wurde. Weder Cycloheximid noch Pifithrin hatten aber einen signifikanten Einfluss auf das Ausmaß der Apoptose-Induktion durch γ-Bestrahlung. Die Herunterregulation der p53-Expression durch siRNA bestätigte diesen Befund. Auch die

generierten p53-*Knock-down* Zellen wurden durch Koffein für die durch γ-Strahlen-induzierte Caspase-Aktivierung und Apoptose sensitiviert. Die Anwesenheit von funktionellem p53 war demnach in MCF7-Zellen für die Aufhebung der Bestrahlungs-Resistenz durch Koffein nicht erforderlich.

Für das untersuchte Zellsystem muss gefolgert werden, dass an der Resistenz zwei unabhängige Mechanismen beteiligt sind: zum einen der Verlust der Caspase-3 und zum anderen ein p53-unabhängiger Mechanismus, der oberhalb der Mitochondrien für deren Aktivierung notwendig ist. Letzterer wird von Koffein moduliert, so dass Apoptose-Induktion durch γ-Bestrahlung in Abhängigkeit von Caspase-3 ermöglicht wird.

2.7 Die Rolle von mitochondrial lokalisiertem p53 bei der Apoptose

Essmann, F., Pohlmann, S., Gillissen, B., Daniel, P.T., Schulze-Osthoff, K. und Jänicke R.U. (2005). Irradiation-induced translocation of p53 to mitochondria in the absence of apoptosis. *J Biol Chem,* **280**: 37169-37177.

Neben der anerkannten transkriptionsabhängigen Funktion von p53 beschreibt eine zunehmende Anzahl von Veröffentlichungen eine transkriptionsunabhängige Rolle von p53 bei der Apoptose (Chipuk und Green, 2003; Erster und Moll, 2005; Moll und Zaika, 2001; Yee und Vousden, 2005). Den Anstoß hierzu hat wohl insbesondere die Beschreibung der Cytochrom c-Freisetzung durch p53 aus isolierten Mitochondrien gegeben (Schuler *et al.*, 2000). Bisher wurden verschiedene Mechanismen vorgeschlagen, die sowohl die mitochondriale Translokation von p53 als auch seine Interaktion mit Bcl-2-Familienproteinen beinhalten. Ungeklärt ist aber, ob p53 eine de-reprimierende oder aktivierende Funktion ausübt (Abbildung 11, 2 und 3).

Vor allem im Zusammenhang mit den oben genannten neuen Befunden zur p53-abhängigen Apoptose erschien eine detaillierte Analyse der Resistenzmechanismen gegen Bestrahlungs-induzierte Apoptose sinnvoll (2.6). Es sollte nun in verschiedenen Zellsystemen die Rolle von p53 auf nicht-transkriptioneller Ebene bei γ-Bestrahlung und auch bei Zytostatika-Behandlung eingehend untersucht werden. Da die verwendeten, gegen strahleninduzierte Apoptose resistenten Zellen ein transaktivierendes p53 exprimieren, könnte die Resistenz in einer defekten p53-Funktion auf nicht-transkriptioneller Ebene begründet liegen. Verschiedene Zelllinien wurden daher sowohl mit γ-Strahlen als auch mit den Zytostatika Camptothecin, einem Topoisomerase-I-Inhibitor, und Etoposid, einem Topoisomerase-II-Inhibitor, behandelt. Es zeigte sich, dass Zytostatika effizient Apoptose in den verwendeten Zelllinien (Kolonkarzinomzelllinie HCT116, Mammakarzinomzelllinie MCF7, Rektumkarzinomzelllinie RKO, B-Zelllymphomlinie SKW 6.4) auslöste, nicht aber γ-

Bestrahlung, die nur in SKW 6.4-Zellen signifikante Apoptoseraten induzierte. Sowohl nach γ-Bestrahlung als auch durch Zytostatika wurde aber die Expression des durch p53 regulierten Proteins Puma induziert. Das BH3-only-Protein Puma wurde zusammen mit p53 in gradientengereinigten Mitochondrienfraktionen verschiedener Zelllinien nach Zytostatika-Behandlung und γ-Bestrahlung detektiert. Dieses Resultat bestätigte einerseits die transaktivierende Wirkung von p53 (Yu *et al.*, 2003) und andererseits die Stress-induzierte mitochondriale Translokation von p53. Der kausale Zusammenhang der mitochondrialen Lokalisation von p53 mit der Induktion von Apoptose konnte allerdings nicht validiert werden, da trotz vergleichbarer Mengen von p53 in den Mitochondrienfraktionen nur die Zytostatika-Behandlung Apoptose hervorrief, während γ-Bestrahlung vorwiegend in der Induktion von Seneszenz resultierte. Auch die Oligomerisierung von Bax wurde nicht in γ-bestrahlten Zellen, wohl aber nach Inkubation mit Etoposid detektiert. Dieses Ergebnis steht ebenfalls im Gegensatz zur ursächlichen Verknüpfung der mitochondrialen Lokalisation von p53 mit der Induktion von Apoptose (Erster *et al.*, 2004; Erster und Moll, 2005; Mihara *et al.*, 2003; Mihara und Moll, 2003).

Eine Erklärung konnte die Expression eines p53-Fusionsproteins liefern, in dem das Tumorsuppressorprotein mit der Transmembrandomäne von Bcl-2 fusioniert wurde. Hierdurch wurde transgenes p53 konstitutiv an den Mitochondrien lokalisiert. Auch die Überexpression dieses transgenen p53-Konstruktes führte in MCF7-Zellen weder zur Oligomerisierung von Bax noch zu einer apoptotischen Zellmorphologie. Beide Veränderungen wurden jedoch nach Überexpression von Wildtyp p53 detektiert. Die pro-apoptotische Funktion von p53 wurde also nur in Gegenwart seiner transaktivierenden Wirkung entfaltet. Es liegt daher der Schluss nahe, dass der radioresistente Phänotyp der MCF7-Zellen nicht durch eine generelle Resistenz gegenüber p53-abhängiger Apoptose verursacht wurde, da sowohl Chemotherapeutika als auch die Überexpression von p53 effizient Apoptose in diesen Zellen induzieren konnten. Weiterhin kann vermutet werden, dass die p53-abhängige Apoptose in diesem Zellsystem in erster Linie transkriptionsabhängig ist, da mitochondrial lokalisiertes p53 nicht zur Apoptose-Induktion führte.

Diese Ergebnisse stimmen mit Daten einer kürzlich veröffentlichten Arbeit überein (Speidel *et al.*, 2006), die beschreibt, dass für die transkriptionsunabhängige Apoptose-Induktion durch p53 große Mengen dieses Proteins notwendig sind. Dies erscheint auch aufgrund der ermittelten geringen Affinitäten von p53 und Bcl-2 mit einer $K_D \approx 0{,}5$ µM einsichtig (Tomita *et al.*, 2006). Mahyar-Roemer *et al.* konnten zeigen, dass die Menge an mitochondrial lokalisiertem p53 nicht zwangsläufig mit der Apoptose-Induktion korreliert,

sondern prinzipiell die zelluläre Menge an p53-Protein wiedergibt (Mahyar-Roemer *et al.*, 2004).

Die Frage nach der physiologischen Bedeutung der transkriptionsunabhängigen Wirkung von p53 ist trotz der steigenden Zahl an Studien zu diesem Thema nicht eindeutig zu beantworten. Einen interessanten Versuch zur Integration der unterschiedlichen Wirkungen von p53 stellt die Kombination transkriptionsabhängiger und –unabhängiger Wirkungen dar (Vousden, 2005). Die synergistische Wirkung beider Mechanismen könnte daher eine Erklärung für die reduzierte Apoptose-Effizienz eines einzelnen der beiden Mechanismen sein.

3 FAZIT

Die vorliegend zusammengefassten Arbeiten behandeln zahlreiche Facetten der Apoptose und spiegeln so auch ihre Bedeutung in der Medizin sowie die komplexe Vernetzung unterschiedlicher Mechanismen und Signalwege wider. Zu Beginn der Untersuchungen waren grundlegende Mechanismen der Apoptose Gegenstand der Forschung, die Familie der Caspasen war noch nicht vollständig bekannt und die Entdeckung neuer Caspase-Substrate vermehrte das Wissen um die Mechanismen der Apoptose beträchtlich. Zum aktuellen Verständnis der Apoptose hat aber nicht zuletzt das Studium der Verknüpfung der Apoptose-Signalkaskade mit anderen Signalwegen maßgeblich beigetragen.

Mittlerweile wurden nicht nur die zentrale Rolle der Caspasen umfassend beschrieben (Fuentes-Prior und Salvesen, 2004), sondern ebenso die an ihrer Regulation beteiligten Proteine wie Adaptoren (z.B. FADD bzw. Apaf-1), Inhibitoren (z.B. FLIP und anti-apoptotische Bcl-2-Proteine) und Aktivatoren (z.B. Puma) (Reed *et al.*, 2004). Daher rücken Fragen nach der klinischen Bedeutung der zugrunde liegenden Signalwege und ihrer Regulationsmechanismen zunehmend in den Mittelpunkt.

Dieser Wandel der Forschungsschwerpunkte macht das Gebiet der Apoptose nach wie vor interessant und bedeutend und kann an den zusammengefassten Arbeiten nachvollzogen werden. In hämatopoetischen Zellen wurde die differenzielle Spaltung homologer Proteine (Rho-GDI-1 und D4-GDI) durch Caspase-3 im Rahmen der Zytostatika-induzierten Apoptose eingehend analysiert (Essmann *et al.*, 2000) und so ein neues regulatorisches Caspase-Substrat identifiziert und charakterisiert. Die Untersuchung der α-Toxin-induzierten Apoptose zeigte nicht nur die Bedeutung des Zelltodes bei bakterieller Infektion, sondern führte auch zu einem genaueren Verständnis des zugrunde liegenden, primär nekrotischen Mechanismus (Essmann *et al.*, 2003). Die Ergebnisse geben zudem Anlass zur kritischen Betrachtung der klassischen Analysemethoden bei der Differenzierung zwischen Apoptose und Nekrose. Da beide Prozesse fließend ineinander übergehen, ist die strikte Trennung von Apoptose und Nekrose nicht mehr aufrecht zu erhalten.

Die Verknüpfungen des intrinsischen und extrinsischen Apoptose-Signalweges sowie die Aufdeckung von Amplifikationsschleifen (Wieder *et al.*, 2001) haben zu einem komplexen Modell der Regulation des programmierten Zelltod beigetragen, deren Kenntnis Voraussetzung für die Entwicklung neuer Therapeutika ist. Die Aufklärung von Resistenzmechanismen gegenüber klassischen Apoptosestimuli wie γ-Bestrahlung kann hierbei der Entwicklung neuer und individualisierter Therapieansätze bedeutenden Vorschub leisten. Hierzu ist allerdings die Aufklärung der regulatorischen Mechanismen zwingend erforderlich. Sowohl die Mitglieder der Bcl-2-Familie (1.5.1, Gillissen *et al.*, 2003) als auch

das vielfach beschriebene Tumorsuppressorprotein p53 (1.7, Essmann *et al.*, 2004) nehmen hierbei eine zentrale Stellung ein. Wie in Abbildung 14 für p53 veranschaulicht, bildet die Vernknüpfung dieser beiden regulatorischen Ebenen aus Genaktivierung und Protein-Interaktionen ein komplexes Netzwerk, das eine feine Regulation des Apoptose ermöglicht (Essmann *et al.*, 2005).

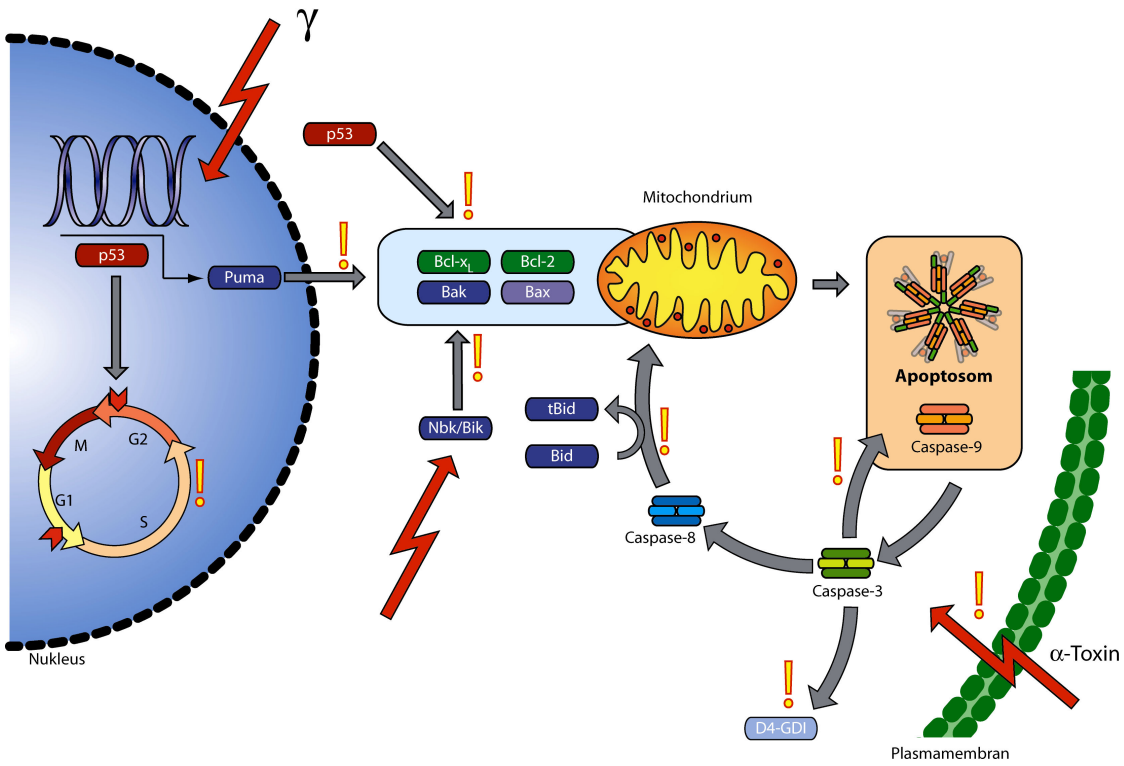

Abbildung 14: Zusammenfassende schematische Darstellung der aus den präsentierten Publikationen gewonnenen Erkenntnisse. Unterschiedliche Stimuli sind durch einen *Blitz* markiert und spezifische Resultate mit einem *!* gekennzeichnet.

Andere Signalwege, die nicht primär mit dem Zelltod in Zusammenhang stehen, wie z.B. der proteasomale Proteinabbau (Sohn *et al.*, 2006b), der NF-κB Signalweg (Totzke *et al.*, 2006) und die Zellzyklusregulation durch Cyclin-abhängige Kinasen (Sohn *et al.*, 2006a), wurden ebenfalls untersucht, da auch diese zunehmend an Bedeutung in dem beschriebenen Forschungsbereich gewinnen. Der hier zusammenfassend wiedergegebene thematische Querschnitt durch das Gebiet der Apoptose beschreibt also die Entwicklung eines hoch aktuellen Forschungsgebietes. Die beschriebenen Erkenntnisse sind in die Entwicklung eines detaillierteren Modells der Apoptose und ihrer Kommunikation mit anderen zellulären Signalprozessen eingeflossen.

4 BIBLIOGRAPHIE

Acehan, D., Jiang, X., Morgan, D. G., Heuser, J. E., Wang, X. und Akey, C. W. (2002). Three-dimensional structure of the apoptosome: implications for assembly, procaspase-9 binding, and activation. *Mol Cell*, **9**: 423-432.

Adams, J. M. und Cory, S. (1998). The Bcl-2 protein family: arbiters of cell survival. *Science*, **281**: 1322-1326.

Alnemri, E. S., Livingston, D. J., Nicholson, D. W., Salvesen, G., Thornberry, N. A., Wong, W. W. und Yuan, J. (1996). Human ICE/CED-3 protease nomenclature. *Cell*, **87**: 171.

Appella, E. und Anderson, C. W. (2001). Post-translational modifications and activation of p53 by genotoxic stresses. *Eur J Biochem*, **268**: 2764-2772.

Ashcroft, M. und Vousden, K. H. (1999). Regulation of p53 stability. *Oncogene*, **18**: 7637-7643.

Ashkenazi, A. und Dixit, V. M. (1998). Death receptors: signaling and modulation. *Science*, **281**: 1305-1308.

Bakhshi, A., Jensen, J. P., Goldman, P., Wright, J. J., McBride, O. W., Epstein, A. L. und Korsmeyer, S. J. (1985). Cloning the chromosomal breakpoint of t(14;18) human lymphomas: clustering around JH on chromosome 14 and near a transcriptional unit on 18. *Cell*, **41**: 899-906.

Balint, E., Bates, S. und Vousden, K. H. (1999). Mdm2 binds p73 alpha without targeting degradation. *Oncogene*, **18**: 3923-3929.

Banda, N. K., Bernier, J., Kurahara, D. K., Kurrle, R., Haigwood, N., Sekaly, R. P. und Finkel, T. H. (1992). Crosslinking CD4 by human immunodeficiency virus gp120 primes T cells for activation-induced apoptosis. *J Exp Med*, **176**: 1099-1106.

Banin, S., Moyal, L., Shieh, S., Taya, Y., Anderson, C. W., Chessa, L., Smorodinsky, N. I., Prives, C., Reiss, Y., Shiloh, Y. und Ziv, Y. (1998). Enhanced phosphorylation of p53 by ATM in response to DNA damage. *Science*, **281**: 1674-1677.

Bantel, H., Sinha, B., Domschke, W., Peters, G., Schulze-Osthoff, K. und Janicke, R. U. (2001). alpha-Toxin is a mediator of Staphylococcus aureus-induced cell death and activates caspases via the intrinsic death pathway independently of death receptor signaling. *J Cell Biol*, **155**: 637-648.

Barak, Y., Gottlieb, E., Juven-Gershon, T. und Oren, M. (1994). Regulation of mdm2 expression by p53: alternative promoters produce transcripts with nonidentical translation potential. *Genes Dev*, **8**: 1739-1749.

Bates, S., Phillips, A. C., Clark, P. A., Stott, F., Peters, G., Ludwig, R. L. und Vousden, K. H. (1998). p14ARF links the tumour suppressors RB and p53. *Nature*, **395**: 124-125.

Bergmann, A., Agapite, J. und Steller, H. (1998). Mechanisms and control of programmed cell death in invertebrates. *Oncogene*, **17**: 3215-3223.

Boatright, K. M., Renatus, M., Scott, F. L., Sperandio, S., Shin, H., Pedersen, I. M., Ricci, J. E., Edris, W. A., Sutherlin, D. P., Green, D. R. und Salvesen, G. S. (2003). A unified model for apical caspase activation. *Mol Cell*, **11**: 529-541.

Boldin, M. P., Goncharov, T. M., Goltsev, Y. V. und Wallach, D. (1996). Involvement of MACH, a novel MORT1/FADD-interacting protease, in Fas/APO-1- and TNF receptor-induced cell death. *Cell*, **85**: 803-815.

Borner, C. und Monney, L. (1999). Apoptosis without caspases: an inefficient molecular guillotine? *Cell Death Differ*, **6**: 497-507.

Boyd, J. M., Gallo, G. J., Elangovan, B., Houghton, A. B., Malstrom, S., Avery, B. J., Ebb, R. G., Subramanian, T., Chittenden, T., Lutz, R. J. und et al. (1995). Bik, a novel death-inducing protein shares a distinct sequence motif with Bcl-2 family proteins and interacts with viral and cellular survival-promoting proteins. *Oncogene*, **11**: 1921-1928.

Brockstedt, E., Rickers, A., Kostka, S., Laubersheimer, A., Dorken, B., Wittmann-Liebold, B., Bommert, K. und Otto, A. (1998). Identification of apoptosis-associated proteins in a human Burkitt lymphoma cell line. Cleavage of heterogeneous nuclear ribonucleoprotein A1 by caspase 3. *J Biol Chem*, **273**: 28057-28064.

Bunch, R. T. und Eastman, A. (1996). Enhancement of cisplatin-induced cytotoxicity by 7-hydroxystaurosporine (UCN-01), a new G2-checkpoint inhibitor. *Clin Cancer Res*, **2**: 791-797.

Burridge, K. und Wennerberg, K. (2004). Rho and Rac take center stage. *Cell*, **116**: 167-179.

Canman, C. E., Lim, D. S., Cimprich, K. A., Taya, Y., Tamai, K., Sakaguchi, K., Appella, E., Kastan, M. B. und Siliciano, J. D. (1998). Activation of the ATM kinase by ionizing radiation and phosphorylation of p53. *Science*, **281**: 1677-1679.

Chai, J., Du, C., Wu, J. W., Kyin, S., Wang, X. und Shi, Y. (2000). Structural and biochemical basis of apoptotic activation by Smac/DIABLO. *Nature*, **406**: 855-862.

Chehab, N. H., Malikzay, A., Appel, M. und Halazonetis, T. D. (2000). Chk2/hCds1 functions as a DNA damage checkpoint in G(1) by stabilizing p53. *Genes Dev*, **14**: 278-288.

Chen, L., Marechal, V., Moreau, J., Levine, A. J. und Chen, J. (1997). Proteolytic cleavage of the mdm2 oncoprotein during apoptosis. *J Biol Chem*, **272**: 22966-22973.

Chen, L., Willis, S. N., Wei, A., Smith, B. J., Fletcher, J. I., Hinds, M. G., Colman, P. M., Day, C. L., Adams, J. M. und Huang, D. C. (2005). Differential targeting of prosurvival Bcl-2 proteins by their BH3-only ligands allows complementary apoptotic function. *Mol Cell*, **17**: 393-403.

Chen, X., Ko, L. J., Jayaraman, L. und Prives, C. (1996). p53 levels, functional domains, and DNA damage determine the extent of the apoptotic response of tumor cells. *Genes Dev*, **10**: 2438-2451.

Chinnaiyan, A. M., O'Rourke, K., Lane, B. R. und Dixit, V. M. (1997). Interaction of CED-4 with CED-3 and CED-9: a molecular framework for cell death. *Science*, **275**: 1122-1126.

Chipuk, J. E. und Green, D. R. (2003). p53's believe it or not: lessons on transcription-independent death. *J Clin Immunol*, **23**: 355-361.

Chipuk, J. E., Maurer, U., Green, D. R. und Schuler, M. (2003). Pharmacologic activation of p53 elicits Bax-dependent apoptosis in the absence of transcription. *Cancer Cell*, **4**: 371-381.

Chittenden, T., Harrington, E. A., O'Connor, R., Flemington, C., Lutz, R. J., Evan, G. I. und Guild, B. C. (1995). Induction of apoptosis by the Bcl-2 homologue Bak. *Nature*, **374**: 733-736.

Colman, M. S., Afshari, C. A. und Barrett, J. C. (2000). Regulation of p53 stability and activity in response to genotoxic stress. *Mutat Res*, **462**: 179-188.

Conradt, B. und Horvitz, H. R. (1998). The C. elegans protein EGL-1 is required for programmed cell death and interacts with the Bcl-2-like protein CED-9. *Cell*, **93**: 519-529.

Cory, S., Huang, D. C. und Adams, J. M. (2003). The Bcl-2 family: roles in cell survival and oncogenesis. *Oncogene*, **22**: 8590-8607.

Councilman, W. (1890). Report on the etiology and prevention of yellow fever. depolarization. Public

Health Bulletin Washington,. *Public Health Bulletin*, **2**: 151-159.

Danial, N. N. und Korsmeyer, S. J. (2004). Cell death: critical control points. *Cell*, **116**: 205-219.

Daniel, P. T., Pun, K. T., Ritschel, S., Sturm, I., Holler, J., Dorken, B. und Brown, R. (1999). Expression of the death gene Bik/Nbk promotes sensitivity to drug-induced apoptosis in corticosteroid-resistant T-cell lymphoma and prevents tumor growth in severe combined immunodeficient mice. *Blood*, **94**: 1100-1107.

Danley, D. E., Chuang, T. H. und Bokoch, G. M. (1996). Defective Rho GTPase regulation by IL-1 beta-converting enzyme-mediated cleavage of D4 GDP dissociation inhibitor. *J Immunol*, **157**: 500-503.

Datta, S. R., Dudek, H., Tao, X., Masters, S., Fu, H., Gotoh, Y. und Greenberg, M. E. (1997). Akt phosphorylation of BAD couples survival signals to the cell-intrinsic death machinery. *Cell*, **91**: 231-241.

Debatin, K. M. und Krammer, P. H. (2004). Death receptors in chemotherapy and cancer. *Oncogene*, **23**: 2950-2966.

Degli Esposti, M., Ferry, G., Masdehors, P., Boutin, J. A., Hickman, J. A. und Dive, C. (2003). Post-translational modification of Bid has differential effects on its susceptibility to cleavage by caspase 8 or caspase 3. *J Biol Chem*, **278**: 15749-15757.

Deng, X., Gao, F., Flagg, T., Anderson, J. und May, W. S. (2006). Bcl2's flexible loop domain regulates p53 binding and survival. *Mol Cell Biol*, **26**: 4421-4434.

Desagher, S., Osen-Sand, A., Montessuit, S., Magnenat, E., Vilbois, F., Hochmann, A., Journot, L., Antonsson, B. und Martinou, J. C. (2001). Phosphorylation of bid by casein kinases I and II regulates its cleavage by caspase 8. *Mol Cell*, **8**: 601-611.

Di Leonardo, A., Linke, S. P., Clarkin, K. und Wahl, G. M. (1994). DNA damage triggers a prolonged p53-dependent G1 arrest and long-term induction of Cip1 in normal human fibroblasts. *Genes Dev*, **8**: 2540-2551.

Du, C., Fang, M., Li, Y., Li, L. und Wang, X. (2000). Smac, a mitochondrial protein that promotes cytochrome c-dependent caspase activation by eliminating IAP inhibition. *Cell*, **102**: 33-42.

Dumont, P., Leu, J. I., Della Pietra, A. C., 3rd, George, D. L. und Murphy, M. (2003). The codon 72 polymorphic variants of p53 have markedly different apoptotic potential. *Nat Genet*, **33**: 357-365.

Ellis, R. E., Yuan, J. Y. und Horvitz, H. R. (1991). Mechanisms and functions of cell death. *Annu Rev Cell Biol*, **7**: 663-698.

Enari, M., Sakahira, H., Yokoyama, H., Okawa, K., Iwamatsu, A. und Nagata, S. (1998). A caspase-activated DNase that degrades DNA during apoptosis, and its inhibitor ICAD. *Nature*, **391**: 43-50.

Engels, I. H., Stepczynska, A., Stroh, C., Lauber, K., Berg, C., Schwenzer, R., Wajant, H., Janicke, R. U., Porter, A. G., Belka, C*., et al.* (2000). Caspase-8/FLICE functions as an executioner caspase in anticancer drug-induced apoptosis. *Oncogene*, **19**: 4563-4573.

Erhardt, P., Tomaselli, K. J. und Cooper, G. M. (1997). Identification of the MDM2 oncoprotein as a substrate for CPP32-like apoptotic proteases. *J Biol Chem*, **272**: 15049-15052.

Erster, S., Mihara, M., Kim, R. H., Petrenko, O. und Moll, U. M. (2004). In vivo mitochondrial p53 translocation triggers a rapid first wave of cell death in response to DNA damage that can precede p53 target gene activation. *Mol Cell Biol*, **24**: 6728-6741.

Erster, S. und Moll, U. M. (2004). Stress-induced p53 runs a direct mitochondrial death program: its role in physiologic and pathophysiologic stress responses in vivo. *Cell Cycle*, **3**: 1492-1495.

Erster, S. und Moll, U. M. (2005). Stress-induced p53 runs a transcription-independent death program. *Biochem Biophys Res Commun*, **331**: 843-850.

Essmann, F., Bantel, H., Totzke, G., Engels, I. H., Sinha, B., Schulze-Osthoff, K. und Janicke, R. U. (2003). Staphylococcus aureus alpha-toxin-induced cell death: predominant necrosis despite apoptotic caspase activation. *Cell Death Differ*, **10**: 1260-1272.

Essmann, F., Wieder, T., Otto, A., Muller, E. C., Dorken, B. und Daniel, P. T. (2000). GDP dissociation inhibitor D4-GDI (Rho-GDI 2), but not the homologous rho-GDI 1, is cleaved by caspase-3 during drug-induced apoptosis. *Biochem J*, **346**: 777-783.

Farrow, S. N., White, J. H., Martinou, I., Raven, T., Pun, K. T., Grinham, C. J., Martinou, J. C. und Brown, R. (1995). Cloning of a bcl-2 homologue by interaction with adenovirus E1B 19K. *Nature*, **374**: 731-733.

Fischer, U., Janicke, R. U. und Schulze-Osthoff, K. (2003). Many cuts to ruin: a comprehensive update of caspase substrates. *Cell Death Differ*, **10**: 76-100.

Fischer, U. und Schulze-Osthoff, K. (2005a). Apoptosis-based therapies and drug targets. *Cell Death Differ*, **12 Suppl 1**: 942-961.

Fischer, U. und Schulze-Osthoff, K. (2005b). New approaches and therapeutics targeting apoptosis in disease. *Pharmacol Rev*, **57**: 187-215.

Fisher, G. H., Rosenberg, F. J., Straus, S. E., Dale, J. K., Middleton, L. A., Lin, A. Y., Strober, W., Lenardo, M. J. und Puck, J. M. (1995). Dominant interfering Fas gene mutations impair apoptosis in a human autoimmune lymphoproliferative syndrome. *Cell*, **81**: 935-946.

Friesen, C., Herr, I., Krammer, P. H. und Debatin, K. M. (1996). Involvement of the CD95 (APO-1/FAS) receptor/ligand system in drug-induced apoptosis in leukemia cells. *Nat Med*, **2**: 574-577.

Fuentes-Prior, P. und Salvesen, G. S. (2004). The protein structures that shape caspase activity, specificity, activation and inhibition. *Biochem J*, **384**: 201-232.

Fulda, S., Strauss, G., Meyer, E. und Debatin, K. M. (2000). Functional CD95 ligand and CD95 death-inducing signaling complex in activation-induced cell death and doxorubicin-induced apoptosis in leukemic T cells. *Blood*, **95**: 301-308.

Garcia-Saez, A. J., Mingarro, I., Perez-Paya, E. und Salgado, J. (2004). Membrane-insertion fragments of Bcl-xL, Bax, and Bid. *Biochemistry*, **43**: 10930-10943.

Geyer, M. und Wittinghofer, A. (1997). GEFs, GAPs, GDIs and effectors: taking a closer (3D) look at the regulation of Ras-related GTP-binding proteins. *Curr Opin Struct Biol*, **7**: 786-792.

Gildea, J. J., Seraj, M. J., Oxford, G., Harding, M. A., Hampton, G. M., Moskaluk, C. A., Frierson, H. F., Conaway, M. R. und Theodorescu, D. (2002). RhoGDI2 is an invasion and metastasis suppressor gene in human cancer. *Cancer Res*, **62**: 6418-6423.

Golks, A., Brenner, D., Fritsch, C., Krammer, P. H. und Lavrik, I. N. (2005). c-FLIPR, a new regulator of death receptor-induced apoptosis. *J Biol Chem*, **280**: 14507-14513.

Goltsev, Y. V., Kovalenko, A. V., Arnold, E., Varfolomeev, E. E., Brodianskii, V. M. und Wallach, D. (1997). CASH, a novel caspase homologue with death effector domains. *J Biol Chem*, **272**: 19641-19644.

Gross, A., Yin, X. M., Wang, K., Wei, M. C., Jockel, J., Milliman, C., Erdjument-Bromage, H., Tempst, P. und Korsmeyer, S. J. (1999). Caspase cleaved BID targets mitochondria and is required for cytochrome c release, while BCL-XL prevents this release but not tumor necrosis factor-R1/Fas death. *J Biol Chem*, **274**: 1156-1163.

Gu, J., Nie, L., Wiederschain, D. und Yuan, Z. M. (2001). Identification of p53 sequence elements that are required for MDM2-mediated nuclear export. *Mol Cell Biol*, **21**: 8533-8546.

Guner, D., Belka, C. und Daniel, P. T. (2003). Disruption of cell death signaling in cancer: impact on disease prognosis and response to therapy. *Curr Med Chem Anticancer Agents*, **3**: 319-326.

Hall, A. (1994). Small GTP-binding proteins and the regulation of the actin cytoskeleton. *Annu Rev Cell Biol*, **10**: 31-54.

Han, J., Sabbatini, P. und White, E. (1996). Induction of apoptosis by human Nbk/Bik, a BH3-containing protein that interacts with E1B 19K. *Mol Cell Biol*, **16**: 5857-5864.

Harada, H., Becknell, B., Wilm, M., Mann, M., Huang, L. J., Taylor, S. S., Scott, J. D. und Korsmeyer, S. J. (1999). Phosphorylation and inactivation of BAD by mitochondria-anchored protein kinase A. *Mol Cell*, **3**: 413-422.

Hengartner, M. O. und Horvitz, H. R. (1994). Programmed cell death in Caenorhabditis elegans. *Curr Opin Genet Dev*, **4**: 581-586.

Hetz, C. A., Torres, V. und Quest, A. F. (2005). Beyond apoptosis: nonapoptotic cell death in physiology and disease. *Biochem Cell Biol*, **83**: 579-588.

Hollstein, M., Sidransky, D., Vogelstein, B. und Harris, C. C. (1991). p53 mutations in human cancers. *Science*, **253**: 49-53.

Hsu, H., Huang, J., Shu, H. B., Baichwal, V. und Goeddel, D. V. (1996a). TNF-dependent recruitment of the protein kinase RIP to the TNF receptor-1 signaling complex. *Immunity*, **4**: 387-396.

Hsu, H., Shu, H. B., Pan, M. G. und Goeddel, D. V. (1996b). TRADD-TRAF2 and TRADD-FADD interactions define two distinct TNF receptor 1 signal transduction pathways. *Cell*, **84**: 299-308.

Hsu, S. Y., Kaipia, A., McGee, E., Lomeli, M. und Hsueh, A. J. (1997). Bok is a pro-apoptotic Bcl-2 protein with restricted expression in reproductive tissues and heterodimerizes with selective anti-apoptotic Bcl-2 family members. *Proc Natl Acad Sci U S A*, **94**: 12401-12406.

Inohara, N., Koseki, T., Hu, Y., Chen, S. und Nunez, G. (1997). CLARP, a death effector domain-containing protein interacts with caspase-8 and regulates apoptosis. *Proc Natl Acad Sci U S A*, **94**: 10717-10722.

Irmler, M., Thome, M., Hahne, M., Schneider, P., Hofmann, K., Steiner, V., Bodmer, J. L., Schroter, M., Burns, K., Mattmann, C.*, et al.* (1997). Inhibition of death receptor signals by cellular FLIP. *Nature*, **388**: 190-195.

Janicke, R. U., Engels, I. H., Dunkern, T., Kaina, B., Schulze-Osthoff, K. und Porter, A. G. (2001). Ionizing radiation but not anticancer drugs causes cell cycle arrest and failure to activate the mitochondrial death pathway in MCF-7 breast carcinoma cells. *Oncogene*, **20**: 5043-5053.

Janicke, R. U., Ng, P., Sprengart, M. L. und Porter, A. G. (1998a). Caspase-3 is required for alpha-fodrin cleavage but dispensable for cleavage of other death substrates in apoptosis. *J Biol Chem*, **273**: 15540-15545.

Janicke, R. U., Sprengart, M. L., Wati, M. R. und Porter, A. G. (1998b). Caspase-3 is required for DNA fragmentation and morphological changes associated with apoptosis. *J Biol Chem*, **273**: 9357-9360.

Jiang, X. und Wang, X. (2004). Cytochrome C-mediated apoptosis. *Annu Rev Biochem*, **73**: 87-106.

Jin, S. und Levine, A. J. (2001). The p53 functional circuit. *J Cell Sci*, **114**: 4139-4140.

Kelliher, M. A., Grimm, S., Ishida, Y., Kuo, F., Stanger, B. Z. und Leder, P. (1998). The death domain kinase RIP mediates the TNF-induced NF-kappaB signal. *Immunity*, **8**: 297-303.

Kerr, J. F., Wyllie, A. H. und Currie, A. R. (1972). Apoptosis: a basic biological phenomenon with wide-ranging implications in tissue kinetics. *Br J Cancer*, **26**: 239-257.

Khanna, K. K. und Jackson, S. P. (2001). DNA double-strand breaks: signaling, repair and the cancer connection. *Nat Genet*, **27**: 247-254.

Kischkel, F. C., Hellbardt, S., Behrmann, I., Germer, M., Pawlita, M., Krammer, P. H. und Peter, M. E. (1995). Cytotoxicity-dependent APO-1 (Fas/CD95)-associated proteins form a death-inducing signaling complex (DISC) with the receptor. *Embo J*, **14**: 5579-5588.

Ko, L. J. und Prives, C. (1996). p53: puzzle and paradigm. *Genes Dev*, **10**: 1054-1072.

Komarov, P. G., Komarova, E. A., Kondratov, R. V., Christov-Tselkov, K., Coon, J. S., Chernov, M. V. und Gudkov, A. V. (1999). A chemical inhibitor of p53 that protects mice from the side effects of cancer therapy. *Science*, **285**: 1733-1737.

Kroemer, G. und Reed, J. C. (2000). Mitochondrial control of cell death. *Nat Med*, **6**: 513-519.

Kwon, K. B., Park, E. K., Ryu, D. G. und Park, B. H. (2002). D4-GDI is cleaved by caspase-3 during daunorubicin-induced apoptosis in HL-60 cells. *Exp Mol Med*, **34**: 32-37.

Lau, C. C. und Pardee, A. B. (1982). Mechanism by which caffeine potentiates lethality of nitrogen mustard. *Proc Natl Acad Sci U S A*, **79**: 2942-2946.

Laurent-Crawford, A. G., Krust, B., Muller, S., Riviere, Y., Rey-Cuille, M. A., Bechet, J. M., Montagnier, L. und Hovanessian, A. G. (1991). The cytopathic effect of HIV is associated with apoptosis. *Virology*, **185**: 829-839.

Lavin, M. F. und Gueven, N. (2006). The complexity of p53 stabilization and activation. *Cell Death Differ*, **13**: 941-950.

Lavrik, I., Golks, A. und Krammer, P. H. (2005). Death receptor signaling. *J Cell Sci*, **118**: 265-267.

Lazebnik, Y. A., Takahashi, A., Poirier, G. G., Kaufmann, S. H. und Earnshaw, W. C. (1995). Characterization of the execution phase of apoptosis in vitro using extracts from condemned-phase cells. *J Cell Sci Suppl*, **19**: 41-49.

Leist, M. und Jaattela, M. (2001). Four deaths and a funeral: from caspases to alternative mechanisms. *Nat Rev Mol Cell Biol*, **2**: 589-598.

Leu, J. I., Dumont, P., Hafey, M., Murphy, M. E. und George, D. L. (2004). Mitochondrial p53 activates Bak and causes disruption of a Bak-Mcl1 complex. *Nat Cell Biol*, **6**: 443-450.

Levine, A. J. (1997). p53, the cellular gatekeeper for growth and division. *Cell*, **88**: 323-331.

Levine, A. J., Hu, W. und Feng, Z. (2006). The P53 pathway: what questions remain to be explored? *Cell Death Differ*, **13**: 1027-1036.

Levine, B. und Yuan, J. (2005). Autophagy in cell death: an innocent convict? *J Clin Invest*, **115**: 2679-2688.

Li, H., Zhu, H., Xu, C. J. und Yuan, J. (1998). Cleavage of BID by caspase 8 mediates the mitochondrial damage in the Fas pathway of apoptosis. *Cell*, **94**: 491-501.

Li, M. O., Sarkisian, M. R., Mehal, W. Z., Rakic, P. und Flavell, R. A. (2003). Phosphatidylserine receptor is required for clearance of apoptotic cells. *Science*, **302**: 1560-1563.

Liu, X., Dai, S., Zhu, Y., Marrack, P. und Kappler, J. W. (2003). The structure of a Bcl-xL/Bim fragment complex: implications for Bim function. *Immunity*, **19**: 341-352.

Liu, X., Zou, H., Slaughter, C. und Wang, X. (1997). DFF, a heterodimeric protein that functions downstream of caspase-3 to trigger DNA fragmentation during apoptosis. *Cell*, **89**: 175-184.

Liu, Z., Sun, C., Olejniczak, E. T., Meadows, R. P., Betz, S. F., Oost, T., Herrmann, J., Wu, J. C. und Fesik, S. W. (2000). Structural basis for binding of Smac/DIABLO to the XIAP BIR3 domain. *Nature*, **408**: 1004-1008.

Luo, X., Budihardjo, I., Zou, H., Slaughter, C. und Wang, X. (1998). Bid, a Bcl2 interacting protein, mediates cytochrome c release from mitochondria in response to activation of cell surface death receptors. *Cell*, **94**: 481-490.

Mahyar-Roemer, M., Fritzsche, C., Wagner, S., Laue, M. und Roemer, K. (2004). Mitochondrial p53 levels parallel total p53 levels independent of stress response in human colorectal carcinoma and glioblastoma cells. *Oncogene*, **23**: 6226-6236.

Malkin, D., Li, F. P., Strong, L. C., Fraumeni, J. F., Jr., Nelson, C. E., Kim, D. H., Kassel, J., Gryka, M. A., Bischoff, F. Z., Tainsky, M. A. und et al. (1990). Germ line p53 mutations in a familial syndrome of breast cancer, sarcomas, and other neoplasms. *Science*, **250**: 1233-1238.

Marani, M., Tenev, T., Hancock, D., Downward, J. und Lemoine, N. R. (2002). Identification of novel isoforms of the BH3 domain protein Bim which directly activate Bax to trigger apoptosis. *Mol Cell Biol*, **22**: 3577-3589.

Marchenko, N. D., Zaika, A. und Moll, U. M. (2000). Death signal-induced localization of p53 protein to mitochondria. A potential role in apoptotic signaling. *J Biol Chem*, **275**: 16202-16212.

Martin, S. J. und Green, D. R. (1995). Protease activation during apoptosis: death by a thousand cuts? *Cell*, **82**: 349-352.

Martinou, J. C. und Green, D. R. (2001). Breaking the mitochondrial barrier. *Nat Rev Mol Cell Biol*, **2**: 63-67.

Mashima, T., Naito, M., Noguchi, K., Miller, D. K., Nicholson, D. W. und Tsuruo, T. (1997). Actin cleavage by CPP-32/apopain during the development of apoptosis. *Oncogene*, **14**: 1007-1012.

Mattson, M. P. (2000). Apoptosis in neurodegenerative disorders. *Nat Rev Mol Cell Biol*, **1**: 120-129.

Melino, G., Bernassola, F., Ranalli, M., Yee, K., Zong, W. X., Corazzari, M., Knight, R. A., Green, D. R., Thompson, C. und Vousden, K. H. (2004). p73 Induces apoptosis via PUMA transactivation and Bax mitochondrial translocation. *J Biol Chem*, **279**: 8076-8083.

Micheau, O. und Tschopp, J. (2003). Induction of TNF receptor I-mediated apoptosis via two sequential signaling complexes. *Cell*, **114**: 181-190.

Midgley, C. A. und Lane, D. P. (1997). p53 protein stability in tumour cells is not determined by mutation but is dependent on Mdm2 binding. *Oncogene*, **15**: 1179-1189.

Mihara, M., Erster, S., Zaika, A., Petrenko, O., Chittenden, T., Pancoska, P. und Moll, U. M. (2003). p53 has a direct apoptogenic role at the mitochondria. *Mol Cell*, **11**: 577-590.

Mihara, M. und Moll, U. M. (2003). Detection of mitochondrial localization of p53. *Methods Mol Biol*, **234**: 203-209.

Ming, L., Wang, P., Bank, A., Yu, J. und Zhang, L. (2006). PUMA Dissociates Bax and Bcl-X(L) to induce apoptosis in colon cancer cells. *J Biol Chem*, **281**: 16034-16042.

Miyashita, T. und Reed, J. C. (1995). Tumor suppressor p53 is a direct transcriptional activator of the human bax gene. *Cell*, **80**: 293-299.

Moll, U. M. und Zaika, A. (2001). Nuclear and mitochondrial apoptotic pathways of p53. *FEBS Lett*, **493**: 65-69.

Muchmore, S. W., Sattler, M., Liang, H., Meadows, R. P., Harlan, J. E., Yoon, H. S., Nettesheim, D., Chang, B. S., Thompson, C. B., Wong, S. L.*, et al.* (1996). X-ray and NMR structure of human Bcl-xL, an inhibitor of programmed cell death. *Nature*, **381**: 335-341.

Muzio, M., Chinnaiyan, A. M., Kischkel, F. C., O'Rourke, K., Shevchenko, A., Ni, J., Scaffidi, C., Bretz, J. D., Zhang, M., Gentz, R.*, et al.* (1996). FLICE, a novel FADD-homologous ICE/CED-3-like protease, is recruited to the CD95 (Fas/APO-1) death--inducing signaling complex. *Cell*, **85**: 817-827.

Na, S., Chuang, T. H., Cunningham, A., Turi, T. G., Hanke, J. H., Bokoch, G. M. und Danley, D. E. (1996). D4-GDI, a substrate of CPP32, is proteolyzed during Fas-induced apoptosis. *J Biol Chem*, **271**: 11209-11213.

Nakanishi, M., Shimada, M. und Niida, H. (2006). Genetic instability in cancer cells by impaired cell cycle checkpoints. *Cancer Sci*, **97**: 984-989.

Nakano, K. und Vousden, K. H. (2001). PUMA, a novel proapoptotic gene, is induced by p53. *Mol Cell*, **7**: 683-694.

Narumiya, S. (1996). The small GTPase Rho: cellular functions and signal transduction. *J Biochem (Tokyo)*, **120**: 215-228.

Nechushtan, A., Smith, C. L., Hsu, Y. T. und Youle, R. J. (1999). Conformation of the Bax C-terminus regulates subcellular location and cell death. *Embo J*, **18**: 2330-2341.

Niida, H. und Nakanishi, M. (2006). DNA damage checkpoints in mammals. *Mutagenesis*, **21**: 3-9.

Normand, G., Hemmati, P. G., Verdoodt, B., von Haefen, C., Wendt, J., Guner, D., May, E., Dorken, B. und Daniel, P. T. (2005). p14ARF induces G2 cell cycle arrest in p53- and p21-deficient cells by down-regulating p34cdc2 kinase activity. *J Biol Chem*, **280**: 7118-7130.

O'Connor, L., Strasser, A., O'Reilly, L. A., Hausmann, G., Adams, J. M., Cory, S. und Huang, D. C. (1998). Bim: a novel member of the Bcl-2 family that promotes apoptosis. *Embo J*, **17**: 384-395.

Oda, E., Ohki, R., Murasawa, H., Nemoto, J., Shibue, T., Yamashita, T., Tokino, T., Taniguchi, T. und Tanaka, N. (2000a). Noxa, a BH3-only member of the Bcl-2 family and candidate mediator of p53-induced apoptosis. *Science*, **288**: 1053-1058.

Oda, K., Arakawa, H., Tanaka, T., Matsuda, K., Tanikawa, C., Mori, T., Nishimori, H., Tamai, K., Tokino, T., Nakamura, Y. und Taya, Y. (2000b). p53AIP1, a potential mediator of p53-dependent apoptosis, and its regulation by Ser-46-phosphorylated p53. *Cell*, **102**: 849-862.

Oltvai, Z. N., Milliman, C. L. und Korsmeyer, S. J. (1993). Bcl-2 heterodimerizes in vivo with a conserved homolog, Bax, that accelerates programmed cell death. *Cell*, **74**: 609-619.

Orth, K., Chinnaiyan, A. M., Garg, M., Froelich, C. J. und Dixit, V. M. (1996). The CED-3/ICE-like protease Mch2 is activated during apoptosis and cleaves the death substrate lamin A. *J Biol Chem*, **271**: 16443-16446.

Pattingre, S., Tassa, A., Qu, X., Garuti, R., Liang, X. H., Mizushima, N., Packer, M., Schneider, M. D. und Levine, B. (2005). Bcl-2 antiapoptotic proteins inhibit Beclin 1-dependent autophagy. *Cell*, **122**: 927-939.

Pomerantz, J., Schreiber-Agus, N., Liegeois, N. J., Silverman, A., Alland, L., Chin, L., Potes, J., Chen, K., Orlow, I., Lee, H. W.*, et al.* (1998). The Ink4a tumor suppressor gene product, p19Arf, interacts with MDM2 and neutralizes MDM2's inhibition of p53. *Cell*, **92**: 713-723.

Pop, C., Timmer, J., Sperandio, S. und Salvesen, G. S. (2006). The apoptosome activates caspase-9 by dimerization. *Mol Cell*, **22**: 269-275.

Prives, C. und Hall, P. A. (1999). The p53 pathway. *J Pathol*, **187**: 112-126.

Puthalakath, H. und Strasser, A. (2002). Keeping killers on a tight leash: transcriptional and post-translational control of the pro-apoptotic activity of BH3-only proteins. *Cell Death Differ*, **9**: 505-512.

Rao, L., Perez, D. und White, E. (1996). Lamin proteolysis facilitates nuclear events during apoptosis. *J Cell Biol*, **135**: 1441-1455.

Rathmell, J. C. und Thompson, C. B. (2002). Pathways of apoptosis in lymphocyte development, homeostasis, and disease. *Cell*, **109 Suppl**: S97-107.

Reed, J. C., Doctor, K. S. und Godzik, A. (2004). The domains of apoptosis: a genomics perspective. *Sci STKE*, **2004**: re9.

Renatus, M., Stennicke, H. R., Scott, F. L., Liddington, R. C. und Salvesen, G. S. (2001). Dimer formation drives the activation of the cell death protease caspase 9. *Proc Natl Acad Sci U S A*, **98**: 14250-14255.

Rickers, A., Brockstedt, E., Mapara, M. Y., Otto, A., Dorken, B. und Bommert, K. (1998). Inhibition of CPP32 blocks surface IgM-mediated apoptosis and D4-GDI cleavage in human BL60 Burkitt lymphoma cells. *Eur J Immunol*, **28**: 296-304.

Riedl, S. J., Fuentes-Prior, P., Renatus, M., Kairies, N., Krapp, S., Huber, R., Salvesen, G. S. und Bode, W. (2001). Structural basis for the activation of human procaspase-7. *Proc Natl Acad Sci U S A*, **98**: 14790-14795.

Riedl, S. J., Li, W., Chao, Y., Schwarzenbacher, R. und Shi, Y. (2005). Structure of the apoptotic protease-activating factor 1 bound to ADP. *Nature*, **434**: 926-933.

Sakahira, H., Enari, M. und Nagata, S. (1998). Cleavage of CAD inhibitor in CAD activation and DNA degradation during apoptosis. *Nature*, **391**: 96-99.

Salvesen, G. S. und Dixit, V. M. (1999). Caspase activation: the induced-proximity model. *Proc Natl Acad Sci U S A*, **96**: 10964-10967.

Sansome, C., Zaika, A., Marchenko, N. D. und Moll, U. M. (2001). Hypoxia death stimulus induces translocation of p53 protein to mitochondria. Detection by immunofluorescence on whole cells. *FEBS Lett*, **488**: 110-115.

Scaffidi, C., Fulda, S., Srinivasan, A., Friesen, C., Li, F., Tomaselli, K. J., Debatin, K. M., Krammer, P. H. und Peter, M. E. (1998). Two CD95 (APO-1/Fas) signaling pathways. *Embo J*, **17**: 1675-1687.

Scaffidi, C., Schmitz, I., Krammer, P. H. und Peter, M. E. (1999a). The role of c-FLIP in modulation of CD95-induced apoptosis. *J Biol Chem*, **274**: 1541-1548.

Scaffidi, C., Schmitz, I., Zha, J., Korsmeyer, S. J., Krammer, P. H. und Peter, M. E. (1999b). Differential modulation of apoptosis sensitivity in CD95 type I and type II cells. *J Biol Chem*, **274**: 22532-22538.

Scaffidi, P., Misteli, T. und Bianchi, M. E. (2002). Release of chromatin protein HMGB1 by necrotic cells triggers inflammation. *Nature*, **418**: 191-195.

Schuler, M., Bossy-Wetzel, E., Goldstein, J. C., Fitzgerald, P. und Green, D. R. (2000). p53 induces apoptosis by caspase activation through mitochondrial cytochrome c release. *J Biol Chem*, **275**: 7337-7342.

Sherr, C. J. (2006). Divorcing ARF and p53: an unsettled case. *Nat Rev Cancer*, **6**: 663-673.

Shieh, S. Y., Ahn, J., Tamai, K., Taya, Y. und Prives, C. (2000). The human homologs of checkpoint kinases Chk1 and Cds1 (Chk2) phosphorylate p53 at multiple DNA damage-inducible sites. *Genes Dev*, **14**: 289-300.

Slee, E. A., Harte, M. T., Kluck, R. M., Wolf, B. B., Casiano, C. A., Newmeyer, D. D., Wang, H. G., Reed, J. C., Nicholson, D. W., Alnemri, E. S.*, et al.* (1999). Ordering the cytochrome c-initiated caspase cascade: hierarchical activation of caspases-2, -3, -6, -7, -8, and -10 in a caspase-9-dependent manner. *J Cell Biol*, **144**: 281-292.

Slee, E. A., Keogh, S. A. und Martin, S. J. (2000). Cleavage of BID during cytotoxic drug and UV radiation-induced apoptosis occurs downstream of the point of Bcl-2 action and is catalysed by caspase-3: a potential feedback loop for amplification of apoptosis-associated mitochondrial cytochrome c release. *Cell Death Differ*, **7**: 556-565.

Smith, G. C., d'Adda di Fagagna, F., Lakin, N. D. und Jackson, S. P. (1999). Cleavage and inactivation of ATM during apoptosis. *Mol Cell Biol*, **19**: 6076-6084.

Smith, M. L., Chen, I. T., Zhan, Q., O'Connor, P. M. und Fornace, A. J., Jr. (1995). Involvement of the p53 tumor suppressor in repair of u.v.-type DNA damage. *Oncogene*, **10**: 1053-1059.

Sohn, D., Essmann, F., Schulze-Osthoff, K. und Janicke, R. U. (2006a). p21 blocks irradiation-induced apoptosis downstream of mitochondria by inhibition of cyclin-dependent kinase-mediated caspase-9 activation. . *Cancer Res*, **In Druck**.

Sohn, D., Schulze-Osthoff, K. und Janicke, R. U. (2005). Caspase-8 can be activated by interchain proteolysis without receptor-triggered dimerization during drug-induced apoptosis. *J Biol Chem*, **280**: 5267-5273.

Sohn, D., Totzke, G., Essmann, F., Schulze-Osthoff, K., Levkau, B. und Janicke, R. U. (2006b). The proteasome is required for rapid initiation of death receptor-induced apoptosis. *Mol Cell Biol*, **26**: 1967-1978.

Song, L., Hobaugh, M. R., Shustak, C., Cheley, S., Bayley, H. und Gouaux, J. E. (1996). Structure of staphylococcal alpha-hemolysin, a heptameric transmembrane pore. *Science*, **274**: 1859-1866.

Speidel, D., Helmbold, H. und Deppert, W. (2006). Dissection of transcriptional and non-transcriptional p53 activities in the response to genotoxic stress. *Oncogene*, **25**: 940-953.

Srinivasula, S. M., Ahmad, M., Ottilie, S., Bullrich, F., Banks, S., Wang, Y., Fernandes-Alnemri, T., Croce, C. M., Litwack, G., Tomaselli, K. J.*, et al.* (1997). FLAME-1, a novel FADD-like anti-apoptotic molecule that regulates Fas/TNFR1-induced apoptosis. *J Biol Chem*, **272**: 18542-18545.

Srinivasula, S. M., Datta, P., Fan, X. J., Fernandes-Alnemri, T., Huang, Z. und Alnemri, E. S. (2000). Molecular determinants of the caspase-promoting activity of Smac/DIABLO and its role in the death receptor pathway. *J Biol Chem*, **275**: 36152-36157.

Stott, F. J., Bates, S., James, M. C., McConnell, B. B., Starborg, M., Brookes, S., Palmero, I., Ryan, K., Hara, E., Vousden, K. H. und Peters, G. (1998). The alternative product from the human CDKN2A locus, p14(ARF), participates in a regulatory feedback loop with p53 and MDM2. *Embo J*, **17**: 5001-5014.

Stroh, C. und Schulze-Osthoff, K. (1998). Death by a thousand cuts: an ever increasing list of caspase substrates. *Cell Death Differ*, **5**: 997-1000.

Sulston, J., Du, Z., Thomas, K., Wilson, R., Hillier, L., Staden, R., Halloran, N., Green, P., Thierry-Mieg, J., Qiu, L. und et al. (1992). The C. elegans genome sequencing project: a beginning. *Nature*, **356**: 37-41.

Thiede, B., Siejak, F., Dimmler, C. und Rudel, T. (2002). Prediction of translocation and cleavage of heterogeneous ribonuclear proteins and Rho guanine nucleotide dissociation inhibitor 2 during apoptosis by subcellular proteome analysis. *Proteomics*, **2**: 996-1006.

Thiede, B., Treumann, A., Kretschmer, A., Sohlke, J. und Rudel, T. (2005). Shotgun proteome analysis of protein cleavage in apoptotic cells. *Proteomics*, **5**: 2123-2130.

Thome, M., Schneider, P., Hofmann, K., Fickenscher, H., Meinl, E., Neipel, F., Mattmann, C., Burns, K., Bodmer, J. L., Schroter, M.*, et al.* (1997). Viral FLICE-inhibitory proteins (FLIPs) prevent apoptosis induced by death receptors. *Nature*, **386**: 517-521.

Thornberry, N. A., Chapman, K. T. und Nicholson, D. W. (2000). Determination of caspase specificities using a peptide combinatorial library. *Methods Enzymol*, **322**: 100-110.

Thornberry, N. A., Rano, T. A., Peterson, E. P., Rasper, D. M., Timkey, T., Garcia-Calvo, M., Houtzager, V. M., Nordstrom, P. A., Roy, S., Vaillancourt, J. P.*, et al.* (1997). A combinatorial approach defines specificities of members of the caspase family and granzyme B. Functional relationships established for key mediators of apoptosis. *J Biol Chem*, **272**: 17907-17911.

Tibbetts, R. S., Brumbaugh, K. M., Williams, J. M., Sarkaria, J. N., Cliby, W. A., Shieh, S. Y., Taya, Y., Prives, C. und Abraham, R. T. (1999). A role for ATR in the DNA damage-induced phosphorylation of p53. *Genes Dev*, **13**: 152-157.

Tomita, Y., Marchenko, N., Erster, S., Nemajerova, A., Dehner, A., Klein, C., Pan, H., Kessler, H., Pancoska, P. und Moll, U. M. (2006). WT p53, but not tumor-derived mutants, bind to Bcl2 via the DNA binding domain and induce mitochondrial permeabilization. *J Biol Chem*, **281**: 8600-8606.

Totzke, G., Essmann, F., Pohlmann, S., Lindenblatt, C., Janicke, R. U. und Schulze-Osthoff, K. (2006). A novel member of the IkappaB family, human IkappaB-zeta, inhibits transactivation of p65 and its DNA binding. *J Biol Chem*, **281**: 12645-12654.

Valeva, A., Palmer, M. und Bhakdi, S. (1997). Staphylococcal alpha-toxin: formation of the heptameric pore is partially cooperative and proceeds through multiple intermediate stages. *Biochemistry*, **36**: 13298-13304.

van Delft, M. F. und Huang, D. C. (2006). How the Bcl-2 family of proteins interact to regulate apoptosis. *Cell Res*, **16**: 203-213.

Vaux, D. L. und Korsmeyer, S. J. (1999). Cell death in development. *Cell*, **96**: 245-254.

Verma, S., Zhao, L. J. und Chinnadurai, G. (2001). Phosphorylation of the pro-apoptotic protein BIK: mapping of phosphorylation sites and effect on apoptosis. *J Biol Chem*, **276**: 4671-4676.

von Haefen, C., Wieder, T., Essmann, F., Schulze-Osthoff, K., Dorken, B. und Daniel, P. T. (2003). Paclitaxel-induced apoptosis in BJAB cells proceeds via a death receptor-independent, caspases-3/-8-driven mitochondrial amplification loop. *Oncogene*, **22**: 2236-2247.

Vousden, K. H. (2005). Apoptosis. p53 and PUMA: a deadly duo. *Science*, **309**: 1685-1686.

Vousden, K. H. und Lu, X. (2002). Live or let die: the cell's response to p53. *Nat Rev Cancer*, **2**: 594-604.

Vousden, K. H. und Prives, C. (2005). P53 and prognosis: new insights and further complexity. *Cell*, **120**: 7-10.

Wahl, G. M. und Carr, A. M. (2001). The evolution of diverse biological responses to DNA damage: insights from yeast and p53. *Nat Cell Biol*, **3**: E277-286.

Wei, M. C., Lindsten, T., Mootha, V. K., Weiler, S., Gross, A., Ashiya, M., Thompson, C. B. und Korsmeyer, S. J. (2000). tBID, a membrane-targeted death ligand, oligomerizes BAK to release cytochrome c. *Genes Dev*, **14**: 2060-2071.

Wennerberg, K. und Der, C. J. (2004). Rho-family GTPases: it's not only Rac and Rho (and I like it). *J Cell Sci*, **117**: 1301-1312.

Wieder, T., Essmann, F., Prokop, A., Schmelz, K., Schulze-Osthoff, K., Beyaert, R., Dorken, B. und Daniel, P. T. (2001). Activation of caspase-8 in drug-induced apoptosis of B-lymphoid cells is independent of CD95/Fas receptor-ligand interaction and occurs downstream of caspase-3. *Blood*, **97**: 1378-1387.

Willis, S. N. und Adams, J. M. (2005). Life in the balance: how BH3-only proteins induce apoptosis. *Curr Opin Cell Biol*, **17**: 617-625.

Xiong, Y., Hannon, G. J., Zhang, H., Casso, D., Kobayashi, R. und Beach, D. (1993). p21 is a universal inhibitor of cyclin kinases. *Nature*, **366**: 701-704.

Yee, K. S. und Vousden, K. H. (2005). Complicating the complexity of p53. *Carcinogenesis*, **26**: 1317-1322.

Yin, L., Schwartzberg, P., Scharton-Kersten, T. M., Staudt, L. und Lenardo, M. (1997). Immune responses in mice deficient in Ly-GDI, a lymphoid-specific regulator of Rho GTPases. *Mol Immunol*, **34**: 481-491.

Yu, J., Wang, Z., Kinzler, K. W., Vogelstein, B. und Zhang, L. (2003). PUMA mediates the apoptotic response to p53 in colorectal cancer cells. *Proc Natl Acad Sci U S A*, **100**: 1931-1936.

Yu, J., Zhang, L., Hwang, P. M., Kinzler, K. W. und Vogelstein, B. (2001). PUMA induces the rapid apoptosis of colorectal cancer cells. *Mol Cell*, **7**: 673-682.

Yu, Q., La Rose, J., Zhang, H., Takemura, H., Kohn, K. W. und Pommier, Y. (2002). UCN-01 inhibits p53 up-regulation and abrogates gamma-radiation-induced G(2)-M checkpoint independently of p53 by targeting both of the checkpoint kinases, Chk2 and Chk1. *Cancer Res*, **62**: 5743-5748.

Zha, J., Harada, H., Yang, E., Jockel, J. und Korsmeyer, S. J. (1996). Serine phosphorylation of death agonist BAD in response to survival factor results in binding to 14-3-3 not BCL-X(L). *Cell*, **87**: 619-628.

5 CURRICULUM VITAE

DR. RER. NAT. FRANK EßMANN

Geburtsdatum: 13.12.1971

Geburtsort: Waltrop, NRW

Ausbildung und beruflicher Werdegang

seit 09/2002	Wissenschaftlicher Angestellter am Institut für Molekulare Medizin des Universitätsklinikums Düsseldorf, Institutsleiter Herr Prof. K. Schulze-Osthoff.
08/2001-08/2002	Mitgründer der Proteome Factory AG, Berlin. Projektleiter Elektrophorese und Bildanalyse.
10/2000-07/2001	Wissenschaftlicher Angestellter an der Charité Berlin, Abteilung für Hämatologie, Onkologie und Tumorimmunologie, Arbeitsgruppe von Herrn Prof. P.T. Daniel.
09/2000	Promotion an der Technischen Universität Berlin, Titel der Arbeit: *Mechanisms of Apoptosis in Cancer: Regulatory Role of Caspases*.
09/1997-09/2000	Promotionsarbeit als Stipendiat im Graduiertenkolleg 331 der DFG an der Charité Berlin, Abteilung Hämatologie, Onkologie und Tumorimmunologie (Prof. B. Dörken), Arbeitsgruppe von Herrn Prof. P.T. Daniel in Kooperation mit der Arbeitsgruppe von Frau Prof. B. Wittmann-Liebold am Max-Delbrueck-Centrum, Berlin.
01/1997-10/1997	Diplomarbeit am Max-Planck-Institut für Molekulare Physiologie, Dortmund, Abteilung für physikalische Biochemie (Prof. R. Goody), Arbeitsgruppe von Herrn Prof. A.J. Scheidig.
10/1992-10/1997	Studium der Chemie an der Universität Dortmund.
07/1991-07/1992	Wehrdienst in Büdel (Niederlande) und Axstedt.
06/1991	Abitur am Theodor-Heuss-Gymnasium, Waltrop.

6 PUBLIKATIONSLISTE

1. Daniel, P.T., Scholz, C., Essmann, F., Westermann, J., Pezzutto, A. und Dörken, B. (1999).
   CD95/Fas-triggered apoptosis of activated T lymphocytes is prevented by dendritic cells through a CD58-dependent mechanism.
   Exp Hematol, **9**:1402-1408.

2. Essmann, F., Wieder, T., Otto, A., Müller, E.C., Dörken, B., Daniel, P.T. (2000).
   GDP dissociation inhibitor D4-GDI (Rho-GDI 2), but not the homologous rho-GDI 1, is cleaved by caspase-3 during drug-induced apoptosis.
   Biochem J, **346**: 777-783

3. Prokop, A., Wieder, T., Sturm, I., Essmann, F., Seeger, K., Wuchter, C., Ludwig, W.D., Henze, G., Dörken, B. und Daniel P.T. (2000).
   Relapse in childhood acute lymphoblastic leukemia is associated with a decrease of the Bax/Bcl-2 ratio and loss of spontaneous caspase-3 processing in vivo.
   Leukemia, **9**: 1606-1613

4. Wieder, T., Essmann, F., Prokop, A., Schmelz, K., Schulze-Osthoff, K., Beyaert, R., Dörken, B. und Daniel P.T. (2001). Activation of caspase-8 in drug-induced apoptosis of B-lymphoid cells is independent of CD95/Fas receptor-ligand interaction and occurs downstream of caspase-3.
   Blood, **97**: 1378-1387.

5. Wieder, T., Prokop, A., Bagci, B., Essmann, F., Bernicke, D., Schulze-Osthoff, K., Dörken, B., Schmalz, H.G., Daniel, P.T. und Henze G. (2001). Piceatannol, a hydroxylated analog of the chemopreventive agent resveratrol, is a potent inducer of apoptosis in the lymphoma cell line BJAB and in primary, leukemic lymphoblasts.
   Leukemia, **15**: 1735-1742.

6. Bosanquet, A.G., Sturm, I., Wieder, T., Essmann, F., Bosanquet, M.I., Head, D.J., Dörken, B. und Daniel, P.T. (2002). Bax expression correlates with cellular drug sensitivity to doxorubicin, cyclophosphamide and chlorambucil but not fludarabine, cladribine or corticosteroids in B cell chronic lymphocytic leukemia.
   Leukemia, **16**: 1035-1044.

7. von Haefen, C., Wieder, T., Essmann, F*., Schulze-Osthoff, K., Dörken, B. und Daniel, P.T. (2003). Paclitaxel-induced apoptosis in BJAB cells proceeds via a death receptor-independent, caspases-3/-8-driven mitochondrial amplification loop.
   Oncogene, **22**: 2236-2247.

8. Zeller, M., Essmann, F*., Jänicke, R.U., Schulze-Osthoff, K. und König, S. (2003). A rapid nonradioactive peptide phosphorylation assay.
J Exp Ther Oncol, **3**: 59-61.

9. Gillissen, B., Essmann, F., Graupner, V., Stärck, L., Radetzki, S., Dörken, B., Schulze-Osthoff, K. und Daniel, P.T. (2003). Induction of cell death by the BH3-only Bcl-2 homolog Nbk/Bik is mediated by an entirely Bax-dependent mitochondrial pathway.
Embo J, **22**: 3580-3590.

10. Essmann, F., Bantel, H., Totzke, G., Engels, I.H., Sinha, B., Schulze-Osthoff, K. und Jänicke R.U. (2003). Staphylococcus aureus alpha-toxin-induced cell death: predominant necrosis despite apoptotic caspase activation.
Cell Death Differ, **10**: 1260-1272.

11. Schmelz, K., Wieder, T., Tamm, I., Müller, A., Essmann, F., Geilen, C.C., Schulze-Osthoff, K., Dörken B. und Daniel P.T. (2004). Tumor necrosis factor alpha sensitizes malignant cells to chemotherapeutic drugs via the mitochondrial apoptosis pathway independently of caspase-8 and NF-kappaB.
Oncogene, **23**: 6743-6759.

12. Essmann, F., Engels, I.H., Totzke, G., Schulze-Osthoff, K. und Jänicke R.U. (2004). Apoptosis resistance of MCF7 breast carcinoma cells to ionizing radiation is independent of p53 and cell cycle control but caused by the lack of caspase-3 and a caffeine-inhibitable event.
Cancer Res, **64**: 7065-7072.

13. Scholz, C., Wieder, T., Stärck, L., Essmann, F., Schulze-Osthoff, K., Dörken, B. und Daniel, P.T. (2005). Arsenic trioxide triggers a regulated form of caspase-independent necrotic cell death via the mitochondrial death pathway.
Oncogene, **24**: 1904-1913.

14. Essmann, F., Pohlmann, S., Gillissen, B., Daniel, P.T., Schulze-Osthoff, K. und Jänicke, R.U. (2005). Irradiation-induced translocation of p53 to mitochondria in the absence of apoptosis.
J Biol Chem, **280**: 37169-37177.

15. Sohn, D., Totzke, G., Essmann, F., Schulze-Osthoff, K., Levkau, B. und Jänicke, R.U. (2006). The proteasome is required for rapid initiation of death receptor-induced apoptosis.
Mol Cell Biol, **26**: 1967-1978.

16. Totzke, G., Essmann, F., Pohlmann, S., Lindenblatt, C., Jänicke, R.U. und Schulze-Osthoff, K. (2006). A novel member of the IkappaB family, human IkappaB-zeta, inhibits transactivation of p65 and its DNA binding.
J Biol Chem, **281**: 12645-12654.

17. Tenenbaum, T., Essmann, F., Adam, R., Seibt, A., Jänicke, R.U., Novotny, G.E., Galla, H.J. und Schroten, H. (2006). Cell death, caspase activation, and HMGB1 release of porcine choroid plexus epithelial cells during Streptococcus suis infection in vitro.
Brain Res, **1100**: 1-12.

18. Sohn, D., Essmann, F., Schulze-Osthoff, K. und Jänicke, R.U. (2006). p21 blocks irradiation-induced apoptosis downstream of mitochondria by inhibition of cyclin-dependent kinase-mediated caspase-9 activation.
Cancer Res, **66**: 11254-11262

19. Werdehausen, R., Braun, S., Essmann, F., Walczak, H., Schulze-Osthoff, K., Lipfert P., Stevens M.F. (2007). Lidocaine Induces Apoptosis via the Mitochondrial Pathway Independently of Caspase-8.
Anesthesiology, In Revision.

20. Schneider, L., Essmann, F., Kletke, A., Rio, P., Hanenberg, H., Wetzel, W., Schulze-Osthoff, K., Nürnberg, B. und Piekorz, R.P. (2006). Compromised checkpoints exacerbate centrosomal abnormalities, polyploidy and cell death upon TACC3 depletion.
J Cell Biol, In Revision.

*: gleichberechtigter Erstautor

GDP dissociation inhibitor D4-GDI (Rho-GDI 2), but not the homologous Rho-GDI 1, is cleaved by caspase-3 during drug-induced apoptosis

Frank ESSMANN*, Thomas WIEDER*, Albrecht OTTO†, Eva-Christina MÜLLER†, Bernd DÖRKEN* and Peter T. DANIEL*[1]

*Department of Hematology, Oncology and Tumor Immunology, University Medical Center Charité, Campus Berlin-Buch, Humboldt University Berlin, Lindenberger Weg 80, 13125 Berlin, Germany, and †Max Delbrück Center for Molecular Medicine, Robert-Rössle-Strasse 10, 13092 Berlin-Buch, Germany

Different cytotoxic drugs induce cell death by activating the apoptotic programme; a family of cysteinyl aspartate proteases named caspases has been shown to be involved in the initiation as well as the execution of this kind of cell death. In the present study, cleavage of D4-GDI (Rho-GDI 2), an abundant haemopoietic-cell GDP dissociation inhibitor for the Ras-related Rho family GTPases, was demonstrated after treatment of BJAB Burkitt-like lymphoma cells with taxol or epirubicin. The cleavage of D4-GDI occurred simultaneously with the activation of caspase-3 but preceded DNA fragmentation and the morphological changes associated with apoptotic cell death. By using high-resolution two-dimensional gel electrophoresis it was shown that this cleavage is specific: whereas the level of the homologous protein Rho-GDI 1 was not significantly altered during drug-induced apoptosis and in cytochrome *c*/dATP-activated cellular extracts, D4-GDI disappeared owing to proteolytic cleavage. Inhibitor experiments with Z-DEVD-fmk (in which Z stands for benzyloxycarbonyl and fmk for fluoromethyl ketone) and microsequencing of the D4-GDI fragment revealed that this occurs at the caspase-3 cleavage site. Our results strongly suggest the differential regulation of the homologous GDP dissociation inhibitors Rho-GDI 1 and D4-GDI during drug-induced apoptosis by proteolysis mediated by caspase-3 but not by caspase-1. Owing to their crucial role as modulators of Rho GTPases, this might in turn have a significant impact on the mechanisms that induce the cytoskeletal and morphological changes in apoptotic cells.

Key words: epirubicin, mass spectrometry, microsequencing, taxol, two-dimensional electrophoresis.

INTRODUCTION

Apoptosis is an important process in a wide variety of biological systems, including physiological cell turnover, the immune system, embryonic development and hormone-dependent atrophy [1–4]. Interestingly, it has been shown that cytostatic agents such as taxotere [5], daunorubicin [6] and synthetic phospholipids [7] induce apoptosis, thereby providing some evidence for their mechanisms of action. The initiation of death signalling and the execution of the apoptotic programme after different death stimuli is mediated in most cases by a family of cysteine proteases called caspases [8]. Although death signalling in apoptosis is relatively well defined, especially for the death receptors located on the cell surface [9], the role of caspases as downstream effectors and the search for specific caspase substrates are continuing fields of research. In this context, the cleavage of the GDP dissociation inhibitor D4-GDI (Rho-GDI 2) has been demonstrated during CD95/Fas-induced and surface IgM-mediated apoptosis [10,11]; the relevance of this cleavage for the marked cytoskeletal changes that accompany apoptosis has been discussed.

Intensive studies have clarified the functions of small GTP-binding proteins, a protein superfamily which consists of the Ras, Rho, Arf, Rab and Ran families. It has been proposed that the Rho family of GTPases is involved in the regulation of integrin activity and in the organization of the actin cytoskeleton [12,13]. The activities of the different Rho proteins are regulated by at least three types of regulator protein: (1) GDP/GTP exchange proteins, (2) GTPase-activating proteins and (3) GDP dissociation inhibitors (GDIs) [14]. The last comprise a family of proteins consisting of three members: Rho-GDI 1, D4-GDI (also named Rho-GDI 2 or Ly-GDI) and Rho-GDI 3. Rho-GDI 1 is expressed ubiquitously, whereas D4-GDI is expressed in haemopoietic tissues and Rho-GDI 3 in brain, lung, kidney, testis and pancreas [15].

The N-terminal cleavage of D4-GDI leads to the defective regulation of Rho-GTPase; truncated D4-GDI is unable to inhibit the dissociation of GDP from RhoA [16]. This might in turn have a negative impact on the organization of actin filaments.

However, the influence of cytostatic drugs on the status of the two members of the GDI family being expressed in lymphoid cells, Rho-GDI 1 and D4-GDI, has not yet been studied. In the present study, cleavage of GDI proteins after incubation of BJAB Burkitt-like lymphoma cells with taxol, a chemotherapeutic agent that perturbs microtubule dynamics [17], was investigated by Western blot analysis, high-resolution two-dimensional gel electrophoresis and subsequent microsequencing of the proteolytic cleavage site. Furthermore, the results were compared with the influence of epirubicin, another chemotherapeutic drug, which targets DNA and also induces G_2/M arrest. Our results demonstrate clearly that D4-GDI, but not Rho-GDI 1, is cleaved during taxol- and epirubicin-induced apoptosis, indicating that the proteolysis of D4-GDI is a highly specific feature of apoptosis, at least in haemopoietic cells.

Although caspase-1 has been shown to be involved mainly in inflammation (reviewed in [18]), previous studies suggested an additional role for caspase-1 in cell death after drug exposure [5,19]. Because D4-GDI contains caspase-1 and caspase-3 cleavage sites [10], we addressed the role of caspase-1 and the central effector caspase-3 in our experimental system. By using cell-

Abbreviations used: BJAB, Burkitt-like lymphoma cell line; Caps, 3-(cyclohexylamino)propane-1-sulphonic acid; CBB, Coomassie Brilliant Blue; crmA, cytokine response modifier A; fmk, fluoromethyl ketone; GDI, GDP dissociation inhibitor; PARP, poly(ADP-ribose) polymerase; pNA, *p*-nitroanilide; Z, benzyloxycarbonyl.

[1] To whom correspondence should be addressed (e-mail pdaniel@mdc-berlin.de).

permeable peptide inhibitors we were able to show that caspase-1 is not involved in D4-GDI cleavage and apoptosis after treatment with taxol. Microsequencing of the resulting D4-GDI fragment led to the identification of the caspase-3 cleavage site. Thus cleavage of D4-GDI is independent from caspase-1 and occurs by a caspase-3-dependent mechanism.

EXPERIMENTAL

Materials

Polyclonal rabbit anti-(human caspase-3) (developed against human recombinant protein), anti-[poly(ADP-ribose) polymerase] (anti-PARP) (clone C2-10) and polyclonal rabbit anti-(human Rho-GDI/D4-GDI) (developed against full-length recombinant human Rho-GDI 1) antibodies were from Pharmingen (Hamburg, Germany). Secondary horseradish-peroxidase-conjugated anti-mouse antibodies and secondary horseradish-peroxidase-conjugated anti-rabbit antibodies were from Promega (Mannheim, Germany). Substrate for caspase-3-like activities, Ac-DEVD-pNA (in which pNA stands for *p*-nitroanilide), and substrate for caspase-1-like activities, Ac-YVAD-pNA, were from Calbiochem-Novabiochem GmbH (Bad Soden, Germany). Inhibitor for caspase-3-like activities, Z-DEVD-fmk (in which Z stands for benzyloxycarbonyl and fmk for fluoromethyl ketone), and caspase-1,4,5 inhibitor, Z-WEHD-fmk, were from Kamiya Biomedical Company (Seattle, WA, U.S.A.); they were dissolved in DMSO to give 20 mM stock solutions. According to the manufacturer, these inhibitors are synthesized as methyl esters to enhance cell permeability and facilitate the penetration of cell membranes; in cells the methyl groups are removed by endogenous enzymes. RNAse A was from Roth (Karlsruhe, Germany). Epirubicin was purchased from Pharmacia Upjohn (Erlangen, Germany); taxol (paclitaxel) was from Bristol Arzneimittel GmbH (München, Germany).

Cell culture

BJAB cells transfected with control vector (mock transfection with pcDNA 3) and with pcDNA 3 crmA (cytokine response modifier A) [20] were kindly provided by Klaus Schulze-Osthoff (University of Tübingen, Tübingen, Germany) and were grown in RPMI 1640 medium supplemented with 10 % (v/v) fetal calf serum, 0.56 g/l L-glutamine, 100 000 i.u. penicillin and 0.1 g/l streptomycin. Media and culture reagents were from Life Technologies GmbH (Karlsruhe, Germany). Confluent cells were subcultured every 5 days by dilution of the cells to a concentration of 10^5 cells/ml.

Measurement of DNA fragmentation

Mock- and crmA-transfected BJAB cells were seeded at a density of 10^5 cells/ml and treated with different concentrations of the respective cytostatic drugs. Cells were harvested after 24, 48 and 72 h of incubation by centrifugation at 300 ***g***. Cells were washed twice with cold PBS and fixed in PBS/2 % (v/v) formaldehyde on ice for 30 min. After fixation, cells were incubated with ethanol/PBS (2:1, v/v) for 15 min, pelleted and resuspended in PBS containing 40 μg/ml RNase A. RNA was digested for 30 min at 37 °C, cells were pelleted again and finally resuspended in PBS containing 50 μg/ml propidium iodide. Nuclear DNA fragmentation was then quantified by flow-cytometric determination of hypodiploid DNA, as described [21]. Data were collected and analysed with a FACScan (Becton Dickinson, Heidelberg, Germany) equipped with CELLQuest software. Data are given as percentages of hypoploidy sub-G_1, which reflects the number of apoptotic cells.

Immunoblotting

After incubation with the respective cytostatic drugs, mock- and crmA-transfected BJAB cells were washed twice with PBS and lysed in buffer L [10 mM Tris/HCl (pH 7.5)/300 mM NaCl/1 % Triton X-100/2 mM $MgCl_2$/5 mM EDTA/1 μM pepstatin/1 μM leupeptin/0.1 mM PMSF]. Protein concentration was determined with the bicinchoninic acid assay [22] (Pierce, Rockford, IL, U.S.A.) and equal amounts of protein (usually 20 μg per lane) were separated by SDS/PAGE [23]; immunoblotting was performed essentially as described [24]. Membranes (Schleicher and Schuell, Dassel, Germany) were swollen in Caps buffer {10 mM Caps [3-(cyclohexylamino) propane-1-sulphonic acid] (pH 11)/10 % (v/v) methanol} for several minutes and blotting was performed at 1 mA/cm² for 1 h in a transblot SD cell (Bio-Rad, München, Germany). The membrane was blocked for 1 h in blocking buffer [PBS/0.05 % (v/v) Tween 20/3 % (w/v) non-fat dried milk] and incubated with primary antibody in blocking buffer for 1 h. After the membrane had been washed three times in PBST [PBS/0.05 % (v/v) Tween 20], secondary antibody was applied in PBST for 1 h. Finally, the membrane was washed in PBST again and bands were detected with the ECL® enhanced chemiluminescence system (Amersham Buchler, Braunschweig, Germany) in accordance with the manufacturer's protocol. Two-dimensional Western blots were prepared in the same way.

Two-dimensional gel electrophoresis

Cell pellets were spun down at 724 ***g*** (3000 rev./min) in an Eppendorf centrifuge and resuspended in 1 μl of buffer PE/mg of cells [PE buffer is 50 mM Tris/HCl (pH 7.1)/100 mM KCl/6 mM EDTA]. Ampholytes (pH 2–4) were added to a final concentration of 2 % (v/v), sulphide bonds were reduced with 70 mM dithiothreitol and the mixture was supplemented with 1 mM PMSF and 1 μg/ml pepstatin. To achieve lysis and denaturing of proteins, urea was added to a final concentration of 9 M. DNA was separated by centrifugation at 70 000 ***g*** for 20 min at 20 °C. Aliquots (10 μl for 0.09 cm rod gels; 20–30 μl for 0.15 cm rod gels) of the samples were separated in the first dimension by using carrier ampholytes of pH 2–11 and 4 % (w/v) gels 23 cm in length. After isoelectric focusing, proteins were separated by SDS/PAGE on 23 cm × 35 cm gels [15 % (v/v) polyacrylamide] [25]. Staining was performed with Coomassie Brilliant Blue (CBB) G250 (0.15 cm rod gels) or silver staining as described by Blum et al. [26].

Identification of spots

Spots were identified by mass spectrometric methods [27] after tryptic digestion as described elsewhere [28]. The measurements were performed with a Q-Tof (Micromass, Manchester, U.K.) equipped with a nanoflow Z spray ion source. An aliquot of 1 μl was sufficient for one mass spectrum and five or six MS/MS experiments to obtain sequence information direct from the peptides in the mixture. Protein identification was possible for the faintest CBB-stained spots and not too weakly silver-stained spots. We used the sequence tag program, which combines partial manual spectrum interpretation of approx. three amino acids (sequence tag) with the residual mass N-terminal and C-terminal of the interpreted region and the peptide mass [29]. This information was then applied to searching in a non-redundant translated nucleotide database (http://www.mann.embl-

heidelberg.de/Services/PeptideSearch/FR_Peptide PatternForm.html).

Preparation of cell extracts and induction of the cell-free apoptotic system

Cell extracts were prepared as described [30]. In brief, BJAB cells were washed twice with PBS, resuspended in buffer A [20 mM Hepes (pH 7.4)/10 mM KCl/2 mM $MgCl_2$/1 mM EDTA] and incubated on ice for 15 min. PMSF was added to give a final concentration of 0.1 mM. Cells were then disrupted by passage 15 times through a 21 G $\times$ $1\frac{1}{2}$ needle (0.80 mm $\times$ 40 mm; Braun, Melsungen, Germany). The homogenates were cleared by centrifugation at 16000 ***g*** and 4 °C for 15 min. The centrifugation step was repeated and the clear supernatants were used for caspase activation *in vitro* or the measurement of caspase activities *in vitro*. For initiating caspase activation *in vitro*, 1 mM dithiothreitol, 1 μM horse heart cytochrome *c* (Sigma, München, Germany) and 1 mM dATP were added and the extracts were incubated at 30 °C for 5 min followed by incubation at 37 °C for different periods.

Measurement of caspase-3-like and caspase-1-like activity

After incubation with the respective cytostatic drugs, the mock- or crmA-transfected BJAB cells were washed twice with PBS and cell extracts were prepared as described above. After determination of the protein concentration with the bicinchoninic acid assay, caspase-3-like activity was measured as described [31], with some modifications. For this, 10 μl of extract, 90 μl of buffer B [50 mM Hepes (pH 7.4)/100 mM NaCl/1 mM EDTA/0.1 % CHAPS/10 % (w/v) sucrose/5 mM dithiothreitol] and 2 μl of colorimetric substrate (10 mM Ac-DEVD-pNA in DMSO) were mixed. Samples were incubated at 37 °C and A_{405} was measured in an ELISA reader every 10 min. From the specific caspase-3 activities (units/mg of protein) the increase of caspase-3 activity in drug-treated cells over the respective controls was calculated.

Similarly, caspase-1-like activity was measured in BJAB cells by using Ac-YVAD-pNA as substrate.

RESULTS AND DISCUSSION

Induction of apoptosis, caspase-3 activation and cleavage of D4-GDI during drug-induced apoptosis

To examine D4-GDI cleavage after treatment with chemotherapeutic drugs, we first determined the concentration-dependent proapoptotic effects of taxol and epirubicin in mock-transfected BJAB cells and found that 0.12 μM taxol and 1.85 μM epirubicin efficiently induced DNA fragmentation (results not shown). Time-course experiments in mock-transfected BJAB cells revealed that DNA fragmentation was hardly observed after 24 h of incubation and increased significantly with time. After 72 h of incubation with 0.12 μM taxol or 1.85 μM epirubicin, the number of apoptotic cells reached 50–60 % (Figure 1A). In a second set of experiments, we examined the cleavage of caspase substrates and the activation of caspase-3 by Western blot analyses with anti-(Rho-GDI) 1/D4-GDI, anti-caspase-3 and anti-PARP antibodies. In mock-transfected BJAB cells, cleavage of Rho-GDI 1/D4-GDI (Figure 1B) and cleavage of the typical death substrate PARP [32] (Figure 1E) were shown to be early events in drug-induced apoptosis occurring after 24 h of incubation and reaching a plateau after 48 h. This coincided with the activation of caspase-3 as shown by the appearance of the active 17 kDa subunit after 24, 48 and 72 h (Figure 1D).

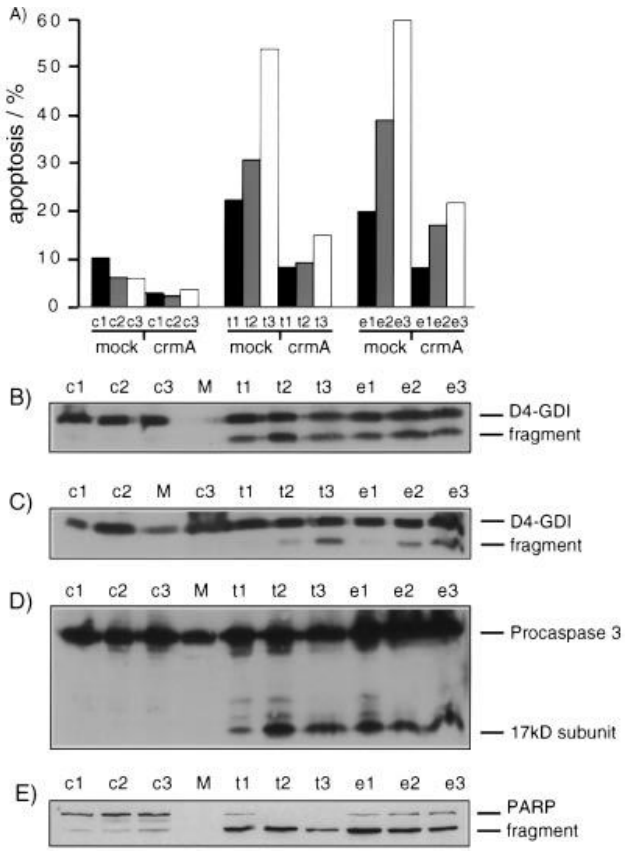

Figure 1 Taxol and epirubicin time-dependently induce DNA fragmentation, cleavage of Rho-GDI 1/D4-GDI, activation of caspase-3 and cleavage of PARP

(**A**) Mock-transfected BJAB cells and BJAB/crmA cells were incubated for 24, 48 and 72 h with control medium (c1, c2 and c3 respectively), 0.12 μM taxol (t1, t2 and t3 respectively) or 1.85 μM epirubicin (e1, e2 and e3 respectively). DNA fragmentation was then determined as described in the Experimental section. Values are given as percentages of apoptosis. Results are representative of three separate experiments. (**B**, **D**, **E**) Extracts from mock-transfected BJAB cells that had been treated as described above were subjected to Western blot analyses with anti-(Rho-GDI 1/D4-GDI) (**B**), anti-(caspase-3) (**D**) and anti-PARP (**E**) antibodies, as described in the Experimental section. Lanes M, molecular mass marker. (**C**) In addition, BJAB/crmA cells were treated in the same way and Western blot analysis was performed with anti-(Rho-GDI 1/D4-GDI) antibody. Results shown are representative of three separate experiments. Lane M, Molecular mass marker. kD, kDa.

Measurement of caspase-3 activity after 48 h of incubation showed 16-fold and 23-fold increases in caspase-3-like activity in taxol- and epirubicin-treated mock-transfected BJAB cells respectively. In these experiments, no activation of caspase-1-like activity was detected (results not shown). Furthermore, we investigated caspase-dependent cleavage of Rho-GDI 1/D4-GDI by using BJAB cells transfected with the cowpox virus gene crmA, which encodes a protease inhibitor of the serpin family. crmA has been described as a potent inhibitor of Fas- and tumour-necrosis-factor-induced apoptosis [20], interfering preferentially with caspase-1 and caspase-8 (reviewed in [33]). As shown in Figure 1(A), crmA inhibited taxol- and epirubicin-induced apoptosis but the inhibition was not complete. The same was true for the cleavage of Rho-GDI 1/D4-GDI which was decreased in crmA-transfected BJAB cells after 24 h of incubation (Figure 1C) in comparison with mock-transfected BJAB cells (Figure 1B). However, significant cleavage of Rho-GDI

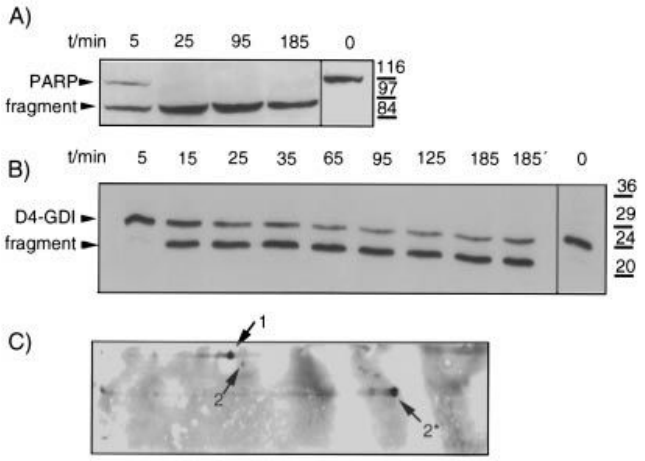

Figure 2 Time-dependent cleavage of PARP and Rho-GDI 1/D4-GDI after activation of caspases *in vitro* and localization of Rho-GDI 1, D4-GDI and D4-GDI fragment on a two-dimensional Western blot

(**A**, **B**) Extracts of mock-transfected BJAB cells were incubated with 10 μM cytochrome *c* and 1 mM dATP for different durations as indicated. The reaction was then stopped by the addition of SDS sample buffer, and Western blot analyses were performed with anti-PARP (**A**) and anti-(Rho-GDI 1/D4-GDI) (**B**) antibodies as described in the Experimental section. The positions of molecular mass markers are indicated (in kDa) at the right. (**C**) Additionally, the cytochrome *c*/dATP-treated extract of mock-transfected BJAB cells was separated by high-resolution two-dimensional gel electrophoresis, and Western blot analysis was performed with anti-(Rho-GDI 1/D4-GDI) as described in the Experimental section. Arrows indicate the positions of spots 1, 2 and 2* (see also Figure 4). The experiments were repeated and yielded similar results.

1/D4-GDI was observed after 48 and 72 h in drug-treated crmA-transfected cells (Figure 1C). Similarly, caspase-3 activation as well as PARP cleavage after 24 h were decreased in crmA-transfected cultures in comparison with mock-transfected BJAB cells but reached the same level as mock-transfected BJAB cells after 72 h (results not shown). Thus the inhibition of caspase-1 by crmA does not prevent the cleavage of D4-GDI, indicating that caspase-1 is not essential for D4-GDI cleavage.

Our results are consistent with earlier reports that demonstrated a rapid, caspase-3-dependent, cleavage of D4-GDI after treatment of lymphoid and myeloid cells with death-inducing stimuli such as CD95/Fas and anti-IgM [10,11]. However, cleavage of Rho-GDI 1/D4-GDI in our experimental system was not complete after 72 h of incubation with taxol or epirubicin (Figure 1B). To exclude the possibility that this was simply due to the presence of non-apoptotic cells in the samples used for the Western blot analyses, we established a cell-free system based on the activation of cytosol with cytochrome *c* and dATP, as described by Liu et al. [34]. In this system *in vitro*, a proteolytic cascade is initiated that leads to the rapid activation of caspase-3 [35]. In contrast with PARP, which was completely cleaved 25 min after the addition of 10 μM cytochrome *c* and 1 mM dATP to the cytosolic extract of mock-transfected BJAB cells (Figure 2A), the band corresponding to Rho-GDI 1/D4-GDI did not disappear, even after 185 min (Figure 2B).

Detecting specific D4-GDI cleavage by two-dimensional gel electrophoresis and MS

Keeping in mind that the antiserum employed for Western blot analysis detects both Rho-GDI 1 and D4-GDI, we decided to study the cleavage of the two related proteins by high-resolution two-dimensional gel electrophoresis. First, the spots representing the two GDI proteins and putative fragments were localized by Western blot analysis of an cell extract activated *in vitro* and separated by two-dimensional gel electrophoresis. With this technique, the two bands detected after one-dimensional separation by SDS/PAGE (Figure 2B) were separated into three spots: 1, 2 and 2* (Figure 2C). The identities of the indicated spots were verified by MS: spot 1 was Rho-GDI 1 and spot 2 was D4-GDI, as was spot 2* (Figure 3). However, the apparent molecular mass of 23 kDa and the pI of approx. 6.4 deduced from the position of spot 2* on the two-dimensional gel matched the theoretically predicted values for the corresponding fragment resulting from the cleavage of D4-GDI at Asp[19], as described by Na et al. [10]. Thus, spot 2* was undoubtedly a fragment of D4-GDI.

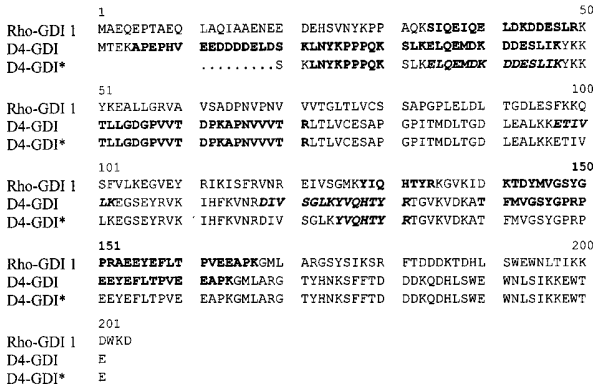

```
          1                                                  50
Rho-GDI 1 MAEQEPTAEQ  LAQIAAENEE  DEHSVNYKPP  AQKSIQEIQE  LDKDDESLRK
D4-GDI    MTEKAPEPHV  EEDDDDELDS  KLNYKPPPQK  SLKELQEMDK  DDESLIKYKK
D4-GDI*               .........S  KLNYKPPPQK  SLKELQEMDK  DDESLIKYKK
          51                                                 100
Rho-GDI 1 YKEALLGRVA  VSADPNVPNV  VVTGLTLVCS  SAPGPLELDL  TGDLESFKKQ
D4-GDI    TLLGDGPVVT  DPKAPNVVVT  RLTLVCESAP  GPITMDLTGD  LEALKKETIV
D4-GDI*   TLLGDGPVVT  DPKAPNVVVT  RLTLVCESAP  GPITMDLTGD  LEALKKETIV
          101                                                150
Rho-GDI 1 SFVLKEGVEY  RIKISFRVNR  EIVSGMKYIQ  HTYRKGVKID  KTDYMVGSYG
D4-GDI    LKEGSEYRVK  IHFKVNRDIV  SGLKYVQHTY  RTGVKVDKAT  FMVGSYGPRP
D4-GDI*   LKEGSEYRVK  IHFKVNRDIV  SGLKYVQHTY  RTGVKVDKAT  FMVGSYGPRP
          151                                                200
Rho-GDI 1 PRAEEYEFLT  PVEEAPKGML  ARGSYSIKSR  FTDDDKTDHL  SWEWNLTIKK
D4-GDI    EEYEFLTPVE  EAPKGMLARG  TYHNKSFFTD  DDKQDHLSWE  WNLSIKKEWT
D4-GDI*   EEYEFLTPVE  EAPKGMLARG  TYHNKSFFTD  DDKQDHLSWE  WNLSIKKEWT
          201
Rho-GDI 1 DWKD
D4-GDI    E
D4-GDI*   E
```

Figure 3 Characterization of spots 1, 2 and 2* by MS

Spots 1, 2 and 2* were cut from a CBB-stained two-dimensional electrophoresis gel. The proteins were digested and peptide masses were detected in the MS spectra (bold italics). Peptide sequences obtained by MS/MS are printed in bold. Aligned sequences of Rho-GDI 1 (spot 1), D4-GDI (spot 2) and fragment of D4-GDI (spot 2*) are shown.

To investigate the specificity of Rho-GDI 1/D4-GDI cleavage, whole-cell lysates from mock-transfected BJAB cells that had been treated with chemotherapeutic drugs were separated by high-resolution two-dimensional gel electrophoresis. Then the intensities of the corresponding spots after silver staining of the proteins were compared with the respective controls. As shown in Figure 4(A) (upper panels), Rho-GDI 1 (spot 1) did not show any decrease in intensity after 72 h of incubation with 0.12 μM taxol, whereas D4-GDI (spot 2) disappeared in the same lysates. Additional time-course experiments revealed that the intensity of D4-GDI was already declining after 24 h of incubation (results not shown). In contrast, the protein levels of Rho-GDI 1 showed only marginal fluctuations after 24, 48 and 72 h of incubation, indicating that this protein was resistant to cleavage by different caspases or even resistant to proteolytic cleavage in general. In contrast, the D4-GDI fragment (spot 2*) was not visible in control cells and appeared only on the induction of apoptosis (Figure 4A, lower panels). Similar results were obtained when the cells were treated with 1.85 μM epirubicin (results not shown). We also analysed the specificity of Rho-GDI 1/D4-GDI cleavage in the cell-free dATP/cytochrome *c*-activated system [34]. The results were virtually the same as described for the lysates of drug-treated cells: whereas the spot intensity of D4-GDI in the activated extract decreased in comparison with the control extract, Rho-GDI 1 remained unchanged (Figure 4B, upper panels). Furthermore, cleavage of D4-GDI in the extract activ-

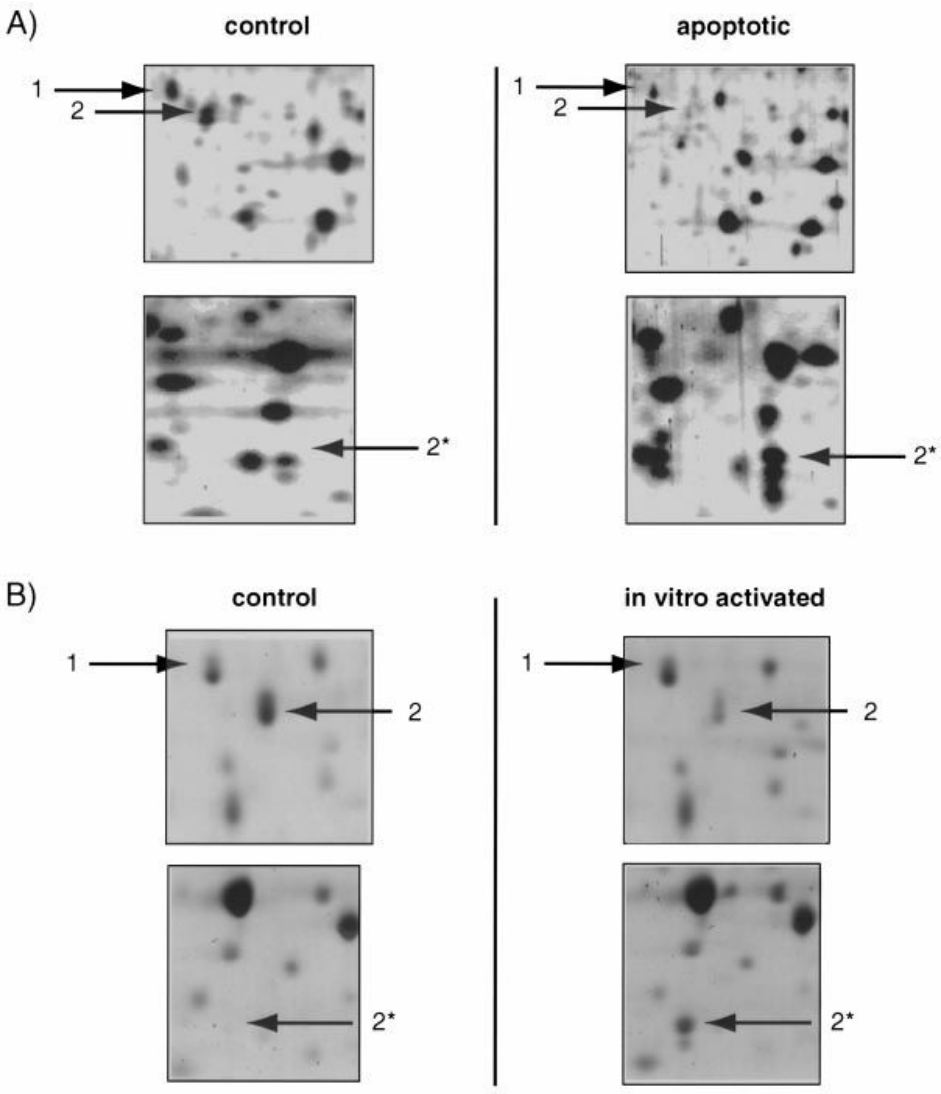

Figure 4 Specific cleavage of D4-GDI in apoptotic cells and in cell extracts activated *in vitro*

(**A**) Mock-transfected BJAB cells were incubated for 72 h with 0.12 μM taxol (apoptotic cells) or no additional supplements (control cells). The cell extracts were then separated by high-resolution two-dimensional gel electrophoresis and proteins were stained with silver as described in the Experimental section. The upper panels show the parts of two-dimensional gels in which spots 1 and 2 migrated; the lower panels show the parts of two-dimensional gels that included spot 2* (see also Figure 2C). Assigned spots were cut from a CBB-stained two-dimensional gel that was run in parallel. The proteins were digested and identified by MS. Spot 1, Rho-GDI 1; spot 2, D4-GDI; spot 2*, fragment of D4-GDI. (**B**) Extracts of mock-transfected BJAB cells were incubated for 3 h with 10 μM cytochrome *c* and 1 mM dATP (*in vitro* activated) or no additional supplements (control). The cell extracts were then separated by high-resolution two-dimensional gel electrophoresis and proteins were stained with silver as described in the Experimental section. The upper panels show the parts of two-dimensional gels in which spots 1 and 2 migrated; the lower panels show the parts of a two-dimensional gel that included spot 2* (see also Figure 2C). Spot assignments are as in (**A**). The experiments were repeated and yielded similar results.

ated *in vitro* was accompanied by the appearance of the corresponding fragment (Figure 4B, lower panels). These results clearly confirmed the specific cleavage of D4-GDI but not Rho-GDI 1 during drug-induced apoptosis, thereby providing further evidence that other potential cleavage sites that are present in Rho-GDI 1 (e.g. LELD^{89}L or DKTD^{143}Y) are not accessible. The experiments *in vitro* with cell-free extracts indicate that cleavage of D4-GDI also occurs downstream of the cytochrome *c*- and dATP-dependent formation of the Apaf-1/caspase-9 complex [36] and is not restricted to death-receptor-mediated apoptosis. The time course of D4-GDI cleavage *in vitro* (see Figure 2B) closely resembled the time courses of other typical death substrates such as Fodrin, U1sn-RNP and PARP [35].

D4-GDI is proteolysed by caspase-3

Triggering of the death cascade by cytotoxic drugs has recently been shown to lead to CD95/Fas-independent caspase activation [37]. In this context, an involvement of caspase-3 in taxol-induced cell death has been demonstrated in different cell types [38,39] but the role of caspase-1 in drug-mediated cytotoxicity is still a matter of debate. For example, in mouse fibroblast L929 cells a time-dependent increase of interleukin-1β-converting enzyme-like activity has been reported after treatment with taxotere [5]. Interestingly, D4-GDI is a substrate for both caspase-1 [16] and caspase-3 [10] and a detailed analysis of D4-GDI cleavage should reveal the role of these proteolytic enzymes

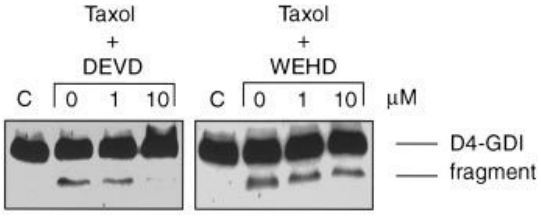

Figure 5 Taxol-induced cleavage of D4-GDI is inhibited by a cell-permeable inhibitor of caspase-3-like activity

Mock-transfected BJAB cells were preincubated for 2 h with different concentrations of Z-DEVD-fmk, Z-WEHD-fmk or diluent alone as indicated. The cells were then treated for 24 h with 0.12 μM taxol. Controls (C) were incubated in the absence of taxol. Cell extracts were prepared and subjected to Western blot analyses with anti-(Rho-GDI 1/D4-GDI) as described in the Experimental section. The experiment was repeated and yielded similar results.

in drug-induced apoptosis. First, we analysed the cleavage site of the D4-GDI fragment that appeared after the treatment of BJAB cells with taxol and also with epirubicin. However, N-terminal sequencing needs approx. 10 pmol of peptide; because it is very difficult to get enough protein from apoptotic cells to do HPLC and N-terminal Edman sequencing we decided to use micro-sequencing by nanospray MS. This method allows sequencing with femtomole amounts of a peptide mixture and enabled us to distinguish between the caspase-1 and caspase-3 cleavage sites of the D4-GDI fragment (spot 2*) in cellular extracts from apoptotic cells. Microsequencing of tryptic peptides of spot 2* by MS/MS led to the identification of the peptide E^{34}LQEMDKDDESLIK^{47} (Figure 3). Because the cleavage site of caspase-3 is represented by DELD^{19}S and the cleavage site of caspase-1 by LLGD^{55}G [10], the detection of this peptide, located between Lys^{33} and Tyr^{48} of spot 2*, was consistent only with the caspase-3-mediated proteolysis of D4-GDI. This was confirmed by inhibitor experiments with cell-permeable peptide inhibitors. Caspases can be divided into different groups on the basis of their substrate specificities (reviewed in [40]). By using a combinatorial approach, specificities of members of the caspase family were defined by Thornberry et al. [41] as follows: caspase-3-like activities display the subsite preference DEXD and caspase-1-like activities (W/L)EHD. We therefore used in our experimental system Z-DEVD-fmk or Z-WEHD-fmk, which irreversibly inhibit caspase-3-like and caspase-1-like activities respectively. As shown in Figure 5, 10 μM Z-DEVD-fmk blocked the taxol-induced cleavage of D4-GDI, whereas Z-WEHD-fmk had little or no effect.

Novel aspects of D4-GDI in comparison with Rho-GDI 1 cleavage in drug-induced apoptosis

As already outlined above, D4-GDI cleavage has been shown to occur after receptor-mediated apoptosis [10,11]. By mixing recombinant proteins in an assay *in vitro*, it has been demonstrated that only D4-GDI, and not Rho-GDI 1, represents a substrate for caspase-mediated cleavage [16]. In our study we used neither purified caspases nor recombinant substrates. In contrast, we analysed cleavage *in vivo* and employed whole-cell lysates without further purification in combination with the described analytical methods and the application of caspase inhibitors. We were thus able to demonstrate for the first time that (1) D4-GDI is cleaved during drug-induced apoptosis, (2) D4-GDI cleavage is specific because Rho-GDI 1 is not cleaved *in vivo* (either by caspases or by other proteases) when BJAB cells undergo apoptosis, (3) D4-GDI is cleaved *in vivo* at the caspase-3 cleavage site after treatment of BJAB cells with drugs, and (4) caspase-1 does not have a role in the taxol-induced cleavage of D4-GDI and the subsequent induction of apoptosis in BJAB cells. The last is of interest for the understanding of taxol-induced cell death because caspase-1 has previously been implicated in the induction of apoptosis by this kind of compound.

Taken together, the differential, caspase-3-mediated cleavage of D4-GDI in comparison with Rho-GDI 1 during drug-induced apoptosis indicates that, despite their high degree of similarity, these proteins display different properties. In this context it is interesting to note that the differential phosphorylation and Rho-GTPase selectivity of D4-GDI compared with Rho-GDI 1 have been shown after the stimulation of U937 cells with phorbol ester [42]. This might also be related to the differential effect of a D4-GDI knock-out in mice on apoptosis regulation. Only the apoptosis induced by IL-2 withdrawal, but not dexamethasone- and T-cell-receptor-induced apoptosis, was affected in lymphocytes from D4-GDI-deficient mice [43]. Thus the relevance of D4-GDI cleavage to the absence of Rho-GDI 1 cleavage for different apoptotic pathways might be an interesting subject for further investigation.

BJAB pcDNA 3-mock-transfected and pcDNA 3-crmA-transfected cells were a gift from Klaus Schulze-Osthoff (University of Tübingen, Tübingen, Germany). This work was supported in part by research grants from the Deutsche Forschungsgemeinschaft [SFB 273 and SFB 506 (to P.T.D.) and OT169/1-1 (to A.O.)] and the European Community TMR Programme (to P.T.D.). F.E. is the recipient of a fellowship from the DFG Graduiertenkolleg 'Temperaturabhängige Effekte für Therapie und Diagnostik' at the University Medical Center Charité.

REFERENCES

1 Arends, M. J. and Wyllie, A. H. (1991) Int. Rev. Exp. Pathol. **32**, 223–254
2 Ellis, R. E., Yuan, J. Y. and Horvitz, H. R. (1991) Annu. Rev. Cell Biol. **7**, 663–698
3 Cohen, J. J., Duke, R. C., Fadok, V. A. and Sellins, K. S. (1992) Annu. Rev. Immunol. **10**, 267–293
4 Krammer, P. H., Behrmann, I., Daniel, P., Dhein, J. and Debatin, K. M. (1994) Curr. Opin. Immunol. **6**, 279–289
5 Suzuki, A., Kawabata, T. and Kato, M. (1998) Eur. J. Pharmacol. **343**, 87–92
6 Palucka, K. A., Knaust, E., Xu, D., Macnamara, B., Porwit-Macdonald, A., Gruber, A., Peterson, C., Bjorkholm, M. and Pisa, P. (1999) Leuk. Lymphoma **32**, 309–316
7 Wieder, T., Orfanos, C. E. and Geilen, C. C. (1998) J. Biol. Chem. **273**, 11025–11031
8 Thornberry, N. A. and Lazebnik, Y. (1998) Science **281**, 1312–1316
9 Ashkenazi, A. and Dixit, V. M. (1998) Science **281**, 1305–1308
10 Na, S., Chuang, T. H., Cunningham, A., Turi, T. G., Hanke, J. H., Bokoch, G. M. and Danley, D. E. (1996) J. Biol. Chem. **271**, 11209–11213
11 Rickers, A., Brockstedt, E., Mapara, M. Y., Otto, A., Dorken, B. and Bommert, K. (1998) Eur. J. Immunol. **28**, 296–304
12 Hall, A. (1994) Annu. Rev. Cell Biol. **10**, 31–54
13 Narumiya, S. (1996) J. Biochem. (Tokyo) **120**, 215–228
14 Geyer, M. and Wittinghofer, A. (1997) Curr. Opin. Struct. Biol. **7**, 786–792
15 Sasaki, T. and Takai, Y. (1998) Biochem. Biophys. Res. Commun. **245**, 641–645
16 Danley, D. E., Chuang, T. H. and Bokoch, G. M. (1996) J. Immunol. **157**, 500–503
17 Sorger, P. K., Dobles, M., Tournebize, R. and Hyman, A. A. (1997) Curr. Opin. Cell Biol. **9**, 807–814
18 Cohen, G. M. (1997) Biochem. J. **326**, 1–16
19 Hiwasa, T., Tokita, H., Sakiyama, S. and Nakagaware, A. (1998) Anticancer Drugs **9**, 82–87
20 Tewari, M. and Dixit, V. M. (1995) J. Biol. Chem. **270**, 3255–3260
21 Nicoletti, I., Migliorati, G., Pagliacci, M. C., Grignani, F. and Riccardi, C. (1991) J. Immunol. Methods **139**, 271–279
22 Smith, P. K., Krohn, R. I., Hermanson, G. T., Mallia, A. K., Gartner, F. H., Provenzano, M. D., Fujimoto, E. K., Goeke, N. M., Olson, B. J. and Klenk, D. C. (1985) Anal. Biochem. **150**, 76–85
23 Laemmli, U. K. (1970) Nature (London) **227**, 680–685

24 Wieder, T., Geilen, C. C., Wieprecht, M., Becker, A. and Orfanos, C. E. (1994) FEBS Lett. **345**, 207–210
25 Klose, J. and Kobalz, U. (1995) Electrophoresis **16**, 1034–1059
26 Blum, H., Beier, H. and Gross, H. J. (1987) Electrophoresis **8**, 93–99
27 Müller, E. C., Schumann, M., Rickers, A., Bommert, K., Wittmann-Liebold, B. and Otto, A. (1999) Electrophoresis **20**, 320–330
28 Otto, A., Thiede, B., Muller, E. C., Scheler, C., Wittmann-Liebold, B. and Jungblut, P. (1996) Electrophoresis **17**, 1643–1650
29 Mann, M. and Wilm, M. (1994) Anal. Chem. **66**, 4390–4399
30 Deveraux, Q. L., Takahashi, R., Salvesen, G. S. and Reed, J. C. (1997) Nature (London) **388**, 300–304
31 Zhou, Q., Snipas, S., Orth, K., Muzio, M., Dixit, V. M. and Salvesen, G. S. (1997) J. Biol. Chem. **272**, 7797–7800
32 Tewari, M., Quan, L. T., O'Rourke, K., Desnoyers, S., Zeng, Z., Beidler, D. R., Poirier, G. G., Salvesen, G. S. and Dixit, V. M. (1995) Cell **81**, 801–809
33 Villa, P., Kaufmann, S. H. and Earnshaw, W. C. (1997) Trends Biochem. Sci. **22**, 388–393
34 Liu, X., Kim, C. N., Yang, J., Jemmerson, R. and Wang, X. (1996) Cell **86**, 147–157
35 Slee, E. A., Harte, M. T., Kluck, R. M., Wolf, B. B., Casiano, C. A., Newmeyer, D. D., Wang, H. G., Reed, J. C., Nicholson, D. W., Alnemri, E. S. et al. (1999) J. Cell Biol. **144**, 281–292
36 Li, P., Nijhawan, D., Budihardjo, I., Srinivasula, S. M., Ahmad, M., Alnemri, E. S. and Wang, X. (1997) Cell **91**, 479–489
37 Wesselborg, S., Engels, I. H., Rossmann, E., Los, M. and Schulze-Osthoff, K. (1999) Blood **93**, 3053–3063
38 Ibrado, A. M., Kim, C. N. and Bhalla, K. (1998) Leukemia **12**, 1930–1936
39 Kottke, T. J., Blajeski, A. L., Martins, L. M., Mesner, Jr, P. W., Davidson, N. E., Earnshaw, W. C., Armstrong, D. K. and Kaufmann, S. H. (1999) J. Biol. Chem. **274**, 15927–15936
40 Salvesen, G. S. and Dixit, V. M. (1997) Cell **91**, 443–446
41 Thornberry, N. A., Rano, T. A., Peterson, E. P., Rasper, D. M., Timkey, T., Garcia-Calvo, M., Houtzager, V. M., Nordstrom, P. A., Roy, S., Vaillancourt, J. P. et al. (1997) J. Biol. Chem. **272**, 17907–17911
42 Gorvel, J. P., Chang, T. C., Boretto, J., Azuma, T. and Chavrier, P. (1998) FEBS Lett. **422**, 269–273
43 Yin, L., Schwartzberg, P., Scharton, K. T., Staudt, L. and Lenardo, M. (1997) Mol. Immunol. **34**, 481–491

Received 11 August 1999/15 November 1999; accepted 4 January 2000

Activation of caspase-8 in drug-induced apoptosis of B-lymphoid cells is independent of CD95/Fas receptor-ligand interaction and occurs downstream of caspase-3

Thomas Wieder, Frank Essmann, Aram Prokop, Karin Schmelz, Klaus Schulze-Osthoff, Rudi Beyaert, Bernd Dörken, and Peter T. Daniel

The activation of caspase-8, a crucial upstream mediator of death receptor signaling, was investigated in epirubicin- and Taxol-induced apoptosis of B-lymphoma cells. This study was performed because the CD95/Fas receptor-ligand interaction, recruitment of the Fas-associated death domain (FADD) adaptor protein, and subsequent activation of procaspase-8 have been implicated in the execution of drug-induced apoptosis in other cell types. Indeed, active caspase-8 was readily detected after treatment of mature and immature B-lymphoid cells with epirubicin or Taxol. However, neither constitutive nor drug-induced expression of the CD95/Fas ligand was detectable in B-lymphoma cells. Furthermore, overexpression of a dominant-negative FADD mutant (FADDdn) did not block caspase-8 processing and subsequent DNA fragmentation, indicating that drug-induced caspase-8 activation was mediated by a CD95/Fas-independent mechanism. Instead, caspase-8 cleavage was slightly preceded by activation of caspase-3, suggesting that drug-induced caspase-8 activation in B-lymphoma cells is a downstream event mediated by other caspases. This assumption was confirmed in 2 experimental systems—zDEVD-fmk, a cell-permeable inhibitor of caspase-3–like activity, blocked drug-induced caspase-8 cleavage, and depletion of caspase-3 from cell extracts impaired caspase-8 cleavage after in vitro activation with dATP and cytochrome c. Thus, these data indicate that drug-induced caspase-8 activation in B-lymphoma cells is independent of death receptor signaling and is mediated by postmitochondrial caspase-3 activation. (Blood. 2001;97: 1378-1387)

Introduction

Apoptosis, a morphologically and biochemically defined form of cell death,[1] plays a role in a wide variety of biologic systems, including tissue homeostasis and regulation of the immune system.[2,3] The process is a highly orchestrated cellular pathway leading to activation of the downstream death machinery. The central mediator and executioner of the death machinery is a proteolytic system involving a family of cysteinyl proteases, called caspases (for review, see Thornberry and Lazebnik[4]). Triggering of the apoptotic cascade by different death stimuli, such as ionizing radiation[5] and chemotherapeutic drugs,[6] culminates in caspase-dependent cleavage of a set of regulatory proteins, degradation of cellular DNA, and complete disassembly of the cell. Thus far, 14 caspase family members have been identified, and some of them, such as caspase-8, mediate apoptotic signals after the activation of death receptors.[7,8] Others, such as caspase-9, are part of the apoptosome and play a role in signal transduction after mitochondrial damage.[9] Recently, an endoplasmic–reticulum-specific pathway of apoptosis has been described that is mediated by caspase-12.[10]

Previous data suggest that cytotoxic drugs induce cell death through CD95/Fas–CD95 ligand interaction,[11] and the relevance of this particular death pathway has been shown, for instance, in doxorubicin-induced apoptosis of leukemic T cells.[12] However, other groups were unable to confirm these findings and showed CD95/Fas-independent induction of apoptosis by chemotherapeutic drugs—for example, doxorubicin and etoposide—in T-lymphoma cells.[13,14] The finding that CD95/Fas-signaling and DNA damage induce different apoptosis-signaling pathways has also been shown in a murine and a human B-lymphoma cell line.[15] Furthermore, experimental evidence has been provided that neither FADD[16] nor caspase-8[17] is required for drug-induced apoptosis.

In B cells, the induction of apoptosis plays important roles in humoral immunity. In this context, it has been shown that the antigen receptor BCR and the CD95/Fas receptor transduce pro-apoptotic signals in mature B cells (for review, see Tsubata[18]). We previously showed that activation-induced apoptosis of normal and malignant B lymphocytes upon antigen-receptor ligation is independent of CD95/Fas and CD95/Fas ligand.[19] This has been confirmed by another study demonstrating that B-cell receptor-mediated apoptosis, in contrast to activation-induced T-cell apoptosis, is not mediated through known death receptor systems, nor does it involve the initial activation of caspase-8.[20] We nevertheless

From the Department of Hematology, Oncology and Tumor Immunology, University Medical Center Charité, Campus Berlin-Buch, and the Department of Pediatric Hematology/Oncology, University Medical Center Charité, Campus Virchow, Humboldt University of Berlin, Germany; the Department of Immunology and Cell Biology, University of Münster, Germany; the Department of Molecular Biology, Flanders Interuniversity Institute for Biotechnology, and University of Gent, Belgium.

Submitted June 1, 2000; accepted October 10, 2000.

Supported by grants from the Deutsche Forschungsgemeinschaft (SFB 273 and SFB 506) (P.T.D.), the European Community TMR Programme (P.T.D., K.S.-O., R.B.), and the Verein zur Förderung der Tagesklinik e. V. (T.W., A.P.). F.E. is a recipient of a fellowship from the DFG Graduiertenkolleg 331 at the University Medical Center Charité.

Reprints: Peter T. Daniel, Department of Hematology, Oncology, and Tumor Immunology, University Medical Center Charité, Campus Berlin-Buch, Humboldt University of Berlin, Lindenberger Weg 80, 13125 Berlin, Germany; e-mail: pdaniel@mdc-berlin.de.

The publication costs of this article were defrayed in part by page charge payment. Therefore, and solely to indicate this fact, this article is hereby marked ''advertisement'' in accordance with 18 U.S.C. section 1734.

observed that drug treatment leads to processing and activation of procaspase-8. We therefore focused our interest on the specific mechanisms leading to apoptotic death after the treatment of immature and mature B-lymphoma cells with cytotoxic drugs. By Northern blot analysis for the detection of CD95 ligand, by blocking of CD95 ligand/CD95 receptor interaction, and by overexpression of dominant-negative FADD (FADDdn), we show here that epirubicin-induced apoptosis in B cells is independent of a functional CD95 ligand–CD95 death-inducing signaling complex. This CD95-independent mechanism was also found after the treatment of B cells with Taxol, a chemotherapeutic agent that perturbs microtubule dynamics.[21] Furthermore, experimental evidence is provided that the activation of caspase-8 in B cells occurs downstream of the mitochondrial apoptosome and caspase-3. Thus, in contrast to the death receptor-mediated activation of apoptosis, caspase-8 appears to function as an amplifying executioner caspase in drug-induced B cell apoptosis.

Materials and methods

Materials

Polyclonal rabbit antihuman caspase-3 (developed against human recombinant protein), monoclonal anti-PARP (clone C2-10), and polyclonal rabbit antihuman Rho-GDI/D4-GDI (developed against full-length recombinant human Rho-GDI-1) antibodies were from Pharmingen (Hamburg, Germany). Monoclonal anti-FADD antibody was from Transduction Laboratories (Lexington, KY). Monoclonal antihuman caspase-8 antibody directed against the active p18 subunit of caspase-8 has been described previously.[22] Agonistic, monoclonal anti-CD95 antibody[13] was diluted into growth medium to give a final concentration of 1 μg/mL. Secondary antimouse horseradish peroxidase-conjugated antibodies and secondary antirabbit horseradish peroxidase-conjugated antibodies were from Promega (Mannheim, Germany). The caspase-3 substrate (Ac-DEVD-*p*NA, in which *p*NA stands for *P*-nitroanilide) and the caspase-8 substrate (Ac-IETD-*p*NA) were from Calbiochem-Novabiochem GmbH (Bad Soden, Germany). The caspase-3 inhibitor zDEVD-fmk (in which z stands for benzyloxycarbonyl and fmk for fluoromethyl ketone) was from Syrinx Diagnostica (Frankfurt, Germany) and was dissolved in dimethyl sulfoxide to give a 20 mM stock solution. According to the manufacturer, this inhibitor was synthesized as a methyl ester to enhance cell permeability. RNase A was from Roth (Karlsruhe, Germany). Epirubicin was purchased from Pharmacia Upjohn (Erlangen, Germany), and Taxol (paclitaxel) was purchased from Bristol Arzneimittel GmbH (Munich, Germany). The dominant-negative FADD construct (FADDdn) was a kind gift from A. M. Chinnaiyan and V. M. Dixit (Ann Arbor, MI).

Cell culture

Control vector- (pcDNA3-mock-transfected), pcDNA3-FADDdn-transfected BJAB cells, which were stably transfected with a dominant-negative FADD mutant lacking the N-terminal death effector domain,[22] Jurkat T-cells, NALM-6, and REH B-lymphoid cells were grown in RPMI 1640 medium supplemented with 10% fetal calf serum, 0.56 g/L L-glutamine, 100 000 U/L penicillin, and 0.1 g/L streptomycin. Media and culture reagents were from Life Technologies GmbH (Karlsruhe, Germany). Cells were subcultured every 3 to 4 days by dilution of the cells to a concentration of 1×10^5 cells/mL.

Additionally, bone marrow material from patients with childhood acute lymphoblastic leukemia (ALL) was obtained by bone marrow aspiration. Lymphoblasts and mononuclear cells were separated by centrifugation over Ficoll. The percentage of leukemic lymphoblasts was greater than 90%, which is in accordance with findings of a former study.[23] The diagnosis was established by immunophenotyping of leukemia cells according to Béné et al.[24] After separation, cells were immediately seeded at a density of 1×10^5 cells/mL in RPMI 1640 complete cell culture medium and treated with epirubicin. Leukemic lymphoblasts were also treated with Taxol. However, because of the missing cell proliferation in this experimental setting, Taxol did not induce significant apoptosis or caspase activation in primary lymphoblasts (data not shown).

CD95/Fas-mediated induction of apoptosis

Anti-CD95 (anti-APO-1 IgG3) or FII23c $F(ab)_2$ fragments were produced as described[25] and were added to the cultures before exposure to the cytostatic drugs. As a positive control for the ability of the $F(ab)_2$ fragments to block CD95/Fas receptor ligand interaction, we used Jurkat T cells induced for apoptosis by immobilized OKT3 anti-CD3 monoclonal antibody.[19]

Measurement of cell death

For the determination of cell death, 3×10^4 cells per well were seeded in microtiter plates and treated for different time periods with 1 μg/mL anti-CD95 or the chemotherapeutic agents. Cell death was assessed by the uptake of propidium iodide (2 μg/mL) in phosphate-buffered saline (PBS) into nonfixed cells and by subsequent flow cytometric analysis using the FSC–FL2 profile. Analyses were performed on a FACScalibur (Becton Dickinson; Heidelberg, Germany) using CellQuest analysis software. Additionally, cell death was determined by trypan blue exclusion as described.[26] Both methods virtually gave the same results.

Measurement of DNA fragmentation

DNA fragmentation was measured essentially as described.[27] Briefly, cells were seeded at a density of 1×10^5 cells/mL and treated with different concentrations of the respective cytotoxic drugs. After 24, 48, and 72 hours, cells were collected by centrifugation at 300*g* for 5 minutes, washed with PBS at 4°C, and fixed in PBS/2% (vol/vol) formaldehyde on ice for 30 minutes. After fixation, cells were incubated with ethanol/PBS (2:1, vol/vol) for 15 minutes, pelleted, and resuspended in PBS containing 40 μg/mL RNase A. After incubation for 30 minutes at 37°C, cells were pelleted again and finally resuspended in PBS containing 50 μg/mL propidium iodide. Nuclear DNA fragmentation was then quantified by flow cytometric determination of hypodiploid DNA. Data were collected and analyzed using a FACScan (Becton Dickinson) equipped with the CELLQuest software. Data are given in percentage hypoploidy (subG1), which reflects the number of apoptotic cells. Specific apoptosis was calculated by subtracting background apoptosis observed in control cells from total apoptosis observed in drug-treated cells. Background apoptosis was approximately 5%, depending on the cell line and the experimental settings.

Northern blotting

Northern blotting and hybridization were performed as previously described.[19] CD95 ligand expression (1.3 kB mRNA) was detected using a 500-bp polymerase chain reaction-cloned fragment, and β-actin was detected with a cloned and sequenced 246-bp fragment obtained by reverse transcriptase polymerase chain reaction as described.[19]

Immunoblotting

After incubation with the respective cytostatic drugs, cells were washed twice with PBS and lysed in buffer containing 10 mM Tris/HCl, pH 7.5, 300 mM NaCl, 1% Triton X-100, 2 mM $MgCl_2$, 5 μM EDTA, 1 μM pepstatin, 1 μM leupeptin, and 0.1 mM phenylmethylsulfonyl fluoride. Protein concentration was determined using the bicinchoninic acid assay[28] from Pierce (Rockford, IL), and equal amounts of protein (usually 20 μg per lane) were separated by SDS-PAGE.[29] Then, immunoblotting was performed as described.[30] Membranes (Schleicher & Schuell, Dassel, Germany) were swollen in CAPS-buffer (10 mM 3-[cyclohexylamino]propane-1-sulfonic acid, pH 11, 10% MeOH) for several minutes, and blotting was performed at 1 mA/cm^2 for 1 hour in a transblot SD cell (Bio-Rad, Munich, Germany). The membrane was blocked for 1 hour in PBST (PBS, 0.05% Tween-20) containing 3% nonfat dry milk and incubated with primary antibody for 1

hour. After the membrane had been washed 3 times in PBST, secondary antibody in PBST was applied for 1 hour. Finally, the membrane was washed in PBST again, and protein bands were detected using the enhanced chemiluminescence system (Amersham Buchler, Braunschweig, Germany).

Preparation of cytoplasmic cell extracts and induction of the cell-free apoptotic system

Cell extracts were prepared as described.[27] Briefly, BJAB cells were washed twice with PBS, resuspended in buffer A containing 20 mM HEPES, pH 7.4, 10 mM KCl, 2 mM $MgCl_2$, and 1 mM EDTA and incubated on ice for 15 minutes. Phenylmethylsulfonyl fluoride was added to give a final concentration of 0.1 mM. Cells were then disrupted by 15 passages through a 21-gauge × 1 1/2 needle (0.80 mm × 40 mm; Braun, Melsungen, Germany). The homogenates were cleared by centrifugation at 16 000*g*, 4°C for 15 minutes. The centrifugation step was repeated, and the clear supernatants were used for in vitro caspase activation, immunoprecipitation of caspase-3, or measurement of caspase activities. For initiating in vitro caspase activation, 1 mM dithiothreitol, 10 μM horse heart cytochrome c (Sigma; Munich, Germany), and 1 mM dATP were added, and the extracts were incubated at 30°C for 5 minutes followed by incubation at 37°C for different time periods. Control extracts were similarly incubated in the absence of cytochrome c and dATP.

Measurement of caspase-3–like and caspase-8–like activities

Caspase-3–like activity was measured in cell extracts from BJAB cells as described[31] with some modifications. To this end, 10 μL extract, 90 μL buffer B containing 50 mM HEPES, pH 7.4, 100 mM NaCl, 1 mM EDTA, 0.1% 3-[(3-cholamidopropyl)dimethyl-ammonio]-1-propanesulfonate, 10% saccharose, 5 mM dithiothreitol, and 2 μL colorimetric substrate (10 mM Ac-DEVD-*p*NA in dimethyl sulfoxide) were mixed. Samples were incubated at 37°C, and the absorbance at 405 nm was measured in an enzyme-linked immunosorbent assay reader every 5 minutes. One unit enzyme activity is defined as μmol Ac-DEVD-*p*NA cleaved per minute. Caspase-8–like activity was measured in BJAB cells using Ac-IETD-*p*NA as substrate.

Immunoprecipitation of caspase-3

Caspase-3 was immunoprecipitated from cellular extracts of BJAB cells essentially as described elsewhere.[32] Briefly, 100 μL cellular extract was incubated with 0.5 mg protein A–Sepharose and 20 μL antihuman caspase-3 antibody at 4°C for 4 hours and moderately shaken. The protein A–Sepharose immune complex was sedimented by centrifugation at 300*g*, 4°C for 5 minutes, and the supernatant was used for in vitro activation by the addition of dATP and cytochrome c as described above. In addition, 100 μL control extract was incubated in the presence of protein A–Sepharose and the absence of antihuman caspase-3 antibody.

Measurement of the mitochondrial permeability transition

After incubation with the respective cytostatic drugs, cells were collected by centrifugation at 300*g*, 4°C for 5 minutes. Mitochondrial permeability transition was then determined by staining the cells with 5,5′,6,6′-tetrachloro-1,1′,3,3′-tetraethyl-benzimidazolylcarbocyanin iodide (JC-1; Molecular Probes, Leiden, The Netherlands) as described.[33,34] 1×10^5 cells were resuspended in 500 μL phenol red-free RPMI 1640 without supplements, and JC-1 was added to give a final concentration of 2.5 μg/mL. The cells were incubated for 30 minutes at 37°C and moderately shaken. Control cells were incubated in the absence of JC-1 dye. The cells were harvested by centrifugation at 300*g,* 4°C for 5 minutes, washed with ice-cold PBS, and resuspended in 200 μL PBS at 4°C. Mitochondrial permeability transition was then quantified by flow cytometric determination of cells with decreased fluorescence—that is, with mitochondria displaying a lower membrane potential. Data were collected and analyzed using a FACScan (Becton Dickinson) equipped with the CELLQuest software. Data are given in percentage cells with low $\Delta\Psi$m, which reflects the number of apoptotic cells.

Results

Anticancer drugs induce apoptosis and caspase-8 activation in CD95/Fas-sensitive and -resistant B-lymphoid cells

To investigate B cell apoptosis induced by anticancer drugs, BJAB cells were treated with 0.1 μg/mL Taxol or 1.0 μg/mL epirubicin for 24 hours, 48 hours, and 72 hours. Apoptosis was determined by flow cytometry using a modified cell cycle assay and measurement of hypodiploid DNA. These experiments revealed that not only BJAB cells (Figure 1A) but also immature B cells, namely NALM-6 (Figure 1B) and REH cells (Figure 1C), and primary B-ALL cells (Table 1) displayed significant DNA fragmentation after treatment with the cytotoxic drugs. To verify that the cells underwent apoptotic cell death, the cleavage of 2 known caspase substrates, poly-(ADP-ribose)polymerase and GDP dissociation inhibitor (D4-GDI),[27] was investigated by Western blot analysis. Cleavage of these proteins occurred in a time-dependent manner corresponding to the results obtained by flow cytometric analysis. Cleavage was detected as early as 24 hours after treatment and

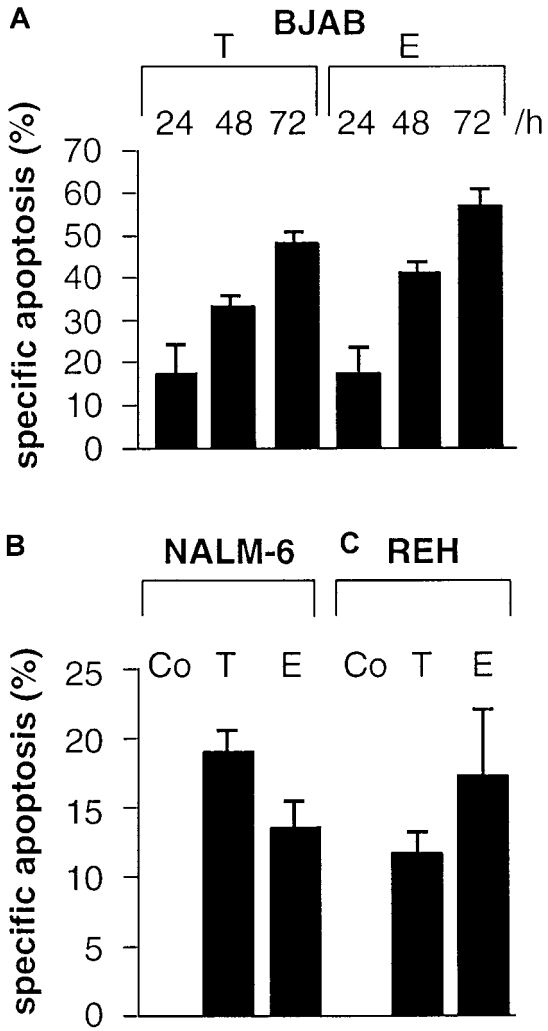

Figure 1. Taxol and epirubicin time-dependently induce DNA fragmentation in B-lymphoid cells. Cells were treated with control medium (Co), 0.1 μg/mL Taxol (T), or 1 μg/mL epirubicin (E). DNA fragmentation was measured in drug-treated BJAB cells (A) after the indicated time, in NALM-6 cells (B) after 48 hours, and in REH cells (C) after 48 hours as described in "Materials and methods." Values are given as percentage of specific apoptosis ± SD (n = 3).

Table 1. Blocking experiments with anti-CD95-Fas-F(ab)$_2$ fragments in primary B-lineage ALL cells

	B-lineage ALL (% apoptosis)				
Patient	1	2	3	4	5
Medium control	35.1 ± 5.8	54.8 ± 5.3	23.9 ± 3.1	44.2 ± 3.7	38.5 ± 4.2
Epirubicin	99.1 ± 9.9	98.1 ± 9.8	92.2 ± 7.2	97.5 ± 4.1	62.3 ± 6.9
Epirubicin + control F(ab)$_2$	99.1 ± 2.9	99.2 ± 6.2	95.6 ± 6.9	98.7 ± 4.7	68.4 ± 7.4
Epirubicin + anti-CD95 F(ab)$_2$	99.3 ± 5.7	95.4 ± 7.9	98.6 ± 8.1	94.7 ± 3	65.4 ± 4.1

B-lineage ALL cells were cultured for 48 hours in the presence or absence of epirubicin (0.1 μg/mL). F(ab)$_2$ fragments were added at 1 μg/mL. Apoptosis was measured on the single-cell level by assessing the nuclear DNA content. Each experiment was performed in triplicate. Mean values for the percentage of apoptotic cells ± SD (n = 3) are shown for 5 patients with childhood B-lineage ALL.

reached a maximum after 48 hours (data not shown). To further examine apoptosis signaling pathways in B cells, we determined drug-induced processing and activation of caspase-3 in our experimental systems. As shown in Figure 2A, the immunoreactive 17-kd active subunit of caspase-3 was detected in BJAB cells as early as 24 hours after treatment and persisted for 72 hours. Furthermore, the appearance of the 17-kd subunit of caspase-3 was observed in drug-treated NALM-6 (Figure 2B, upper panel), REH (Figure 2C, upper panel), and primary B ALL cells (Figure 2D, upper panel) after 48 hours.

We also detected caspase-8 processing in all B-lineage cells tested in this study (Figure 2A-C, lower panel). Interestingly, prolonged incubation of primary childhood B-lineage ALL blasts for 48 hours in the presence of epirubicin led to complete processing of procaspase-8, as evidenced by the disappearance of the proenzyme (Figure 2D, lower panel). However, more detailed time-course experiments in BJAB cells revealed that caspase-8 cleavage was delayed compared with that of caspase-3. Whereas the 17-kd active subunit of caspase-3 was already observed after 24 hours of Taxol and epirubicin treatment (Figure 3A), caspase-8 processing and detection of the 18-kd active subunit of caspase-8 was only marginal at this time point (Figure 3B). After 6 hours and 10 hours of drug treatment, we could not detect any processing of caspase-3 (Figure 3A) or caspase-8 (Figure 3B). To further substantiate these data, caspase-3–like and caspase-8–like activities were measured in Taxol- and epirubicin-treated BJAB cells. Again, Taxol- and epirubicin-induced caspase-3–like activity preceded caspase-8–like activity. After 24 hours of treatment with both drugs, caspase-3–like activity was enhanced 4 times compared with control cells (Figure 4A). On the other hand, no significant increase of caspase-8 activity was observed at time points up to 24 hours

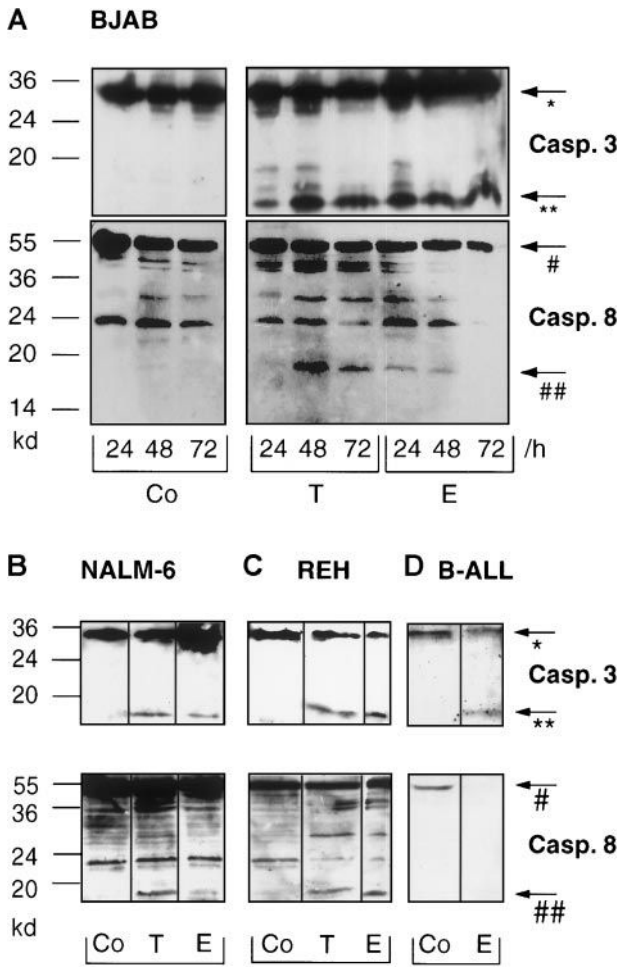

Figure 2. Taxol and epirubicin induce processing of caspase-3 and caspase-8 in different B-lymphoid cell lines and in primary B-lineage ALL cells. BJAB cells (A) were cultured in control medium (Co), 0.1 μg/mL Taxol (T), or 1 μg/mL epirubicin (E) for different time intervals as indicated. NALM-6 (B), REH (C), and primary B-ALL cells (D) were treated with control medium (Co), 0.1 μg/mL Taxol (T), or 1 μg/mL epirubicin (E) for 48 hours. Western blot analyses were performed as described in "Materials and methods" with antihuman caspase-3 and antihuman caspase-8 antibodies. Positions of molecular mass markers are indicated at the left. Arrows indicate the positions of procaspase-3 (*), the 17-kd active subunit of caspase-3 (**), procaspase-8 (#), and the 18-kd active subunit of caspase-8 (##). Experiments were repeated twice and yielded similar results.

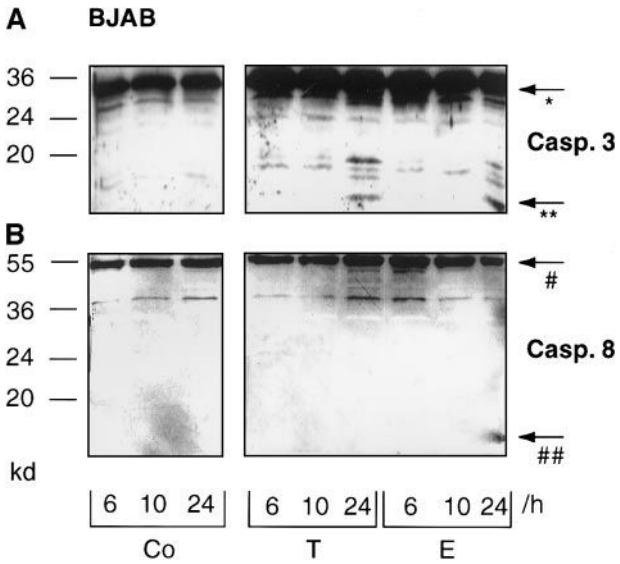

Figure 3. Time-course of Taxol- and epirubicin-induced processing of caspase-3 and caspase-8 in BJAB cells. BJAB cells were cultured in control medium (Co), 0.1 μg/mL Taxol (T), or 1 μg/mL epirubicin (E) for different time intervals as indicated. Western blot analyses were performed as described in "Materials and methods" with antihuman caspase-3 (A) and antihuman caspase-8 antibodies (B). Positions of the molecular mass markers are indicated at the left. Arrows indicate the positions of procaspase-3 (*), the 17-kd active subunit of caspase-3 (**), procaspase-8 (#), and the 18-kd active subunit of caspase-8 (##). Experiments were repeated twice and yielded similar results.

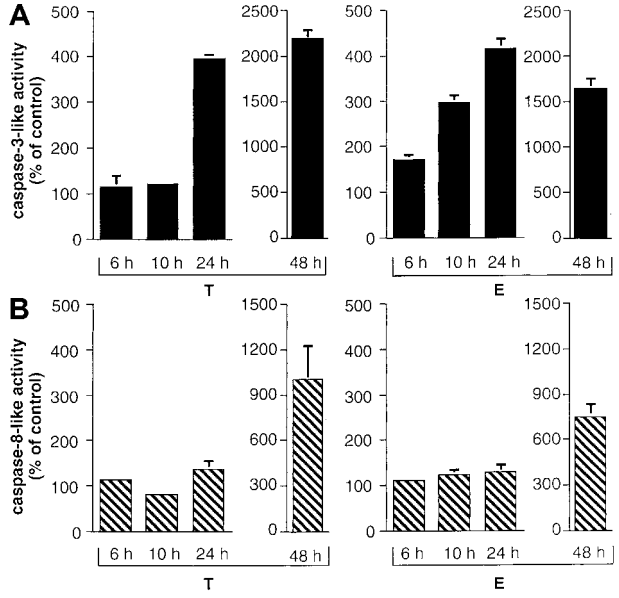

Figure 4. Time-course of Taxol- and epirubicin-induced caspase-3– and caspase-8–like activity in BJAB cells. BJAB cells were cultured in control medium, 0.1 μg/mL Taxol (T), or 1 μg/mL epirubicin (E) for different time intervals as indicated. Caspase-3–like activity was determined as described in "Materials and methods" using Ac-DEVD-*p*NA (A). Caspase-8–like activity was assessed in parallel using Ac-IETD-*p*NA (B). Caspase-3– and caspase-8–like activities are given as percentage of control ± SD (n = 3).

(Figure 4B). At a later time point, however, the processing of procaspase-8 and the appearance of the 18-kd active subunit of caspase-8 coincided with an elevation of caspase-8–like enzyme activity in drug-treated BJAB cells. After 48 hours of incubation, the measurement of Ac-IETD-*p*NA cleavage showed 7.9-fold and 10.2-fold increases in caspase-8–like activity in epirubicin- and Taxol-treated BJAB cells, respectively (Figure 4B). A significant increase in caspase-8–like activity was also measured after the treatment of NALM-6 and REH cells with epirubicin and Taxol (data not shown).

Drug-induced apoptosis in B-lineage leukemia is independent of CD95 ligand and CD95 death-inducing signaling complex

In previous studies, it has been demonstrated that cytotoxic drugs strongly stimulate CD95 ligand messenger RNA expression in human leukemia T-cell lines.[11] To test whether CD95 ligand expression in B-lineage leukemia cells after challenge with epirubicin correlates with the activation of caspase-8, we performed Northern blot analyses for CD95 ligand expression and blocking experiments to assess the requirement of CD95/Fas–CD95 ligand interaction in our system. As already shown above, the onset of the apoptotic program after treatment with epirubicin takes at least 24 hours, and no evidence for induction of the initiator caspase-8 at earlier time points could be found. Nevertheless, we performed control experiments to check the time frame of epirubicin-induced CD95 ligand expression, and significant levels of CD95 ligand mRNA were detected in primary leukemic T-lineage ALL cells after 24 hours of incubation with this drug (data not shown). In clear contrast, Northern blot analyses revealed that neither primary leukemic cell samples of patients with childhood B-lineage ALL (Figure 5A) nor BJAB (Figure 5B) and REH cells (Figure 5C) expressed significant levels of CD95 ligand mRNA after drug exposure. However, using cross-linking of Jurkat T cells by anti-CD3 as an additional control, we could clearly demonstrate CD95 ligand mRNA expression (Figure 5D).

In another set of experiments, we used anti-CD95/Fas $F(ab)_2$ fragments to block CD95 ligand–CD95 receptor interaction. In accordance with the lack of CD95 ligand expression, epirubicin-induced apoptosis of BJAB (Figure 6A) and REH cells (Figure 6B) was not influenced by neutralizing anti-CD95 antibody $F(ab)_2$ fragments. The same was true for primary B-lineage ALL cells, which also showed epirubicin-induced DNA fragmentation that could not be inhibited by neutralizing anti-CD95 antibody $F(ab)_2$ fragments (Table 1). As a positive control for these blocking experiments, again Jurkat T cells were treated with immobilized anti-CD3 monoclonal antibody OKT3 to trigger activation-induced cell death (see also the control experiment shown in Figure 5D). In this experimental setup, anti-CD3–triggered cell death was inhibited in a concentration-dependent manner by the addition of anti-CD95 $F(ab)_2$ fragments (Figure 6C), thereby confirming that this approach allows discrimination between CD95-dependent and

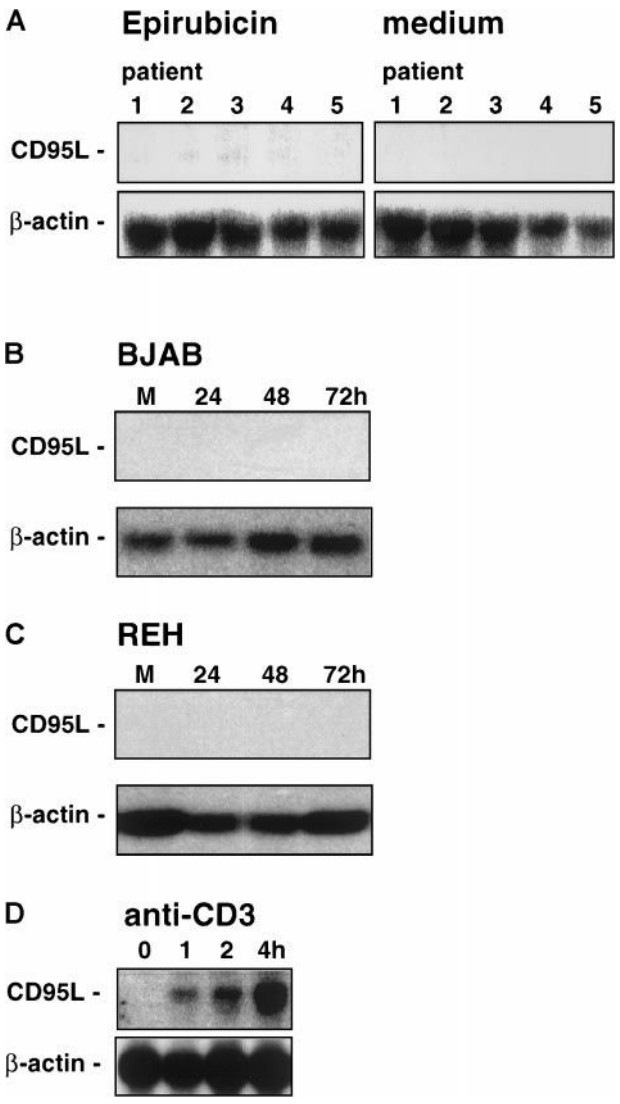

Figure 5. Northern blot analysis of CD95/Fas ligand expression in epirubicin-induced cells. Leukemic cell samples of 5 patients (the same as in Table 1) with childhood B-lineage ALL (A) were induced for 24 hours in the presence of epirubicin (0.1 μg/mL) or medium alone. BJAB (B) or REH cells (C) were induced for 24 to 72 hours in the presence of epirubicin. M, medium control at 72 hours. (D) As a positive control for the induction of CD95/Fas ligand expression, Jurkat T cells were cultured in the presence of plastic-immobilized anti-CD3 monoclonal antibody OKT3 for 0, 1, 2, or 4 hours. To control for equal amounts and the integrity of the RNA, the blots were rehybridized with a cDNA probe for β-actin.

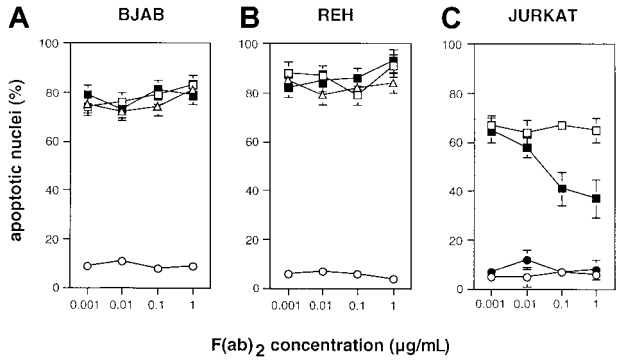

Figure 6. Effects of blocking of CD95 ligand–CD95 receptor interaction. BJAB (A) or REH (B) B cells were induced for apoptosis by epirubicin (0.1 μg/mL) in the presence or absence of neutralizing anti-CD95/Fas or control $F(ab)_2$ fragments. Open circles, medium control; open triangles, epirubicin; open squares, epirubicin plus control $F(ab)_2$; filled squares, epirubicin plus anti-CD95/Fas $F(ab)_2$ fragments. Jurkat T-cells (C) were induced for apoptosis for 24 hours in the presence (squares) or absence (circles) of immobilized anti-CD3 as described.[19] Control (open circles, open squares) or anti-CD95/Fas $F(ab)_2$ fragments (filled circles, filled squares) were present in the cultures at 1 μg/mL. Apoptosis was measured at the single cell level by assessing the nuclear DNA content as described in "Materials and methods." Mean values for the percentage of apoptotic cells ± SD (n = 3) are shown.

CD95-independent signaling pathways. Thus, epirubicin-induced apoptosis in B lymphoid cells is not functionally linked to CD95 ligand–CD95 receptor interaction.

Processing of caspase-8 occurs independently of CD95 signaling in BJAB cells

As shown above, drug-induced apoptosis in B cells was not accompanied by the expression of CD95 ligand mRNA and occurred independently of CD95 ligand–CD95 receptor interaction. Nevertheless, the induction of apoptosis in these cells also led to the cleavage of caspase-8. To further exclude an involvement of the CD95 or other death receptor systems, we used BJAB cells overexpressing a dominant-negative FADD mutant (FADDdn). Both mock and FADDdn transfectants express endogenous FADD (27 kd), whereas the FADDdn transfectants also show a lower band representing the truncated FADDdn (see Figure 7A). This FADD mutant blocks CD95-induced apoptosis[22] and completely prevents caspase-3 activation upon triggering of the BJAB transfectants with agonistic anti-CD95 antibodies.[35] In our hands, BJAB/FADDdn cells were completely resistant to treatment with 1 μg/mL agonistic anti-CD95 antibody, whereas approximately 70% of the control vector-transfected BJAB/mock cells were killed under the same conditions (Figure 7B), thereby demonstrating the efficacy of FADDdn in this cell line. However, in accordance with the hypothesis that drug-induced caspase-8 processing in BJAB cells is independent of CD95 signaling, the active 18-kd subunit of caspase-8 was detected in BJAB/FADDdn cells after challenge with Taxol and epirubicin (Figure 8B). The cleavage of caspase-8 in these cells coincided with the appearance of the 17-kd active subunit of caspase-3 (Figure 8A). CD95-independent apoptosis

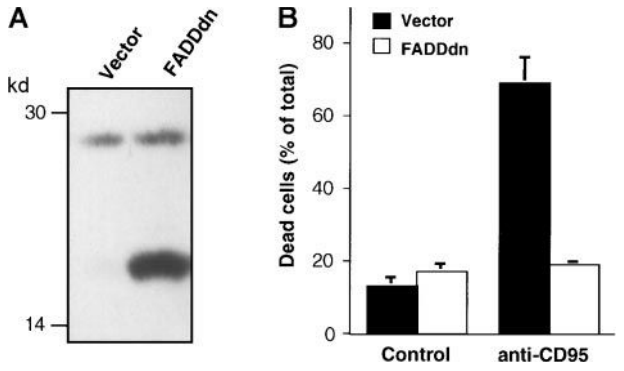

Figure 7. BJAB cells overexpressing a dominant-negative FADD mutant (FADDdn) are resistant to CD95-mediated apoptosis. (A) Expression of FADDdn. Lysates of vector-transfected BJAB cells and BJAB cells stably expressing FADDdn were subjected to immunoblotting using a monoclonal anti-FADD antibody. The positions of molecular mass markers are indicated at the left. (B) Apoptosis induction. BJAB vector control or FADDdn-expressing cells were either left untreated (Control) or were stimulated for 30 hours with 1 μg/mL anti-CD95 antibody. Then cell death was assessed by the uptake of propidium iodide and flow cytometry as described in "Materials and methods." Values are given as percentage of dead cells ± SD (n = 3).

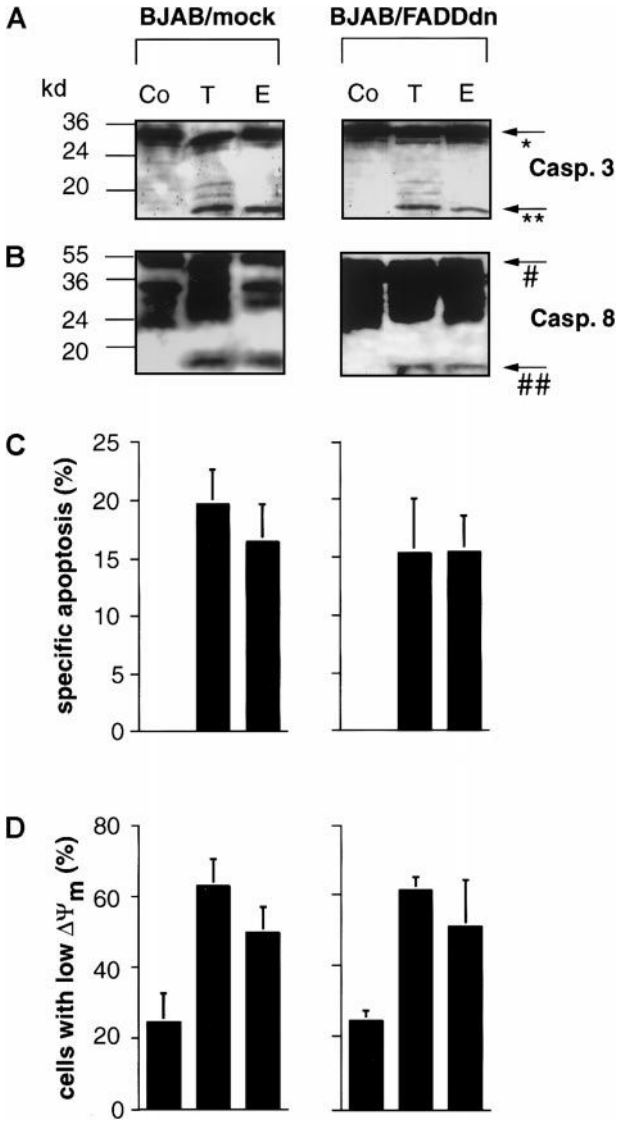

Figure 8. Overexpression of dominant-negative FADD in BJAB cells does not impair drug-induced processing of caspase-3, caspase-8, DNA fragmentation, and mitochondrial activation. Mock- or dominant-negative FADD (FADDdn)-transfected BJAB cells were either left untreated (Co) or were incubated with 0.1 μg/mL Taxol (T) or 1 μg/mL epirubicin (E) for 48 hours. Then Western blot analyses were performed with antihuman caspase-3 (A) and antihuman caspase-8 antibodies (B). Positions of molecular mass markers are indicated at the left. Arrows indicate the positions of procaspase-3 (*), the 17-kd active subunit of caspase-3 (**), procaspase-8 (#), and the 18-kd active subunit of caspase-8 (##). The experiments were repeated and yielded similar results. Additionally, DNA fragmentation (C) and mitochondrial permeability transition (D) in drug-treated BJAB cells were measured as described in "Materials and methods." Values are given as percentage of specific apoptosis ± SD (n = 3) and as percentage of cells with low $\Delta\Psi m$ ± SD (n = 3), respectively.

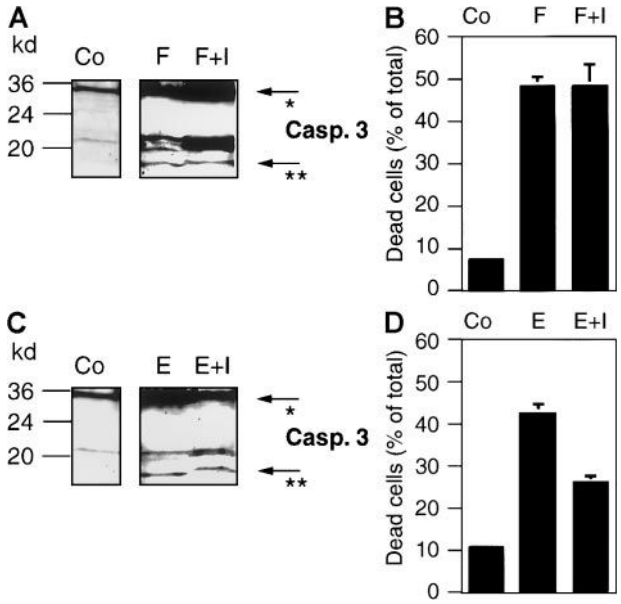

Figure 9. The caspase-3 inhibitor zDEVD-fmk does not interfere with CD95- or epirubicin-induced processing of caspase-3 in BJAB cells. BJAB cells were either incubated in control medium (Co) or stimulated with 1 μg/mL anti-CD95/Fas antibody (F) or 1 μg/mL epirubicin (E). Some cultures were preincubated with 10 μM of the caspase-3 inhibitor zDEVD-fmk (I) 2 hours before anti-CD95 or drug treatment. After 24 hours of incubation, Western blot analyses were performed with antihuman caspase-3 (A, C). The positions of molecular mass markers are indicated at the left. Arrows indicate the positions of procaspase-3 (*) and the 17-kd active subunit of caspase-3 (**). The experiments were repeated and yielded similar results. Additionally, cell death was determined in the cultures after 24 hours of anti-CD95 or epirubicin treatment by trypan blue exclusion (B, D). Values are given as percentage of dead cells ± SD (n = 3).

was further supported by the assessment of drug-induced DNA fragmentation in BJAB/FADDdn cells as compared with control vector-transfected BJAB/mock cells. As shown in Figure 8C, Taxol- and epirubicin-induced apoptosis was not significantly influenced by the overexpression of FADDdn. In recent publications, the critical role of mitochondrial damage for drug-induced apoptosis[36,37] and CD95-dependent signaling to mitochondria through caspase-8–mediated cleavage of Bid has been demonstrated.[38] We thus measured mitochondrial activation after treatment with Taxol and epirubicin in our experimental system. Treatment of BJAB/mock cells with both agents led to significant mitochondrial permeability transition and to an approximately 2.5-fold increase of cells with low $\Delta\Psi$m after 48 hours (Figure 8D). This drug-induced mitochondrial permeability transition was not influenced by the overexpression of FADDdn (Figure 8D), thereby excluding the possibility that the mitochondrial activation in BJAB cells was mediated by a CD95-dependent mechanism. Time-course experiments in BJAB/mock, BJAB/FADDdn, NALM-6, and REH cells revealed that the mitochondrial permeability transition already occurred 24 hours after the addition of epirubicin and Taxol to the culture medium and thus preceded, or at least coincided with, the processing of procaspase-8 (data not shown).

Caspase-3 triggers activation of caspase-8 in vivo and in vitro

Different death stimuli activate mitochondria, which in turn release cytochrome c. The latter triggers an apoptotic cascade through Apaf-1–caspase-9 complex formation,[9] leading to the subsequent activation of the main executioner of the apoptotic machinery, caspase-3. From the results described above, we reasoned that the processing of procaspase-8 to the active caspase-8 occurs downstream of caspase-3. To verify this hypothesis, we used zDEVD-fmk, a cell-permeable peptide-inhibitor that specifically inhibits caspase-3–like enzyme activities by irreversibly binding to the active site of caspase-3. In a control experiment, we first excluded that zDEVD-fmk interferes with upstream initiator caspases, for example, caspase-8. Indeed, this inhibitor did not inhibit CD95- or epirubicin-induced cleavage of caspase-3 (Figure 9A and C, respectively). Addition of the inhibitor to anti-CD95 antibody- and drug-treated cells led to a clear shift of the 17-kd active subunit of caspase-3 to a higher apparent molecular weight of approximately 18 kd (Figures 9A and C, 10A), indicating that the inhibitor had irreversibly bound to the enzyme. Interestingly, zDEVD-fmk only inhibited drug-induced cell-death (Figures 9D, 10C), whereas CD95-induced cell death was not influenced (Figure 9B). This might be explained by the recent finding that caspase-3 is involved in a feedback loop for the amplification of drug-induced mitochondrial cytochrome c release.[39] Furthermore, the inhibition of caspase-3–like activity by zDEVD-fmk in this experimental setting was confirmed by Western blot analysis of the cleavage of the caspase-3

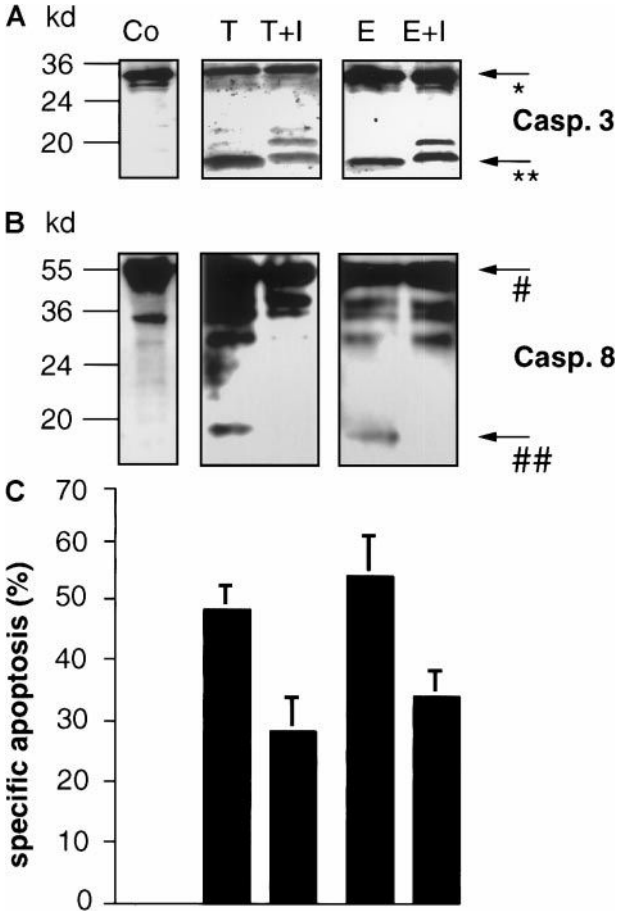

Figure 10. The caspase-3 inhibitor zDEVD-fmk blocks drug-induced processing of caspase-8 and inhibits DNA fragmentation in BJAB cells. BJAB cells were either incubated in control medium (Co) or stimulated with 0.1 μg/mL Taxol (T) or 1 μg/mL epirubicin (E). Some cultures were preincubated with 10 μM caspase-3 inhibitor zDEVD-fmk (I) 2 hours before drug treatment. After 48 hours of incubation, Western blot analyses were performed with antihuman caspase-3 (A) and antihuman caspase-8 antibodies (B). Positions of molecular mass markers are indicated at the left. Arrows indicate the positions of procaspase-3 (*), the 17-kd active subunit of caspase-3 (**), procaspase-8 (#), and the 18-kd active subunit of caspase-8 (##). The experiments were repeated and yielded similar results. Additionally, DNA fragmentation (C) was measured in the cultures after 48 hours of drug treatment. Values are given as percentage of specific apoptosis ± SD (n = 3).

substrate D4-GDI, which was completely inhibited when drug-treated cells were incubated in the presence of the peptide inhibitor (data not shown). Thus, zDEVD-fmk represents a suitable tool to investigate apoptosis-associated events located downstream of caspase-3. As shown in Figure 10B, the treatment of BJAB cells with zDEVD-fmk completely blocked Taxol- and epirubicin-induced processing of procaspase-8, and its 18-kd active cleavage product was no longer detected. This again provided evidence that drug-induced activation of caspase-8 occurred downstream of caspase-3. To further investigate the mechanism of caspase-8 processing in vitro, a cell-free system based on the activation of BJAB cytosol with cytochrome c and dATP[40] was established. As shown in Figure 11A, the addition of cytochrome c and dATP to cellular extracts led to the rapid cleavage of procaspase-3 and to the appearance of the 17-kd active cleavage product of caspase-3 after

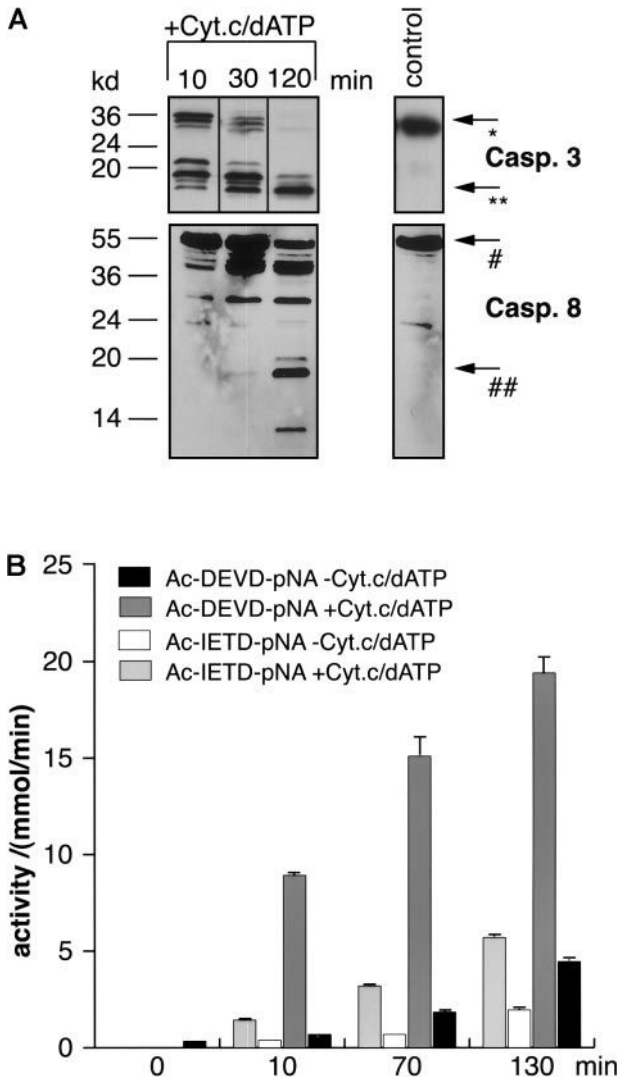

Figure 11. Time-dependent in vitro activation of caspase-8 by cytochrome c and dATP in extracts of BJAB cells. Extracts from BJAB cells were incubated for different time periods in the presence or absence of 10 μM cytochrome c and 1 mM dATP. Then Western blot analyses were performed by the use of antihuman caspase-3 (A, upper panel) or antihuman caspase-8 antibodies (A, lower panel). Positions of molecular mass markers are indicated at the left. Arrows indicate the positions of procaspase-3 (*), the 17-kd active subunit of caspase-3 (**), procaspase-8 (#), and the 18-kd active subunit of caspase-8 (##). The experiments were repeated twice and yielded similar results. Additionally, caspase-3–like or caspase-8–like activities were measured in a colorimetric assay using Ac-DEVD-*p*NA or Ac-IETD-*p*NA, respectively (B). Caspase activities are given as mmol substrate cleaved per minute ± SD (n = 3).

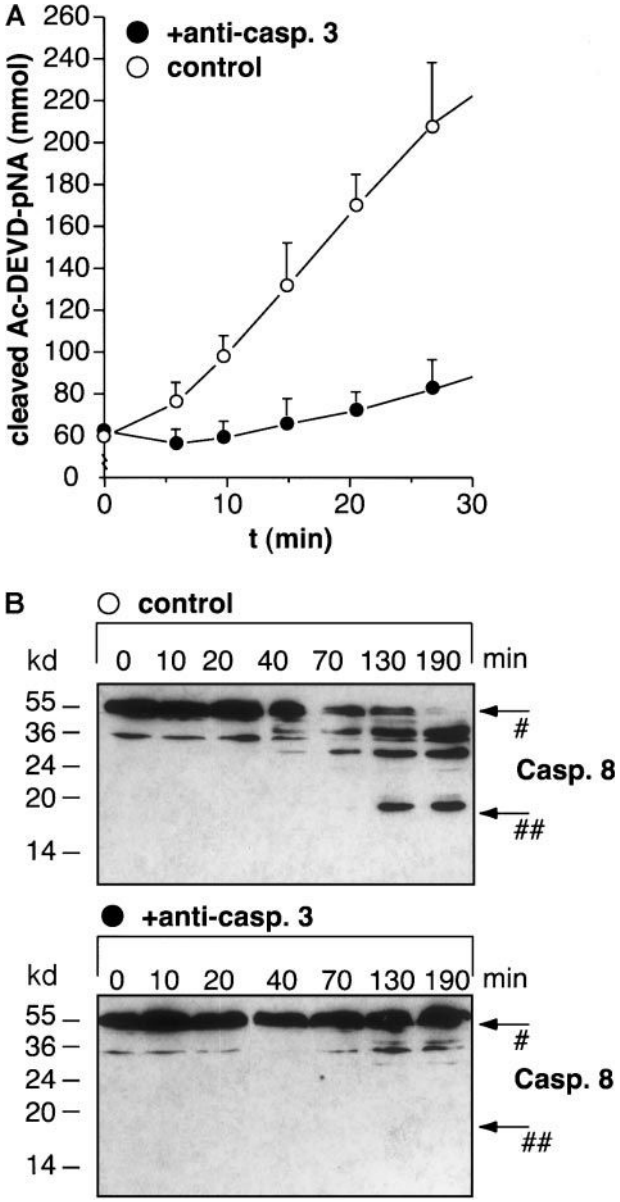

Figure 12. Immunoprecipitation of caspase-3 abolishes in vitro activation of caspase-8 by cytochrome c and dATP in BJAB cell extracts. Caspase-3 was immunoprecipitated from cellular extracts as described in "Materials and methods." After in vitro activation with 10 μM cytochrome c and 1 mM dATP for 10 minutes, cleavage of Ac-DEVD-*p*NA in control (A, open circles) and immunoprecipitated (A, filled circles) extracts was determined after the indicated times. Values are given as mmol cleaved Ac-DEVD-*p*NA ± SD (n = 3). Furthermore, control extracts (B, upper panel) and caspase-3–depleted extracts (B, lower panel) were activated with 10 μM cytochrome c and 1 mM dATP for different time points and analyzed for caspase-8 processing by Western blot analysis. Positions of molecular mass markers are indicated at the left. Arrows indicate the positions of procaspase-8 (#) and the 18-kd active subunit of caspase-8 (##). The experiments were repeated twice and yielded similar results.

10 minutes. Interestingly, processing of procaspase-8 was delayed compared with that of caspase-3, and the 18-kd active subunit of caspase-8 was detected after 120 minutes of incubation (Figure 11A, lower panel). This was verified by the measurement of caspase-3– and caspase-8–like enzyme activities using the colorimetric peptide substrates Ac-DEVD-*p*NA and Ac-IETD-*p*NA, respectively. Again, the activation of caspase-3 preceded the activation of caspase-8 (Figure 11B). This was reflected by a steady increase of the caspase-8–caspase-3 ratio from 0.156 after 10

minutes to 0.215 after 70 minutes and to 0.290 after 130 minutes of incubation with cytochrome c and dATP.

To order the processing of procaspase-8 within the cytochrome c–initiated caspase cascade, we immunoprecipitated caspase-3 from BJAB cell extracts. Measurement of caspase-3–like enzyme activity in extracts that had been treated with anti–caspase-3 antibodies, followed by sedimentation of the immune complex using protein A–Sepharose, showed that 90% of the total caspase-3 activity was successfully precipitated (Figure 12A). Although caspase-8 processing was detected in control extracts after 130 and 190 minutes of incubation with cytochrome c and dATP (Figure 12B, upper panel), the processing of procaspase-8 and the appearance of the active 18-kd subunit of caspase-8 was completely blocked in caspase-3–depleted cell extracts (Figure 12B, lower panel). Thus, both the experiments in intact B cells and in the cell-free system indicate that caspase-8 activation through the mitochondrial pathway is an event occurring downstream of caspase-3 activation.

Discussion

Recently, a controversial discussion about the role of the CD95 receptor–ligand system in drug-induced apoptosis in human leukemia T-cell lines was raised, and it is still a matter of debate whether CD95-mediated signaling is functionally involved in the propagation of death signals after drug treatment. Although an involvement of CD95–CD95 ligand was originally demonstrated,[11] other groups could not confirm drug-induced CD95 ligand expression and inhibition of drug-induced apoptosis by the use of blocking anti-CD95 antibodies, and they showed CD95-independent death signaling after the exposure of malignant T cells to cytotoxic drugs.[13,14,41,42] However, Fulda et al[12] insisted that a functional CD95 ligand and CD95 death-inducing signaling complex plays an important role in activation-induced and doxorubicin-induced apoptosis in leukemic T cells. These conflicting data might in part be explained by the concept of CD95 type 1 and type 2 cells.[43] CD95-mediated apoptosis in type 1 cells is suggested to be initiated by large amounts of caspase-8 formed at the death-inducing signaling complex at the plasma membrane, whereas in type 2 cells small amounts of active caspase-8 are believed to induce the apoptogenic activity of mitochondria. However, many experiments have documented that CD95/Fas-deficient, FADD-deficient, and caspase-8–deficient cells are normally sensitive to chemotherapeutic drugs. Because all these molecules were reported to be essential for CD95-induced apoptosis in type 1 and type 2 cells, even the type 1–type 2 paradigm has recently been questioned.[44] Nevertheless, the use of different experimental approaches—for example, CD95-resistant cell clones[13] or T cells from CD95-deficient *lpr* mice,[14] might be one possible reason for these controversial results. In the current study, we investigated drug-induced death pathways in B-lymphoid cells that, unlike in T cells, have been less intensively characterized. In contrast to T cells, B-lymphoid cells did not express significant amounts of CD95 ligand after challenge with the cytotoxic drug epirubicin. Additionally, epirubicin-induced cell death was not influenced by antagonistic anti-CD95 antibodies, even at low drug concentrations. We therefore conclude that B-lymphoid cells represent a suitable model system to elaborate CD95-independent apoptosis without manipulating cells by means such as the generation of resistant cell clones or the generation of transgenic mice.

In principle, mature B cells can undergo apoptosis by signaling through CD95.[18,19,25,45,46] However, most B-lineage ALL cells are negative or only express low amounts of CD95/Fas and are constitutively resistant toward CD95-induced death but can be sensitized for this signaling pathway by pretreatment with chemotherapeutic drugs.[47] We report here that epirubicin and Taxol, 2 different kinds of drugs that target the nucleus or the cytoskeleton, respectively, are effective inducers of apoptotic cell death in B-lymphoid cell lines and in primary B-lineage tumor cells. Apoptosis and activation of distinct caspases by these drugs occurred in a CD95-independent manner, as further evidenced by the use of a dominant-negative FADD mutant (FADDdn). Overexpression of FADDdn did not influence caspase-3 or mitochondrial activation as early events nor DNA fragmentation as a late event in drug-induced apoptosis. Interestingly, we also observed processing and activation of procaspase-8 after the addition of cytotoxic drugs to the culture medium of B-lymphoid cells. In all cases, the processing of procaspase-8 was either preceded or paralleled by mitochondrial permeability transition. These results suggest that the mitochondrial apoptosome is a main player in drug-induced apoptosis of B-lymphoid cells, thereby confirming other data that point to the critical role for mitochondria in the apoptotic pathways of other cell types, such as HeLa cells[37] and malignant melanoma.[48]

Caspases with long prodomains, such as caspase-8, are generally considered to be upstream (inducer) caspases because of their ability to associate with cell surface death-receptor molecules. However, it has been shown that the addition of cytochrome c to Jurkat cell-free extracts initiates a cascade of protease activation events in vitro involving caspases-2, -3, -6, -7, -8, -9, and -10.[49] We therefore reasoned that the molecular order in our experimental system is represented by the hierarchical activation of mitochondria, caspase-3, and caspase-8. This hypothesis was further substantiated by 2 different experimental approaches: (1) the cell-permeable peptide zDEVD-fmk, which irreversibly inhibits caspase-3–like enzyme activities, blocked processing of procaspase-8 in drug-treated BJAB cells, and (2) the depletion of caspase-3 from BJAB cell extracts abrogated cytochrome c-induced processing of procaspase-8. Thus, unlike its role as an inducer caspase in death receptor-triggered apoptosis, caspase-8 appears to function as a downstream (executioner) caspase during drug-induced apoptosis.

The potential relevance of apoptosis signaling for clinical practice has recently been demonstrated in a patient with B-cell lymphoma. In this study, the protein kinase inhibitor 7-hydroxystaurosporine sensitized the lymphoma cells to the cytotoxic effects of multi-agent chemotherapy, presumably by modulating the threshold for apoptosis.[50] Our results, that the drug-induced activation of caspase-8 in B-lymphoid cells occurs independently of the CD95/Fas death-inducing signaling complex and downstream of the main executioner of the mitochondrial apoptosis signaling complex, caspase-3, provide new insights into the molecular cascade of apoptosis signaling in this important cellular system.

Acknowledgments

We thank Clarissa von Haefen and Verena Lehmann for their expert technical assistance.

References

1. Kerr J, Wyllie A, Currie A. Apoptosis: a basic biological phenomenon with wide-ranging implications in tissue kinetics. Br J Cancer. 1972;26:239-257.
2. Krammer PH, Behrmann I, Daniel P, Dhein J, Debatin KM. Regulation of apoptosis in the immune system. Curr Opin Immunol. 1994;6:279-289.
3. Ellis RE, Yuan JY, Horvitz HR. Mechanisms and functions of cell death. Annu Rev Cell Biol. 1991; 7:663-698.
4. Thornberry NA, Lazebnik Y. Caspases: enemies within. Science. 1998;281:1312-1316.
5. Findley HW, Gu L, Yeager AM, Zhou M. Expression and regulation of Bcl-2, Bcl-xl, and Bax correlate with p53 status and sensitivity to apoptosis in childhood acute lymphoblastic leukemia. Blood. 1997;89:2986-2993.
6. Hannun YA. Apoptosis and the dilemma of cancer chemotherapy. Blood. 1997;89:1845-1853.
7. Boldin MP, Goncharov TM, Goltsev YV, Wallach D. Involvement of MACH, a novel MORT1/FADD-interacting protease, in Fas/APO-1- and TNF receptor-induced cell death. Cell. 1996;85:803-815.
8. Muzio M, Chinnaiyan AM, Kischkel FC, et al. FLICE, a novel FADD-homologous ICE/CED-3-like protease, is recruited to the CD95 (Fas/APO-1) death-inducing signaling complex. Cell. 1996;85:817-827.
9. Li P, Nijhawan D, Budihardjo I, et al. Cytochrome c and dATP-dependent formation of Apaf-1/caspase-9 complex initiates an apoptotic protease cascade. Cell. 1997;91:479-489.
10. Nakagawa T, Zhu H, Morishima N, et al. Caspase-12 mediates endoplasmic-reticulum-specific apoptosis and cytotoxicity by amyloid-beta. Nature. 2000;403:98-103.
11. Friesen C, Herr I, Krammer PH, Debatin KM. Involvement of the CD95 (APO-1/FAS) receptor/Ligand system in drug-induced apoptosis in leukemia cells. Nat Med. 1996;2:574-577.
12. Fulda S, Strauss G, Meyer E, Debatin KM. Functional CD95 ligand and CD95 death-inducing signaling complex in activation-induced cell death and doxorubicin-induced apoptosis in leukemic T cells. Blood. 2000;95:301-308.
13. Wesselborg S, Engels IH, Rossmann E, Los M, Schulze-Osthoff K. Anticancer drugs induce caspase-8/FLICE activation and apoptosis in the absence of CD95 receptor/Ligand interaction. Blood. 1999;93:3053-3063.
14. Newton K, Strasser A. Ionizing radiation and chemotherapeutic drugs induce apoptosis in lymphocytes in the absence of Fas or FADD/MORT1 signaling: implications for cancer therapy. J Exp Med. 2000;191:195-200.
15. Strasser A, Harris AW, Huang DC, Krammer PH, Cory S. Bcl-2 and Fas/APO-1 regulate distinct pathways to lymphocyte apoptosis. EMBO J. 1995;14:6136-6147.
16. Newton K, Harris AW, Bath ML, Smith KGC, Strasser A. A dominant interfering mutant of FADD/MORT1 enhances deletion of autoreactive thymocytes and inhibits proliferation of mature T lymphocytes. EMBO J. 1998;17:706-718.
17. Varfolomeev EE, Schuchmann M, Luria V, et al. Targeted disruption of the mouse caspase 8 gene ablates cell death induction by the TNF receptors, Fas/Apo1, and DR3 and is lethal prenatally. Immunity. 1998;9:267-276.
18. Tsubata T. Apotosis of mature B cells. Int Rev Immunol. 1999;18:347-365.
19. Daniel PT, Oettinger U, Mapara MY, Bommert K, Bargou R, Dörken B. Activation and activation-induced death of human tonsillar B cells and Burkitt lymphoma cells: lack of CD95 (Fas/APO-1) ligand expression and function. Eur J Immunol. 1997;27:1029-1034.
20. Bouchon A, Krammer PH, Walczak H. Critical role for mitochondria in B cell receptor-mediated apoptosis. Eur J Immunol. 2000;30:69-77.
21. Sorger PK, Dobles M, Tournebize R, Hyman AA. Coupling cell division and cell death to microtubule dynamics. Curr Opin Cell Biol. 1997;9:807-814.
22. Bantel H, Engels IH, Voelter W, Schulze-Osthoff K, Wesselborg S. Mistletoe lectin activates caspase-8/FLICE independently of death receptor signaling and enhances anticancer drug-induced apoptosis. Cancer Res. 1999;59:2083-2090.
23. Prokop A, Wieder T, Sturm I, et al. Relapse in childhood acute lymphoblastic leukemia is associated with a decrease of the Bax/Bcl-2-ratio and loss of spontaneous caspase-3 processing in vivo. Leukemia. 2000;14:1606-1613.
24. Béné MC, Castoldi G, Knapp W, et al. Proposals for the immunological classification of acute leukemias: European Group for the Immunological Characterization of Leukemias (EGIL). Leukemia. 1995;9:1783-1786.
25. Dhein J, Daniel PT, Trauth BC, Oehm A, Moller P, Krammer PH. Induction of apoptosis by monoclonal antibody anti–APO-1 class switch variants is dependent on cross-linking of APO-1 cell surface antigens. J Immunol. 1992;149:3166-3173.
26. Wieder T, Perlitz C, Wieprecht M, Huang RT, Geilen CC, Orfanos CE. Two new sphingomyelin analogues inhibit phosphatidylcholine biosynthesis by decreasing membrane-bound CTP: phosphocholine cytidylyltransferase levels in HaCaT cells. Biochem J. 1995;311:873-879.
27. Essmann F, Wieder T, Otto A, Müller EC, Dörken B, Daniel PT. GDP dissociation inhibitor D4-GDI (Rho-GDI 2), but not the homologous Rho-GDI 1, is cleaved by caspase-3 during drug-induced apoptosis. Biochem J. 2000;346:777-783.
28. Smith PK, Krohn RI, Hermanson GT, et al. Measurement of protein using bicinchoninic acid. Anal Biochem. 1985;150:76-85.
29. Laemmli UK. Cleavage of structural proteins during the assembly of the head of bacteriophage T4. Nature. 1970;227:680-685.
30. Wieder T, Geilen CC, Wieprecht M, Becker A, Orfanos CE. Identification of a putative membrane-interacting domain of CTP: phosphocholine cytidylyltransferase from rat liver. FEBS Lett. 1994; 345:207-210.
31. Zhou Q, Snipas S, Orth K, Muzio M, Dixit VM, Salvesen GS. Target protease specificity of the viral serpin CrmA: analysis of five caspases. J Biol Chem. 1997;272:7797-7800.
32. Geilen CC, Bektas M, Wieder T, Kodelja V, Goerdt S, Orfanos CE. 1α,25-dihydroxyvitamin D3 induces sphingomyelin hydrolysis in HaCaT cells via tumor necrosis factor alpha. J Biol Chem. 1997;272:8997-9001.
33. Lambert IH, Hoffmann EK, Jorgensen F. Membrane potential, anion and cation conductances in Ehrlich ascites tumor cells. J Membr Biol. 1989; 111:113-131.
34. Reers M, Smiley ST, Mottola-Hartshorn C, Chen A, Lin M, Chen LB. Mitochondrial membrane potential monitored by JC-1 dye. Methods Enzymol. 1995;260:406-417.
35. Chinnaiyan AM, Tepper CG, Seldin MF, et al. FADD/MORT1 is a common mediator of CD95 (Fas/APO-1) and tumor necrosis factor receptor-induced apoptosis. J Biol Chem. 1996;271:4961-4965.
36. Fulda S, Susin SA, Kroemer G, Debatin KM. Molecular ordering of apoptosis induced by anticancer drugs in neuroblastoma cells. Cancer Res. 1998;58:4453-4460.
37. Melendez-Zajgla J, Cruz E, Maldonado V, Espinoza AM. Mitochondrial changes during the apoptotic process of HeLa cells exposed to cisplatin. Biochem Mol Biol Int. 1999;47:765-771.
38. Li H, Zhu H, Xu CJ, Yuan J. Cleavage of BID by caspase 8 mediates the mitochondrial damage in the Fas pathway of apoptosis. Cell. 1998;94:491-501.
39. Slee EA, Keogh SA, Martin SJ. Cleavage of BID during cytotoxic drug and UV radiation-induced apoptosis occurs downstream of the point of Bcl-2 action and is catalysed by caspase-3: a potential feedback loop for amplification of apoptosis-associated mitochondrial cytochrome c release. Cell Death Differ. 2000;7:556-565.
40. Liu X, Kim CN, Yang J, Jemmerson R, Wang X. Induction of apoptotic program in cell-free extracts: requirement for dATP and cytochrome c. Cell. 1996;86:147-157.
41. Eischen CM, Kottke TJ, Martins LM, et al. Comparison of apoptosis in wild-type and Fas-resistant cells: chemotherapy-induced apoptosis is not dependent on Fas/Fas ligand interactions. Blood. 1997;90:935-943.
42. Cuvillier O, Mayhew E, Janoff AS, Spiegel S. Liposomal ET-18-OCH(3) induces cytochrome c-mediated apoptosis independently of CD95 (APO-1/Fas) signaling. Blood. 1999;94:3583-3592.
43. Scaffidi C, Schmitz I, Zha J, Korsmeyer SJ, Krammer PH, Peter ME. Differential modulation of apoptosis sensitivity in CD95 type I and type II cells. J Biol Chem. 1999;274:22532-22538.
44. Huang DC, Hahne M, Schroeter M, et al. Activation of Fas by FasL induces apoptosis by a mechanism that cannot be blocked by Bcl-2 or Bcl-x(L). Proc Natl Acad Sci U S A. 1999;96: 14871-14876.
45. Daniel PT, Krammer PH. Activation induces sensitivity toward APO-1 (CD95)-mediated apoptosis in human B cells. J Immunol. 1994;152:5624-5632.
46. Lagresle C, Bella C, Daniel PT, Krammer PH, Defrance T. Regulation of germinal center B cell differentiation: role of the human APO-1/Fas (CD95) molecule. J Immunol. 1995;154:5746-5756.
47. Posovszky C, Friesen C, Herr I, Debatin KM. Chemotherapeutic drugs sensitize pre-B ALL cells for CD95- and cytotoxic T-lymphocyte-mediated apoptosis. Leukemia. 1999;13:400-409.
48. Raisova M, Bektas M, Wieder T, et al. Resistance to CD95/Fas-induced and ceramide-mediated apoptosis of human melanoma cells is caused by a defective mitochondrial cytochrome c release. FEBS Lett. 2000;473:27-32.
49. Slee EA, Harte MT, Kluck RM, et al. Ordering the cytochrome c-initiated caspase cascade: hierarchical activation of caspases-2, -3, -6, -7, -8, and -10 in a caspase-9–dependent manner. J Cell Biol. 1999;144:281-292.
50. Wilson WH, Sorbara L, Figg WD, et al. Modulation of clinical drug resistance in a B cell lymphoma patient by the protein kinase inhibitor 7-hydroxystaurosporine: presentation of a novel therapeutic paradigm. Clin Cancer Res. 2000;6: 415-421.

Oncogene (2003) 22, 2236–2247

www.nature.com/onc

Paclitaxel-induced apoptosis in BJAB cells proceeds via a death receptor-independent, caspases-3/-8-driven mitochondrial amplification loop

Clarissa von Haefen[1,3], Thomas Wieder[1,3], Frank Essmann[1,3], Klaus Schulze-Osthoff[2], Bernd Dörken[1] and Peter T Daniel[1]

[1]*Department of Hematology, Oncology and Tumor Immunology, University Medical Center Charité, Campus Berlin-Buch, Humboldt University of Berlin, Germany;* [2]*Institute for Molecular Medicine, University of Düsseldorf, Germany*

Caspase-8 is a key effector of death-receptor-triggered apoptosis. In a previous study, we demonstrated, however, that caspase-8 can also be activated in a death receptor-independent manner via the mitochondrial apoptosis pathway, downstream of caspase-3. Here, we show that caspases-3 and -8 mediate a mitochondrial amplification loop that is required for the optimal release of cytochrome *c*, mitochondrial permeability shift transition, and cell death during apoptosis induced by treatment with the microtubule-damaging agent paclitaxel (Taxol). In contrast, Smac release from mitochondria followed a different pattern, and therefore seems to be regulated independently from cytochrome *c* release. Taxol-induced cell death was inhibited by the use of synthetic, cell-permeable caspase-3- (zDEVD-fmk) or caspase-8-specific (zIETD-fmk) inhibitors. Apoptosis signaling was not affected by a dominant-negative FADD mutant (FADD-DN), thereby excluding a role of death receptor signaling in the amplification loop and drug-induced apoptosis. The inhibitor experiments were corroborated by the use of BJAB cells overexpressing the natural serpin protease inhibitor, cytokine response modifier A. These data demonstrate that the complete activation of mitochondria, release of cytochrome *c*, and execution of drug-induced apoptosis require a mitochondrial amplification loop that depends on caspases-3 and -8 activation. In addition, this is the first report to demonstrate death receptor-independent caspase-8 autoprocessing *in vivo*.
Oncogene (2003) **22,** 2236–2247. doi:10.1038/sj.onc.1206280

Keywords: chemotherapy; apoptosis; mitochondria; amplification loop; BJAB cells; caspase-3; caspase-8; cytochrome *c*; Bcl-x_L; Taxol; paclitaxel

*Correspondence: PT Daniel, Molecular Hematology and Oncology, University Medical Center Charité, Campus Berlin-Buch, Humboldt University of Berlin, Lindenberger We.g. 80, 13125 Berlin, Germany; E-mail: pdaniel@mdc-berlin.de

[3]These authors contributed equally to the present study
Received 22 April 2002; revised 28 November 2002; accepted 28 November 2002

Introduction

Triggering of apoptotic cell death by different stimuli, such as death ligands, ionizing irradiation or chemotherapeutic drugs, leads to the activation of a family of cysteine proteases with an absolute requirement of aspartate residues at the substrate cleavage site which are thus called caspases (Nicholson, 1999). Caspases form the core of the apoptotic machinery and are involved both in initiation of receptor-mediated apoptotic signaling cascades as well as in the execution of the apoptotic program (Cohen, 1997; Thornberry and Lazebnik, 1998; Fadeel *et al*., 2000; Daniel *et al*., 2001).

Depending on the death stimulus, one of these two major pathways is activated, that is, death receptor-dependent signaling and death receptor-independent signaling via the mitochondria (Los *et al*., 1999; Daniel, 2000; Daniel *et al*., 2001). In both cases, stimulation of the death pathway leads to processing and activation of initiator caspases, for example, caspases-8 or -9, which subsequently transmit the signal to downstream effector caspases, for example, caspases-3, -6, or -7.

Interestingly, inactivation of apoptosis signaling pathways at the level of caspases might play a role in the development of cytotoxic drug resistance. Loss of caspase-3 impairs drug-induced apoptosis and reconstitution of caspase-3 reverts drug resistance in breast cancer cells with acquired drug resistance (Friedrich *et al*., 2001). We previously demonstrated that a severe disturbance of the mitochondrial apoptosis pathway occurs during relapse of childhood acute lymphoblastic leukemia (ALL). In this setting, chemoresistant relapse is associated with a decrease of the Bax/Bcl-2 ratio and a concomitant impaired caspase-3 processing (Prokop *et al*., 2000).

Caspase-8 has been shown to act as initiator caspase in the signal transduction of death receptor-triggered apoptosis, that is, by CD95/Fas, the tumor necrosis factor (TNF)-related apoptosis-inducing ligand (TRAIL) receptors, and TNF-receptor-1 (for a review, see Daniel *et al*., 2001). Furthermore, it was suggested that cytotoxic drug-induced apoptosis is mediated by a CD95/Fas-dependent mechanism in T cells (Friesen *et al*., 1999; Nomura *et al*., 2000; Fulda *et al*., 2001b).

However, other groups were not able to confirm these findings and showed CD95/Fas-independent caspase-8 activation and induction of apoptosis by different chemotherapeutics, for example, daunorubicin, doxorubicin, etoposide, mitomycin C (Wesselborg *et al*., 1999), cisplatin (Newton and Strasser, 2000), or arsenic trioxide (Kitamura *et al*., 2000). In this line, a careful analysis of drug-induced cell death in malignant B lymphoid cells demonstrated that caspase-8 activation in these cells is independent of CD95/Fas signaling and occurs downstream of caspase-3 (Wieder *et al*., 2001). In fact, re-expression of procaspase-8 sensitizes cancer cells for drug-induced apoptosis (Fulda *et al*., 2001a).

In the present study, we investigated the functional role of caspases-3 and -8 as downstream amplifiers and executioner caspases in Taxol-induced apoptosis. To this end, we used the synthetic caspase inhibitors zDEVD-fmk (caspase-3) and zIETD-fmk (caspase-8), and the serpin protease inhibitor, cytokine response modifier A (crmA), in Taxol-treated B lymphoid BJAB cells. We show in this experimental setup that activation of caspases-9, -3, and -8 is almost completely inhibited by Bcl-x_L and is therefore initiated downstream of the mitochondria. Inhibition of caspases-3 and -8 interfered, however, with mitochondrial cytochrome *c* release, permeability transition and with downstream DNA fragmentation, thereby indicating that both caspases-3 and -8 are part of a mitochondrial feedback amplification loop of apoptosis. Furthermore, we exclude an involvement of death receptor signaling pathways in this amplification loop by inhibitor experiments in BJAB cell transfectants overexpressing a dominant-negative FADD mutant (FADD-DN). Our data clearly demonstrate that Taxol-induced cytochrome *c* release, mitochondrial membrane potential breakdown, and apoptosis can be partially blocked by the caspase-3 inhibitor zDEVD-fmk and the caspase-8 inhibitor zIETD-fmk, irrespective of disrupted or functional death receptor signaling. Apart from this evidence for a functional role of caspase-8 in drug-induced apoptosis and feedback amplification, our data also suggest an autoamplification loop of caspase-8 activation since caspase-8 processing could be blocked by addition of the caspase-8 inhibitor zIETD-fmk. To date, this is the first report about a possible autoprocessing of caspase-8 *in vivo* during drug-induced apoptosis in the absence of death receptor signaling.

Results

Caspase-8 activation is independent from death receptor signaling and occurs downstream of caspase-3 in BJAB cells

Death receptor-independent activation of caspase-8 has been observed after treatment with chemotherapeutics in different cell types, for example, Jurkat T cells (Wesselborg *et al*., 1999; Engels *et al*., 2000) and malignant B lymphoid cells (Wieder *et al*., 2001). Previous reports suggested that caspase-8 is induced via a death receptor-dependent pathway during drug-induced apoptosis. To exclude involvement of death receptor signaling via FADD-mediated signals, for example, by CD95/Fas in drug-induced activation of caspase-8, we employed BJAB cells overexpressing a dominant-negative FADD mutant (FADD-DN). Apoptosis was induced by treatment of BJAB cells with the microtubule disrupting agent pacilitaxel (Taxol). First, we determined the susceptibility of these cells towards CD95/Fas-mediated apoptosis. Whereas BJAB mock cells were CD95/Fas-sensitive, the BJAB FADD-DN cells displayed complete resistance to CD95/Fas-induced caspase-3 processing (Figure 1a), mitochondrial permeability transition (Figure 1b), and cell death (Figure 1c). Figure 1d shows that the FADD-DN transfectants express both the wild-type and the truncated FADD-DN protein lacking the death effector domain (DED) required for recruitment of procaspase-8. In contrast, the mock transfectants and the Bcl-x_L transfectants (see below) only express the endogenous wild-type FADD protein at comparable levels. Dominant-negative FADD was shown previously to impair recruitment of procaspases-8 and -10 to death receptor/FADD death-inducing signaling complexes (DISC). Thus, BJAB FADD-DN cells represent a suitable cellular system to investigate mechanisms of caspase activation in a death receptor-independent setting.

To demonstrate a functional role of caspases-3 and -8 in the caspase cascade, we used zDEVD-fmk or zIETD-fmk, two peptide inhibitors specific for caspases-3 and -8, respectively. Previously, it was reported that high concentrations (100 μM) of both inhibitors may block several caspases, but that low concentrations (10 μM) are rather specific for the individual caspases (Walczak *et al*., 2000). In this line, we could show that 10 μM zIETD-fmk significantly inhibits CD95/Fas-induced apoptosis by 72%, whereas 10 μM zDEVD-fmk only had a marginal inhibitory effect of 9% (Figure 2). In accordance with these results, we previously demonstrated that zDEVD-fmk at 10 μM efficiently blocks caspase-3, while caspase-8 activity remained unaffected (Wieder *et al*., 2001). Likewise, 10–20 μM zDEVD-fmk efficiently inhibited caspase-3 activities during ceramide-induced apoptosis (von Haefen *et al*., 2002). We therefore conclude that zIETD-fmk and zDEVD-fmk are specific tools to unravel the role of caspases-8 and -3 during drug-induced cell death.

We then investigated whether activation of caspase-8 (1) occurs independently of CD95/Fas signaling, (2) is located downstream of caspase-3, and (3) is functionally involved in drug-induced apoptosis. In accordance with our previous findings (Wieder *et al*., 2001), caspase-8 activation upon Taxol treatment was not affected by the complete blocking of death receptor-induced apoptosis in BJAB cells overexpressing FADD-DN, a dominant-negative FADD mutant lacking the DED domain required for caspases-8 or -10 recruitment (Muzio *et al*., 1996; Kischkel *et al*., 2001) (Figure 3b). This formally excludes a significant role of FADD-mediated death receptor signaling in drug-induced apoptosis. Interestingly, pretreatment of BJAB mock as well as

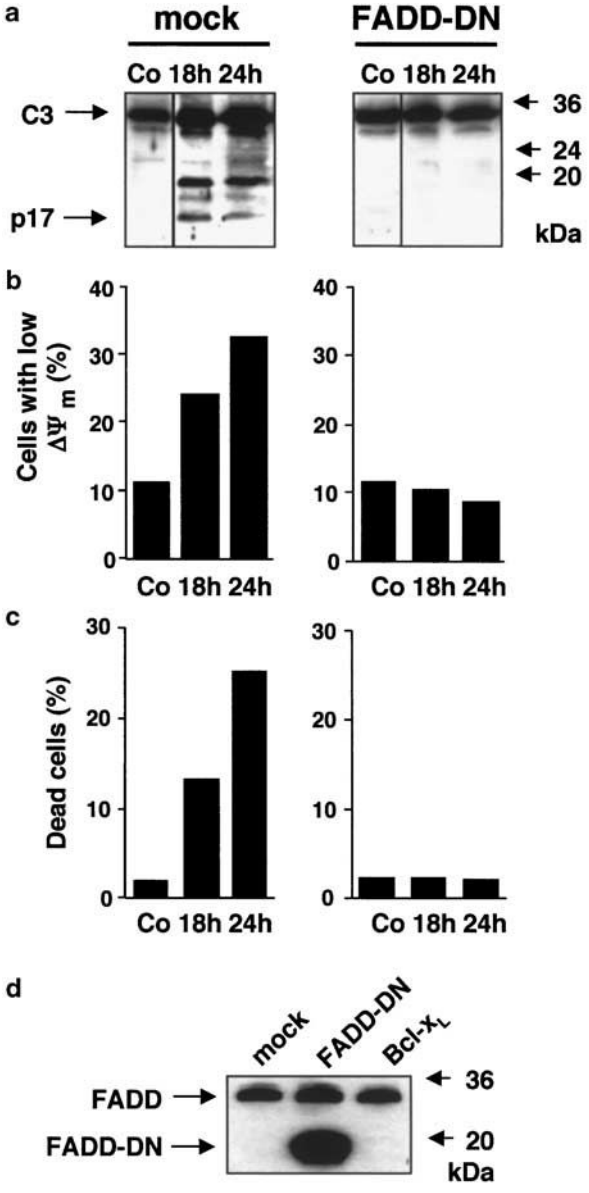

Figure 1 CD95/Fas-mediated processing of caspase-3, mitochondrial membrane permeability transition, and cell death is completely blocked in BJAB cells overexpressing a dominant-negative FADD mutant (FADD-DN). BJAB vector control (BJAB mock) or FADD-DN expressing cells (BJAB FADD-DN) were either incubated in control medium (Co) or stimulated for 18 or 24 h with 1 μg/ml anti-CD95 antibody. (**a**) Caspase-3 activation was assessed by Western blot analysis. Arrows indicate the positions of procaspase-3 (C3) and the 17 kDa active subunit of caspase-3 (p17). (**b**) Mitochondrial permeability transition was measured by staining with JC-1 as described in Materials and methods. Mean values of two determinations are given as percentage of cells with low $\Delta\Psi_m$. (**c**) Overall cell death was determined by Trypan blue exclusion. Mean values of two determinations are given as percentage of dead cells of the total cell population. (**d**) Western blot analysis for wild-type FADD and FADD-DN (lacking the death effector domain, DED) in mock, FADD-DN, and Bcl-x_L-transfected BJAB cells. The experiments were repeated twice and yielded similar results

BJAB FADD-DN cells with 10 μM of the caspase-3 inhibitor zDEVD-fmk completely blocked Taxol-induced caspase-8 processing (Figure 3a and b, respectively). This clearly indicates that Taxol-induced caspase-8 processing occurs downstream of caspase-3. However, the caspase-8 inhibitor zIETD-fmk also displayed a significant inhibitory effect on Taxol-induced caspase-8 activation in both CD95/Fas-sensitive BJAB mock cells and CD95/Fas-insensitive BJAB FADD-DN cells (Figure 3a and b, respectively). This somewhat surprising result may be explained by CD95/Fas-independent autoprocessing of caspase-8 during Taxol-induced apoptosis.

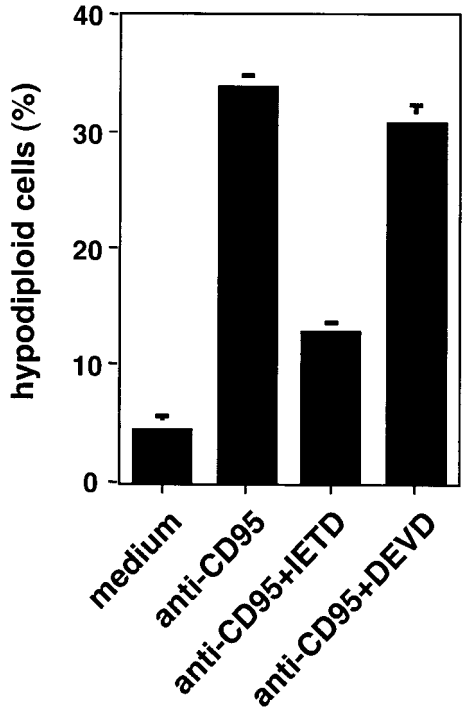

Figure 2 CD95/Fas-mediated apoptosis is inhibited by caspase-8-specific but not by caspase-3-specific inhibitors in BJAB cells. BJAB cells were either incubated in control medium (Co), medium containing 1 μg/ml anti-CD95 antibody (anti-CD95), 1 μg/ml anti-CD95 antibody plus 10 μM zIETD-fmk (anti-CD95 + IETD) or 1 μg/ml anti-CD95 antibody plus 10 μM zDEVD-fmk (anti-CD95 + DEVD) as indicated. Apoptotic DNA fragmentation was measured after 24 h of incubation by staining genomic DNA content using propidium iodide. Values are given as percentage of cells with hypodiploid DNA $\pm$ s.d. ($n = 3$)

Taxol-induced apoptosis is mediated via the mitochondrial pathway

We previously demonstrated that apoptosis induction by the anticancer drugs epirubicin and Taxol is independent from death receptor signaling (Wieder *et al*., 2001). As expected, Taxol triggers the mitochondrial pathway of apoptosis and this can be inhibited by overexpression of the antiapoptotic Bcl-x_L (Figure 4). Figure 4a shows overexpression of Bcl-x_L protein in the Bcl-x_L transfectants, while the mock transfectants and the FADD-DN transfectants only express low levels of endogenous Bcl-x_L. Overexpression of Bcl-x_L almost completely abrogated pan-caspase activation upon Taxol exposure as measured by flow cytometric staining

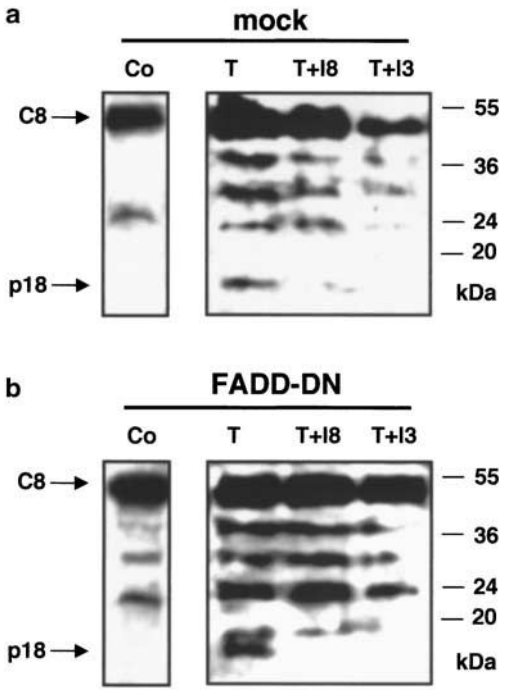

Figure 3 Taxol-induced processing of caspase-8 is independent from CD95/Fas and is abrogated by caspases-3 or -8 inhibitors. BJAB mock cells (**a**) or BJAB FADD-DN cells (**b**) were cultured for 48 h in control medium (Co), in medium containing 0.1 μg/ml Taxol (T) or in medium containing Taxol and caspase-8 inhibitor zIETD-fmk (T + I8) or Taxol and caspase-3 inhibitor zDEVD-fmk (T + I3) as indicated. Western blot analyses were performed by the use of anti-human caspase-8 mab. Arrows indicate the positions of procaspase-8 (C8) and the 18 kDa active subunit of caspase-8 (p18). The experiments were repeated twice and yielded similar results

for binding of the pan-caspase substrate FITC-VAD-fmk (Figure 4c) as compared to the control transfectants (Figure 4b). This drastic inhibition of overall caspase activities was paralleled by a decrease in drug-induced apoptosis (not shown).

To dissect functionally the steps leading to caspase activation, we performed a Western blot analysis to assess release of cytochrome *c* and second mitochondrial activator of caspases (Smac) and processing of individual procaspases (9, 3, and 8), and the caspases-3 and -8 substrate Bid, a known activator of mitochondrial apoptosis (Belka *et al*., 2001; Rokhlin *et al*., 2001; Stepczynska *et al*., 2001; Suliman *et al*., 2001) (Figure 5). Bcl-x_L inhibited Taxol-induced mitochondrial activation as measured by Western blot analysis for cytochrome *c* release at 24–48 h after exposure to Taxol. This was paralleled by an almost complete inhibition of caspases-9, -3, and -8 processing in the Bcl-x_L transfectants (Figure 5). This clearly demonstrates that activation of caspases-9, -3, and -8 occurs secondary to cytochrome *c* release, that is, downstream of the mitochondrial activation, presumably via an APAF-1-dependent mechanism (Perkins *et al*., 2000). Caspase processing was paralleled by cleavage of the 22 kDa BH3-only protein Bid to tBid. Figure 5 shows occurrence of the 15 kDa tBid cleavage product in the mock transfectants at 36

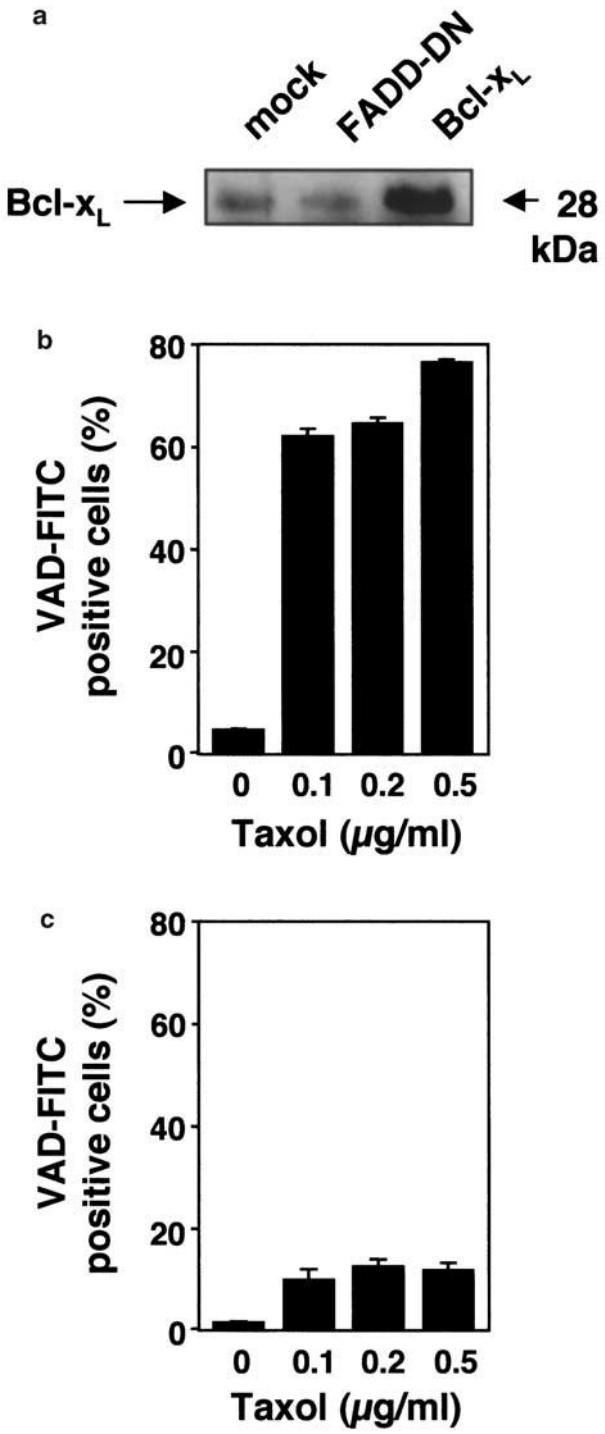

Figure 4 Inhibition of Taxol-induced caspase activity by Bcl-x_L. (**a**) Western blot analysis shows Bcl-x_L overexpression in the BJAB Bcl-x_L transfectants while BJAB mock transfectants and BJAB FADD-DN cells express low levels of endogenous Bcl-x_L. Pan-caspase activities were measured by flow cytometry on the single-cell level by the use of a cell permeable fluorescent FITC-VAD-fmk pan-caspase substrate binding to activated caspases. BJAB cells were cultured in the presence of Taxol for 24 h. Data are given in percentage of fluorescent cells. (**b**) Neo control transfectants. (**c**) Bcl-x_L BJAB transfectants. Taxol-triggered pan-caspase activities were significantly decreased at all concentrations tested in the Bcl-x_L transfectants ($n = 3$, $P < 0.001$)

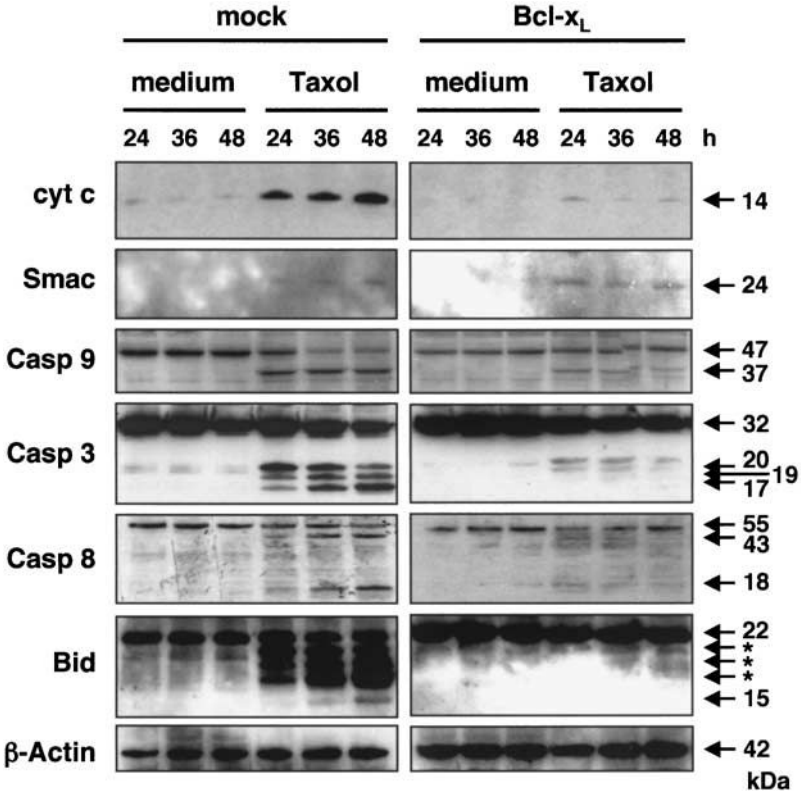

Figure 5 Taxol-induced apoptotic events in BJAB mock and Bcl-x_L transfectants. BJAB Neo control transfectants or Bcl-x_L transfectants were cultured in the absence or presence of Taxol (0.1 μg/ml) for 24, 36, or 48 h. Release of cytochrome *c* or Smac from mitochondria to the cytosol, processing of procaspase-9 (47 kDa, cleavage product: 37 kDa), procaspase-3 (32 kDa, cleavage products: 20, 19, and 17 kDa), and procaspase-8 (55 kDa, cleavage products: 43 and 18 kDa), and cleavage of Bid (22 kDa) to t-Bid (15 kDa) were detected by Western blot analysis. In the case of Bid, nonspecific bands are visible (*) corresponding to the 20, 19, and 17 kDa caspase-3 cleavage products as the blot employed for caspase-3 detection was stripped (incompletely) and subsequently re-exposed with the anti-Bid antibody

and 48 h, whereas no Bid cleavage and occurrence of tBid could be detected in the Bcl-x_L transfectants.

Interestingly, we observed only a rather weak release of Smac from mitochondria and this weak Smac release could not be inhibited by Bcl-x_L (Figure 5). This indicates that Smac release is regulated by different events as compared to cytochrome *c* and that Smac release does not play a major role in the mitochondrial amplification loop.

Blocking of caspases-8 and -3 by cell permeable inhibitors reduces Taxol-induced mitochondrial activation in a CD95/Fas-independent manner

Previous studies described the hierarchical activation of mitochondria and caspase-3 after treatment of cells with cytotoxic drugs (Wieder *et al*., 2001) and a potential feedback loop for amplification of apoptotic signals (Slee *et al*., 2000). As shown in Figure 6a, pretreatment of BJAB mock cells with the caspase-3 inhibitor zDEVD-fmk significantly reduced the Taxol-induced mitochondrial permeability transition by 65$\pm$7.3%. A similar effect was observed using the caspase-8 inhibitor zIETD-fmk. These data clearly indicate that Taxol-induced breakdown of the mitochondrial membrane

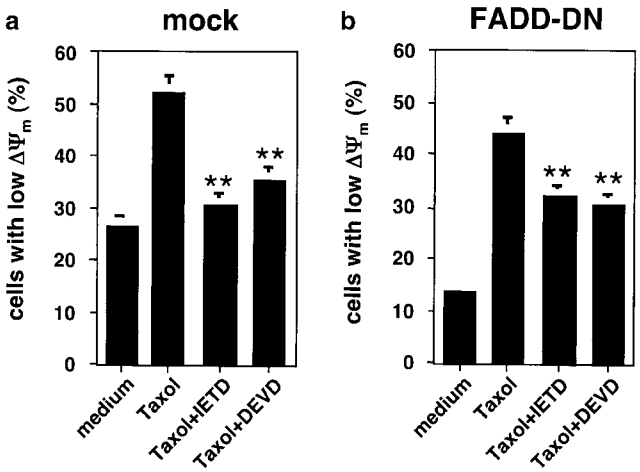

Figure 6 Taxol-induced mitochondrial activation is reduced by caspases-8- and -3-specific inhibitors independently from CD95/Fas signaling. BJAB mock cells (**a**) or BJAB FADD-DN cells (**b**) were treated with medium alone, medium containing 0.1 μg/ml Taxol, 0.1 μg/ml Taxol (Taxol) plus 10 μM zIETD-fmk (Taxol+IETD) or 0.1 μg/ml Taxol plus 10 μM zDEVD-fmk (Taxol+DEVD) as indicated. Breakdown of the mitochondrial membrane potential (mitochondrial permeability transition) was measured after 48 h of incubation by staining with JC-1. Values are given as percentage of cells with low $\Delta\Psi_m\pm$s.d. ($n=3$). **, significantly different from Taxol-treated cells with $P<0.01$

potential is driven by a caspases-3/-8-dependent mitochondrial amplification loop.

To exclude that caspases-3 or -8 are activated via death receptor-mediated signals during drug-induced apoptosis, the experiments described above were repeated in the CD95/Fas-insensitive BJAB FADD-DN cells. Like in the BJAB mock cells, both caspase inhibitors significantly reduced the Taxol-triggered mitochondrial permeability transition in BJAB FADD-DN cells by $43 \pm 6.1\%$ (Figure 6b). Thus, we conclude that amplification of the apoptotic signal after Taxol treatment is independent from signaling by CD95/Fas or other FADD-dependent death receptors.

Caspase-8 is functionally relevant as a downstream effector caspase in Taxol-induced apoptosis

To investigate the functional relevance of caspase-8 activation during drug-induced apoptosis, we measured the impact of caspase inhibitors on Taxol-induced DNA fragmentation. As shown in Figure 7a, preincubation of BJAB mock cells with the caspase-8 inhibitor zIETD-fmk significantly inhibited apoptotic DNA fragmentation by $55 \pm 13.2\%$. Interestingly, the inhibitory effect of zIETD-fmk was in the same range as compared with the caspase-3 inhibitor zDEVD-fmk, that is, an inhibitor for a typical effector caspase that was used as a positive control (Figure 7a). These data clearly demonstrate that activation of caspase-8 plays a functional role during Taxol-induced apoptotic cell death. Furthermore, inhibition of caspase-8 led to a significant reduction of Taxol-induced DNA fragmentation by $50 \pm 6.1\%$ in CD95/Fas-resistant BJAB FADD-DN cells (Figure 7b). This result confirms that the functional role of caspase-8 in this experimental setup is independent from FADD-mediated death receptor signaling.

In line with these findings, a Western blot analysis demonstrates that cytochrome *c* and Smac release, processing of procaspases-9, -3, and -8 and cleavage of Bid to tBid are independent from death receptor signaling (Figure 8).

To further dissect the signaling events involved in the drug-induced amplification loop, we analysed whether caspases-3 and -8 affect the release of cytochrome *c* from mitochondria. To this end, we incubated BJAB cells in the presence or absence of Taxol and peptide caspase inhibitors. Figure 9 shows that incubation of BJAB cells with 0.1 μg/ml Taxol for 24 h triggers release of

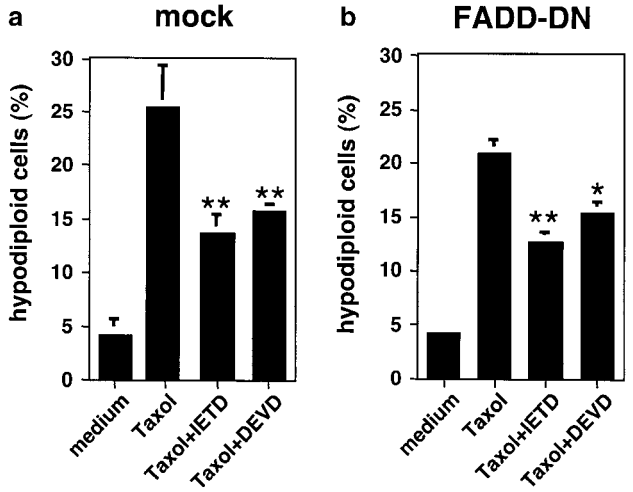

Figure 7 Taxol-induced DNA fragmentation is significantly reduced by caspases-8- and -3-specific inhibitors independently of CD95/Fas signaling. BJAB mock cells (**a**) or BJAB FADD-DN cells (**b**) were treated with medium alone, medium containing 0.1 μg/ml Taxol, 0.1 μg/ml Taxol (Taxol) plus 10 μM zIETD-fmk (Taxol + IETD) or 0.1 μg/ml Taxol plus 10 μM zDEVD-fmk (Taxol + DEVD) as indicated. DNA fragmentation was measured after 48 h of incubation by staining DNA using propidium iodide as described in Materials and methods. Values are given as percentage of cells with hypodiploid DNA $\pm$ s.d. ($n = 3$). **, significantly different from Taxol-treated cells with $P < 0.01$; *, significantly different from Taxol-treated cells with $P < 0.05$

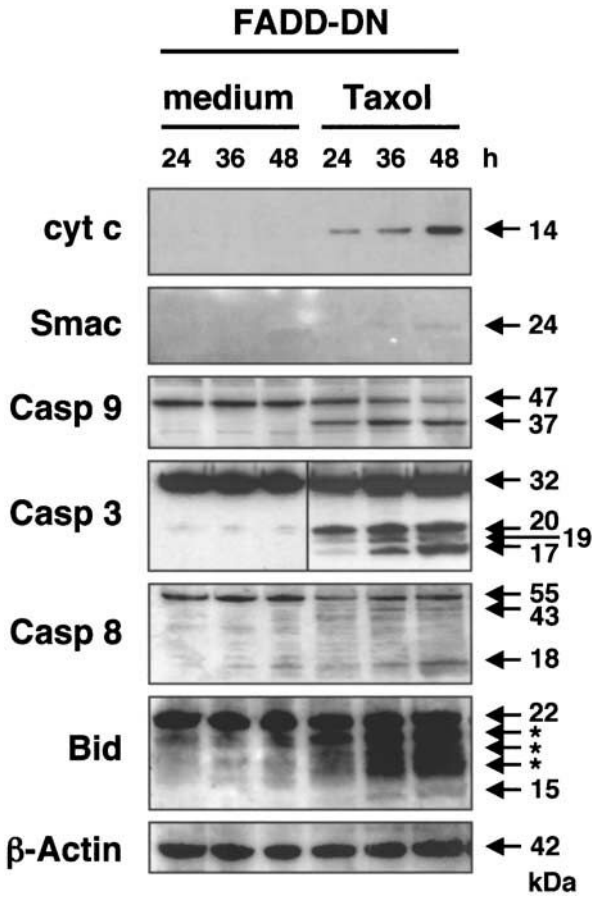

Figure 8 Western blot analysis for Taxol-induced apoptotic events in BJAB FADD-DN transfectants. BJAB FADD-DN transfectants were cultured in the absence or presence of Taxol (0.1 μg/ml) for 24, 36, or 48 h. Release of cytochrome *c* or Smac from mitochondria to the cytosol, processing of procaspase-9 (47 kDa, cleavage product: 37 kDa), procaspase-3 (32 kDa, cleavage products: 20, 19, and 17 kDa), and procaspase-8 (55 kDa, cleavage products: 43 and 18 kDa), and cleavage of Bid (22 kDa) to t-Bid (15 kDa) were detected by Western blot analysis. In the case of Bid, nonspecific bands are visible (*) corresponding to the 20, 19, and 17 kDa caspase-3 cleavage products as the blot employed for caspase-3 detection was stripped (incompletely) and subsequently re-exposed with the anti-Bid antibody

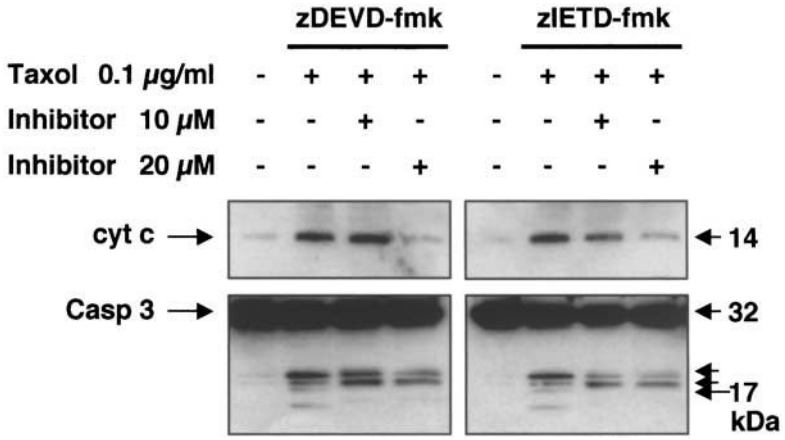

Figure 9 Inhibition of cytochrome *c* release by caspases-3 or -8 inhibitors. Cells were cultured in the absence or presence of Taxol (0.1 μg/ml) for 24 h. Peptide caspase inhibitors specific for caspase-3-like activities (zDEVD-fmk) or caspase-8 (zIETD-fmk) were added at 10–20 μM. Release of cytochrome *c* was detected in cytosolic extracts. In parallel cultures, the cleavage of procaspase-3 was analysed as a surrogate marker for apoptotic cell death

cytochrome *c* into the cytosol. This is paralleled by the processing of procaspase-3 to the active 17 kDa subunit. Addition of both zDEVD-fmk or zIETD-fmk inhibited cleavage of procaspase-3 to the 17 kDa subunit and almost completely impaired cytochrome *c* release at 20 μM inhibitor concentration. This inhibitor experiment demonstrates that both caspases-3 and -8 activities are required for full release of cytochrome *c* from the mitochondria and processing of caspase-3 during Taxol-induced apoptosis. In addition, this inhibitor experiment suggests that caspase-3-like activities are required for full processing of procaspase-3 during drug-induced apoptosis as the zDEVD-fmk inhibits caspase-3 processing to the active 17 kDa subunit.

Cytokine response modifier A blocks Taxol-induced mitochondrial activation and inhibits Taxol-induced DNA fragmentation

To confirm the role of caspase-8 during Taxol-induced apoptosis, we investigated the impact of the cowpox serpin crmA on Taxol-induced DNA fragmentation. This viral caspase inhibitor shows a high target protease specifity for caspase-8 (Zhou *et al*., 1997; Garcia-Calvo *et al*., 1998). As shown in Figure 10a, Taxol-induced mitochondrial permeability transition is blocked in crmA-expressing BJAB cells. This further supports the model of caspase-8 mediating a mitochondrial feedback loop during drug-induced apoptosis. In addition, we demonstrated that CD95/Fas-mediated mitochondrial permeability transition is completely abrogated by crmA and this serves as a further positive control for the efficiency of this caspase-8 inhibitor (Figure 10b). Interestingly, crmA also interfered with downstream DNA fragmentation (Figure 10c). Inhibition of Taxol-induced DNA fragmentation by expression of crmA was in the range between 30 and 46%. This corresponds well to the efficiency of the synthetic caspase-8 inhibitor zIETD-fmk as described above. Likewise, crmA potently inhibited CD95/Fas-mediated DNA fragmentation by 82% (Figure 10d).

Discussion

In the present study, we investigated the functional role of caspase-8 in drug-induced apoptosis of B-lymphoid cells. In detail, we demonstrate that caspases-8 and -3 are activated via the mitochondrial pathway of apoptosis in a death receptor-independent manner. The activated caspases then mediate a mitochondrial auto-amplification loop that is required for optimal release of cytochrome *c* and mitochondrial permeability shift transition. This pathway involves release of cytochrome *c*, processing of caspases-9, -3, and –8, and cleavage of the BH3-only protein Bid to tBid (Figure 11).

Taxol-treated BJAB cells were employed as a model system since we had demonstrated in a previous study that Taxol-induced apoptosis in these cells is characterized by the hierarchical activation of mitochondria, caspases-3, and -8 (Wieder *et al*., 2001). Furthermore, it is well known that Taxol, which primarily targets the microtubule components of the cytoskeleton (for a review see Wang *et al*., 1999), preferentially induces apoptotic and not necrotic cell death at concentrations below 1 μg/ml in a variety of cell types, for example, B-lymphoid cells (Essmann *et al*., 2000; Wieder *et al*., 2001), human breast cancer cells (Charles *et al*., 2001), and lung cancer cells (Das *et al*., 2001). In addition, it is well established that Taxol-induced cell death depends in part on the activation of caspase-3-like protease activities (Suzuki *et al*., 1998; Essmann *et al*., 2000).

In a first set of experiments, we observed that Taxol-induced apoptosis is accompanied not only by processing and activation of caspase-3 but also by cleavage of caspase-8 to the active p18 subunit. This is concordant with previous reports demonstrating activation of caspase-8 in drug-induced apoptosis via the mitochondrial pathway (Wesselborg *et al*., 1999; Belka *et al*., 2000; Engels *et al*., 2000; Wieder *et al*., 2001). Apoptosis induction and caspase-8 processing by Taxol or other drugs such as anthracyclines or nucleoside analogs (Friesen *et al*., 1999; Nomura *et al*., 2000; Biswas *et al*.,

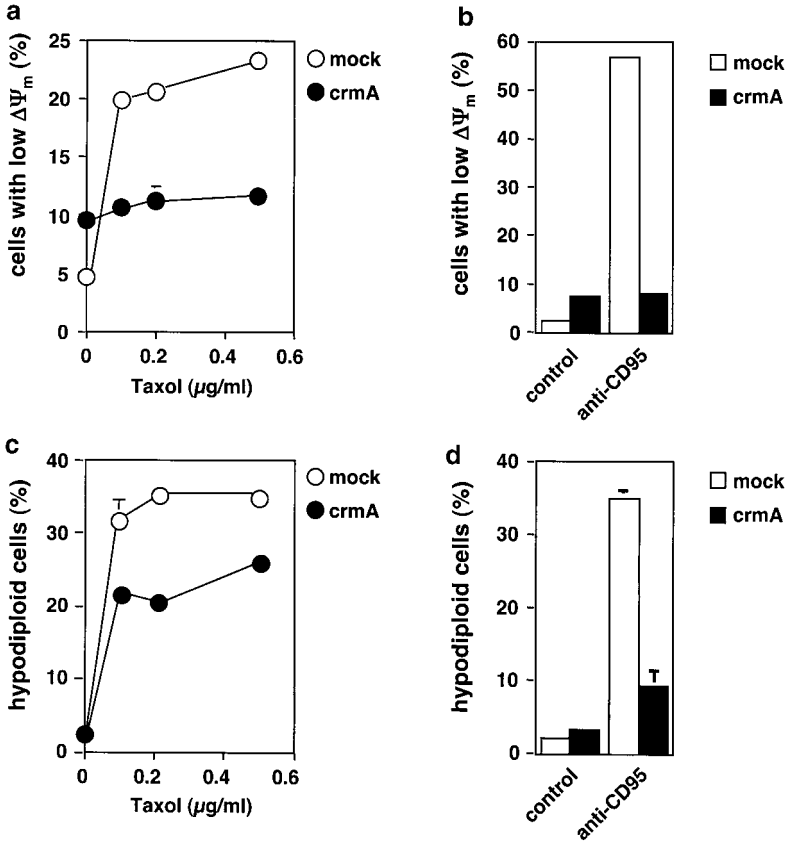

Figure 10 Taxol-induced mitochondrial transmembrane permeability transition and DNA fragmentation is abrogated in BJAB cells expressing cytokine response modifier A (crmA). BJAB vector control (mock) or crmA expressing cells (crmA) were incubated in the presence of different concentrations of Taxol for 48 h. As a positive control for the efficacy of crmA, BJAB vector control (mock) or crmA expressing cells (crmA) were incubated for 24 h in the presence or absence of 1 μg/ml anti-CD95 antibody. (**a**) and (**b**) Mitochondrial permeability transition was measured by staining with JC-1. Values are given as percentage of cells with low $\Delta\Psi_m \pm$ s.d. ($n = 3$). (**c**) and (**d**) DNA fragmentation was measured by staining DNA using propidium iodide. Values are given as percentage of cells with hypodiploid DNA $\pm$ s.d. ($n = 3$)

2001; Fulda *et al*., 2001a, b) was suggested to occur via the CD95/Fas receptor/ligand system. Nevertheless, we and others previously demonstrated that caspase-8 is activated downstream of caspase-3 during drug-induced apoptosis (reviewed in Daniel *et al*., 2001) including cell death activated by Taxol (Wieder *et al*., 2001). In detail, this activation of caspase-8 was also found in CD95/Fas-resistant BJAB FADD-DN cells, thereby confirming that signaling by CD95/Fas or other death receptors utilizing the FADD adaptor molecule is not involved in the activation of the caspase cascade in drug-induced apoptosis. Likewise, the caspase-8 inhibitor zIETD-fmk inhibited caspase-8 processing in BJAB mock as well as in BJAB FADD-DN cells. This finding indicates that caspase-8 is an essential part of a feedback loop that seems to also include autoprocessing of the enzyme. Such caspase-8 autoprocessing may involve modulation of the Bcl-2/Bcl-x_L/BAR rheostat (Stegh *et al*., 2002). Our data regarding the inhibition of procaspase-8 processing in the Bcl-x_L transfectants indirectly support this hypothesis. Thus, caspase-8 autoprocessing may take place at the mitochondria where caspase-8 activation could occur through an induced proximity model as described earlier for the death-receptor associated DISC (Muzio *et al*., 1998). In fact, the present work is the first report to demonstrate death-receptor independent autoprocessing of caspase-8 *in vivo*.

As shown previously, Taxol-induced apoptosis is mediated via the mitochondrial death pathway and can be inhibited by Bcl-x_L. Here, overexpression of Bcl-x_L not only inhibited Taxol-induced cell death but also abrogated caspase activation upon Taxol exposure. This clearly demonstrates that caspase activation is initiated in consequence of mitochondrial activation. Thus, Bcl-x_L almost completely inhibited the release of cytochrome *c* from the mitochondria into the cytosol and this was paralleled by a drastic decrease in processing of the procaspases-9, -3, and -8.

Further experiments revealed that inhibition of caspases-8 and -3 clearly inhibited cytochrome *c* release and mitochondrial permeability transition. Activation of caspases-9, -3, -and -8 occurred in a death receptor-independent manner. This demonstrates, together with the data showing Bcl-x_L acting upstream of the caspase cascade, that caspases-3 and -8 mediate a feedback amplification loop that is required for full activation of cytochrome *c*, caspase activation and execution of cell death.

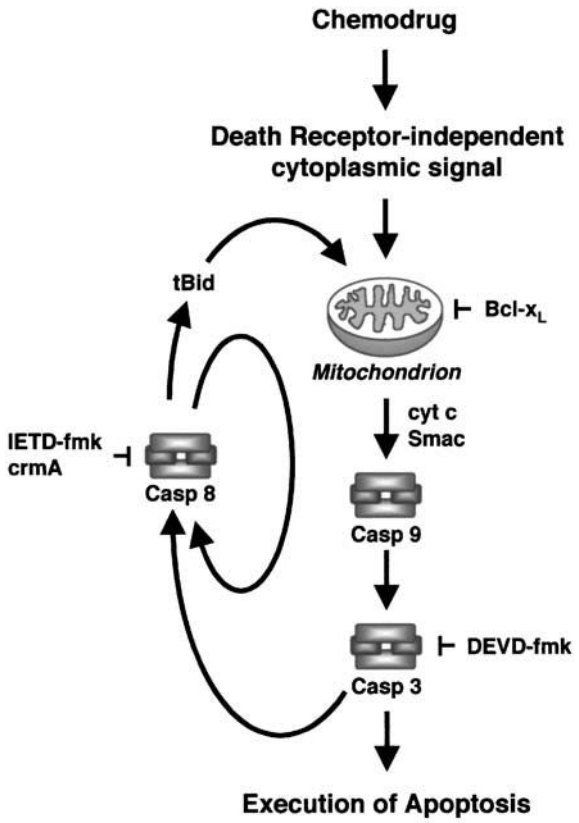

Figure 11 Schematic illustration of a caspases-3/-8-driven amplification loop during drug-induced apoptosis. Treatment of cells with death receptor-independent stimuli, for example, cytotoxic drugs, leads to activation of mitochondria and release of cytochrome *c* and Smac. Cytochrome *c* release and breakdown of the mitochondrial membrane potential is inhibited by Bcl-x_L. Formation of the apoptosome, consisting of cytochrome *c*, (d)ATP, APAF-1, and procaspase-9, triggers activation of initiator caspase-9 followed by activation of effector caspase-3 and consecutive processing and activation of procaspase-8. Caspase-8 processing can occur autocatalytically. Bid is cleaved by a caspases-3 and -8 dependent mechanism and can activate mitochondrial apoptosis. This scheme delineates a positive feedback loop for mitochondrial activation that is required for full cytochrome *c* release and mitochondrial permeability transition. The sites of action of the synthetic caspase inhibitors are indicated. Casp 9: caspase-9; Casp 3, caspase-3; Casp 8, caspase-8; DEVD-fmk, caspase-3 inhibitor; IETD-fmk, caspase-8 inhibitor

This is well in line with data obtained in lung adenocarcinoma cells where caspases-3 and -8 inhibition inhibited breakdown of the mitochondrial membrane potential upon Taxol exposure (Oyaizu *et al*., 1999). Cytochrome *c* release was shown to occur upstream of caspases-9, -3, and -8 activation in anaplastic thyroid carcinoma cells (Pan *et al*., 2001). In this report, no inhibition of cytochrome *c* release was observed, however, when caspases-3, -8, and -9 were inhibited. Experiments in APAF-1 overexpressing HL-60 and in APAF-1 knockout mouse embryonal fibroblasts showed that Taxol-induced apoptosis and caspase-8 cleavage occurs via an APAF-1- and caspase-9-dependent pathway (Perkins *et al*., 2000).

Furthermore, Bcl-x_L completely inhibited cleavage of the BH3-only protein to tBid, a known activator of the mitochondrial apoptosis cascade that is generated via caspases-3- or -8-dependent cleavage of Bid during anticancer drug exposure, irradiation and death receptor triggering (Belka *et al*., 2000, 2001; Engels *et al*., 2000; Rokhlin *et al*., 2001; Stepczynska *et al*., 2001; Suliman *et al*., 2001). Again, this event was independent from death receptor signaling as cleavage of Bid to the 15 kDa tBid occurred to a similar extent in the FADD-DN transfected BJAB cells (Figure 8) as compared with the mock transfectants (Figure 5) upon treatment with Taxol.

Our data are also in line with a previous report demonstrating that cleavage of the proapoptotic protein Bid during drug-induced apoptosis occurs downstream of Bcl-2 action and is catalysed by caspase-3. According to their results, the authors suggested a potential feedback loop for amplification of apoptosis-associated mitochondrial activation (Slee *et al*., 2000). Here, we provide evidence that this amplification loop really exists and extend this model in a therapeutically relevant setting. The significant reduction of Taxol-induced cytochrome *c* release and mitochondrial permeability transition by zIETD-fmk, zDEVD-fmk or crmA shows that this caspase-driven mitochondrial amplification loop is death receptor-independent and not only involves caspase-8 but also caspase-3.

Caspase-8 activation has been shown after drug treatment or ionizing irradiation in different cell types, for example, leukemic T cells (Wesselborg *et al*., 1999; Belka *et al*., 2000), breast cancer cells (Engels *et al*., 2000), and B lymphoid cells (Wieder *et al*., 2001). There was, however, no convincing evidence for a functional role of caspase-8 in drug-induced apoptosis. Our results intriguingly show that inhibition of caspase-8 results in impaired mitochondrial activation and DNA fragmentation in BJAB cells. Nevertheless, neither the caspase-3- nor the caspase-8-specific inhibitors completely blocked cytochrome *c* release, breakdown of the mitochondrial membrane potential or Taxol-induced DNA fragmentation. This phenomenon can be explained at least in part by the fact that probably other caspases, such as caspases-6 and -7, or other proteases, such as serine proteases (Huang *et al*., 1999) can do the job. Furthermore, it is possible that a significant part of Taxol-mediated DNA fragmentation is mediated via caspase-independent death pathways. In addition, tBid preferentially activates mitochondria to release cytochrome *c* in a Bax/Bak-dependent manner (Korsmeyer *et al*., 2000; Zamzami *et al*., 2000; Sugiyama *et al*., 2002). Nevertheless, we and others demonstrated that mitochondria can be activated by Bax/Bak-dependent or-independent mechanisms (Hemmati *et al*., 2002; Radetzki *et al*., 2002; von Haefen *et al*., 2002). In addition, such Bax/Bak-independent pathways may not be subject to regulation by the amplification loop.

In addition, microtubule-damaging agents induce serine/threonine phosphorylation of Bcl-2 through the c-Raf-1 and the mTOR kinases (Huang *et al*., 1999; Calastretti *et al*., 2001), presumably in consequence of the induction of M-phase arrest. Bcl-2 phosphorylation inhibits degradation of Bcl-2 via the proteasome and

thereby stabilizes Bcl-2 protein expression. The functional consequences of Bcl-2 phosphorylation are, however, discussed controversially. While some authors observe inactivation of Bcl-2 upon phosphorylation other reports don't. Importantly, Taxol-induced Bcl-2 phosphorylation was shown to be irrelevant for the sensitivity of mitochondria to undergo apoptotic activation upon exposure to Bid in a cell-free system. Thus, Bcl-2 phosphorylation does not appear to be functionally relevant in the amplification loop as described in the present work (Brichese *et al*., 2002).

Another interesting aspect of our study comes from the observation that Smac release is rather weak and could not be inhibited by Bcl-x_L. This suggests that Smac is not a major player in our experimental system. In addition, our observation indicates that the mechanisms for the release of cytochrome *c* and Smac differ significantly even while Bid was shown previously to mediate release of both cytochrome *c* and Smac (Madesh *et al*., 2002).

In summary, the data presented in the present study provide experimental evidence that Taxol-induced apoptosis proceeds via a caspases-8/-3-driven mitochondrial amplification loop as outlined in Figure 11. Our data clearly delineate that caspases-3 and -8 are required for full activation of cytochrome *c* release and mitochondrial permeabilty transition. These results substantiate the hypothesis that, besides its role as an initiator caspase in death receptor signaling cascades, caspase-8 functions as a downstream amplificator and executioner in drug-induced apoptosis.

Materials and methods

Materials

The murine monoclonal antibody (mab) against against the active p18 subunit of human caspase-8 has been described previously (Engels *et al*., 2000). Antibodies against caspase-9 (goat polyclonal IgG), caspase-3 (goat polyclonal IgG), Bid (rabbit polyclonal IgG), Smac (rabbit polyclonal IgG) were from R&D Systems, Wiesbaden-Nordenstadt, Germany. Anti-cytochrome *c* (mouse mab clone 7H8.2C12) was from BD Biosciences, Heidelberg, Germany and anti-β-actin (rabbit polyclonal IgG) was purchased from Sigma-Aldrich (Taufkirchen, Germany). Agonistic, monoclonal anti-CD95 antibody (Dhein *et al*., 1992) was diluted into growth medium to give a final concentration of 1 μg/ml. As a control, isotype-matched control antibody FII23c (Dhein *et al*., 1992) was used. FII23c did not induce significant DNA fragmentation as compared with medium treated cells (data not shown). Secondary horseradish peroxidase (HRP)-conjugated antibodies (anti-mouse and anti-rabbit IgG) were from Promega (Mannheim, Germany) and donkey anti-goat-HRP conjugate was from Santa Cruz, Heidelberg, Germany. RNase A was from Roth (Karlsruhe, Germany). Taxol (paclitaxel) was purchased from Bristol Arzneimittel GmbH (München, Germany). The caspase-3 inhibitor zDEVD-fmk and the caspase-8 inhibitor zIETD-fmk (in which z stands for benzyloxycarbonyl and fmk for fluoromethyl ketone) were from Kamiya Biomedical Company (Seattle, WA, USA) and dissolved in dimethyl sulfoxide (DMSO) to give 20 mM stock solutions. DMSO (vehicle) was added to controls and was present at 0.1% or less in the experiments. DMSO of 0.1% did not induce significant DNA fragmentation as compared with medium treated cells (data not shown). The dominant-negative FADD construct (FADD-DN) was a kind gift from AM Chinnaiyan and VM Dixit (Ann Arbor, MI, USA).

Cell culture

Control vector-(pcDNA3-mock-transfected), pcDNA3-FADD-DN-cells stably transfected with a dominant-negative FADD mutant lacking the N-terminal death effector domain (Wieder *et al*., 2001), pcDNA3-crmA-transfected BJAB cells (Essmann *et al*., 2000), and Bcl-x_L-transfected and Neo-vector controls (Fulda *et al*. 2001b, kindly provided by S Fulda, University of Ulm, Germany) were grown in RPMI 1640 medium supplemented with 10% fetal calf serum, 0.56 g/l L-glutamine, 100 000 U/l penicillin, and 0.1 g/l streptomycin. Media and culture reagents were from Life Technologies GmbH (Karlsruhe, Germany). BJAB cells were subcultured every 3–4 days by dilution of the cells to a concentration of 1×10^5 cells/ml.

Measurement of CD95/Fas-mediated cell death

For determination of CD95/Fas-mediated cell death in BJAB mock, BJAB FADD-DN cells, and BJAB crmA cells, 1×10^5 cells/ml were treated for different time periods with 1 μg/ml anti-CD95. Then, overall cell death was assessed by Trypan blue exclusion as described. Additionally, measurements of DNA fragmentation, immunoblotting or measurements of mitochondrial permeability transition were performed as described below.

Measurement of the mitochondrial permeability transition

After incubation with the respective compounds for 48 h, BJAB cells were collected by centrifugation at 300 *g*, 4°C for 5 min. Mitochondrial permeability transition was then determined by staining the cells with 5,5′,6,6′-tetrachloro-1,1′,3,3′-tetraethyl-benzimidazolylcarbocyanin iodide (JC-1; Molecular Probes, Leiden, The Netherlands) as described (Lambert *et al*., 1989; Reers *et al*., 1995). The cells (1×10^5) were resuspended in 500 μl phenol red-free RPMI 1640 without supplements and JC-1 was added to give a final concentration of 2.5 μg/ml. The cells were incubated for 30 min at 37°C and moderate shaking. Control cells were likewise incubated in the absence of JC-1 dye. The cells were harvested by centrifugation at 300 *g*, 4°C for 5 min, washed with ice-cold PBS and resuspended in 200 μl PBS at 4°C. Mitochondrial permeability transition was then quantified by flow cytometric determination of cells with decreased fluorescence as measured in the FL2 channel (550–650 nm), that is, with mitochondria displaying a lower membrane potential. Data were collected and analysed using a FACScan (Becton Dickinson, Heidelberg, Germany) equipped with the CELLQuest software. Data are given in percentage of cells with low $\Delta\Psi_m$ which reflects the number of cells undergoing mitochondrial apoptosis.

Measurement of caspase activation on the single-cell level

Cells were cultured for 48 h in the presence or absence of Taxol. Thereafter, cells were harvested by trypsinization and washed twice in PBS. Caspase activation was determined by incubation of cells with a fluoresceinisothiocyanate (FITC)-labelled conjugate of the cell permeable pan-caspase substrate VAD-fmk (valyl-alanyl-aspartyl-(*O*-methyl)-fluoromethylketone) purchased from Promega Corporation (Madison, WI, USA). Equal numbers of cells (5×10^5) were resuspended in 500 μl PBS containing FITC-VAD-fmk at a final concentra-

tion of 10 μM followed by incubation for 20 min at 37°C with moderate shaking. Thereafter, cells were centrifuged at 300 *g* at room temperature for 5 min, washed twice with PBS, and finally resuspended in 200 μl PBS. Caspase activation was subsequently quantified by flow cytometric detection of cells with increased fluorescence, that is, through binding of FITC-labelled VAD-fmk to activated caspases *in situ*. Data are given in percentage of fluorescent cells.

Measurement of DNA fragmentation

DNA fragmentation was measured essentially as described (Essmann *et al*., 2000). For this, BJAB cells were seeded at a density of 1×10^5 cells/ml. After incubation for 48 h with the respective compounds, the cells were collected by centrifugation at 300 *g* for 5 min, washed with phosphate-buffered saline (PBS) at 4°C, and fixed in PBS/0.7% (v/v) formaldehyde on ice for 30 min. After fixation, the cells were incubated with ethanol/PBS (2 : 1, v/v) for 15 min, pelleted, and resuspended in PBS containing 40 μg/ml RNase A. After incubation for 30 min at 37°C, the cells were pelleted again and finally resuspended in PBS containing 50 μg/ml propidium iodide. Nuclear DNA fragmentation was then quantified by flow cytometric determination of hypodiploid DNA. Data were collected and analysed using a FACScan (Becton Dickinson, Heidelberg, Germany) equipped with the CELLQuest software. Data are given in percentage hypoploidy (subG1), which reflects the number of apoptotic cells.

Immunoblotting

After incubation for 48 h with control medium, 0.1 μg/ml Taxol, 0.1 μg/ml Taxol plus 10 μM zDEVD-fmk or 0.1 μg/ml Taxol plus 10 μM zIETD-fmk, BJAB cells were washed twice with PBS and lysed in buffer containing 10 mM Tris/HCl, pH 7.5, 300 mM NaCl, 1% Triton X-100, 2 mM $MgCl_2$, 5 μM [ethylenediamino]tetraacetic acid (EDTA), 1 μM pepstatin, 1 μM leupeptin, and 0.1 mM phenylmethylsulfonyl fluoride. Protein concentration was determined using the bicinchoninic acid assay (Smith *et al*., 1985) from Pierce (Rockford, IL, USA) and equal amounts of protein (usually 20 μg per lane) were separated by SDS–PAGE as described (Essmann *et al*., 2000). Thereafter, immunoblotting was performed as described (Wieder *et al*., 2001). Membranes (Schleicher & Schuell, Dassel, Germany) were swollen in CAPS-buffer (10 mM 3-(cyclohexylamino)propane-1-sulfonic acid (CAPS), pH 11, 10% MeOH) for several minutes and blotting was performed at 1 mA/cm^2 for 1 h in a transblot SD cell (BioRad, München, Germany). The membrane was blocked for 1 h in PBST (PBS, 0.05% Tween-20) containing 3% nonfat dry milk and incubated with primary antibodies for 1 h. After the membrane had been washed three times in PBST, the respective secondary antibody in PBST was applied for 1 h. Finally, the membrane was washed again in PBST and protein bands were detected using the ECL enhanced chemiluminescence system (Amersham Buchler, Braunschweig, Germany).

Preparation of cytosolic extracts and cytochrome c/Smac Western blot analysis

Cytosolic extracts for measurement of cytochrome *c* and Smac release from mitochondria were prepared according to a method described previously. After incubation of cells for 24–48 h, cells were harvested in PBS, equilibrated in hypotonic buffer (20 mM HEPES (pH 7.4), 10 mM KCl, 2 mM $MgCl_2$, 1 mM EDTA), and centrifuged at 300 *g* for 5 min. The resulting cell pellets were then resuspended in hypotonic buffer containing phenylmethyl sulfonylfluoride (final concentration 0.1 mM) and incubated on ice for 15 min. Cells were then homogenized by passing the cells through a syringe (gauge 20) approximately 20 times. The homogenates were centrifuged twice at 10 000 *g* at 4°C for 10 min and the supernatant of the second centrifugation was used as cytosolic extract. After determination of the protein concentration, Western blot analyses with 30 μg cytosolic protein were performed as described above and conducted with anticytochrome *c* antibodies or anti-Smac antibodies.

Statistical analysis

Statistical comparisons were made by the use of Student's *t*-test.

Acknowledgements
The technical assistance of Antje Richter is gratefully acknowledged. We thank AM Chinnaiyan and VM Dixit (Ann Arbor, MI, USA) for providing the dominant-negative FADD (FADD-DN) construct. BJAB Bcl-x_L and vector controls were kindly provided by S Fulda, University of Ulm, Germany. This work was supported by grants from the Deutsche Forschungsgemeinschaft (SFB 506 and Da238/4-1), the European Union TMR program, and the Deutsche José Carreras Leukämie-Stiftung e. V. (DJCLS-R01/02).

References

Belka C, Rudner J, Wesselborg S, Stepczynska A, Marini P, Lepple-Wienhues A, Faltin H, Bamberg M, Budach W and Schulze-Osthoff K. (2000). *Oncogene*, **19,** 1181–1190.

Belka C, Schmid B, Marini P, Durand E, Rudner J, Faltin H, Bamberg M, Schulze-Osthoff K and Budach W. (2001). *Oncogene*, **20,** 2190–2196.

Biswas RS, Cha HJ, Hardwick JM and Srivastava RK. (2001). *Mol. Cell. Biochem.*, **225,** 7–20.

Brichese L, Barboule N, Heliez C and Valette A. (2002). *Exp. Cell Res.*, **278,** 101–111.

Calastretti A, Bevilacqua A, Ceriani C, Vigano S, Zancai P, Capaccioli S and Nicolin A. (2001). *Oncogene*, **20,** 6172–6180.

Charles AG, Han TY, Liu YY, Hansen N, Giuliano AE and Cabot MC. (2001). *Cancer Chemother. Pharmacol*, **47,** 444–450.

Cohen GM. (1997). *Biochem. J.*, **326,** 1–16.

Daniel PT. (2000). *Leukemia*, **14,** 2035–2044.

Daniel PT, Sturm I, Wieder T and Schulze-Osthoff K. (2001). *Leukemia*, **15,** 1022–1032.

Das GC, Holiday D, Gallardo R and Haas C. (2001). *Cancer Lett.*, **165,** 147–153.

Dhein J, Daniel PT, Trauth BC, Oehm A, Moller P and Krammer PH. (1992). *J. Immunol*, **149,** 3166–3173.

Engels IH, Stepczynska A, Stroh C, Lauber K, Berg C, Schwenzer R, Wajant H, Janicke RU, Porter AG, Belka C, Gregor M, Schulze-Osthoff K and Wesselborg S. (2000). *Oncogene*, **19,** 4563–4573.

Essmann F, Wieder T, Otto A, Muller EC, Dorken B and Daniel PT. (2000). *Biochem. J.*, **346,** 777–783.

Fadeel B, Orrenius S and Zhivotovsky B. (2000). *Leukemia*, **14,** 1514–1525.

Friedrich K, Wieder T, von Haefen C, Radetzki S, Jänicke R, Schulze-Osthoff K, Dörken B and Daniel PT. (2001). *Oncogene*, **20,** 2749–2760.
Friesen C, Fulda S and Debatin KM. (1999). *Leukemia*, **13,** 1854–1858.
Fulda S, Kufer MU, Meyer E, van Valen F, Dockhorn-Dworniczak B and Debatin KM. (2001a). *Oncogene*, **20,** 5865–5877.
Fulda S, Meyer E, Friesen C, Susin SA, Kroemer G and Debatin KM. (2001b). *Oncogene*, **20,** 1063–1075.
Garcia-Calvo M, Peterson EP, Leiting B, Ruel R, Nicholson DW and Thornberry NA. (1998). *J. Biol. Chem*., **273,** 32608–32613.
Hemmati PG, Gillissen B, von Haefen C, Wendt J, Stärck L, Güner D, Dörken B and Daniel PT. (2002). *Oncogene*, **21,** 3149–3161.
Huang Y, Sheikh MS, Fornace Jr AJ and Holbrook NJ. (1999). *Oncogene*, **18,** 3431–3439.
Kischkel FC, Lawrence DA, Tinel A, LeBlanc H, Virmani A, Schow P, Gazdar A, Blenis J, Arnott D and Ashkenazi A. (2001). *J. Biol. Chem.*, **276,** 46639–46646.
Kitamura K, Minami Y, Yamamoto K, Akao Y, Kiyoi H, Saito H and Naoe T. (2000). *Leukemia*, **14,** 1743–1750.
Korsmeyer SJ, Wei MC, Saito M, Weiler S, Oh KJ and Schlesinger PH. (2000). *Cell Death Differ.*, **7,** 1166–1173.
Lambert IH, Hoffmann EK and Jorgensen F. (1989). *J Membr Biol*., **111,** 113–131.
Los M, Wesselborg S and Schulze-Osthoff K. (1999). *Immunity*, **10,** 629–639.
Madesh M, Antonsson B, Srinivasula SM, Alnemri ES and Hajnoczky G. (2002). *J. Biol. Chem.*, **277,** 5651–5659.
Muzio M, Chinnaiyan AM, Kischkel FC, O'Rourke K, Shevchenko A, Ni J, Scaffidi C, Bretz JD, Zhang M, Gentz R, Mann M, Krammer PH, Peter ME and Dixit VM. (1996). *Cell*, **85,** 817–827.
Muzio M, Stockwell BR, Stennicke HR, Salvesen GS and Dixit VM. (1998). *J Biol Chem*., **273,** 2926–2930.
Newton K and Strasser A. (2000). *J. Exp. Med*., **191,** 195–200.
Nicholson DW. (1999). *Cell Death Differ.*, **6,** 1028–1042.
Nomura Y, Inanami O, Takahashi K, Matsuda A and Kuwabara M. (2000). *Leukemia*, **14,** 299–306.
Oyaizu H, Adachi Y, Taketani S, Tokunaga R, Fukuhara S and Ikehara S. (1999). *Mol. Cell. Biol. Res. Commun.*, **2,** 36–41.
Pan J, Xu G and Yeung SC. (2001). *J. Clin. Endocrinol. Metab.*, **86,** 4731–4740.
Perkins CL, Fang G, Kim CN and Bhalla KN. (2000). *Cancer Res.*, **60,** 1645–1653.
Prokop A, Wieder T, Sturm I, Essmann F, Seeger K, Wuchter C, Ludwig W-D, Henze G, Dörken B and Daniel PT. (2000). *Leukemia*, **14,** 1606–1613.
Radetzki S, Köhne CH, von Haefen C, Gillissen B, Sturm I, Dörken B and Daniel PT. (2002). *Oncogene*, **21,** 227–238.
Reers M, Smiley ST, Mottola-Hartshorn C, Chen A, Lin M and Chen LB. (1995). *Methods Enzymol*., **260,** 406–417.
Rokhlin OW, Guseva N, Tagiyev A, Knudson CM and Cohen MB. (2001). *Oncogene*, **20,** 2836–2843.
Slee EA, Keogh SA and Martin SJ. (2000). *Cell Death Differ*., **7,** 556–565.
Smith PK, Krohn RI, Hermanson GT, Mallia AK, Gartner FH, Provenzano MD, Fuijmoto EK, Geoke NM, Olson BJ and Klenk DC. (1985). *Anal Bicohem*., **150,** 76–85.
Stepczynska A, Lauber K, Engels IH, Janssen O, Kabelitz D, Wesselborg S and Schulze-Osthoff K. (2001). *Oncogene*, **20,** 1193–1202.
Sugiyama T, Shimizu S, Matsuoka Y, Yoneda Y and Tsujimoto Y. (2002). *Oncogene*, **21,** 4944–4956.
Suliman A, Lam A, Datta R and Srivastava RK. (2001). *Oncogene*, **20,** 2122–2133.
Suzuki A, Kawabata T and Kato M. (1998). *Eur. J. Pharmacol*., **343,** 87–92.
Thornberry NA and Lazebnik Y. (1998). *Science*, **281,** 1312–1316.
von Haefen C, Wieder T, Gillissen B, Stärck L, Graupner V, Dörken B and Daniel PT. (2002). *Oncogene*, **21,** 4009–4019.
Wang LG, Liu XM, Kreis W and Budman DR. (1999). *Cancer Chemother. Pharmacol*., **44,** 355–361.
Wesselborg S, Engels IH, Rossmann E, Los M and Schulze-Osthoff K. (1999). *Blood*, **93,** 3053–3063.
Wieder T, Essmann F, Prokop A, Schmelz K, Schulze-Osthoff K, Beyaert R, Dörken B and Daniel PT. (2001). *Blood*, **97,** 1378–1387.
Zamzami N, El Hamel C, Maisse C, Brenner C, Munoz-Pinedo C, Belzacq AS, Costantini P, Vieira H, Loeffler M, Molle G and Kroemer G. (2000). *Oncogene*, **19,** 6342–6350.
Zhou Q, Snipas S, Orth K, Muzio M, Dixit VM and Salvesen GS. (1997). *J. Biol. Chem*., **272,** 7797–7800.

Cell Death and Differentiation (2003) 10, 1260–1272

www.nature.com/cdd

Staphylococcus aureus α-toxin-induced cell death: predominant necrosis despite apoptotic caspase activation

F Essmann[1,3], H Bantel[1,4,3], G Totzke[1], IH Engels[1,5], B Sinha[2], K Schulze-Osthoff[1] and RU Jänicke[*,1]

[1] Institute of Molecular Medicine, University of Düsseldorf, Germany
[2] Institute of Medical Microbiology, University of Münster, Germany
[3] These two authors contributed equally to this work.
[4] Current address: Department of Gastroenterology and Hepatology, Medical University of Hannover, Germany
[5] Current address: Genomics Institute of the Novartis Research Foundation, Department of Cancer and Cell Biology, 10675 John Jay Hopkins Drive, San Diego, CA 92121, USA
[*] Corresponding author: RU Jänicke, Institute of Molecular Medicine, University of Düsseldorf, Universitätsstrasse 1, Bldg. 23.12, 40225 Düsseldorf, Germany. Tel: +49 211 8115895; Fax: +49 211 8115892; E-mail: janicke@uni-duesseldorf.de

Received 06.3.03; revised 11.6.03; accepted 19.6.03; published online 1 August 2003
Edited by RA Knight

Abstract

Recent data suggest that α-toxin, the major hemolysin of *Staphylococcus aureus*, induces cell death via the classical apoptotic pathway. Here we demonstrate, however, that although zVAD-fmk or overexpression of Bcl-2 completely abrogated caspase activation and internucleosomal DNA fragmentation, they did not significantly affect α-toxin-induced death of Jurkat T or MCF-7 breast carcinoma cells. Caspase inhibition had also no effect on α-toxin-induced lactate dehydrogenase release and ATP depletion. Furthermore, whereas early assessment of apoptosis induction by CD95 resulted solely in the generation of cells positive for active caspases that were, however, not yet permeable for propidium iodide, a substantial proportion of α-toxin-treated cells were positive for both active caspases and PI. Finally, electron microscopy demonstrated that even in the presence of active caspases, α-toxin-treated cells displayed a necrotic morphology characterized by cell swelling and cytoplasmic vacuolation. Together, our data suggest that α-toxin-induced cell death proceeds even in the presence of activated caspases, at least partially, in a caspase-independent, necrotic-like manner.
Cell Death and Differentiation (2003) **10,** 1260–1272, doi:10.1038/sj.cdd.4401301
Published online 1 August 2003

Keywords: caspase-independent death; necrosis; zVAD-fmk; Bcl-2; α-toxin; DNA fragmentation

Abbreviations: FACS, fluorescence-activated cell sorter; FITC, fluorescein isothiocyanate; HMGB1, high-mobility group 1; LDH, lactate dehydrogenase; PFGE, pulsed-field gel electrophoresis; PI, propidium iodide; TNF, tumor necrosis factor; zVAD-fmk, benzoyl-Val-Ala-Asp-fluoromethylketone

Introduction

Cells can die in two fundamental ways: by a yet ill-defined necrotic pathway following damage of their cell membrane or by a well-characterized process, called programmed cell death or apoptosis that includes the shrinkage and blebbing of the intact cell membrane.[1] Necrotic cell death results from physical or chemical injury, and is accompanied by swelling of the cells and organelles, as well as by cytoplasmic vacuolation and increased permeability of the plasma membrane allowing the passive diffusion of ions. Apoptosis, on the other hand, is characterized by stereotypic biochemical and morphological changes including chromatin condensation, oligonucleosomal DNA fragmentation and formation of apoptotic bodies that can be cleared by phagocytes without producing an inflammatory response.[1] Most of these alterations are due to the activation of a class of intracellular cysteine proteases, called caspases that cleave cellular substrates after aspartate residues.[2,3]

Apoptosis can be achieved by a variety of stimuli such as death receptors, DNA-damaging agents, cytokine withdrawal, etc., all of which efficiently activate caspases. As cell death can be blocked in many apoptotic, but not necrotic systems by caspase inhibitors, it was widely accepted that these proteases are indispensable for apoptosis, and hence activation of caspases classified a particular mode of cell death as apoptosis. However, recent reports suggest the existence of intermediate cell death forms, making it sometimes difficult to unambiguously define the mode of death a particular cell is undergoing.[1,4] Perhaps, two of the first clear demonstrations of caspase-independent programmed cell death were apoptosis induced by the proapoptotic Bcl-2 homologues Bax[5,6] and Bak.[7] Although cell death mediated by both molecules was accompanied by caspase activation, the inhibition of these enzymes only blocked the apoptotic morphology, but not cell death itself. More recent examples include apoptosis induced during thymocyte development,[8] HIV-1 infection of primary T cells,[9] stimulation of surface antigens such as CD4, CD47 and CD99,[10–12] or CTL-mediated target cell lysis.[13] In parallel, it became evident that apoptosis can also occur in the complete absence of caspase activation.[14,15] Even death receptors such as CD95 or TNF receptor-1, which were originally believed to mediate cell death exclusively via the direct activation of the caspase cascade, were shown to simultaneously activate mechanistically different death pathways leading either to necrosis or apoptosis.[16–19] Thus, the presence or absence of active caspases alone does not qualify a particular cell death system as apoptosis or necrosis, respectively. In most of the above-mentioned systems, however, cell death could be blocked by

the antiapoptotic protein Bcl-2, thereby clearly distinguishing these systems from necrosis in which cell death is merely a result of the damage *per se*. Therefore, the term apoptosis-like programmed cell death[1] appears to be appropriate for death events that are under tight regulation of intracellular survival mechanisms.

Staphylococcus aureus is one of the most common gram-positive bacterial pathogens that plays an increasing role in nosocomial infections such as abscess formation, osteomyelitis, endocarditis or pneumonia, which often require a prolonged and aggressive antibiotic treatment.[20] Among the most serious complications of *S. aureus* infections are manifestations of septic and toxic shock syndromes that may lead to multiple organ failure.[21] As tissue injury and a depletion of immune cells are characteristic features of septic and toxic shock syndromes, several studies have focused on cell death induction following exposure to microbial pathogens.[22,23] Indeed, it was shown that *S. aureus* is able to induce apoptosis in various cell types including epithelial cells, endothelial cells, keratinocytes, osteoblasts as well as lymphocytes and macrophages.[24–29] One of the key virulence determinants of *S. aureus* is α-toxin, a pore-forming protein of 34 kDa. At low doses, the toxin was shown to bind to specific, as yet unidentified cell surface receptors, and to produce small heptameric pores that selectively facilitate the release of monovalent ions, resulting in DNA fragmentation and apoptosis.[24,30,31] At high doses ($>6\,\mu$g/ml), in contrast, α-toxin nonspecifically adsorbs to the lipid bilayer, forming larger pores that are Ca^{2+}-permissive, which results in massive necrosis. In addition, we have recently demonstrated that only low α-toxin doses activate caspases, and that this activation is mediated via the intrinsic pathway independently of death receptors.[32] Thus, it appears that the mode of cell death critically depends on the concentration of α-toxin.

However, as discussed above, both oligonucleosomal DNA fragmentation and caspase activation are not necessarily required for apoptotic processes. Therefore, we analyzed this system in more detail, resulting in some intriguing findings that challenge the current concept of cell death induced by α-toxin. Using various methods for cell death assessment, we found that inhibition of caspases did not protect cells from α-toxin-induced death. Moreover, and most interestingly, our results suggest that even in the presence of active caspases α-toxin induces cell death via a necrotic pathway. Thus, our findings are in sharp contrast to numerous death models in which the caspase-independent mode of cell death only surfaces when the activation of caspases is inhibited, and therefore indicate that inhibition of caspases might not be sufficient to prevent the demise of *S. aureus*-infected cells.

Results

Caspase inhibition by zVAD-fmk only partially prevents *S. aureus* α-toxin-induced DNA fragmentation

Recently, we demonstrated that α-toxin, a major hemolysin of *S. aureus*, induces caspase activation via the mitochondrial pathway independently of death receptor signaling.[32] During this work, however, we also noticed that although *S. aureus*-induced caspase activation was almost completely blocked in Bcl-2-overexpressing Jurkat cells, the formation of hypodiploid nuclei as measured by FACS analysis could only be partially prevented in these cells. These results indicated that caspases might not be required for *S. aureus*-induced DNA fragmentation and cell death. To investigate this hypothesis in more detail, we first analyzed hypodiploid nuclei formation induced by either α-toxin or by a supernatant of the cytotoxic *S. aureus* strain Wood 46 in the absence or presence of the broad spectrum caspase inhibitor zVAD-fmk. Similar to the results obtained with Jurkat Bcl-2 cells,[32] caspase inhibition by zVAD-fmk resulted in only a partial decrease of *S. aureus*-induced DNA fragmentation (Figure 1a). Even with the lowest Wood 46 or α-toxin concentrations that efficiently induced

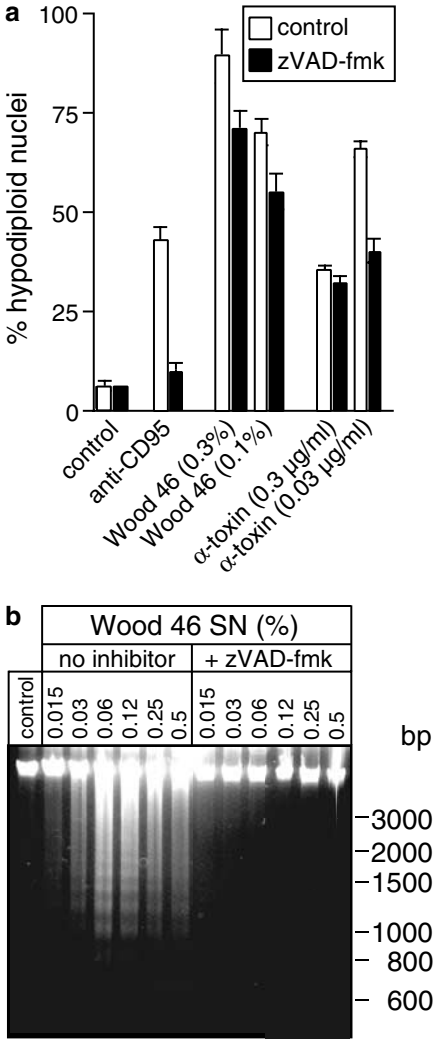

Figure 1 α-toxin-induced DNA fragmentation is only partially prevented by zVAD-fmk. Jurkat cells were either left untreated (control) or incubated with anti-CD95, or with supernatant (SN) of the cytotoxic *S. aureus* strain Wood 46 or with purified α-toxin at the indicated concentrations in the absence or presence of zVAD-fmk. The proportion of hypodiploid nuclei (**a**) and internucleosomal DNA fragmentation (**b**) were determined by flow cytometric analysis (**a**) after 24 h and by CAGE (**b**) after 6 h, respectively. In (**a**), one representative experiment out of three is shown. In (**b**), the positions of the DNA molecular size marker are indicated to the right

caspase-3 activation (Figure 2; Bantel *et al.*[32]), zVAD-fmk reduced hypodiploid nuclei formation by only 22 and 40%, respectively. In contrast, CD95-induced DNA fragmentation in Jurkat cells was almost completely blocked in the presence of zVAD-fmk (Figure 1a). Interestingly, although *S. aureus*-induced formation of hypodiploid nuclei was only partially inhibited by zVAD-fmk, internucleosomal DNA fragmentation in Jurkat cells treated with various concentrations of the *S. aureus* strain Wood 46 was completely abrogated in the presence of this caspase inhibitor (Figure 1b). Thus, our results indicate that *S. aureus* α-toxin induces DNA fragmentation in a caspase-dependent and -independent manner.

Caspase inhibition by zVAD-fmk or overexpression of Bcl-2 does not prevent α-toxin-induced cell death

To verify these results in another experimental setting, we analyzed the effect of zVAD-fmk on α-toxin-induced caspase-3 activation, the caspase responsible for internucleosomal DNA fragmentation during apoptosis.[33] The neutralizing anti-α-toxin antibody was included as a control.[32] As expected, the addition of zVAD-fmk completely abolished α-toxin- and Wood 46-induced caspase-3 activation, as demonstrated by Western blot analysis (Figure 2a) and by the fluorogenic substrate assay, respectively (Figure 2b and d). Caspase-3 activation was also efficiently blocked by the anti-α-toxin antibody when low α-toxin (<0.1 μg/ml) or Wood 46 ($<0.5\%$) concentrations were used, whereas higher α-toxin or Wood 46 doses resulted in a partial activation of caspase-3 (Figure 2a, b and d). Both zVAD-fmk and anti-α-toxin also prevented the activation of the initiator caspases 8 and 9 (data not shown). CD95-induced caspase-3 activation, in contrast, was only blocked by zVAD-fmk, but not by the anti-α-toxin antibody, demonstrating the specificity of this antibody (Figure 2a).

Remarkably, although both zVAD-fmk and the anti-α-toxin antibody efficiently blocked α-toxin- and Wood 46-mediated caspase activation, cell death was dose-dependently inhibited only by the anti-α-toxin antibody but not by zVAD-fmk, as determined by the trypan blue exclusion assay (Figure 2c and e). It is noteworthy that zVAD-fmk also had no effect on the progression of cell death, even when low α-toxin or Wood 46 doses that are known to efficiently activate caspase-3 were used. Therefore, these results indicate that caspases are dispensable for *S. aureus*-mediated cell death.

Next, we compared cell death and DNA fragmentation in Jurkat and Jurkat Bcl-2 cells treated with α-toxin in the presence or absence of zVAD-fmk. Consistent with our previous results (Figure 1a), we observed that α-toxin induced two different DNA fragmentation events in Jurkat cells, which could be easily distinguished based on the inhibitory potential of zVAD-fmk (Figure 3a). The zVAD-fmk-inhibitable and therefore caspase-dependent DNA fragmentation was, however, only evident when low α-toxin concentrations ranging from 0.01 to 0.03 μg/ml were used. This is in agreement with our previous report that caspases are only activated when low α-toxin doses were used.[32] Treatment of Jurkat cells with higher α-toxin doses (>0.03 μg/ml) additionally resulted in a caspase-independent DNA fragmentation that could not be

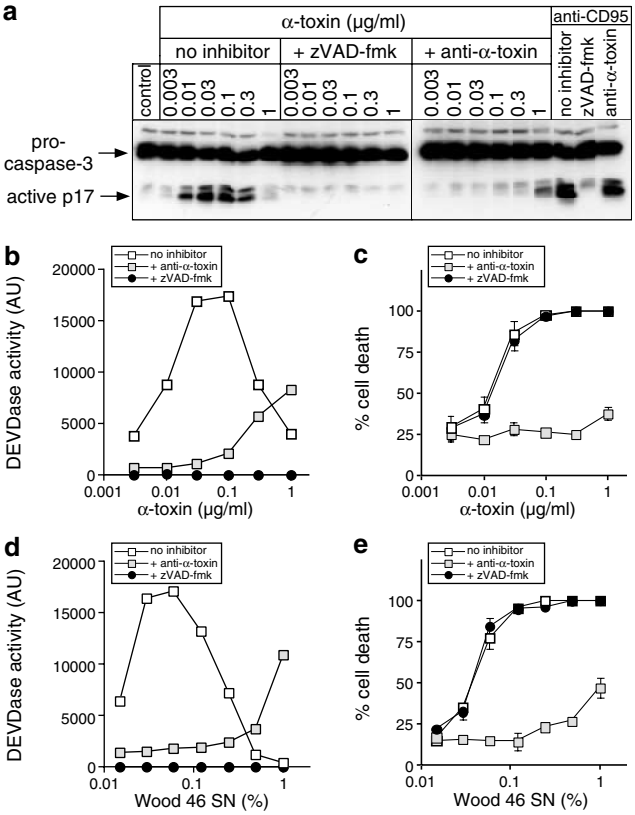

Figure 2 zVAD-fmk completely abrogates α-toxin-induced caspase-3 activation, but not cell death. (**a**) Western blot analysis demonstrating the status of caspase-3 in Jurkat cells that were either left untreated (control) or incubated for 4 h with the indicated concentrations of α-toxin in the absence or presence of zVAD-fmk or the anti-α-toxin antibody. As a control, Jurkat cells were also incubated for 4 h with anti-CD95 in the absence or presence of zVAD-fmk or the anti-α-toxin antibody. The caspase-3 proform and the active p17 subunit are indicated. (**b**, **d**) DEVDase activity in extracts of Jurkat cells incubated for 4 h with the indicated concentrations of α-toxin (**b**) or Wood 46 supernatant (SN) (**d**) in the absence or presence of zVAD-fmk or the anti-α-toxin antibody. One representative experiment out of six performed in triplicates is shown. (**c**, **e**) Assessment of cell death by trypan-blue uptake of Jurkat cells incubated for 4 h with the indicated concentrations of α-toxin (**c**) or Wood 46 supernatant (SN) (**e**) in the absence or presence of zVAD-fmk or the anti-α-toxin antibody. One representative experiment out of six performed in triplicates is shown

blocked by zVAD-fmk (Figure 3a). In Jurkat Bcl-2 cells, however, α-toxin induced only a caspase-independent DNA fragmentation (Figure 3b), which is consistent with our previous finding that α-toxin is unable to induce caspase activation in these cells.[32] In contrast to zVAD-fmk, the anti-α-toxin antibody completely blocked both caspase-dependent and -independent DNA fragmentation, demonstrating that both processes were indeed mediated by α-toxin (Figure 3a and b). As a control, induction of apoptosis in Jurkat and Jurkat Bcl-2 cells by either anti-CD95 or the anti-cancer drug etoposide resulted exclusively in caspase-dependent DNA fragmentation, as it could be completely blocked by zVAD-fmk but not by the anti-α-toxin antibody (Figure 3a and b inlets).

To analyze whether the caspase-dependent apoptotic pathway contributes to cell death induced by α-toxin, we employed an FACS-based method using propidium iodide

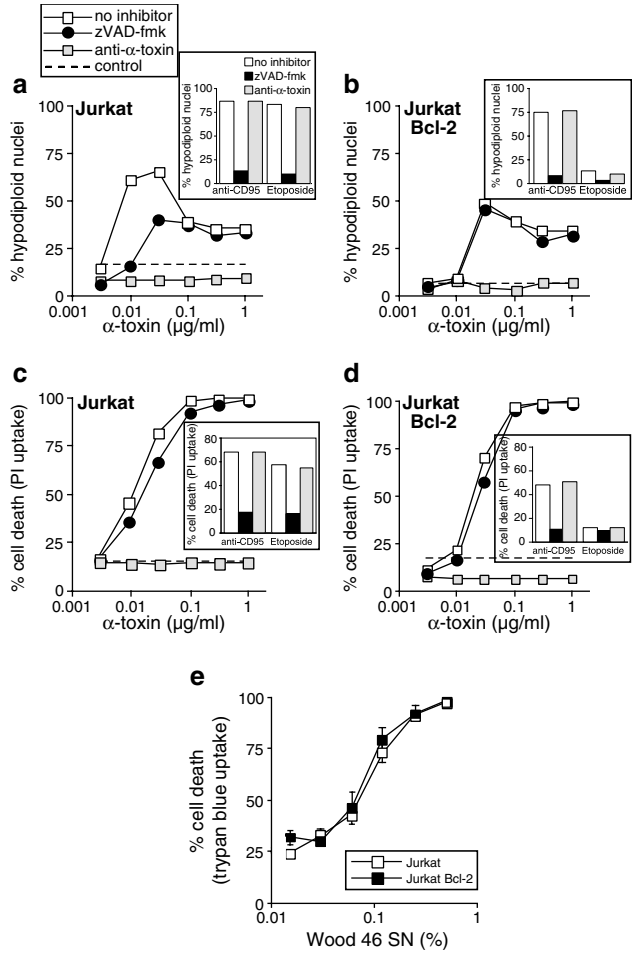

Figure 3 α-toxin induces caspase-dependent and -independent DNA fragmentation. Jurkat (**a**) and Jurkat Bcl-2 cells (**b**) were incubated at 37°C with the indicated concentrations of α-toxin in the absence or presence of zVAD-fmk or the anti-α-toxin antibody. As a control, both cell lines were also incubated with anti-CD95 or etoposide in the absence or presence of zVAD-fmk or the anti-α-toxin antibody (inlets of (**a**, **b**)). The proportion of hypodiploid nuclei was determined by flow cytometric analysis after 24 h. (**c**, **d**) Cell death assessment of Jurkat (**c**) and Jurkat Bcl-2 cells (**d**) treated as above. Cell death was determined after 24 h by flow cytometric analysis based on the uptake of PI. (**e**) Assessment of cell death by trypan-blue uptake of Jurkat and Jurkat Bcl-2 cells incubated for 4 h with the indicated dilutions of Wood 46 supernatant (SN). One representative experiment out of three is shown

(PI)-stained cells. This assay system allows determination of the total percentage of cell death, regardless of whether the cells died via an apoptotic or necrotic pathway. Using this method, we could demonstrate that zVAD-fmk had no effect on α-toxin-mediated killing of Jurkat and Jurkat Bcl-2 cells, whereas CD95- or etoposide-induced death were significantly blocked by this caspase inhibitory peptide (Figure 3c, d). Even with α-toxin concentrations ranging from 0.01 to 0.1 μg/ml that efficiently induced caspase activation (Figure 2a) and hence were expected to mediate apoptosis, zVAD-fmk was not able to diminish Jurkat cell death. In contrast, anti-α-toxin completely blocked α-toxin-induced death of both cell lines, but had no effect on CD95- or etoposide-induced apoptosis (Figure 3c, d). In addition, cell death assessment by the trypan blue exclusion assay confirmed these results and revealed no differences in the susceptibility of both Jurkat cell lines to the cytotoxic activity of *S. aureus* Wood 46 supernatant (Figure 3e). Together, these results demonstrate that although *S. aureus* α-toxin efficiently induces caspase activation, cell death induced by this pathogen proceeds most likely in a caspase-independent manner.

S. aureus α-toxin induces caspase-independent high molecular weight DNA fragmentation

As zVAD-fmk completely blocked α-toxin-induced internucleosomal DNA fragmentation, but only partially prevented the formation of hypodiploid nuclei (Figure 1), we assessed the possibility of high molecular weight DNA breaks induced by this toxin. For this purpose, DNA from Jurkat cells treated for 4 h with various concentrations of α-toxin in the absence or presence of zVAD-fmk or the anti-α-toxin antibody was analyzed by pulsed field gel electrophoresis. Compared to untreated cells, all concentrations of α-toxin markedly induced high molecular weight DNA breaks in Jurkat cells, ranging from approximately 700 to 50 kb in size (Figure 4a, lanes 2–5). Remarkably, even at an α-toxin concentration of 3 ng/ml that did not induce caspase activation (Figure 2), a high molecular weight DNA fragmentation that was efficiently blocked by the anti-α-toxin antibody was observed (Figure 4a, lanes 10–13), but not by zVAD-fmk (Figure 4a, lanes 6–9). In contrast, zVAD-fmk significantly increased the accumulation of α-toxin-induced high molecular weight DNA fragments, most likely caused by the inhibition of caspases required for the further degradation of the DNA into oligonucleosomal fragments.

A similar phenomenon was also observed when DNA from anti-CD95-treated Jurkat cells was analyzed. In this case, we could not detect any high molecular weight DNA fragmentation (Figure 4a, lane 14), because at this time point most of the DNA was already cleaved into the internucleosomal fragments (data not shown), and almost no intact DNA remained in the gel slot. Although the addition of zVAD-fmk completely prevented anti-CD95-induced internucleosomal DNA fragmentation (data not shown), it also resulted in the appearance of the 700 and 50 kb DNA fragments (Figure 4a, lane 15). These results indicate that also during CD95-induced apoptosis, signals that lead to caspase-dependent and-independent DNA fragmentation are generated. In contrast, H_2O_2-induced DNA fragmentation appears to proceed solely via a caspase-independent pathway, as zVAD-fmk did not change the pattern of high molecular weight DNA breaks (Figure 4a, compare lanes 16 and 17).

In addition to α-toxin, *S. aureus* also secretes a nuclease. To investigate whether our α-toxin preparation or the cytotoxic supernatant of *S. aureus* cultures exhibit intrinsic DNA fragmentation activity, we analyzed DNA isolated from untreated Jurkat cells, which was incubated with various concentrations of α-toxin or Wood 46 supernatant by pulsed field and by conventional gel electrophoresis. As shown in Figure 4b, DNA was only excessively fragmented by DNase I, but remained fully intact even in the presence of high α-toxin or Wood 46 concentrations. Thus, we conclude that α-toxin- and Wood 46-induced DNA fragmentation is not mediated by a contaminating nuclease, but most likely by activation of an as yet unknown intracellular caspase-independent DNase.

S. aureus α-toxin mediates cell death via a necrotic pathway

So far, all experiments performed point to a caspase-independent cell death induced by α-toxin. To verify these results in other experimental settings, we also assessed cell death by alternative methods. First, we measured the release of lactate dehydrogenase (LDH), an event that appears to be more closely associated with necrosis than apoptosis. Consistent with this, we observed a dramatic increase of LDH activity in supernatants of Jurkat and Jurkat Bcl-2 cells incubated with H_2O_2, a typical inducer of necrosis, whereas treatment of the cells with the apoptotic inducer CD95 did not result in a significant release of this enzyme (Figure 5b, d). In

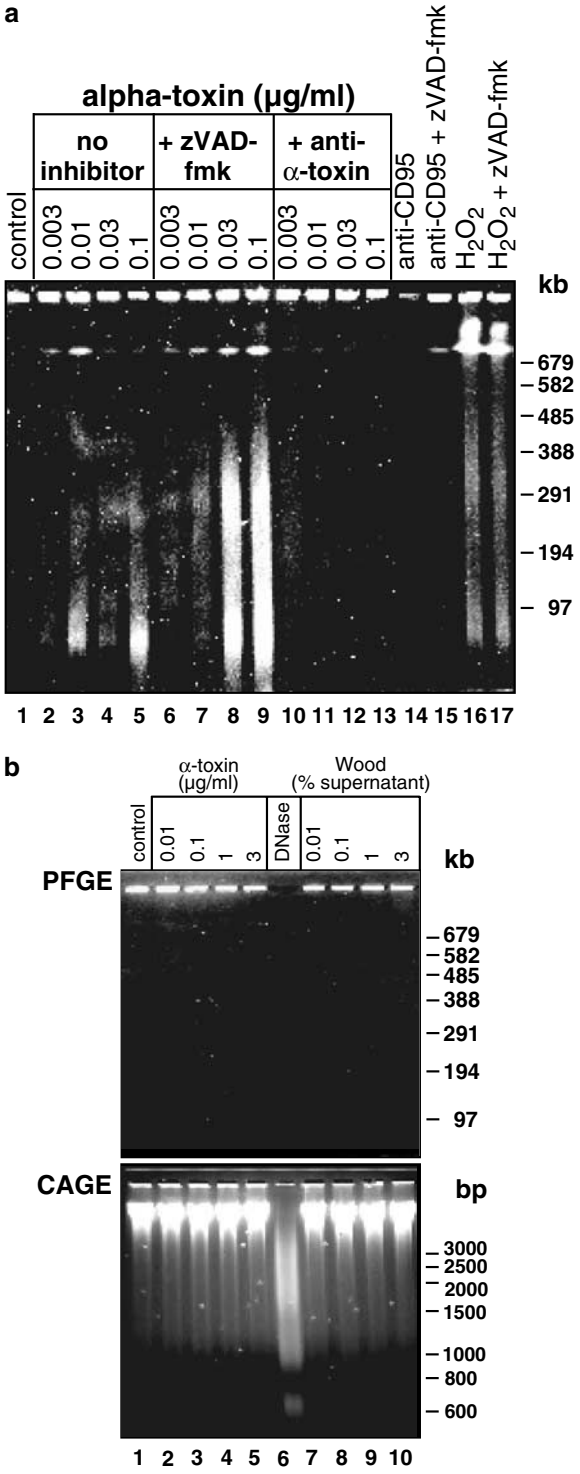

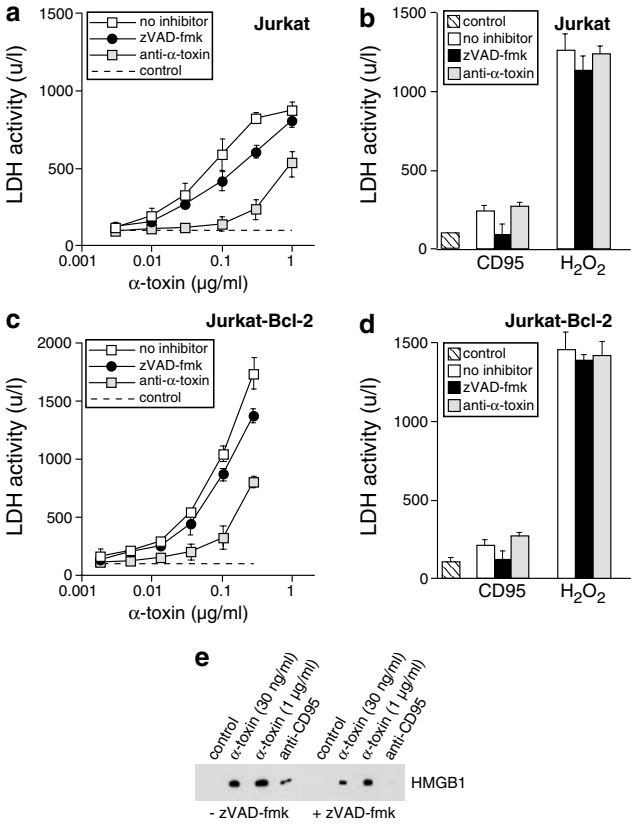

Figure 5 α-toxin induces the release of LDH and HMGB1 independently of caspases. (**a**, **c**) Measurement of LDH release in supernatants of Jurkat (**a**) and Jurkat Bcl-2 cells (**c**) that were incubated for 4 h with the indicated concentrations of α-toxin in the absence or presence of zVAD-fmk or the anti-α-toxin antibody. (**b**, **d**) Supernatants of both cell lines were also analyzed for LDH activity following treatment with anti-CD95 or H_2O_2 in the absence or presence of zVAD-fmk or the anti-α-toxin antibody. One representative experiment out of three is shown. (**e**) Jurkat cells were either treated with low (30 ng/ml) or high (1 µg/ml) α-toxin concentrations or with anti-CD95 (500 ng/ml) in the absence or presence of zVAD-fmk. After 16 h, cells were pelleted at 1200 rpm, and the supernatants were analyzed for the release of HMGB1 by Western blotting

Figure 4 α-toxin induces high molecular DNA fragmentation. (**a**) Jurkat cells were either left untreated (control) or incubated for 2 h with the indicated concentrations of α-toxin in the absence (lanes 2–5) or presence of zVAD-fmk (lanes 6–9) or the anti-α-toxin antibody (lanes 10–13). Cells were also treated for 2 h with anti-CD95 (lane 14 and 15) or H_2O_2 (lane 16 and 17) in the absence or presence of zVAD-fmk. High molecular weight DNA fragmentation was determined by PFGE. The positions of the DNA molecular size marker are indicated on the right. (**b**) α-toxin or Wood-46 supernatants do not exhibit intrinsic DNase activity. Isolated DNA from untreated Jurkat cells was either left untreated (control), or incubated for 2 h at 37°C with the indicated concentrations of α-toxin or Wood 46 supernatant. As a control, DNA was incubated with DNaseI (400 U/ml). High molecular weight and internucleosomal DNA fragmentation were determined by PFGE (top) and CAGE (bottom), respectively. The positions of the DNA molecular size markers are indicated on the right

addition, the caspase inhibitor zVAD-fmk had only a marginal effect on LDH release induced by both death stimuli, implying that this assay might be suitable to distinguish necrotic from apoptotic forms of cell death.

When Jurkat or Jurkat Bcl-2 cells were incubated with the indicated concentrations of α-toxin, a dose-dependent increase in LDH activity was observed in their supernatants (Figure 5a, c). Interestingly, this effect was even more pronounced in Jurkat Bcl-2 cells, a cell line in which *S. aureus* fails to induce caspase activation.[32] More important, however, was our finding that α-toxin-induced LDH release from both cell lines was only blocked in the presence of the anti-α-toxin antibody, but not by zVAD-fmk. In agreement with our previous data (Figures 2 and 3), zVAD-fmk also had no effect even when low, caspase-activating α-toxin concentrations were used, confirming that α-toxin induces a caspase-independent mode of cell death.

Recently, the high-mobility group 1 (HMGB1) protein was identified as another specific marker to distinguish necrosis from apoptosis.[34] It was shown that HMGB1 is only released into the supernatant of necrotic cells, but barely in the supernatant of apoptotic cells due to its tight association with chromatin. In agreement with this report, we observed only a slight release of HMGB1 into the supernatant of Jurkat cells stimulated for 14 h with anti-CD95 that was completely abrogated by zVAD-fmk (Figure 5e). In contrast, when the cells were treated with either 30 μg/ml or 1 μg/ml α-toxin, a substantial HMGB1 release could be detected, which was only marginally affected by the presence of zVAD-fmk (Figure 5e), further supporting the above drawn conclusion.

Intracellular (d)ATP is a critical coactivator of caspases required for the formation of the apoptosome in the mitochondrial death pathway.[2] Hence, in caspase-dependent apoptosis systems, inhibition of caspase activation by either Bcl-2 or zVAD-fmk should maintain the intracellular ATP levels. Based on this assumption, we monitored the ATP content of anti-CD95- or H_2O_2-treated Jurkat cells, which are considered to be type II cells in which CD95-induced apoptosis is mediated also via the intrinsic death pathway.[35] Indeed, anti-CD95-induced ATP depletion in Jurkat cells was completely abrogated in the presence of either zVAD-fmk or Bcl-2, confirming our assumption (Figure 6c). In contrast, both caspase inhibitors had no effect on H_2O_2-induced ATP depletion, clearly demonstrating the caspase-independent necrotic mode of cell death (Figure 6c). Therefore, measurement of the intracellular ATP content in the presence of caspase inhibitors represents an efficient assay to distinguish whether a particular cell death system requires active caspases or not.

In Jurkat cells, α-toxin mediates caspase activation solely via the mitochondrial death pathway, independently of death receptor signaling.[32] In contrast to the caspase-dependent mode of cell death instigated by anti-CD95, α-toxin induced a dose-dependent ATP depletion in Jurkat cells that could only be blocked by anti-α-toxin, but not by zVAD-fmk or Bcl-2 (Figures 6a and b, respectively). In addition, our data reveal that also in contrast to CD95, α-toxin induced the intracellular loss of ATP in Jurkat and in Jurkat Bcl-2 cells with a similar dose dependency. Thus, with regard to some biochemical criteria, our data demonstrate that cell death induced by

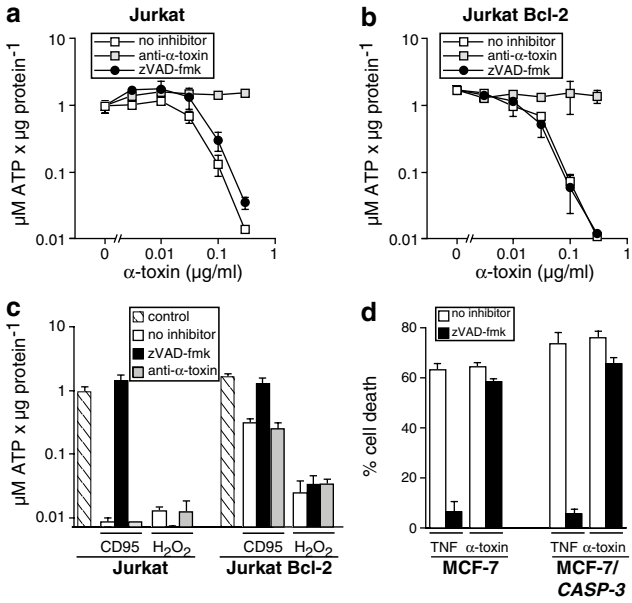

Figure 6 α-toxin induces intracellular ATP depletion independently of caspases. (**a**, **b**) Determination of the intracellular ATP content present in Jurkat (**a**) and Jurkat Bcl-2 cells (**b**) following a 4 h exposure to the indicated concentrations of α-toxin in the absence or presence of zVAD-fmk or the anti-α-toxin antibody. (**c**) Determination of the intracellular ATP content present in Jurkat and Jurkat Bcl-2 cells following a 4 h exposure to anti-CD95 or H_2O_2 in the absence or presence of zVAD-fmk or the anti-α-toxin antibody. Control bars represent the intracellular ATP content in untreated cells. One representative experiment out of three is shown. (**d**) α-toxin also induces in MCF-7 cells a caspase-independent form of cell death. Determination of cell death of MCF-7 and MCF-7/*CASP-3* cells treated for 16 h with TNF (30 ng/ml) or α-toxin (30 ng/ml) in the absence or presence of zVAD-fmk. Cell death was assessed by the crystal violet assay that is based on the staining of viable cells

α-toxin resembles rather the caspase-independent necrotic death induced by H_2O_2 than that of the caspase-dependent CD95-mediated apoptotic pathway.

So far, α-toxin-induced cell death was only assessed in Jurkat cells and with methods based on the uptake or release of small molecules through the cellular membrane. As α-toxin is a pore-forming toxin, these measurements may not accurately reflect the nature of cell death induced by this staphylococcal toxin. Therefore, α-toxin-induced cell death was also assessed in MCF-7 and MCF-7/*CASP-3* breast carcinoma cells[33] by the crystal violet assay that is based on the staining of adherent and hence viable cells. In agreement with our previous results, we found that although both cell lines were efficiently killed by TNF or α-toxin, zVAD-fmk rescued only TNF-treated cells, but had no effect on cell death induced by α-toxin (Figure 6d). Owing to a 47 bp deletion in the *casp-3* gene, MCF-7 cells completely lack caspase-3 protein, which is required for internucleosomal DNA fragmentation.[33] However, caspase-3-deficient MCF-7 cells were killed by α-toxin to a similar extent as caspase-3-expressing MCF-7 cells, clearly demonstrating that α-toxin-induced death is not only independent of caspase-3, but also independent of the characteristic apoptotic events mediated by this protease. Therefore, our data indicate that α-toxin induces a caspase-independent necrotic death pathway.

α-toxin induces a necrotic form of cell death that is biochemically and morphologically distinct from apoptosis even in the presence of active caspases

Numerous studies have described caspase-independent apoptosis pathways that, however, only surface in the presence of zVAD-fmk.[5–7,16–19] Common to all these systems was the observation that zVAD-fmk did not prevent cell death, but changed the apoptotic morphology to a necrotic phenotype. Having clearly established that inhibition of caspases does not protect cells from α-toxin-mediated cytotoxicity, the question still remained whether the same scenario applies to cell death induced by α-toxin, or whether α-toxin induces necrosis even in the presence of active caspases. In an attempt to answer this question, we first compared the cell death patterns induced by low (30 ng/ml) and high (1 μg/ml) α-toxin concentrations with the apoptotic mode of cell death induced by anti-CD95 using the conventional annexin V/PI double-staining technique. This method allows to follow the fate of dying cells that under typical apoptotic conditions first stain positive for annexin V (early apoptotic cells) and then become double positive for annexin V and PI (late apoptotic or secondary necrotic cells). Anti-CD95 induced equal proportions of single- and double-positive cells that could be completely blocked by zVAD-fmk (Figure 7). Overexpression of Bcl-2, however, only partially prevented anti-CD95-induced cell death (double-positive cells), but not the generation of single-positive annexin V-stained cells, which is consistent with the death receptor-mediated pathway. On the other hand, treatment of Jurkat cells with the low, caspase-activating dose of α-toxin did not result in the generation of annexin V single-positive cells, but predominantly in annexin V/PI double-

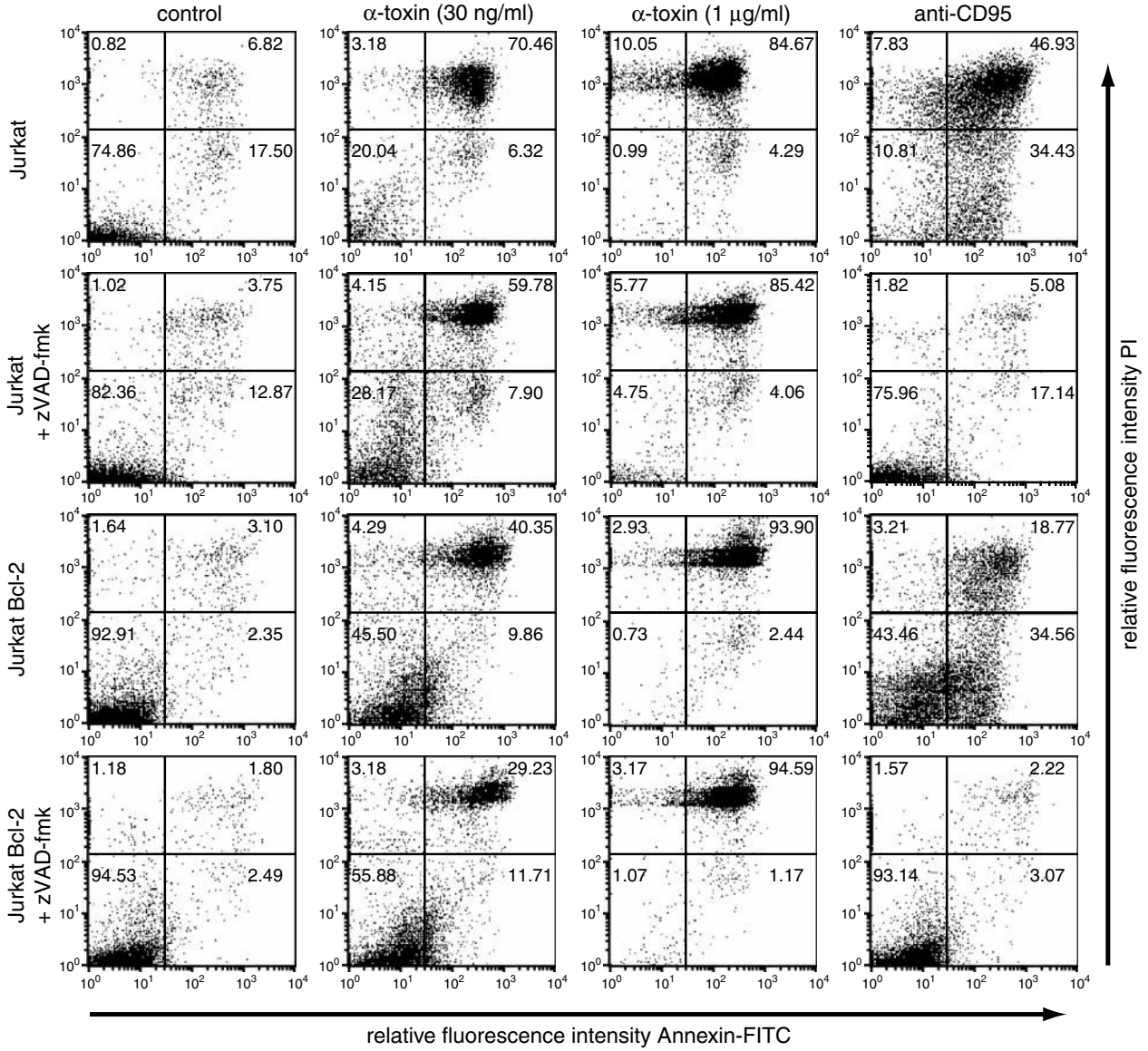

Figure 7 Comparison of α-toxin- and anti-CD95-induced cell death by annexin V and PI double staining. Following treatment of Jurkat cells with the indicated concentrations of anti-CD95 or α-toxin for 14 h, the cells were double stained with propidium iodide and the fluorescence-labeled annexin V-FITC. Cell death and caspase activation were assessed in parallel by flow cytometric analyses. One representative experiment of two performed in duplicates is shown

positive cells, an event that was also observed at 4 h (data not shown). This cell population was, in contrast to anti-CD95, not substantially decreased in the presence of zVAD-fmk and only partially reduced by Bcl-2. As expected, both means of caspase inhibition had also no effect on cell death induced by the higher α-toxin dose of 1 μg/ml (Figure 7). Of note, however, is our observation that the high α-toxin dose of 1 μg/ml, which is not capable of activating caspases (Figure 2) does not only induce the uptake of PI, but also the binding of annexin V (double-positive cells). This suggests that annexin V staining might be unrelated to caspases in α-toxin-induced cell death. Together, these results provide further evidence that α-toxin-induced cell death differs greatly from the classical apoptotic pattern induced by anti-CD95.

Next, we assessed the possible heterogeneity of α-toxin- and anti-CD95-treated Jurkat cells by double staining them with PI, and a fluorescence-labeled pan caspase peptide, FITC-VAD-fmk, that recognizes active caspases. FACS analysis of Jurkat cells that were treated for 4 h with anti-CD95 showed a dose-dependent increase only of FITC-positive cells, whereas the proportion of PI-stained cells (necrotic cells) was only marginally elevated over background levels (Figure 8a, upper left panel). Further dissection of the data revealed that these caspase-positive cells were single FITC-positive cells (apoptotic cells), as the 4 h treatment with anti-CD95 did neither result in an increase of single PI- or double (FITC/PI)-stained cells (Figure 8b, upper left panel). After a 16 h treatment with anti-CD95, however, both FITC- and PI-positive cells increased to the same extent (Figure 8a, lower left panel). These cells were exclusively double (FITC/PI)-stained cells (Figure 8b, lower left panel), indicating a process called secondary necrosis, which is known to occur at a later stage in CD95-induced apoptosis. Thus, our results clearly demonstrate that truly apoptotic cells only display caspase activation, but are not yet permeable for PI.

When similar experiments were performed with α-toxin-treated Jurkat cells, the results differed greatly from those obtained following anti-CD95 treatment. Here, a 4 h treatment with α-toxin induced a dose-dependent increase of cells positive for active caspases, which was exactly paralleled by PI-stained cells (Figure 8a, upper right panel). The difference to the profile obtained with active caspase-3 (Figure 2) is most likely due to the fact that besides caspase-3, α-toxin induces also the activation of other caspases such as caspase-8, -9,[32] -6, and -7, which can be all detected by the FITC-VAD-fmk substrate. Nevertheless, this result is in sharp contrast to CD95-induced apoptosis, and indicates that α-toxin-treated cells die via necrosis, despite the presence of active caspases. This assumption was further supported when the data were plotted in a manner that allows to assess the heterogeneity within the α-toxin-treated cell population in more detail. In contrast to anti-CD95, a 4 h treatment with α-toxin significantly increased the proportion of double-positive cells, whereas both single-positive cell populations even decreased after a slight initial rise (Figure 8b, upper right panel). Interestingly, when the cells were treated for 4 h with an α-toxin concentration of 30 ng/ml, all the three cell populations were present to approximately the same extent (Figure 8b, upper right panel), indicating not only the parallel occurrence of apoptosis and necrosis, but also confirming the process of necrosis in the presence of active caspases. Similar results were obtained when the cells were exposed to α-toxin for shorter times (data not shown). In contrast, a prolonged treatment for 16 h (Figure 8b, lower right panel) or higher α-toxin doses (Figure 8b, right panels) yielded preferentially in the generation of double-positive cells. As

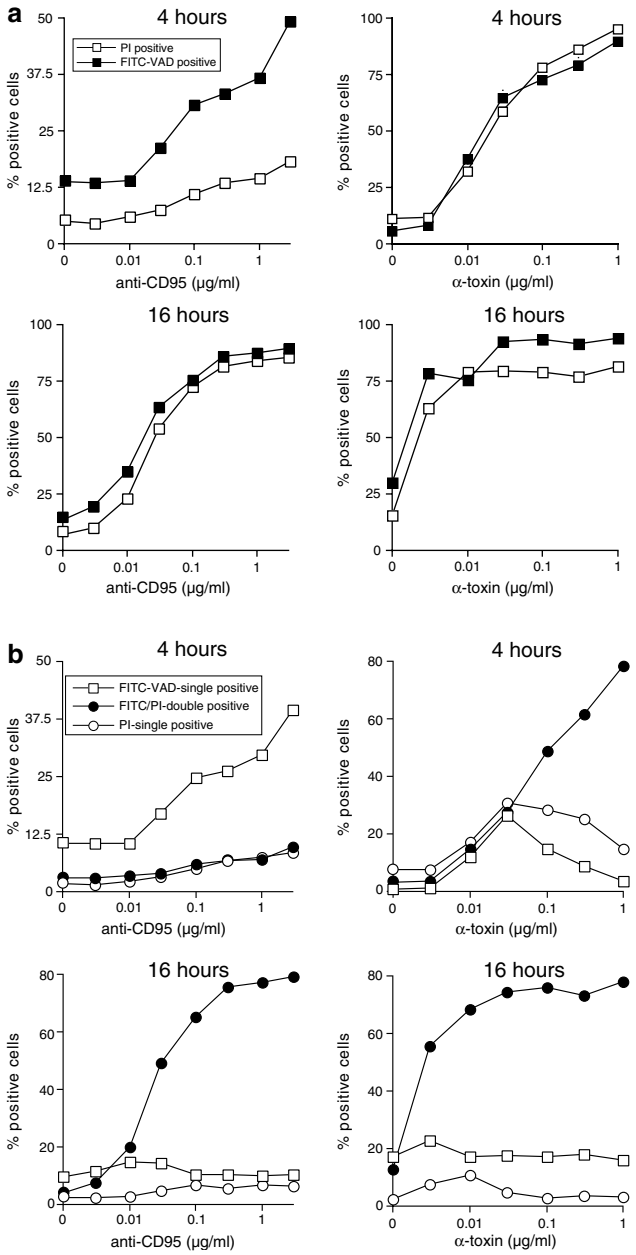

Figure 8 α-toxin induces necrosis even in the presence of active caspases. Following treatment of Jurkat cells with the indicated concentrations of anti-CD95 or α-toxin for 4 and 16 h, the cells were double stained with PI and the fluorescence-labeled pan caspase-peptide FITC-VAD-fmk. Cell death and caspase activation were assessed in parallel by flow cytometric analyses. Note that in (**a**) each line represents the whole population of PI- or FITC-stained cells including single- and double-positive cells, whereas in (**b**) the three subpopulations are plotted individually. One representative experiment of two performed in duplicates is shown

overexpression of Bcl-2 or cotreatment with zVAD-fmk completely abrogated α-toxin-induced caspase activation without exhibiting a dramatic influence on the percentage of PI- and annexin V-positive cells (Figures 2, 3, 7), we conclude that caspases, although efficiently activated, are dispensible for α-toxin-induced cell death. More importantly, our data demonstrate that α-toxin at least partially mediates a necrotic form of cell death even in the presence of active caspases.

To confirm these findings at the ultrastructural level, we finally analyzed α-toxin- and anti-CD95-treated Jurkat cells by electron microscopy. Anti-CD95-treated Jurkat cells showed the typical morphological characteristics of apoptotic cells such as shrinkage, chromatin condensation and fragmentation into apoptotic bodies (Figure 9a, e). As expected, all these events were completely abrogated in the presence of zVAD-fmk (Figure 9b, f). However, a completely different picture emerged when the cells were treated with 30 ng/ml α-toxin, a dose that induces not only caspase activation, but also the uptake of PI (Figures 2, 7, 8). Here we observed a swelling not only of the cytoplasm, but also of the nucleus and nuclear envelope (Figure 9c). In addition, excessive cytoplasmic vacuolation was visible, resembling a necrotic morphology. Moreover, the chromatin of α-toxin-treated cells was only partially condensed, whereas the mitochondria appeared extremely electron dense. As expected, inhibition of caspases by zVAD-fmk did not prevent these events and, most importantly, these cells appeared with a similar morphology as those treated with α-toxin alone (Figure 9d). The phenomenon that α-toxin-treated Jurkat cells displayed prominent necrotic features (swelling of the nucleus, vacuolization) in the presence or absence of active caspases was observed throughout the entire preparations (Figure 9g, h). Thus, our data reveal that caspase activation does not necessarily lead to an apoptotic mode of cell death.

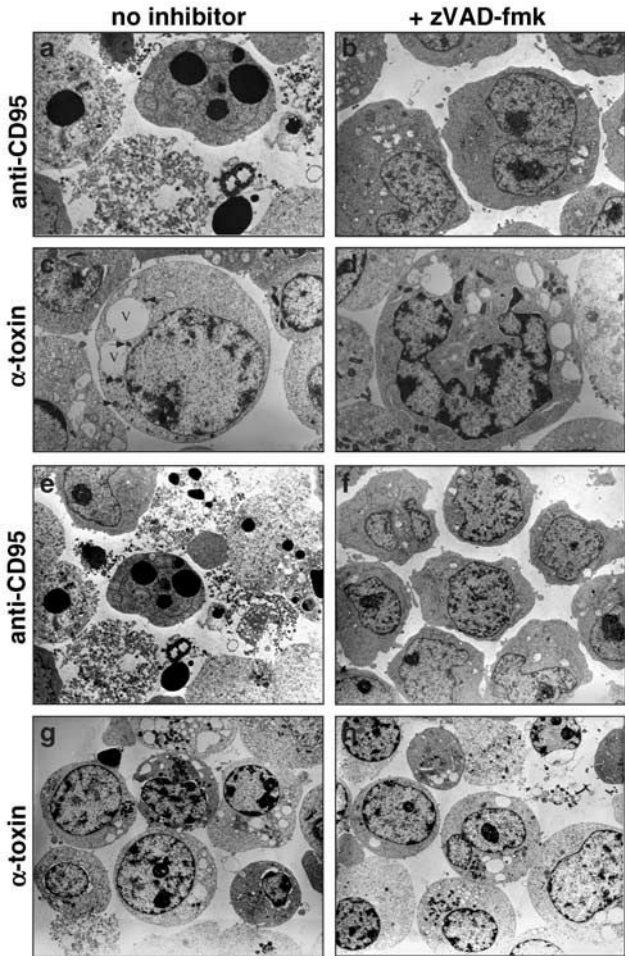

Figure 9 α-toxin induces a necrotic cell morphology even in the presence of active caspases. Ultrastructural analysis of Jurkat cells treated for 4 h with anti-CD95 (**a**, **b**, **e**, **f**) or with 30 ng/ml α-toxin (**c**, **d**, **g**, **h**) in the absence (**a**, **c**, **e**, **g**) or presence (**b**, **d**, **f**, **h**) of zVAD-fmk. Note that the dose of 30 ng/ml α-toxin efficiently induces the activation of caspase-3 as shown in Figure 2. In (**c**), condensed mitochondria are marked by an arrow and vacuoles by a V (magnification, × 2600)

Discussion

α-toxin, the major hemolysin of *S. aureus*, is a pore-forming protein, which was shown to evoke the typical apoptotic alterations such as oligonucleosomal DNA fragmentation and caspase activation in a variety of cell types.[24,25,32] Previously, we have demonstrated that α-toxin is a mediator of *S. aureus*-induced cell death, and that it activates caspases via the mitochondrial pathway.[32] Caspase activation and subsequent apoptotic alterations such as oligonucleosomal DNA fragmentation and substrate cleavage were, however, only observed with low (<300 ng/ml) α-toxin doses. These findings are consistent with the current concept of α-toxin-induced cell death that only low α-toxin doses induce apoptosis, whereas treatment with higher doses results in massive necrosis.[24,30,31] Therefore, it was postulated that the mode of cell death might critically depend on the concentration of α-toxin.

This view, however, is now being challenged by our present study, showing that low α-toxin concentrations also induce, at least partially, a necrotic form of cell death even in the presence of activated caspases. This could be readily demonstrated in various cell death assays including the microscopic assessment of trypan blue-stained cells or in FACS analyses based on the uptake of PI into dead cells. Although caspase activation and subsequent apoptotic alterations such as oligonucleosomal DNA fragmentation and substrate cleavage in α-toxin-treated Jurkat cells were completely blocked by the broad-spectrum caspase-inhibitory peptide zVAD-fmk or by overexpression of Bcl-2, they could not prevent final cell death. Similar results were obtained by measuring the release of LDH and HMGB1 in cell supernatants. Regardless of whether caspases were inhibited or not, LDH activity and HMGB1 protein were predominantly detected in supernatants of α-toxin-treated cells, but barely in supernatants of apoptotic CD95-treated cells. Although it was recently shown that LDH can be also released by late apoptotic cells,[34] together our data suggest that, at all concentrations tested, α-toxin induces a necrotic rather than an apoptotic form of cell death. Furthermore, in contrast to the CD95-induced ATP depletion that was clearly dependent on the activation of caspases, caspase inhibition had no effect on the loss of intracellular ATP levels observed in α-toxin-treated Jurkat cells. As ATP is required for most apoptotic

processes,[17,36] the caspase-independent loss of ATP also explains the inability of high α-toxin doses (>300 ng/ml) to activate caspase-3. Interestingly, in all assays performed, we did not detect any significant differences in the dose- and time (data not shown)-dependent α-toxin-induced cell death rates in the presence or absence of zVAD-fmk or Bcl-2. These results clearly demonstrate that caspases are not required for α-toxin-induced cell death and, furthermore, suggest that cell death may proceed even in the presence of active caspases independently of them.

As all these measurements are based on either the release or uptake of molecules through the cellular membrane, one could argue that they might not be adequate assessments of cell death induced by a pore-forming toxin. However, in contrast to TNF, α-toxin-induced death of MCF-7 breast carcinoma cells could not be blocked by zVAD-fmk, as assessed by the crystal violet assay that is based on the staining of viable adherent cells independently of pore formation. Importantly, α-toxin induced similar cell death rates in caspase-3-deficient and -proficient MCF-7 cells, clearly demonstrating that even low α-toxin concentrations induce cell death in a caspase-3-independent manner.

Caspase-independent apoptosis was recently observed in a variety of *in vitro* systems, including that induced by Bax-related proteins,[5–7] oncogenes and DNA-damaging agents,[7] and even death receptors.[16–19] In addition, caspase-independent death pathways also appear to be involved in the negative selection of lymphocytes,[8,37] and the embryonic removal of interdigital webs.[38] Caspase inhibition by zVAD-fmk efficiently blocked the typical apoptotic alterations in all of these systems, but could not prevent cell death itself. Instead, addition of zVAD-fmk changed the phenotype of the dying cell from the apoptotic into the necrotic morphology. As cell death, however, could be completely blocked by Bcl-2, and hence is under the tight control of an intrinsic survival program, they are considered as apoptosis-like programmed cell deaths.[1] This is in sharp contrast to cell death induced by α-toxin. Firstly, α-toxin-induced cell death is not inhibitable by Bcl-2. Secondly, α-toxin concentrations up to 30 ng/ml induced an equal mixture of single caspase- and PI-positive cells as well as double-positive cells after 4 h, and the latter cell population was even further increased when higher α-toxin doses were applied. In contrast, CD95-induced apoptosis resulted after 4 h exclusively in the generation of single caspase-positive cells that were not yet permeable for PI, demonstrating that at least early apoptosis is solely characterized by caspase activation and not by membrane damage. However, it should be noted that FITC-VAD-fmk might also detect other proteases than caspases. Finally, and most importantly, ultrastructural analysis revealed that even Jurkat cells treated with low α-toxin doses (30 ng/ml) in the absence of caspase inhibitors displayed a prominent necrotic phenotype, characterized by swelling of the cytoplasm and nuclei as well as by cytoplasmic vacuolation. These intriguing observations demonstrate that α-toxin induces predominantly a necrotic form of cell death even in the presence of active caspases, which is unlike other caspase-independent apoptosis systems not under the control of an intrinsic survival program.

Why are caspases then activated so efficiently by *S. aureus* α-toxin? The answer might lie in the molecular properties of α-toxin itself. Insertion of α-toxin into the plasma membrane and subsequent pore formation will lead to K^+ efflux and Na^+ influx.[24,30,31] Potassium efflux has been described as an important event in the progression of apoptosis,[39] and prevention of this efflux was shown to inhibit death receptor- and chemical-induced apoptosis.[40,41] Potassium depletion may even be required for apoptosis, since normal intracellular K^+ concentrations inhibited caspase activation and DNA fragmentation,[42] whereas the depletion of potassium ions with depolarizing drugs was shown to cause caspase activation.[43] Therefore, caspase activation by α-toxin might be only a side effect caused by the pore-forming properties of this molecule.

Treatment of Jurkat cells with α-toxin resulted in both oligonucleosomal and high molecular weight DNA fragmentation, and only the former event could be inhibited by zVAD-fmk. This is consistent with the caspase-3-dependent activation of ICAD/DFF45 that is necessary for the apoptosis-specific oligonucleosomal DNA fragmentation.[44,45] As neither the α-toxin preparation nor supernatants of the cytotoxic *S. aureus* strain Wood 46 exhibited any intrinsic DNase activity, it is likely that α-toxin induces an as yet unknown factor that mediates high molecular weight DNA fragmentation. One possible candidate might be the recently identified apoptosis-inducing factor (AIF). Upon treatment of cells with various stimuli, AIF was shown to be released from the mitochondria and to translocate to the nucleus, where it mediates via an as yet unknown factor high molecular weight DNA fragmentation.[46] Indeed, a similar scenario was described in cell death induced by *S. pneumoniae* which is also not inhibitable by zVAD-fmk.[47] In this study, exposure of microglia or neurons to live pneumococci caused the mitochondrial release of AIF and high molecular weight DNA fragmentation, which was blocked by microinjection of AIF-specific antiserum. As α-toxin can directly target mitochondria leading to cytochrome *c* release,[32] one might speculate that α-toxin-induced AIF translocation might be particularly important in those cell types, in which cell death induction may require internalization of *S. aureus*.[25–28]

In view of the fact that AIF does not exhibit intrinsic DNase activity, the downstream effectors remain obscure. Although several noncaspase proteases such as calpains, serine proteases and cathepsins have been implicated in cell death processes,[48–51] and even the loading of any type of protease into cells provoked apoptosis-like morphologies,[52] it is presently unknown whether any of these proteases are involved in α-toxin-induced cell death. Nevertheless, the results presented here suggest that *S. aureus* α-toxin induces cell death independently of caspases. In addition, we provide strong evidence that this cell death proceeds via the necrotic pathway even in the presence of active caspases. On first glance, our previous report[32] and the present study appear to be contradictory. This is, however, not the case, as we demonstrate in both studies the efficient activation of caspases by α-toxin. Previously, we focused our investigations solely on the caspase activation pathway, but not on the mode of cell death induced by α-toxin. Therefore, the use of zVAD-fmk was not essential for these experiments. Having noticed, however, that the α-toxin-induced formation of hypodiploid nuclei was only partially inhibited in Jurkat-Bcl-2 cells, we performed additional studies using the pan caspase-

inhibitory peptide zVAD-fmk, which enabled us to clearly demonstrate that caspases, although efficiently activated, are not essential for α-toxin-induced cell death. Hence, our findings deliver a cautionary note that even caspase activation might not always be linked to an apoptotic phenotype, and should help to better understand the pathophysiological function of *S. aureus*.

Materials and Methods

Cells, reagents and antibodies

All cell lines were maintained in RPMI 1640, supplemented with 10% fetal calf serum, 10 mM glutamine and antibiotics (all from Gibco BRL, Eggenstein, Germany). MCF-7 and MCF-7/*CASP-3* breast carcinoma cells were described recently.[33] Jurkat cells stably transfected with Bcl-2 or empty vector alone were a gift from H Walczak (Heidelberg, Germany). The protease inhibitors aprotinin, antipain, pepstatin, leupeptin and phenylmethylsulfonyl fluoride (PMSF) as well as etoposide, RNase A, proteinase K and *S. aureus* α-toxin that showed a single band on a SDS polyacrylamide gel[32] were purchased from Sigma (Deisenhofen, Germany). The neutralizing polyclonal sheep anti-α-toxin antibody that was used at a 1 : 100 dilution was from Toxin Technology (Sarasota, FL, USA). The various death stimuli such as anti-CD95 mAb (BioCheck, Münster, Germany), H_2O_2 and etoposide were always used at concentrations of 1 μg/ml, 200 μM and 100 μM, respectively. DNase I, which was used at a concentration of 400 U/ml was purchased from Roche Molecular Biochemicals (Mannheim, Germany). The fluorogenic caspase substrate DEVD-AMC (*N*-acetyl-Asp-Glu-Val-Asp-aminomethyl-coumarin) was from BIOMOL (Hamburg, Germany), FITC-VAD-fmk was from Promega and annexin V-FITC was purchased from BD Biosciences (Heidelberg, Germany). The caspase-inhibitory peptide zVAD-fmk that was always used at 50 μM was from Enzyme Systems (Dublin, CA, USA). The polyclonal goat antibodies recognizing the proform and the active subunits of caspase-3 were from R&D Systems (Minneapolis, USA) and the monoclonal HMGB1 antibody was from Pharmingen.

Bacterial strains, cultures and supernatants

Culture conditions and preparation of the supernatant of the *S. aureus* strain Wood 46 were described previously.[32]

Preparation of cell extracts and Western blotting

Cell extracts were prepared as described.[53] To confirm equal loading, protein concentrations were determined with the BioRad protein assay (BioRad, Munich, Germany). Proteins were separated in SDS-polyacrylamide gels, and subjected to Western blotting. The proteins were visualized by enhanced chemiluminescent staining using ECL reagents (Amersham, Freiburg, Germany).

Cell death assays

Cell death was assessed by various methods including microscopic examination of trypan blue-stained cells, in which a minimum of 100 cells, each on four different fields of a hemocytometer, was counted. Cell death was also determined by the uptake of PI (2 μg/ml; Sigma) in the absence or presence of annexin V-FITC into nonfixed cells, and subsequent flow cytometric analyses using the FSC/FL2 profile as described previously.[54] For each determination, a minimum of 10 000 cells was analysed. Lactate dehydrogenase (LDH) activity in supernatants of cells was assessed according to the protocol of the manufacturer (Roche Molecular Biochemicals). The standard crystal violet assay was employed as an alternative cell death measurement that is based on the staining of viable cells, and was performed as described.[53]

Determination of intracellular ATP levels

ATP levels were determined using the ATP Bioluminescence Assay Kit CLS II (Roche Molecular Biochemicals). Cells were collected by centrifugation at 4°C and washed with PBS. The cell pellet was resuspended in 50 μl of ice-cold lysis buffer (100 mM Tris-HCl and 4 mM EDTA, pH 7.75), followed by the addition of 150 μl of boiling lysis buffer. The samples were incubated for 2 min at 99°C. Cell lysates were centrifuged at 10 000 rpm for 1 min at 4°C, and supernatants were collected. ATP measurement was performed using 50 μl of supernatant and 50 μl of luciferase reagent. The chemiluminescence was measured in a luminometer.

Determination of DNA fragmentation

The proportion of nuclei containing hypodiploid DNA was determined as previously described.[54] Briefly, apoptotic nuclei were prepared by lysing cells in a hypotonic lysis buffer (0.1% sodium citrate, 0.1% Triton X-100, 50 μg/ml propidium iodide), and subsequently analysed by flow cytometry on a FACScalibur (Becton Dickinson, Heidelberg, Germany) using CellQuest analysis software. For each determination, a minimum of 10 000 cells was analyzed. Internucleosomal DNA fragmentation was assessed using conventional agarose gel electrophoresis (CAGE). Cellular DNA was prepared by lysing 5×10^6 Jurkat cells in 0.2 ml of 0.5 × TE buffer (20 mM Tris, 0.5 mM EDTA, pH 8.0) containing 0.25% NP-40 and 50 μg RNase A at 37°C for 30 min. Proteinase K (200 μg/sample) was added, and the samples were incubated for another 30 min at 37°C. DNA sample buffer was added and aliquots were analyzed on 1.6% agarose gels. High molecular weight DNA fragmentation was determined by pulsed field gel electrophoresis (PFGE) as described.[55] Jurkat cells were resuspended in PBS, mixed with low melting agarose, cast into blocks and cut into slices. The slices were incubated in EC buffer (pH 7.5; 6 mM Tris-HCl, 1 M NaCl, 0.1 M EDTA, 0.5% Brij-58, 0.2% Na deoxycholate, 0.5% Na lauroyl sarcosine, 35 μg/ml RNase H) at 37°C for 2 h, followed by TE buffer (10 mM Tris-HCl, 1 mM EDTA, 100 μg/ml proteinase K) at 50°C overnight. Agarose slices of stimulated cells were loaded directly into the gel slots; those of unstimulated cells were incubated at 37°C for 2 h with the respective agents, as detailed in the figure legends. Agarose gels (1%) were run in 0.5 × TBE buffer (pH 8; 45 mM Tris, 45 mM boric acid, 1 mM EDTA) using a CHEF-DR II electrophoresis cell (BioRad) under the following conditions: 14°C, 5–50 s switch time, 120° angle and 6 V/cm.

Fluorimetric determination of caspase-3 activity and caspase staining

Caspase-3 activity was measured using the fluorogenic DEVD-AMC substrate as previously described.[32] The catalytic activities are given in arbitrary units (AU). For double stainings of necrotic membrane damage and caspase activation, cells were incubated for 20 min at 37°C with the pan-caspase *in situ* marker FITC-VAD-fmk in PBS at a final concentration of 10 μM, followed by staining with propidium iodide and subsequent flow cytometric analyses as described above.

Electron microscopy

Cells were fixed in 2.5% glutaraldehyde in 100 mM cacodylate buffer, pH 7.35, for 1 h at room temperature. After six washes of 15 min with 100 mM cacodylate buffer, the cells were incubated with 1% osmium tetroxide for 1 h at room temperature. The cells were then washed five times for 10 min in water before embedding, and all other procedures were essentially performed as described.[56]

Acknowledgements

We thank W Magura and C Reimertz for assistance with the ATP assays, V Buchwalow for electron microscopy and S Weber for PFGE. This work was supported by grants from the Interdisciplinary Center of Clinical Research of the University of Münster and the Deutsche Forschungsgemeinschaft.

References

1. Leist M and Jäättelä M (2001) Four deaths and a funeral: from caspases to alternative mechanisms. Nat. Rev. 2: 1–10
2. Cryns V and Yuan J (1998) Proteases to die for. Genes Dev. 12: 1551–1570
3. Stroh C and Schulze-Osthoff K (1998) Death by a thousand cuts: an ever increasing list of caspase substrates. Cell Death Differ. 5: 997–1000
4. Borner C and Monney L (1999) Apoptosis without caspases: an inefficient molecular guillotine? Cell Death Differ. 6: 497–507
5. Xiang J, Chao DT and Korsmeyer SJ (1996) Bax-induced cell death may not require interleukin 1-converting enzyme-like proteases. Proc. Natl. Acad. Sci. USA 93: 14559–14563
6. Miller TM, Mouldner KL, Knudson CM, Creedon DJ, Deshmukh M, Korsmeyer SJ and Johnson Jr EM (1997) Bax deletion further orders the cell death pathway in cerebellar granule cells and suggests a caspase-independent pathway to cell death. J. Cell Biol. 139: 205–217
7. McCarthy NJ, Whyte MKB, Gilbert CS and Evan GI (1997) Inhibition of Ced-3/ICE-related proteases does not prevent cell death induced by oncogenes, DNA damage, or the Bcl-2 homologue Bak. J. Cell Biol. 136: 215–227
8. Doerfler P, Forbush KA and Perlmutter RM (2000) Caspase enzyme activity is not essential for apoptosis during thymocyte development. J. Immunol. 164: 4071–4079
9. Petit F, Arnoult D, Lelievre JD, Parseval LM, Hance AJ, Schneider P, Corbeil J, Ameisen JC and Estaquier J (2001) Productive HIV-1 infection of primary CD4+ T cells induces mitochondrial membrane permeabilization leading to a caspase-independent cell death. J. Biol. Chem. 277: 1477–1487
10. Berndt C, Mopps B, Angermuller S, Gierschik P and Krammer PH (1998) CXCR4 and CD4 mediate a rapid CD95-independent cell death in $CD4^+$ T cells. Proc. Natl. Acad. Sci. USA 95: 12556–12561
11. Mateo V, Lagneaux L, Bron D, Biron G, Armant M, Delespesse G and Sarfati M (1999) CD47 ligation induces caspase-independent cell death in chronic lymphocytic leukemia. Nat. Med. 5: 1277–1284
12. Pettersen RD, Bernard G, Olafsen MK, Pourtein M and Lie SO (2001) CD99 signals caspase-independent T cell death. J. Immunol. 166: 4931–4942
13. Sarin A, Williams MS, Alexander-Miller MA, Berzofsky JA, Zacharchuk CM and Henkart PA (1997) Target cell lysis by CTL granule exocytosis is independent of ICE/Ced-3 family proteases. Immunity 6: 209–215
14. Lavoie JN, Nguyen M, Marcellus RC, Branton PE and Shore GC (1998) E4orf4, a novel adenovirus death factor that induces p53-independent apoptosis by a pathway that is not inhibited by zVAD-fmk. J. Cell Biol. 140: 637–645
15. Nylandsted J, Rohde M, Brand K, Bastholm L, Elling F and Jäättelä M (2000) Selective depletion of heat shock protein 70 (Hsp70) activates a tumor-specific death program that is independent of caspases and bypasses Bcl-2. Proc. Natl. Acad. Sci. USA 97: 7871–7876
16. Eguchi Y, Shimizu S and Tsujimoto Y (1997) Intracellular ATP levels determine cell death fate by apoptosis or necrosis. Cancer Res. 57: 1835–1840
17. Leist M, Single B, Castoldi AF, Kuhnle S and Nicotera P (1997) Intracellular adenosine triphosphate (ATP) concentration: a switch in the decision between apoptosis and necrosis. J. Exp. Med. 185: 1481–1486
18. Holler N, Zaru R, Micheau O, Thome M, Attinger A, Valitutti S, Bodmer JL, Schneider P, Seed B and Tschopp J (2000) Fas triggers an alternative, caspase-8-independent cell death pathway using the kinase RIP as effector molecule. Nat. Immunol. 1: 489–495
19. Denecker G, Vercammen D, Declercq W and Vandenabeele P (2001) Apoptotic and necrotic cell death induced by death domain receptors. Cell. Mol. Life Sci. 58: 356–370
20. Lowy FD (1998) *Staphylococcus aureus* infections. N. Engl. J. Med. 339: 520–532
21. Marrack P and Kappler J (1990) The staphylococcal enterotoxins and their relatives. Science 240: 705–711
22. Weinrauch Y and Zychlinsky A (1999) The induction of apoptosis by bacterial pathogens. Annu. Rev. Microbiol. 53: 155–187
23. Gao LY and Kwaik YA (2000) Hijacking of apoptotic pathways by bacterial pathogens. Microbes Infect. 2: 1705–1719
24. Jonas D, Walev I, Berger T, Liebetrau M, Palmer M and Bhakdi S (1994) Novel path to apoptosis: small transmembrane pores created by staphylococcal α-toxin in T lymphocytes evoke internucleosomal DNA degradation. Infect. Immun. 62: 1304–1312
25. Bayles KW, Wesson CA, Liou LE, Fox LK, Bohach GA and Trumble WR (1998) Intracellular *Staphylococcus aureus* escapes the endosome and induces apoptosis in epithelial cells. Infect. Immun. 66: 336–342
26. Menzies BE and Kourteva I (1998) Internalization of *Staphylococcus aureus* by endothelial cells induces apoptosis. Infect. Immun. 66: 5994–5998
27. Tucker KA, Reilly SS, Leslie CS and Hudson MC (2000) Intracellular *Staphylococcus aureus* induces apoptosis in mouse osteoblasts. FEMS Microbiol. Lett. 186: 151–156
28. Nuzzo I, Sanges MR, Folgore A and Carratelli CR (2000) Apoptosis of human keratinocytes after bacterial invasion. FEMS Immunol. Med. Microbiol. 27: 235–240
29. Wesson CA, Deringer J, Liou LE, Bayles KW, Bohach GA and Trumble WR (2000) Apoptosis induced by *Staphylococcus aureus* in epithelial cells utilizes a mechanism involving caspases 8 and 3. Infect. Immun. 68: 2998–3001
30. Song L, Hobaugh MR, Shustak C, Cheley S, Bayley H and Gouaux JE (1996) Structure of staphylococcal α-hemolysin, a heptameric transmembrane pore. Science 274: 1859–1866
31. Valeva A, Palmer M and Bhakdi S (1997) Staphylococcal α-toxin: formation of the heptameric pore is partially cooperative and proceeds through multiple intermediate stages. Biochemistry 36: 13298–13304
32. Bantel H, Sinha B, Domschke W, Peters G, Schulze-Osthoff K and Jänicke RU (2001) α-toxin is a mediator of *Staphylococcus aureus*-induced cell death and activates caspases via the intrinsic death pathway independently of death receptor signaling. J. Cell Biol. 155: 637–647
33. Jänicke RU, Sprengart ML, Wati MR and Porter AG (1998) Caspase-3 is required for DNA fragmentation and morphological changes associated with apoptosis. J. Biol. Chem. 273: 9357–9360
34. Scaffidi P, Mistell T and Blanchi ME (2002) Release of chromatin protein HMGB1 by necrotic cells triggers inflammation. Nature 488: 191–195
35. Scaffidi C, Fulda S, Srinivasan A, Friesen C, Li F, Tomaselli KJ, Debatin KM, Krammer PH and Peter ME (1998) Two CD95 (APO-1/Fas) signaling pathways. EMBO J. 17: 1675–1687
36. Ferrari D, Stepczynska A, Los M, Wesselborg S and Schulze-Osthoff K (1998) Differential regulation and ATP requirement for caspase-8 and caspase-3 activation during CD95- and anticancer drug-induced apoptosis. J. Exp. Med. 188: 979–984
37. Smith KG, Strasser A and Vaux DL (1996) CrmA expression in T lymphocytes of transgenic mice inhibits CD95 (Fas/APO-1)-transduced apoptosis, but does not cause lymphadenopathy or autoimmune disease. EMBO J. 15: 5167–5176
38. Chautan M, Chazal G, Cecconi F, Gruss P and Golstein P (1999) Interdigital cell death can occur through a necrotic and caspase-independent pathway. Curr. Biol. 9: 967–970
39. Bortner CD, Hughes FM and Cidlowski JA (1997) A primary role for K^+ and Na^+ efflux in the activation of apoptosis. J. Biol. Chem. 272: 32436–32442

40. Dallaporta B, Marchetti P, de Pablo MA, Maisse C, Duc HT, Métivier D, Zamzami N, Geuskens M and Kroemer G (1999) Plasma membrane potential in thymocyte apoptosis. J. Immunol. 162: 6534–6542
41. Maeno E, Ishizaki Y, Kanaseki T, Hazama A and Okada Y (2000) Normotonic cell shrinkage because of disordered volume regulation is an early prerequisite to apoptosis. Proc. Natl. Acad. Sci. USA 97: 9487–9492
42. Hughes Jr FM, Bortner CD, Purdy GD and Cidlowski JA (1997) Intracellular K^+ suppresses the activation of apoptosis in lymphocytes. J. Biol. Chem. 272: 30567–30576
43. Warny M and Kelly CP (1999) Monocytic cell necrosis is mediated by potassium depletion and caspase-like proteases. Am. J. Physiol. 276: 717–724
44. Liu X, Zou H, Slaughter C and Wang X (1997) DFF, a heterodimeric protein that functions downstream of caspase-3 to trigger DNA fragmentation during apoptosis. Cell 89: 175–184
45. Enari M, Sakahira H, Yokoyama H, Okawa K, Iwamatsu A and Nagata S (1998) A caspase-activated DNase that degrades DNA during apoptosis, and its inhibitor ICAD. Nature 391: 43–50
46. Daugas E, Susin SA, Zamzami N, Ferri KF, Irinopoulou T, Larochette N, Prevost MC, Leber B, Andrews D, Penninger J and Kroemer G (2000) Mitochondrio-nuclear translocation of AIF in apoptosis and necrosis. FASEB J. 14: 729–739
47. Braun JS, Novak R, Murray PJ, Eischen CM, Susin SA, Kroemer G, Halle A, Weber JR, Tuomanen EI and Cleveland JL (2001) Apoptosis-inducing factor mediates microglial and neuronal apoptosis caused by pneumococcus. J. Infect. Dis. 184: 1300–1309
48. Squier MKT and Cohen JJ (1996) Calpain and cell death. Cell Death Differ. 3: 275–283
49. Deis LP, Galinka H, Berissi H, Cohen O and Kimchi A (1996) Cathepsin D protease mediates programmed cell death induced by interferon, Fas/APO-1 and TNF-alpha. EMBO J. 15: 3861–3870
50. Foghsgaard L, Wissing D, Mauch D, Lademann U, Bastholm L, Boes M, Elling F, Leist M and Jäättelä M (2001) Cathepsin B acts as a dominant execution protease in tumor cell apoptosis induced by tumor necrosis factor. J. Cell Biol. 153: 999–1009
51. Wright SC, Schellenberger U, Wang H, Kinder DH, Talhouk JW and Larrick JW (1997) Activation of CPP32-like proteases is not sufficient to trigger apoptosis: inhibition of apoptosis by agents that suppress activation of AP24, but not CPP32-like activity. J. Exp. Med. 186: 1107–1117
52. Williams MS and Henkart PA (1994) Apoptotic cell death induced by intracellular proteolysis. J. Immunol. 153: 4247–4255
53. Jänicke RU, Lin XY, Lee FHH and Porter AG (1996) Cyclin D3 sensitizes tumor cells to tumor necrosis factor-induced, c-Myc-dependent apoptosis. Mol. Cell Biol. 16: 5245–5253
54. Wesselborg S, Engels IH, Rossmann E, Los M and Schulze-Osthoff K (1999) Anticancer drugs induce caspase-8/FLICE activation and apoptosis in the absence of CD95 receptor/ligand interaction. Blood 93: 3053–3063
55. Goering RV and Winters MA (1992) Rapid method for epidemiological evaluation of gram-positive cocci by field inversion gel electrophoresis. J. Clin. Microbiol. 30: 577–580
56. Schulze-Osthoff K, Krammer PH and Dröge W (1994) Divergent signalling via APO-1/Fas and the TNF receptor, two homologous molecules involved in physiological cell death. EMBO J. 13: 4587–4596

The EMBO Journal Vol. 22 No. 14 pp. 3580–3590, 2003

Induction of cell death by the BH3-only Bcl-2 homolog Nbk/Bik is mediated by an entirely Bax-dependent mitochondrial pathway

Bernhard Gillissen[1], Frank Essmann[1,2], Vilma Graupner[1], Lilian Stärck[1], Silke Radetzki[1], Bernd Dörken[1], Klaus Schulze-Osthoff[2] and Peter T.Daniel[1,3]

[1]Department of Hematology, Oncology and Tumor Immunology, Charité–Campus Berlin-Buch, Humboldt University, D-13125 Berlin-Buch and [2]Institute of Molecular Medicine, University of Düsseldorf, Düsseldorf, Germany

[3]Corresponding author
e-mail: pdaniel@mdc-berlin.de

Nbk/Bik (natural born killer/Bcl-2-interacting killer) is a tissue-specific BH3-only protein whose molecular function is still largely unknown. To investigate the mechanism of Nbk action, we established a single-vector adenoviral system based on the Tet-off conditional expression of Nbk. Upon Nbk expression, only Bax-positive, but not Bax-deficient cells were found to undergo apoptosis. Interestingly, Nbk failed to induce apoptosis in the absence of Bax, even despite expression of the related molecule Bak. Re-expression of Bax restored the sensitivity to Nbk. Similarly, Bax wild-type HCT116 cells were highly susceptible, whereas HCT116 Bax knock-out cells remained resistant to Nbk-induced apoptosis. In Bax-positive cells, Nbk induced a conformational switch in the Bax N-terminus coinciding with cytochrome *c* release, mitochondrial permeability transition and caspase-9 processing. Immunoprecipitation studies revealed that Nbk interacts with Bcl-x_L and Bcl-2 but not with Bax. Since, in addition, Nbk did not localize to the mitochondria, our data suggest a model in which Nbk acts as an indirect killer to trigger Bax-dependent apoptosis, whereas Bak is not sufficient to confer sensitivity to Nbk.

Keywords: apoptosis/Bax/Bik/mitochondria/Nbk

Introduction

Bcl-2 proteins are essential mediators of death pathways initiated at the mitochondrial level. Structural analyses revealed that the apoptosis-promoting Bcl-2 members can be subdivided into two subfamilies: (i) the Bax homologs including Bax, Bak and Bok/Mtd, and (ii) the BH3-only subfamily (reviewed in Huang and Strasser, 2000; Puthalakath and Strasser, 2002; Borner, 2003; Daniel *et al*., 2003).

Unlike several other members of the BH3-only family, the function and regulation of Nbk/Bik (natural born killer/Bcl-2-interacting killer) (Boyd *et al*., 1995; Han *et al*., 1996) are still poorly defined. Nbk shows a rather tissue-specific expression pattern which is restricted to a subset of human epithelial tissues and activated lymphoid B cells (Daniel *et al*., 1999), suggesting that Nbk plays a role in tissue-specific regulation of apoptosis. Ectopic expression of Nbk restored sensitivity to anti-cancer drugs in resistant tumor cells and impaired tumorigenicity in a mouse xenotransplant model (Daniel *et al*., 1999; Radetzki *et al*., 2002).

A recent report showed that the Nbk BH3 domain is essential for apoptosis induction and its interaction with Bcl-x_L (Tong *et al*., 2001). Similarly, the BH3-only protein Bad interacts via its BH3 domain with Bcl-x_L (Kelekar *et al*., 1997). It has also been proposed that the activity of Nbk is regulated by phosphorylation. Unlike in the case of Bad, phosphorylation increases the pro-apoptotic potency of Nbk by a presently unknown mechanism that does not affect its affinity for anti-apoptotic Bcl-2 members (Verma *et al*., 2001). Altogether, the mechanisms by which Nbk is restrained in healthy cells and by which it induces apoptosis remain largely unclear.

In order to investigate the mechanism of Nbk action and to explore a potential use of Nbk in experimental cancer models, we established a single-vector conditional adenoviral expression system based on the Tet-off system (Gossen and Bujard, 1992). Employing this conditional expression system, we show that Nbk acts as an activator of the mitochondrial apoptotic pathway through a strictly Bax-dependent mechanism. Bax-negative carcinoma cells were completely refractory to Nbk-induced apoptosis, even though they expressed the Bax-related molecule Bak. Further analyses indicated that the proapoptotic effect of Nbk was mediated by an indirect effect on Bax: Nbk did not interact directly with Bax, but instead bound to Bcl-x_L and Bcl-2. Thus, our data suggest a model in which Nbk acts as an indirect killer that triggers Bax-dependent, but Bak-independent apoptosis.

Results

Conditional expression of Nbk

We previously showed that Nbk enhances the sensitivity to different apoptosis stimuli such as CD95/Fas ligation or anti-cancer drugs (Daniel *et al*., 1999a; Radetzki *et al*., 2002). To investigate further the mechanism of this effect and to explore a potential use of Nbk gene transfer in cancer therapy, we aimed at establishing an adenoviral expression system. To circumvent the problem of induction of apoptosis in the HEK293 packaging cell line by Nbk, we constructed a conditional Tet-off expression system. To this end, the E3 region of Ad5 was replaced by the reverse tetracyclin-controlled transactivator (tTA) under the control of a cytomegalovirus (CMV) promoter and an SV40 poly(A) tail. To facilitate detection of the virally transduced Nbk, we introduced a myc tag 5′ of the Nbk cDNA and introduced the myc-Nbk cDNA into

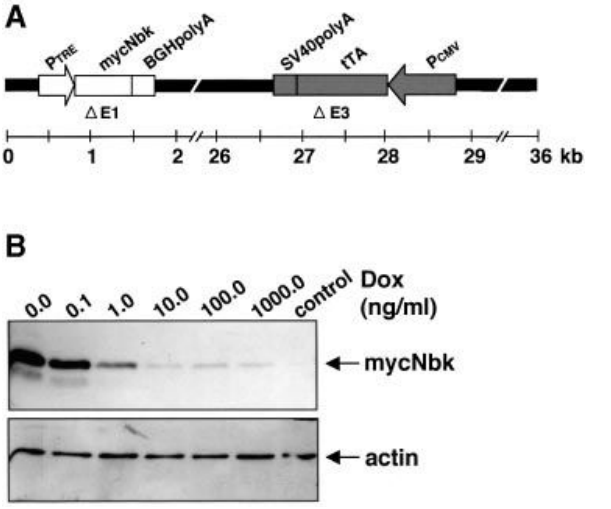

Fig. 1. Inducible Nbk expression mediated by Ad5-myc-Nbk-tTA. (**A**) Genomic structure of recombinant adenovirus Ad5-myc-Nbk-tTA. Ad5 sequences are indicated by black dashes. E1 and E3 regions of Ad5 are replaced by the myc-NBK expression cassette (white boxes) and tTA expression cassette (shaded boxes), respectively. [P_{CMV}, immediate-early promoter of cytomegalovirus; tTA, tetracyclin-controlled (Tet-off) transactivator; P_{TRE}, tetracyclin-responsive element located 5′ of the minimal immediate-early CMV promoter.] (**B**) Western blot analysis of Nbk expression in DU145 cells. Cells were infected with Ad5-myc-NBK-tTA at an m.o.i. of 25 (except control) and treated with increasing concentrations of doxycyclin (Dox) for 24 h. Equal protein loading was confirmed by immunoblotting using an anti-actin antibody. Strong induction of Nbk protein can be detected after doxycyclin withdrawal (Tet-on condition) whereas, in the presence of doxycyclin (Tet-off condition), Nbk expression is repressed to a weak background signal.

the E1 region under control of the Tet-off system to achieve conditional expression in the absence of doxycyclin (Figure 1A). The resulting Ad5-myc-Nbk-tTA DNA construct was transfected in HEK293 packaging cells to produce vector stocks. Transduction of DU145 prostate carcinoma cells with Ad5-myc-Nbk-tTA resulted in high expression of the 24 kDa myc-Nbk protein in the absence of doxycyclin, i.e. the Tet-on condition. Expression of Nbk was almost completely repressed at doxycyclin concentrations of ⩾10 ng/ml (Tet-off condition; Figure 1B).

Induction of apoptosis by Nbk gene transfer

To analyze the effect of adenoviral gene transfer of Nbk, we transduced a panel of carcinoma cells including the colon carcinoma lines LoVo, SW48 and SW480, as well as the prostate carcinoma line DU145. Adenoviral transduction in the presence of doxycyclin did not induce apoptosis and resulted in no or only marginal expression of the myc-Nbk transgene (Figures 1B and 2A). In the absence of doxycyclin, high levels of myc-Nbk (24 kDa) were expressed in all cell lines (Figure 2A). As previously shown (Daniel *et al.*, 1999), SW480 cells expressed low levels of endogenous (22 kDa) Nbk which was not affected by the adenoviral gene transfer of Nbk.

In DU145 and LoVo cells, myc-Nbk gene transfer and expression of the 24 kDa myc-Nbk also increased the intensity of a 22 kDa band. Immunoprecipitation studies (see Figures 8 and 9) showed that only the upper band, i.e. myc-Nbk, could be precipitated by an anti-myc antibody.

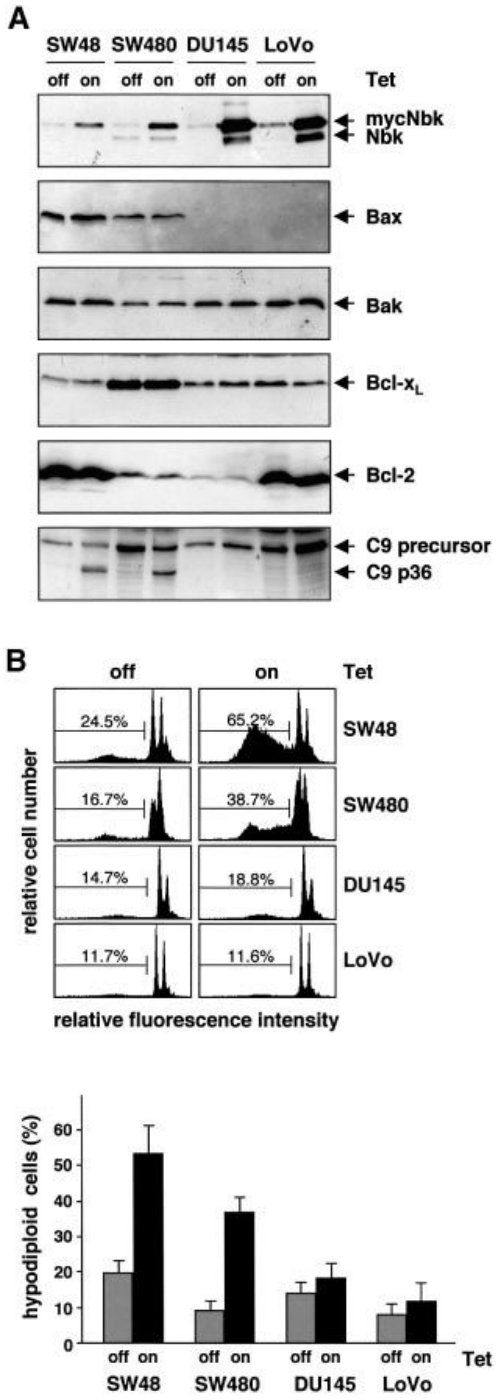

Fig. 2. Nbk expression induces apoptosis in Bax-positive but not in Bax-negative cells. Lovo, DU145, SW480 and SW48 cells were infected with Ad5-myc-NBK-tTA and cultured for 24 h in the presence (Tet-off condition) or absence of doxycyclin (Tet-on condition). (**A**) Western blot analysis for Nbk, Bax, Bak, Bcl-x_L and Bcl-2 expression and processing of procaspase-9. (**B**) Flow cytometric detection of apoptotic cells based on measurement of the cellular DNA content. Upper panel: representative experiment. The percentage of hypodiploid, apoptotic cells is indicated between markers. Lower panel: means ± SD of the percentage of hypodiploid cells from three independent experiments.

The lower band co-precipitated with Bcl-x_L and was recognized by an anti-Nbk antibody. Neither the pan-

caspase inhibitor zVAD-fmk nor calpain or cathepsin inhibitors prevented the appearance of the low molecular weight Nbk in transduced cells, suggesting that it was not generated by proteolytic cleavage (data not shown). It is known that eukaryotic ribosomes can ignore the first AUG and initiate translation at the next start codon, a phenomenon known as 'leaky scanning' (Saito and Tomita, 1999). As the start codon of endogenous Nbk is retained downstream and in-frame in the myc-tagged construct, the smaller form of Nbk was presumably generated from translation at the second AUG.

To measure induction of apoptosis upon Nbk expression, we performed flow cytometric analyses and assessed fragmentation of genomic DNA. Apoptotic cells were identified as cells with a hypodiploid, i.e. a sub-G_1, DNA content. After 24 h of transduction with Ad5-myc-Nbk-tTA, a mean of 53.2% of the SW48 and 36.7% of the SW480 cells became apoptotic when doxycyclin was absent from the culture medium (Figure 2B). In contrast, a much smaller number of cells underwent cell death in the presence of doxycyclin, which inhibits Nbk transgene expression. To our surprise, transduction of Nbk did not significantly induce apoptosis in LoVo and DU145 cells, in both the absence and presence of doxycyclin. This was not due to defective Nbk expression, as both cell lines expressed large amounts of Nbk (Figure 2A). The observation that Nbk was even expressed at higher levels in apoptosis-resistant LoVo and DU145 cells as compared with the sensitive cell lines SW48 and SW480 suggests that there is a selection pressure against the expression of Nbk.

Since DU145 cells and LoVo cells carry frameshift mutations in the Bax gene, they do not express Bax protein (Figure 2A). In contrast, SW48 and SW480 cells do express Bax, and this clear difference indicated that Bax might be required for apoptosis induction by Nbk. In addition, the higher expression level of Bcl-x_L (Figure 2A) could also contribute to the weaker induction of apoptosis in SW480 cells as compared with the SW48 cells (Figure 2B). However, there was no correlation between the expression levels of Bcl-2 and sensitivity to apoptosis induced by Nbk expression. Among the two Nbk-sensitive and Bax-positive lines, SW48 expressed high levels of Bcl-2, whereas SW480 showed low Bcl-2 expression. From the two Nbk-resistant and Bax-negative lines, DU145 cells marginally expressed Bcl-2, whereas LoVo cells showed high Bcl-2 expression (Figure 2A). Interestingly, both LoVo and DU145 cells expressed detectable levels of the Bax-related protein Bak (Figure 2A). Thus, the pro-apoptotic Bak alone was not sufficient to mediate Nbk-induced apoptosis. In turn, this indirectly indicated that Nbk might signal specifically via Bax and not through a Bak-dependent pathway.

Expression of Bax sensitizes for apoptosis induction by Nbk

To support the hypothesis that apoptosis induction by Nbk is mediated by a Bax-dependent mechanism, we overexpressed wild-type Bax in the Bax-mutated DU145 cells. To this end, we employed a retroviral vector, HyTK-Bax (Hemmati *et al*., 2002), containing the Bax-α cDNA under the control of a CMV promoter. Cells were retrovirally transduced, selected with hygromycin and screened for transgene expression by western blot analysis. Three clones were selected, DU145-Bax 2, 3 and 4, and compared with vector-transduced mock controls. The clones DU145 Bax 2 and 4 constitutively expressed high levels of Bax, whereas clone 3 showed a much lower expression level (Figure 3A).

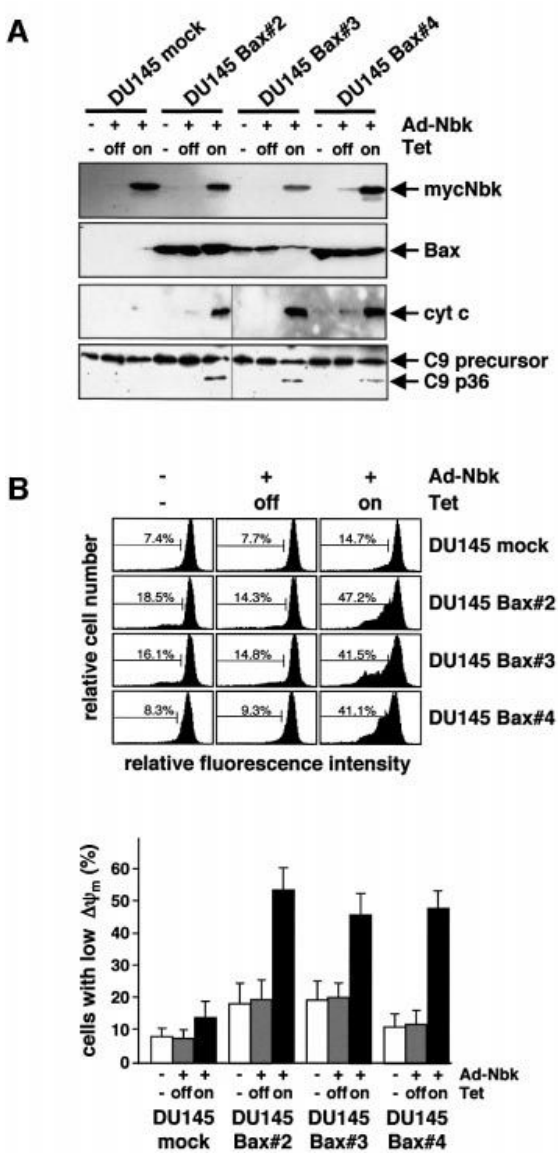

Fig. 3. Apoptotic alterations induced by Nbk in Bax-expressing DU145 clones. DU145 clones expressing exogenous Bax were generated by retroviral transfer of the Bax cDNA under control of the CMV promoter. The DU145-mock clone was generated by transduction with control HyTK retrovirus. Stable clones were transduced with Ad5-myc-Nbk-tTA and cultured for 24 h in the presence (Tet-off condition) or absence of doxycyclin (Tet-on condition). Control cells were mock treated and grown in the absence of doxycyclin. (**A**) Western blot analysis of Bax and Nbk expression, cytochrome *c* release and procaspase-9 processing in DU145-Bax clones 24 h after infection with Ad5-myc-NBK-tTA. (**B**) Disruption of mitochondrial membrane potential ($\Delta\psi_m$) by mycNbk in DU145-Bax cells. Cells were incubated with JC-1, a cationic dye that exhibits potential-dependent accumulation in mitochondria, and fluorescence intensity was measured by flow cytometry. Upper panel: representative experiment. The percentage of cells with $\Delta\psi_m$ loss is indicated between markers. Lower panel: means ± SD of the percentages of cells with $\Delta\psi_m$ loss from three independent experiments.

Consistent with a requirement for Bax for Nbk-induced apoptosis, adenoviral Nbk expression triggered the release of cytochrome *c* in the absence of doxycyclin (Tet-on condition, Figure 3A). Transduction with Ad5-myc-Nbk-tTA induced the release of cytochrome *c* to a similar extent in all three Bax clones, but not in the mock transfectants. This indicated that the relatively low Bax expression in clone 3 was sufficient to restore Nbk-induced mitochondrial activation. Likewise, all Bax clones exhibited processing of procaspase-9 upon expression of Nbk (Figure 3A).

To analyze mitochondrial permeability transition and loss of mitochondrial membrane potential ($\Delta\Psi_m$) during apoptosis, cells were incubated with JC-1 (5,5′,6,6′-tetrachloro-1,1′,3,3′-tetraethyl-benzimidazolylcarbocyanin iodide), a cationic dye that exhibits membrane potential-dependent accumulation in mitochondria. JC-1 fluorescence intensity was measured by flow cytometry on a single-cell level. The analysis of loss in $\Delta\Psi_m$ showed that all DU145 Bax transfectants underwent disruption of the mitochondrial membrane potential upon myc-Nbk expression to a similar extent. This loss of $\Delta\Psi_m$ occurred in a mean of 44.7–52.8% of the individual Bax transfectants as compared with 13.6% of the mock transfectants after Ad5-myc-Nbk-tTA transduction in the absence of doxycyclin (Figure 3B).

A sensitization for Nbk in the Bax transfectants was also apparent when apoptosis induction was analyzed by measurements of either DNA fragmentation or phosphatidylserine exposure. Adenoviral Nbk expression induced formation of hypodiploid DNA in the Bax transfectants: a mean of 31.3% (Bax clone 2), 36.2% (Bax clone 3) or 17.3% (Bax clone 4) of the cells underwent apoptosis in the absence of doxycyclin, while only 7.2% of the mock transfectants died as determined by flow cytometric analysis of apoptotic sub-G_1 cells (Figure 4A). Likewise, after transduction with Ad5-myc-Nbk-tTA and 18 h of incubation in the absence of doxycyclin, all DU145 transfectants showed an increased percentage of propidium iodide (PI)-negative cells exhibiting exposure of phosphatidylserine to the outer cell membrane (Figure 4B).

The rates of apoptosis as measured by annexin V–fluorescein isothiocyanate (FITC) staining (Figure 4B) correlated with the extent of DNA fragmentation induced by Nbk in the DU145 clones (Figure 4A). As in the DNA fragmentation assays, clone 4 showed a lower induction of apoptosis as compared with clones 2 and 3 even despite high Bax expression. Nevertheless, Bax clone 4 revealed a loss of $\Delta\Psi_m$ and release of cytochrome *c* similar to the other Bax clones. This observation is in line with an assumable selection disadvantage for cells with high Bax expression and an intact downstream signaling cascade. Clone 4 also showed impaired procaspase-9 cleavage (Figure 3A), indicating that it had presumably acquired a defect downstream of cytochrome *c* release resulting in decreased caspase activation and cell death.

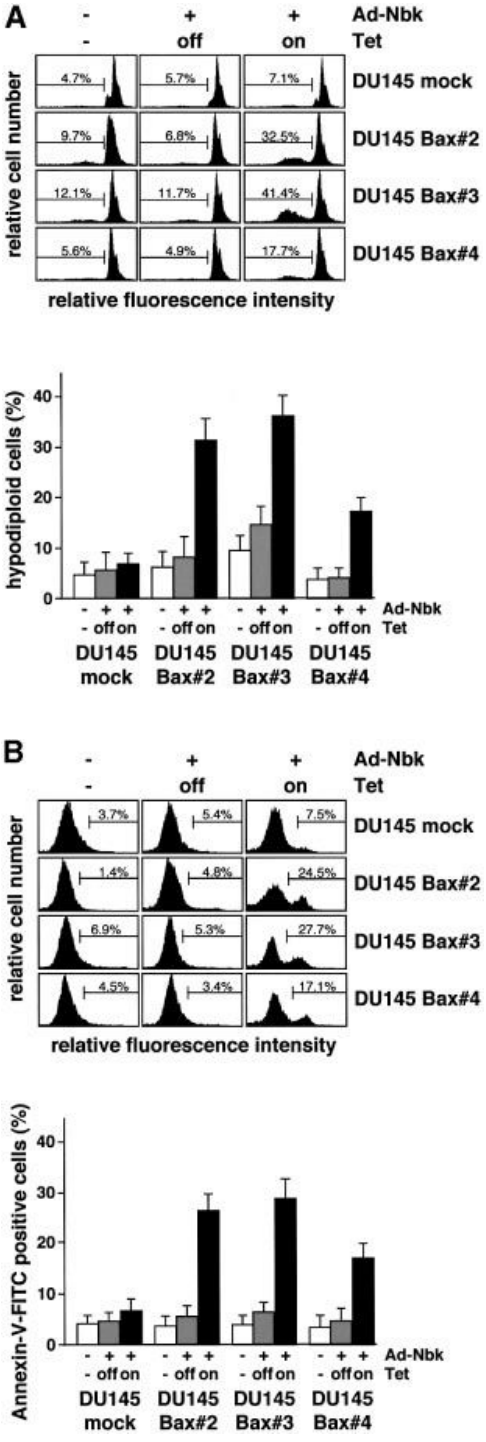

Fig. 4. Bax is required for Nbk-induced apoptosis. Stable Bax-expressing clones were transduced with Ad5-myc-Nbk-tTA as described in Figure 3 and cultured in the presence (Tet-off condition) or absence of doxycyclin (Tet-on condition). Control cells were mock treated and grown in the absence of doxycyclin. (**A**) Flow cytometric measurement of hypodiploid DNA. Upper panel: representative experiment. The percentage of apoptotic cells in a representative experiment was measured 24 h after adenoviral tranduction and is indicated between markers. Lower panel: means ± SD from three independent experiments. (**B**) Detection of phosphatidlyserine exposure: flow cytometric detection of apoptotic cells was performed by staining with annexin V–FITC to detect exposure of phosphatidylserine onto the cell surface 18 h after transduction. Cells were counterstained with propidium iodide (PI) to detect membrane damage. PI-positive cells were considered as necrotic and excluded from the analysis. The percentage of apoptotic cells is indicated between markers. Upper panel: representative experiment. Lower panel: means ± SD from three independent experiments.

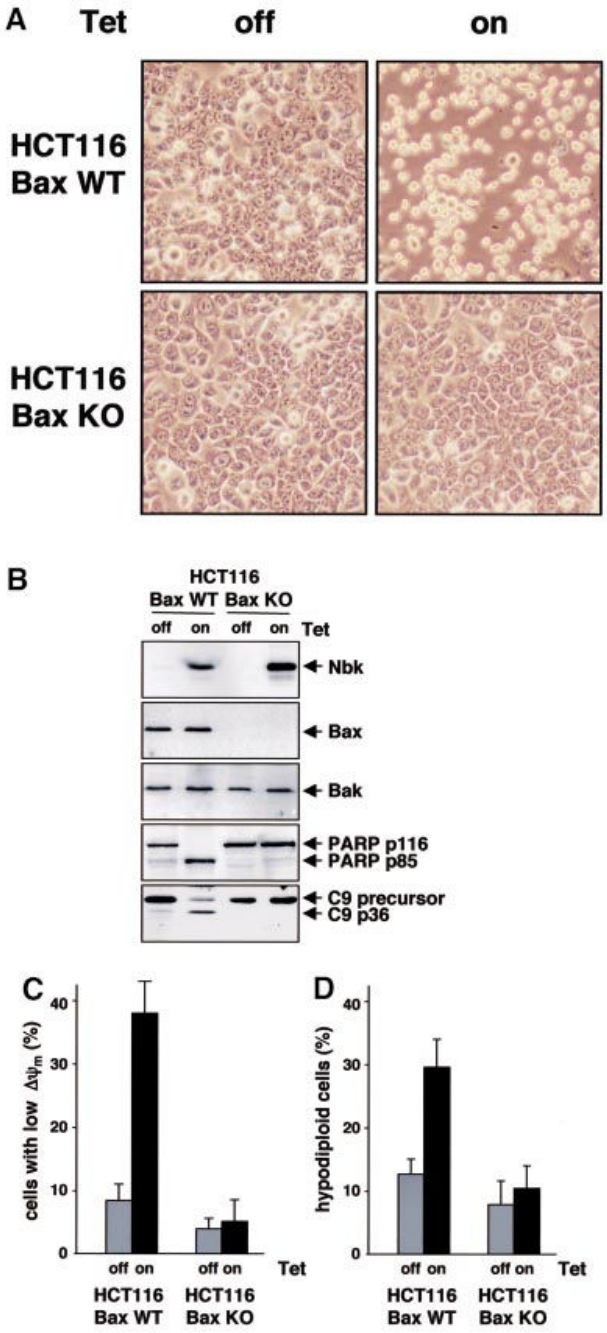

Fig. 5. Induction of apoptosis by Nbk is entirely Bax dependent in HCT116 cells. HCT116 Bax wild-type (WT) and HCT116 Bax knock-out (k.o.) cells were transduced with Ad5-myc-Nbk-tTA and cultured for 24 h in the presence (Tet-off condition) or absence of doxycyclin (Tet-on condition). (**A**) Morphology of HCT116 cells. (**B**) Western blot analyses of Nbk, Bax, Bak expression, PARP and procaspase-9 cleavage. (**C**) Breakdown of the mitochondrial membrane potential. Loss of $\Delta\psi_m$ was measured on the single-cell level by the use of the cationic dye JC-1. Means ± SD were calculated from three independent experiments. (**D**) Apoptosis induction by Nbk. Genomic DNA fragmentation was measured on a single-cell level by determination of cells with a hypodiploid DNA content. Means ± SD were calculated from three independent experiments.

To exclude potential clonal selection artifacts, we determined the role of Bax in an independent cell system. HCT116 cells express the wild-type Bax protein, whereas

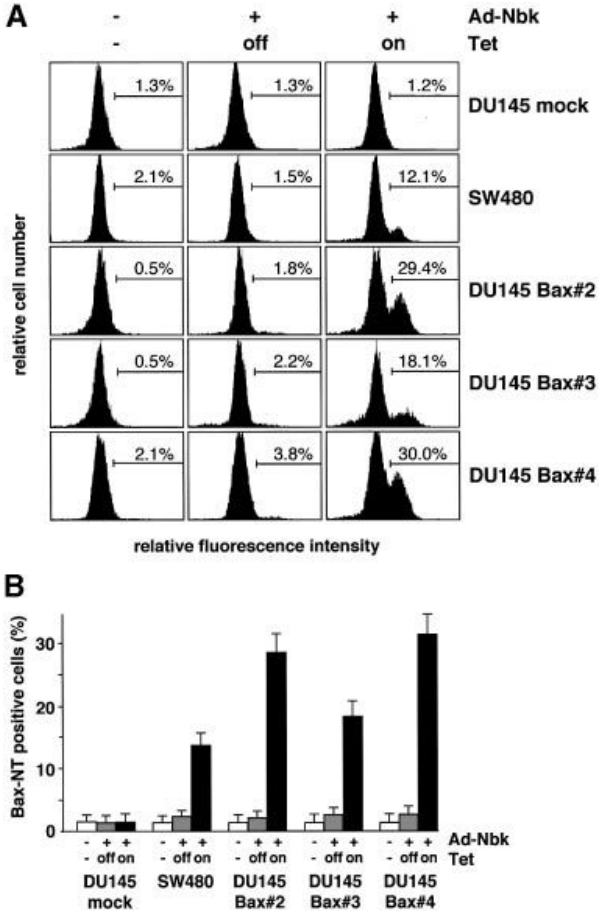

Fig. 6. Bax undergoes a conformational change in response to Nbk expression. SW480 cells, Bax-negative DU145 mock transfectants and DU145-Bax clones 2, 3 and 4 were transduced with Ad5-myc-NBK-tTA and cultured for 24 h in the presence (Tet-off condition) or absence of vector and doxycyclin (Tet-on condition). Control cells were grown in the absence of doxycyclin. (**A**) Cells were stained with a conformation-specific antibody against the Bax N-terminus and analyzed by flow cytometry. The percentage of immunostained cells is indicated between markers. (**B**) Bar chart showing mean ± SD of cells expressing activated Bax. Data were obtained from three independent experiments.

HCT116 Bax knock-out cells are devoid of Bax (Zhang *et al.*, 2000). Similar to DU145 cells, we observed that conditional Nbk expression induced apoptosis in HCT116 colon carcinoma cells carrying the wild-type Bax gene, whereas Bax knock-out cells were resistant against induction of apoptosis (Figure 5A and D). Likewise, Ad5-myc-Nbk-tTA induced mitochondrial permeability transition, caspase-9 processing and poly(ADP-ribose)-polymerase (PARP) cleavage only in the Bax wild-type cells, but not in the congeneic HCT116 Bax-deficient cells (Figure 5B and C). Notably, HCT116 cells expressed significant levels of Bak that were similar irrespective of the Bax status. These experiments therefore indicate that a sensitization to Nbk-induced apoptosis is observed not only after Bax overexpression, but also in the presence of endogenous Bax levels. Furthermore, the results are consistent with the assumption that Nbk-induced apoptosis proceeds in an entirely Bax-dependent manner which cannot be substituted by the presence of Bak.

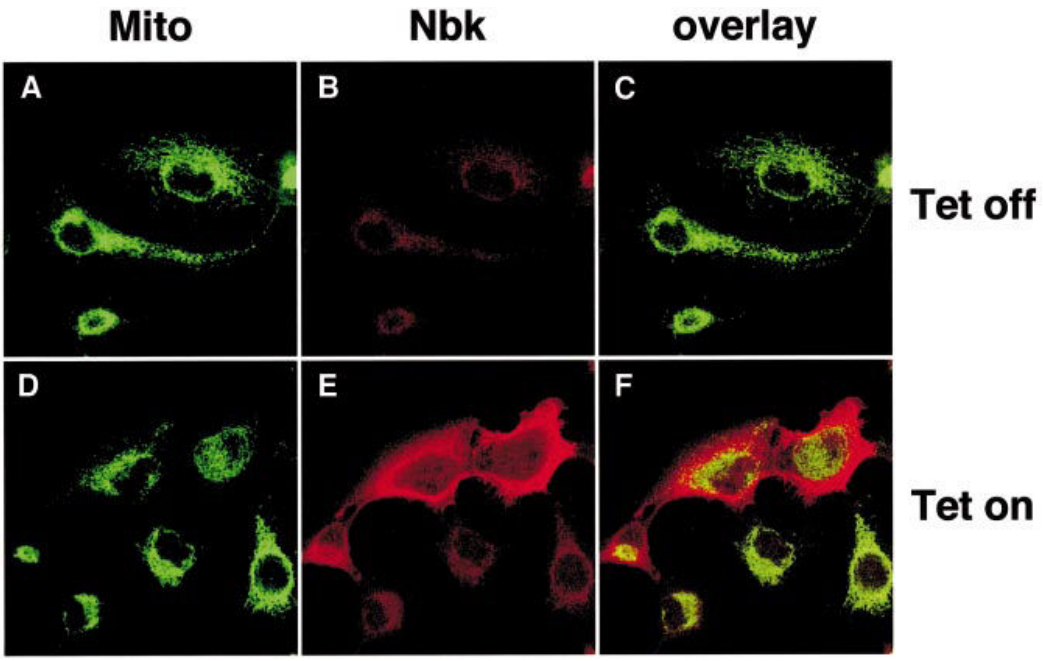

Fig. 7. Subcellular localization pattern of Nbk. Bax-expressing DU145 cells (clone 3) were transduced with Ad5-myc-Nbk-tTA. Cells were stained for Nbk protein expression after 16 h culture in the presence (Tet-off condition, **A**–**C**) or absence of doxycyclin (Tet-on condition, **D**–**F**). Nbk was visualized by goat-anti-Nbk followed by Alexa Fluor 594-conjugated chicken anti-goat IgG (red fluorescence; B and E). Cells were counterstained with MitoTracker Green (A and D). (C and F) The overlay of the Nbk and MitoTracker Green signals.

Nbk induces exposure of an N-terminal Bax epitope

The experiments described above clearly revealed that Nbk is not a direct activator of the mitochondrial pathway, but strongly depends on the presence of Bax. Recent studies reported that during apoptosis, Bax undergoes a conformational change leading to the exposure of an N-terminal epitope and insertion of cytosolic Bax into the outer mitochondrial membrane (Desagher *et al*., 1999; Eskes *et al*., 2000). Therefore, we performed immunofluorescent stainings with a conformation-specific antibody directed against the Bax N-terminus (Desagher *et al*., 1999). Figure 6 shows that this antibody stained permeabilized SW480 cells (mean 13.6%) after Ad5-myc-Nbk-tTA transduction in the absence of doxycyclin. In contrast, no staining was seen in Bax-negative DU145 cells or in Bax-positive SW480 cells in the presence of doxycyclin.

We also analyzed this conformational change in Bax-expressing DU145 cells after Ad5-myc-Nbk-tTA transduction. Staining of DU145 Bax clones showed an average of 28.2% positive cells for Bax clone 2, 18.4% for Bax clone 3 and 32.0% for Bax clone 4 in the absence of doxycyclin, i.e. the Tet-on condition (Figure 6). In contrast, only 1.8–3.8% of the cells displayed exposure of the N-terminal conformational Bax epitope in the presence of doxycyclin, i.e. in the absence of Nbk expression. Upon Nbk expression, the number of cells displaying a Bax conformational change was lower than the number of apoptotic cells. This can be explained by the fact that the exposure of the Bax N-terminus is a dynamic event. In addition, Bax can be cleaved by calpains at its N-terminus, generating a fragment that is not recognized by the antibody, but which is an even more potent inducer of apoptotic cell death than wild-type Bax (Toyota *et al*., 2003). Thus, the number of cells displaying the N-terminal switch of Bax may be lower than the extent of apoptosis detected by DNA fragmentation.

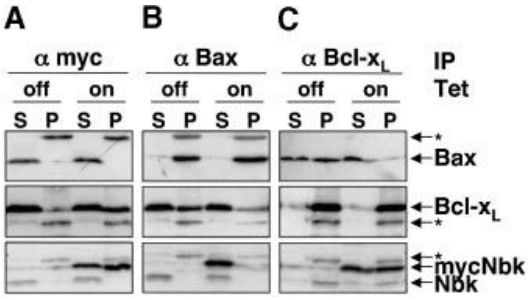

Fig. 8. Co-immunoprecipitation analyses show Nbk binding to Bcl-x_L but not to Bax. SW480 cells were transduced with Ad5-myc-Nbk-tTA in the presence (Tet-off condition) or absence of doxycyclin (Tet-on condition) for 24 h. Lysates of cells solubilized in Triton X-100 buffer were immunoprecipitated with an anti-pan-Bax, anti-Bcl-x_L or anti-c-Myc antibody. Immune complexes were resolved by SDS–PAGE and the presence of the respective protein was detected by immunoblotting, as indicated by arrows. Migration of the immunoglobulin light chain is indicated by an asterisk. S, supernatant; P, immunoprecipitate.

Interaction of Nbk with other Bcl-2 proteins

The conformational switch of the Bax N-terminus mediates its insertion into the outer mitochondrial membrane. We therefore determined the subcellular localization of Nbk in relation to staining of mitochondria with MitoTracker Green (Figure 7A and D). Confocal microscopy showed an almost complete suppression of

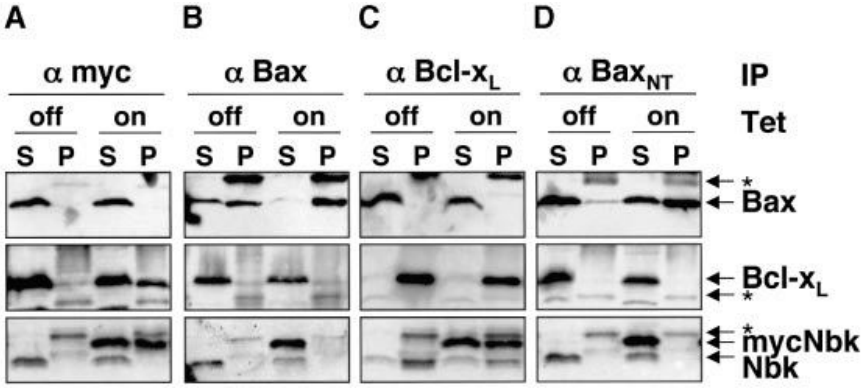

Fig. 9. Conformation-specific immunoprecipitation in CHAPS buffer. SW480 cells were infected with Ad5-myc-Nbk-tTA in the presence (Tet-off condition) or absence of doxycyclin (Tet-on condition) for 24 h, followed by cell lysis in CHAPS buffer. Immunoprecipitation was performed with antibodies against pan-Bax, activated Bax (conformation-specific antibody against the N-terminal epitope Bax-NT), Bcl-x_L or c-myc. Immune complexes were resolved by SDS–PAGE, and the presence of each protein was detected by immunoblotting as indicated by arrows. Migration of the immunoglobulin light chain is indicated by an asterisk. S, supernatant; P, immunoprecipitate.

Nbk expression in the presence of doxycyclin (Tet-off condition, Figure 7B) and strong expression of Nbk in the absence of doxycyclin (Tet-on condition, Figure 7E). Prior to the onset of apoptosis (e.g. 16 h after viral transduction) and also at later time points (data not shown), Nbk expression was confined to the cytoplasm. An overlay of the Nbk and the MitoTracker Green stainings demonstrated a complete segregation of the two signals (Figure 7F).

The immunocytochemical stainings indicated that Nbk was obviously not translocated to mitochondria. In contrast, Bid mediates exposure of the N-terminal Bax epitope upon its cleavage by caspase-8 and co-localizes with Bax to the mitochondria (Desagher *et al.*, 1999). Therefore, Nbk mediates the conformational switch in the Bax N-terminus presumably through an indirect mechanism, e.g. by the interaction of Nbk with other Bcl-2 members. We therefore next performed co-immunoprecipitation experiments for Bcl-x_L, Bax and Nbk. Immunoprecipitation of Nbk was performed with an anti-myc antibody that precipitated the transduced myc-Nbk but not the endogenous Nbk (Figure 8A, lower panel). Bcl-x_L readily co-immunoprecipitated with myc-Nbk (Figure 8A, middle panel). In contrast, immunoprecipitation of myc-Nbk showed no interaction with Bax (Figure 8A, upper panel). Bcl-x_L, however, co-immunoprecipitated with Bax, which interestingly became less evident when Nbk was expressed (Figure 8B, middle panel). Also, in the reverse experiment, Bax showed co-immunoprecipitation with Bcl-x_L and, again, this interaction was clearly weaker upon Nbk expression (Figure 8C, upper panel). Myc-Nbk also showed a strong co-precipitation with Bcl-x_L, even when Triton X-100 was used as a detergent (Figure 8C, lower panel). Under these stringent conditions, Nbk did not co-immunoprecipitate with Bax (Figure 8B, lower panel). Notably, the co-immunoprecipitations between Bcl-x_L and Bax or between Bcl-x_L and Nbk were not complete, and part of the proteins remained in the supernatant. This might be explained by the possibilities that the proteins are not expressed in equimolar quantities or that additional interactions exist which prevented a quantitative immunoprecipitation.

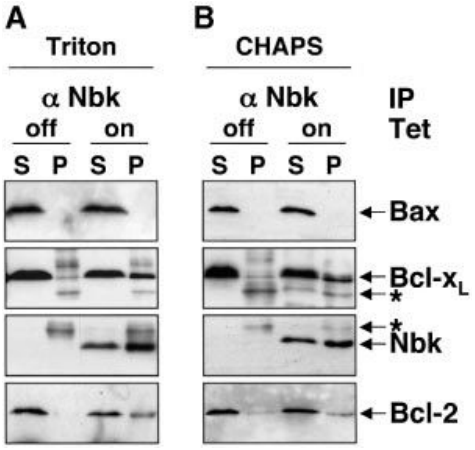

Fig. 10. Interaction between Nbk and Bcl-2. SW48 cells expressing high levels of endogenous Bcl-2 were transduced with Ad5-myc-Nbk-tTA in the presence (Tet-off condition) or absence of doxycyclin (Tet-on condition) for 24 h, followed by cell lysis in (**A**) Triton X-100 or (**B**) CHAPS buffer. Immunoprecipitation was performed with antibodies against pan-Bax, Bcl-x_L, Bcl-2 or c-myc. Immune complexes were resolved by SDS–PAGE, and the presence of each protein was detected by immunoblotting as indicated by arrows. Migration of the immunoglobulin light chain is indicated by an asterisk. S, supernatant; P, immunoprecipitate.

Previous reports showed that detergents such as Triton X-100 trigger the conformational switch of the Bax N-terminus *in vitro*, facilitating Bax oligomerization (Hsu and Youle, 1998; Antonsson *et al.*, 2000). Such Bax alterations do not occur when CHAPS is used as detergent, which should therefore allow a conformation-specific immunoprecipitation of Bax. Under CHAPS conditions, activated Bax was precipitated efficiently by a conformation-specific Bax antibody recognizing the N-terminal epitope when Nbk was expressed, but only weakly when Nbk expression was turned off by doxycyclin (Figure 9D, upper panel). Pan-Bax was precipitated efficiently by a pan-Bax antibody under both conditions (Figure 9B, upper panel). Similarly to the case in Triton X-100, in CHAPS buffer Bax did not co-precipitate with

myc-Nbk, and vice versa (Figure 9A, upper panel; B, lower panel). Furthermore, the precipitation of activated Bax by the conformation-specific anti-Bax antibody did not result in immunoprecipitation of Nbk (Figure 9D, lower panel). Immunoprecipitation of Bcl-x_L showed co-precipitation of Nbk, and vice versa (Figure 9A, middle panel; C, lower panel). In contrast to the experiments with Triton X-100 but consistent with previous reports (Hsu and Youle, 1998; Antonsson *et al*., 2000), we did not observe a co-immunoprecipitation of Bcl-x_L with Bax and vice versa under CHAPS conditions (Figure 9B, middle panel; C, upper panel). As CHAPS can disrupt protein interactions, this does not exclude the possibility that Bax and Bcl-x_L could interact *in vivo*. In this regard, Bcl-x_L interaction with Bax was initially described in yeast two-hybrid studies (Sato *et al*., 1994; Yang *et al*., 1995) and confirmed by fluorescence resonance energy transfer (FRET) analyses in mammalian cells (Mahajan *et al*., 1998).

To address a potential interaction between Nbk and Bcl-2 in addition to Bcl-x_L, we performed co-immunoprecipitation experiments in SW48 cells that demonstrate considerable expression of Bcl-2 (Figure 2). These results showed that Nbk interacts with both Bcl-x_L and Bcl-2 under CHAPS or Triton X-100 conditions (Figure 10). No co-immunoprecipitation was observed between Nbk and Bcl-2 in SW480 cells that express low levels of Bcl-2 (data not shown). In summary, these results demonstrate that Nbk does not physically interact with Bax but induces the activation of Bax through an indirect mechanism. Moreover, Nbk interacts with Bcl-x_L and Bcl-2 under both Triton X-100 and CHAPS buffer conditions, an event which presumably interferes with interaction of anti-apoptotic Bcl-2 proteins and Bax. Whether the interaction of Nbk with anti-apoptotic Bcl-2 homologs is strictly mandatory for the activation of Bax and the mitochondrial death cascade remains to be elucidated.

Discussion

Members of the Bcl-2 family are key regulators of apoptosis. Tremendous progress has been made in elucidating the molecular basis of apoptosis regulation through both pro- and anti-apoptotic Bcl-2 family members. Nevertheless, the mechanism of action of the pro-apoptotic Bcl-2 homologs is still not completely understood. Bax has been shown to be a direct activator of mitochondria which triggers release of cytochrome *c* (Jürgensmeier *et al*., 1998) and other mitochondrial events such as permeability shift transition and the release of a variety of pro-apoptotic factors including AIF, Smac/Diablo and others. The Bax homologs Bak and Bok/Mtd that carry, like Bax, a BH1, BH2 and BH3 domain are believed to exert similar functions (Martinou and Green, 2001).

The mechanisms of apoptosis induction by Nbk, however, remain enigmatic. Nbk contains only one of the signature domains of the Bcl-2-family, the BH3 domain, and therefore might display a mode of action similar to other members of the BH3-only subfamily. Recently, an indirect mode of apoptosis induction was established for the BH3-only proteins Bad, Bid, Bim and Noxa that occurs via a Bax- or Bak-dependent pathway (Cheng *et al*., 2001; Zong *et al*., 2001). In the case of Bid, a truncated caspase cleavage product of Bid, tBid, triggers a conformational switch in the N-terminus of Bax (Desagher *et al*., 1999) or Bak (Wei *et al*., 2000), leading to activation of mitochondrial apoptosis signaling. Experiments in mouse embryonal fibroblasts showed that the activity of these BH3-only proteins in inducing apoptosis depends on the presence of Bax or Bak to trigger cytochrome *c* release and the mitochondrial apoptosis cascade (Cheng *et al*., 2001; Zong *et al*., 2001). This led to the hypothesis that all BH3-only proteins might share a similar mode of action, i.e. depend on Bax and its homologs to trigger apoptosis.

In the present study, we addressed the mechanism of action of Nbk in relation to Bax and the activation of the mitochondrial apoptosis cascade. To this end, we constructed a conditional adenoviral expression system based on the Tet-off system. The prominent finding of the present work is the fact that Nbk did not induce apoptosis in the Bax-negative carcinoma cells including Bax-mutated LoVo and DU145 cells, as well as HCT116 Bax knock-out cells.

The re-expression of Bax in DU145 cells restored the sensitivity for Ad5-myc-Nbk-tTA-induced apoptosis in these cells. Similarly, Bax wild-type HCT116 cells displayed high sensitivity to Nbk-induced apoptosis. Upon Nbk expression, the Bax-positive but not the Bax-negative cells showed release of cytochrome *c*, breakdown of the mitochondrial membrane potential and processing of procaspase-9. This formally demonstrates that Nbk acts via a Bax-dependent mechanism to activate the mitochondrial apoptosis pathway. Western blot analyses showed that the Bax-negative cell lines DU145, LoVo and HCT116 all express Bak. Thus, Bak could not compensate for the loss of Bax in these cells, indicating that Nbk signals preferentially via Bax and not Bak. In the case of other BH3-only proteins, such as Bad, Bid, Bim and Noxa, only the combined inactivation of both Bax and Bak significantly impaired apoptosis induction (Cheng *et al*., 2001; Zong *et al*., 2001). Altogether, Nbk appears to be an indirect inducer of mitochondrial apoptosis that entirely depends on Bax to exert its effect.

The BH3-only protein Bid induces cytochrome *c* release through a Bax-dependent mechanism (Desagher *et al*., 1999). This occurs by relieving inhibition of the Bax transmembrane signal anchor by the N-terminal domain, resulting in integration of Bax into the outer mitochondrial membrane (Eskes *et al*., 2000; Ruffolo *et al*., 2000). A recent report pointed out that Bax-independent mechanisms might also be relevant for Bid-induced mitochondrial activation. In this line, Bid was shown to activate mitochondria and cytochrome *c* release independently of Bax (Kim *et al*., 2000). Recently, it was even suggested that Bid by itself may possess channel-forming capabilities and may thus mediate cytochrome *c* release (Zhai *et al*., 2000) but does not interact with the voltage-dependent anion channel (Sugiyama *et al*., 2002).

Nbk differs from Bid in that it does not physically interact with Bax. In addition, Nbk does not localize to the mitochondria, whereas Bax does (Eskes *et al*., 2000; Ruffolo *et al*., 2000). Furthermore, so far we have found no evidence that Nbk is cleaved during apoptosis. This is in line with data from other BH3-only Bcl-2 homologs such as Bim and Bad. Both proteins have been shown to impair the anti-apoptotic effect of Bcl-2 or Bcl-x_L and both

also depend on Bax or Bak to exert their apoptosis-promoting effect (Cheng *et al*., 2001; Zong *et al*., 2001). Like in the case of Bad, Nbk might act via sequestration of Bcl-x_L and Bcl-2, as suggested by the co-immunoprecipitation of Nbk and Bcl-2 or Bcl-x_L, respectively, that was observed under both Triton X-100 and CHAPS buffer conditions. An interaction of Bax and Bcl-x_L was observed, however, only in co-immunoprecipitation studies based on Triton X-100 as detergent, but not when CHAPS was employed.

It is conceivable that the binding of Nbk to Bcl-x_L or Bcl-2 alone is sufficient to promote the conformational change of Bax, or that additional factors are required which would then, upon sequestration of Bcl-x_L by Nbk, bind to Bax to trigger the pro-apoptotic conformation. Thus, the exact functional role of the interaction between Nbk and Bcl-x_L or Bcl-2 remains to be determined. Evidence for a more complex mode of action comes from the observation that mutation of the phosphorylation sites at residues 33 (threonine) and 35 (serine) reduced the apoptotic activity of Nbk without significantly affecting its ability to heterodimerize with Bcl-2 (Verma *et al*., 2001). Thus, unlike Bad where serine phosphorylation results in inactivation and sequestration via 14-3-3 proteins, Nbk phosphorylation appears to result in a gain of function. A recent report showed that Nbk localizes to the endoplasmic reticulum (ER) membrane upon ectopic overexpression. Furthermore, ER-targeted Nbk could induce secondary activation of mitochondria and cytochrome *c* release in a cell-free system (Germain *et al*., 2002). This observation suggests that Nbk might be involved in a cross-talk of the ER with the mitochondrial apoptosis pathway. Moreover, the activation of mitochondria via artificially ER-targeted Nbk was independent from Bax as assessed in $Bax^{-/-}$ murine hepatocytes. This is in contrast to our data in several human Bax-negative carcinoma lines and the respective congeneic Bax-positive cells.

In conclusion, we provide evidence that Nbk induces apoptosis in Bax-proficient carcinoma cells tested, while Bax-negative cells were refractory. This corroborates a model of BH3-only proteins as indirect activators of the mitochondrial apoptosis signaling cascade that mediate their effects through Bax and its homologs. Interestingly, the Bax-negative cells investigated here express significant levels of Bak. Thus, Bak by itself appears to be insufficient to confer sensitivity for Nbk-induced apoptosis. We demonstrate that the BH3-only protein Nbk/Bik entirely depends on Bax but apparently not on Bak. Therefore, functional interactions between BH3-only proteins and Bax and its homologs might be more complex, as initially believed, and could occur in a subfamily-specific manner.

Recently published data support our notion that Bax and Bak differentially regulate apoptosis (Panaretakis *et al*., 2002). Interestingly, overexpression of Bcl-2 blocked the conformational activation of Bak upon treatment with the anti-cancer drug doxorubicin, whereas the Bax N-terminal switch was still partially activated. As doxorubicin also led to a strong increase in the expression of Nbk/Bik, this may indicate a differential regulation of Bax and Bak by Bcl-2 and Nbk.

Pro-apoptotic stimuli such as antigen receptor-mediated activation of B-lymphoid cells or induction of p53 by anti-cancer drugs may trigger induction of Nbk expression. The exact requirements for induction and transcriptional regulation of this killer protein remain, however, to be established. Evidence is accumulating that BH3 proteins link different cellular compartments or signal transduction machineries to the mitochondrial apoptosome. Our interest is therefore to elucidate the upstream signals regulating Nbk gene expression and activity, especially in view of its restricted tissue expression pattern.

Materials and methods

Cell culture

HEK293, SW48, SW480, DU145, LoVo and HCT116 cells were grown in Dulbecco's modified Eagle's medium (DMEM) high-glucose supplemented with 10% fetal calf serum (FCS), 100 U/ml penicillin and 0.1 μg/ml streptomycin (all from Gibco, Karlsruhe, Germany). Cells were transduced with Ad5-myc-Nbk by incubation for 2 h at an m.o.i. of 25 in growth medium without FCS. Expression of myc-Nbk was suppressed by addition of 1 μg/ml doxycyclin to the culture medium (Tet-off condition).

Antibodies

Monoclonal mouse anti-Bax antibody (clone YTH-2D2, raised against a peptide corresponding to amino acids 3–16) was purchased from Trevigen (Gaithersburg, MD) and the conformation-specific polyclonal rabbit anti-Bax antibody (raised against a peptide corresponding to amino acids 1–21) was from Upstate Biotechnology (Lake Placid, NY). Polyclonal rabbit anti-myc antibody (A-14; raised against the 9E10 myc epitope) and goat anti-Nbk antibody (N-19; raised against an epitope mapping to the 19 amino acid N-terminus of human Nbk) were from Santa Cruz Biotechnology (Santa Cruz, CA), and polyclonal rabbit anti-Bcl-$x_{S/L}$ antibody (raised against amino acids 18–233 of rat Bcl-x_L), monoclonal mouse anti-human cytochrome *c* (clone 7H8.2C12) and monoclonal mouse anti-human PARP antibody (clone C2-10) were from BD Biosciences Pharmingen (San Diego, CA). Monoclonal mouse anti-Bcl-2 antibody (NCL-bcl-2, raised against amino acids 41–55 of human Bcl-2) was purchased from Novocastra Laboratories (Newcastle, UK). Goat anti-caspase-9 antibody (raised against human caspase-9 amino acids 139–330) was from R&D Systems (Minneapolis, MN). The polyclonal rabbit anti-Bak antibody (raised against a peptide corresponding to amino acids 14–36) was from DAKO Corporation (Carpinteria, CA). Secondary anti-mouse, anti-rabbit and anti-goat IgG coupled to horseradish peroxidase were from Promega Corporation (Madison, WI) or Santa Cruz Biotechnology.

Construction of recombinant adenovirus

To insert the tTA expression unit into the adenovirus genome, the tTA expression cassette from pTet-Off (BD Biosciences Clontech, Palo Alto, CA) was first cloned as an *Xho*I–*Pvu*II fragment into pHVAd3, an adenoviral shuttle vector for the E3 region. The virus genome containing the tTA expression unit was generated in the *Escherichia coli* strain BJ5183 RecBC-sbcB by homologous recombination of the shuttle plasmid with pHVAd1 containing the complete adenovirus genome, resulting in the plasmid pAd-tTA. To create an inducible myc-Nbk expression cassette, the *Xho*I–*Eco*RI fragment from pTRE containing the tetracyclin-responsive element (TRE) upstream of the CMV minimal promoter was inserted into the adenoviral shuttle vector pHVAd2. A myc-Nbk construct containing the full-length Nbk cDNA fused to an N-terminal myc tag was first cloned into pSL1180 (Amersham Pharmacia Biotech, Freiburg, Germany) and then inserted as a *Hin*dIII–*Sal*I fragment into the TRE-containing pHVAd2 shuttle vector. The resulting TRE-myc-Nbk expression unit was inserted into the Ad5 virus genome by homologous recombination of the shuttle plasmid with pAd-tTA, thereby replacing the E1 region and creating pAd5-myc-Nbk-tTA (Figure 1A). The viral DNA was transfected into HEK293 cells and adenoviral plaques were propagated as described (Hemmati *et al*., 2002).

Stable expression of Bax by retroviral infection of DU145 cells

For expression of Bax in the Bax-negative DU145 cells, we employed the retroviral vector HyTK-Bax containing the human Bax-α cDNA under the control of a CMV promoter as described (Hemmati *et al*., 2002).

Measurement of apoptotic cell death by flow cytometry

Apoptosis was determined on a single-cell level by measuring the DNA content of individual cells with a FACScan (BD Biosciences) as described (Wieder *et al*., 2001). Alternatively, apoptotic cell death was determined by measuring binding of annexin V–FITC upon exposure of phosphatidylserine to the cell surface. PI-positive cells that had lost membrane integrity were considered as late apoptotic or necrotic cells and therefore excluded from the analysis. Data are given in percentage of cells with increased fluorescence reflecting the number of annexin V–FITC-stained, PI-negative cells.

Measurement of cytochrome c release

Cytosolic extracts were prepared according to a method described previously (von Haefen *et al*., 2003). After induction of apoptosis, cells were harvested in phosphate-buffered saline (PBS), equilibrated in hypotonic buffer (20 mM HEPES pH 7.4, 10 mM KCl, 2 mM $MgCl_2$, 1 mM EDTA) supplemented with 0.1 mM phenylmethylsulfonyl fluoride (PMSF) and 0.75 mg/ml digitonin (Sigma-Aldrich) and incubated on ice for 3 min. Debris was pelleted by centrifugation at 10 000 *g* at 4°C for 5 min and the supernatant was subjected to western blot analysis.

Measurement of mitochondrial permeability transition

After infection with recombinant adenoviruses Ad5-myc-Nbk-tTA at an m.o.i. of 25, cells were collected by centrifugation at 300 *g* at 4°C for 5 min. The mitochondrial permeability transition was determined by staining the cells with JC-1 (Molecular Probes, Leiden, The Netherlands) as described (Wieder *et al*., 2001). Mitochondrial permeability transition was quantified by flow cytometric determination of cells with decreased red fluorescence, i.e. with mitochondria displaying a lower membrane potential ($\Delta\Psi_m$).

Measurement of conformational change of Bax by flow cytometry

A total of 2.5×10^5 cells (25 cm^2 flask) were infected with Ad5-mycNbk-tTA in the presence or absence of doxycyclin and harvested 24 h after infection by trypsination. Quantification of cells showing exposure of the N-terminal epitope detected by the conformation-specific Bax antibody was performed by flow cytometry. Data are given in percentage of cells containing Bax with a conformational change in the N-terminal region.

Immunoblotting

After trypsination, cells were washed twice with ice-cold PBS and lysed in buffer L (10 mM Tris–HCl pH 7.5, 137 mM NaCl, 1% Triton X-100, 2 mM EDTA, 1 μM pepstatin, 1 μM leupeptin and 0.1 mM PMSF). Protein concentration was determined using the bicinchoninic acid assay. Equal amounts of protein (20 μg per lane) were separated by SDS–PAGE, electroblotted and visualized as described (Wieder *et al*., 2001).

Immunocytochemistry

SW480 cells were seeded on coverslips in 6-well plates and infected with Ad5-myc-Nbk-tTA in the presence or absence of doxycyclin. At 24 h post-infection, cells were washed three times with PBS and fixed for 30 min with ice-cold 1% paraformaldehyde. After two washing steps in PBS, the cells were permeabilized with ice-cold 100% methanol for 1 min. Cells were washed again twice and non-specific binding of antibodies was blocked by incubation with 8% bovine serum albumin (BSA) for 30 min at room temperature. The primary antibodies were diluted in 1% BSA in PBS and added to the cells overnight at 4°C. Incubation with secondary antibodies was performed for 1 h at room temperature. Then, cells were washed three times in PBS. The labeling of Nbk was performed by the use of goat anti-Nbk (1:50) followed by incubation with Alexa Fluor 594-conjugated chicken anti-goat IgG. Mitochondria were stained by the use of MitoTracker Green (Molecular Probes, Inc.) After staining, the cells were mounted in Aquamount and inspected in a Leica TCS SP2 confocal microscope.

Immunoprecipitation

A total of 1.5×10^6 cells per 75 cm^2 flask were infected with Ad5-myc-Nbk-tTA and cultured for 24 h with or without doxycyclin. Cells were harvested, washed in ice-cold PBS and resuspended in 800 μl of either Triton X-100- or CHAPS-containing lysis buffer (20 mM Tris–HCl pH 7.5, 137 mM NaCl, 1% Triton X-100, 2 mM EDTA or 10 mM HEPES pH 7.4, 140 mM NaCl, 1% CHAPS) in the presence of protease inhibitors (1 μM pepstatin, 1 μM leupeptin and 0.1 mM PMSF). Lysates were pre-cleared with 40 μg of protein A– and protein G–Sepharose each (Sigma-Aldrich). A 150 μl aliquot of the pre-cleared cellular extract was shaken in the presence of 3 μg of the primary antibody and 0.5 mg of protein A/G–Sepharose at 4°C for 4 h. The protein A/G immune complex was sedimented by centrifugation at 15 000 *g* at 4°C for 20 s and washed three times in lysis buffer. Proteins bound to the protein A/G–Sepharose were eluted in 50 μl of sample buffer (62.5 mM Tris–HCl pH 6.8, 2% SDS, 2% β-mercaptoethanol, 10% glycerol and 1% bromophenol blue) and analyzed by western blot analysis.

Acknowledgements

We would like to thank Verena Lehmann and Karin Schmelz for expert technical assistance, the late Michael Strauss, Max Delbrück Center, Berlin for providing part of the Ad vector components, Dr Karsten Brand, Max Delbrück Center, Berlin for helpful discussions, Christopher Stroh, University of Düsseldorf for help with confocal microscopy, and Bert Vogelstein (Johns Hopkins University School of Medicine, Baltimore) for kindly providing HCT116 cells. This work was supported by the Deutsche Forschungsgemeinschaft grants SFB506 and Da 238/4.

References

Antonsson,B., Montessuit,S., Lauper,S., Eskes,R. and Martinou,J.C. (2000) Bax oligomerization is required for channel-forming activity in liposomes and to trigger cytochrome *c* release from mitochondria. *Biochem. J.*, **345**, 271–278.

Borner,C. (2003) The Bcl-2 protein family: sensors and checkpoints for life-or-death decisions. *Mol. Immunol.*, **39**, 615–647.

Boyd,J.M. *et al*. (1995) Bik, a novel death-inducing protein shares a distinct sequence motif with Bcl-2 family proteins and interacts with viral and cellular survival-promoting proteins. *Oncogene*, **11**, 1921–1928.

Cheng,E.H., Wei,M.C., Weiler,S., Flavell,R.A., Mak,T.W., Lindsten,T. and Korsmeyer,S.J. (2001) Bcl-2, Bcl-xL sequester BH3 domain-only molecules preventing Bax- and Bak-mediated mitochondrial apoptosis. *Mol. Cell*, **8**, 705–711.

Daniel,P.T., Pun,K.T., Ritschel,S., Sturm,I., Holler,J., Dörken,B. and Brown,R. (1999) Expression of the death gene Bik/Nbk promotes sensitivity to drug-induced apoptosis in corticosteroid-resistant T-cell lymphoma and prevents tumor growth in severe combined immunodeficient mice. *Blood*, **94**, 1100–1107.

Daniel,P.T., Schulze-Osthoff,K., Belka,C. and Güner,D. (2003) Guardians of cell death: the Bcl-2 family proteins. *Essays Biochem.*, **39**, in press.

Desagher,S., Osen-Sand,A., Nichols,A., Eskes,R., Montessuit,S., Lauper,S., Maundrell,K., Antonsson,B. and Martinou,J. (1999) Bid-induced conformational change of Bax is responsible for mitochondrial cytochrome *c* release during apoptosis. *J. Cell Biol.*, **144**, 891–901.

Eskes,R., Desagher,S., Antonsson,B. and Martinou,J.C. (2000) Bid induces the oligomerization and insertion of Bax into the outer mitochondrial membrane. *Mol. Cell. Biol.*, **20**, 929–935.

Germain,M., Mathai,J.P. and Shore,G.C. (2002) BH-3 only BIK functions at the endoplasmic reticulum to stimulate cytochrome *c* release from mitochondria. *J. Biol. Chem.*, **277**, 18053–18060.

Gossen,M. and Bujard,H. (1992) Tight control of gene expression in mammalian cells by tetracycline-responsive promoters. *Proc. Natl Acad. Sci. USA*, **89**, 5547–5551.

Han,J., Sabbatini,P. and White,E. (1996) Induction of apoptosis by human Nbk/Bik, a BH3-containing protein that interacts with E1B 19K. *Mol. Cell. Biol.*, **16**, 5857–5864.

Hemmati,P.G., Gillissen,B., von Haefen,C., Wendt,J., Stärck,L., Güner,D., Dörken,B. and Daniel,P.T. (2002) Adenovirus-mediated overexpression of p14ARF induces p53 and Bax-independent apoptosis. *Oncogene*, **21**, 3149–3161.

Hsu,Y.T. and Youle,R.J. (1998) Bax in murine thymus is a soluble monomeric protein that displays differential detergent-induced conformations. *J. Biol. Chem.*, **273**, 10777–10783.

Huang,D.C. and Strasser,A. (2000) BH3-only proteins—essential initiators of apoptotic cell death. *Cell*, **103**, 839–842.

Jürgensmeier,J.M., Xie,Z.H., Deveraux,Q., Ellerby,L., Bredesen,D. and Reed,J.C. (1998) Bax directly induces release of cytochrome *c* from isolated mitochondria. *Proc. Natl Acad. Sci. USA*, **95**, 4997–5002.

Kelekar,A., Chang,B.S., Harlan,J.E., Fesik,S.W. and Thompson,C.B. (1997) Bad is a BH3 domain-containing protein that forms an inactivating dimer with Bcl-xL. *Mol. Cell. Biol.*, **17**, 7040–7046.

Kim,T.H., Zhao,Y., Barber,M.J., Kuharsky,D.K. and Yin,X.M. (2000)

Bid-induced cytochrome *c* release is mediated by a pathway independent of mitochondrial permeability transition pore and Bax. *J. Biol. Chem.*, **275**, 39474–39481.

Mahajan,N.P., Linder,K., Berry,G., Gordon,G.W., Heim,R. and Herman,B. (1998) Bcl-2 and Bax interactions in mitochondria probed with green fluorescent protein and fluorescence resonance energy transfer. *Nat. Biotechnol.*, **16**, 547–552.

Martinou,J.C. and Green,D.R. (2001) Breaking the mitochondrial barrier. *Nat. Rev. Mol. Cell Biol.*, **2**, 63–67.

Panaretakis,T., Pokrovskaja,K., Shoshan,M.C. and Grander,D. (2002) Activation of Bak, Bax and BH3-only proteins in the apoptotic response to doxorubicin. *J. Biol. Chem.*, **277**, 44317–44326.

Puthalakath,H. and Strasser,A. (2002) Keeping killers on a tight leash: transcriptional and post-translational control of the pro-apoptotic activity of BH3-only proteins. *Cell Death Differ.*, **9**, 505–512.

Radetzki,S., Köhne,C.H., von Haefen,C., Gillissen,B., Sturm,I., Dörken,B. and Daniel,P.T. (2002) The apoptosis promoting Bcl-2 homologues Bak and Nbk/Bik overcome drug resistance in Mdr-1-negative and Mdr-1 overexpressing breast cancer cell lines. *Oncogene*, **21**, 227–238.

Ruffolo,S.C., Breckenridge,D.G., Nguyen,M., Goping,I.S., Gross,A., Korsmeyer,S.J., Li,H., Yuan,J. and Shore,G.C. (2000) Bid-dependent and Bid-independent pathways for Bax insertion into mitochondria. *Cell Death Differ.*, **7**, 1101–1108.

Saito,R. and Tomita,M. (1999) On negative selection against ATG triplets near start codons in eukaryotic and prokaryotic genomes. *J. Mol. Evol.*, **48**, 213–217.

Sato,T. *et al*. (1994) Interactions among members of the Bcl-2 protein family analyzed with a yeast two-hybrid system. *Proc. Natl Acad. Sci. USA*, **91**, 9238–9242.

Sugiyama,T., Shimizu,S., Matsuoka,Y., Yoneda,Y. and Tsujimoto,Y. (2002) Activation of mitochondrial voltage-dependent anion channel by a pro-apoptotic BH3-only protein Bim. *Oncogene*, **21**, 4944–4956.

Tong,Y., Yang,Q., Vater,C., Venkateah,L.K., Custeau,D., Chittenden,T., Chinnadurai,G. and Gourdeau,H. (2001) The pro-apoptotic protein Bik exhibits potent antitumor activity that is dependent on its BH3 domain. *Mol. Cancer Ther.*, **1**, 95–102.

Toyota,H., Yanase,N., Yoshimoto,T., Moriyama,M., Sudo,T. and Mizuguchi,J. (2003) Calpain-induced Bax-cleavage product is a more potent inducer of apoptotic cell death than wild-type Bax. *Cancer Lett.*, **189**, 221–230.

Verma,S., Zhao,L. and Chinnadurai,G. (2001) Phosphorylation of the pro-apoptotic protein Bik: mapping of phosphorylation sites and effect on apoptosis. *J. Biol. Chem.*, **276**, 4671–4676.

von Haefen,C., Wieder,T., Essmann,F., Schulze-Osthoff,K., Dörken,B. and Daniel,P.T. (2003) Paclitaxel-induced apoptosis in BJAB cells proceeds via a death receptor-independent, caspase-3/caspase-8-driven mitochondrial amplification loop. *Oncogene*, **22**, 2236–2247.

Wei,M.C., Lindsten,T., Mootha,V.K., Weiler,S., Gross,A., Ashiya,M., Thompson,C.B. and Korsmeyer,S.J. (2000) tBID, a membrane-targeted death ligand, oligomerizes BAK to release cytochrome *c*. *Genes Dev.*, **14**, 2060–2071.

Wieder,T., Essmann,F., Prokop,A., Schmelz,K., Schulze-Osthoff,K., Beyaert,R., Dörken,B. and Daniel,P.T. (2001) Activation of caspase-8 in drug-induced apoptosis of B-lymphoid cells is independent of CD95/Fas receptor ligand interaction and occurs downstream of caspase-3. *Blood*, **97**, 1378–1387.

Yang,E., Zha,J., Jockel,J., Boise,L.H., Thompson,C.B. and Korsmeyer, S.J. (1995) Bad, a heterodimeric partner for Bcl-xL and Bcl-2, displaces Bax and promotes cell death. *Cell*, **80**, 285–291.

Zhai,D., Huang,X., Han,X. and Yang,F. (2000) Characterization of tBid-induced cytochrome *c* release from mitochondria and liposomes. *FEBS Lett.*, **472**, 293–296.

Zhang,L., Yu,J., Park,B.H., Kinzler,K.W. and Vogelstein,B. (2000) Role of Bax in the apoptotic response to anticancer agents. *Science*, **290**, 989–992.

Zong,W.X., Lindsten,T., Ross,A.J., MacGregor,G.R. and Thompson, C.B. (2001) BH3-only proteins that bind pro-survival Bcl-2 family members fail to induce apoptosis in the absence of Bax and Bak. *Genes Dev.*, **15**, 1481–1486.

Received July 17, 2002; revised April 24, 2003;
accepted May 19, 2003

[CANCER RESEARCH 64, 7065–7072, October 1, 2004]

Apoptosis Resistance of MCF-7 Breast Carcinoma Cells to Ionizing Radiation Is Independent of p53 and Cell Cycle Control but Caused by the Lack of Caspase-3 and a Caffeine-Inhibitable Event

Frank Essmann, Ingo H. Engels, Gudrun Totzke, Klaus Schulze-Osthoff, and Reiner U. Jänicke

University of Düsseldorf, Institute of Molecular Medicine, Düsseldorf, Germany

ABSTRACT

We have shown previously that ionizing radiation (IR) induces a persistent G_2-M arrest but not cell death in MCF-7 breast carcinoma cells that harbor functional p53 but lack caspase-3. In the present study, we investigated the mechanisms of apoptosis resistance and the roles of p53, caspase-3, and cell cycle arrest in IR-induced apoptosis. The methylxanthine caffeine and the staurosporine analog UCN-01, which can inhibit ATM and Chk kinases, efficiently abrogated the IR-induced G_2-M arrest and induced mitochondrial activation as judged by the loss of the mitochondrial membrane potential and the release of cytochrome *c* and Smac/Diablo. However, despite these proapoptotic alterations, cell death and activation of the initiator caspase-9 were not induced in MCF-7 cells but were interestingly only observed after reexpression of caspase-3. Sensitization to IR-induced apoptosis by caffeine or UCN-01 was abrogated neither by cycloheximide nor by pifithrin-α, an inhibitor of the transcriptional activity of p53. Furthermore, suppression of p53 by RNA interference could not prevent caffeine- and IR-induced mitochondrial alterations and apoptosis but resulted in an even more pronounced G_2-M arrest. Collectively, our results clearly show that the resistance of MCF-7 cells to IR-induced apoptosis is caused by two independent events; one of them is a caffeine- or UCN-01–inhibitable event that does not depend on p53 or a release of the G_2-M arrest. The second event is the loss of caspase-3 that surprisingly seems essential for a fully functional caspase-9 pathway, even despite the previous release of mitochondrial proapoptotic proteins.

INTRODUCTION

Intrinsic or acquired resistance of tumor cells to chemotherapy or radiotherapy remains a major obstacle to successful cancer management. Mechanisms causing resistance are diverse and poorly defined; however, recent evidence suggests that aberrant apoptosis contributes to this phenomenon. DNA-damaging agents, such as chemotherapeutic drugs or ionizing radiation (IR), are known to induce apoptosis via the intrinsic mitochondrial death pathway, in which a class of cysteine proteases, called caspases, plays a crucial role (1, 2). This pathway is initiated at the mitochondrion by the release of cytochrome *c*, which, together with dATP and apoptotic protease-activating factor 1, binds to procaspase-9 to form the apoptosome (3). On formation of the apoptosome, procaspase-9 is autoproteolytically processed, resulting in the activation of downstream caspases such as caspase-3, -6, and -7 (4). Hence, caspase-9 constitutes a crucial component of the intrinsic death pathway. The finding that cells from caspase-9 knockout mice are resistant to various death stimuli, including IR, further emphasizes this (5). Conversely, caspase-3, although required for some of the typical hallmarks of apoptosis (6, 7), seems to be dispensable for cell death induced by a variety of stimuli, such as tumor necrosis factor, CD95 ligand, or anticancer drugs (6–8). This is consistent with the observations that other effector caspases, such as caspase-6 or -7, can compensate for the lack of caspase-3, at least to some extent, in a stimulus- and cell type-dependent manner (9).

Whereas the pathways leading to caspase activation and cell death are mainly resolved, the sequence of events that take place upstream of the mitochondria following DNA damage is less well defined. Depending on the stimulus and cell type, DNA-damaged cells arrest in various phases of the cell cycle to ensure proper repair of damaged DNA (10). Whereas the G_1 arrest is mediated by the transcription factor p53 via induction of the cyclin-dependent kinase inhibitor p21, the G_2 checkpoint seems to be mainly controlled by the phosphoinositide 3-kinases ATM and ATR (11). Through a series of phosphorylation events involving the Chk1 and Chk2 kinases, ATM and ATR prevent activation of the cyclin B/Cdc2 complex that is essential for the cells to enter mitosis. Although not required for the initialization of this process, p53 seems to be necessary for the maintenance of the IR-induced G_2-M arrest (12). This is achieved via the p53-dependent induction of 14-3-3 ó and GADD45, which specifically interfere with the ATM/ATR-controlled pathway. Together with its multiple activities that result in apoptosis induction, these functions make p53 a powerful tumor suppressor (13). The loss or functional inactivation of p53 that is observed in >50% of all of the human tumors correlates in many cases with apoptosis resistance.

However, apoptosis susceptibility does not always correlate with the status of p53 expression (14–16). We also have reported recently that MCF-7 breast carcinoma cells, regardless of whether they express caspase-3, are especially resistant to IR-induced apoptosis, although they harbor a functional *p53* gene (8). Because the radioresistant phenotype of these cells was accompanied by a persistent arrest in the G_2 phase of the cell cycle, we postulated that this event prevents the generation of an as yet unknown apoptotic signal. Several reports showed that abrogation of the G_2 checkpoint by either the methylxanthine caffeine or the staurosporine analog UCN-01 correlated with a marked increase in the sensitivity of various tumor cells to ionizing radiation and certain chemotherapeutic agents (17–20). Although both compounds probably target several proteins, the release of the G_2 block by caffeine and UCN-01 is most likely mediated by inhibition of the ATM/ATR and Chk1 kinases, respectively (21, 22). In further studies it was reported that the sensitizing effect of caffeine and UCN-01 is based on their ability to release cells from the IR-induced G_2-M arrest and was preferentially observed in cells lacking functional p53 (23–26). In contrast, other reports suggested that caffeine overrides the G_2-M block independently of the p53 status of the cell; however, these cell cycle control modifications by caffeine were not associated with enhancement of radiation-induced apoptosis or reduction of clonogenic growth (27, 28). Thus, these conflicting results suggest that the relationship between the radiosensitizing effect of caffeine, the G_2-M checkpoint, and p53 is far from being elucidated.

On the basis of our previous findings that revealed a persistent irradiation-induced G_2-M arrest in MCF-7 cells (8), we further inves-

Received 3/26/04; revised 7/19/04; accepted 7/29/04.

Grant support: Grants from the Deutsche Forschungsgemeinschaft (SFB 503) and the Deutsche Krebshilfe.

The costs of publication of this article were defrayed in part by the payment of page charges. This article must therefore be hereby marked *advertisement* in accordance with 18 U.S.C. Section 1734 solely to indicate this fact.

Note: F. Essmann and I. H. Engels contributed equally to this work; I. H. Engels is currently at the Genomics Institute of the Novartis Research Foundation, Department of Cancer and Cell Biology, San Diego, California.

Requests for reprints: Reiner U. Jänicke, Institute of Molecular Medicine, University of Düsseldorf, Universitätsstrasse 1, 40225 Düsseldorf, Germany. Phone: 49-211-811-5973; Fax: 49-211-811-5892; E-mail: janicke@uni-duesseldorf.de.

tigated the role of p53 and the G_2-M block with regard to the apoptosis-resistant phenotype of these cells following exposure to IR. To this end, the effects of caffeine and UCN-01 were studied in irradiated MCF-7 and MCF-7/CASP-3 cells in combination with agents that interfere with p53 function and expression. Using this approach, we found that the sensitizing effect of caffeine and UCN-01 to IR-induced apoptosis is mediated independently of p53 and their ability to release cells from the IR-induced G_2-M arrest. We also show that sensitization by caffeine or UCN-01 requires the presence of caspase-3 because only caspase-3–expressing MCF-7 cells, but not MCF-7 cells lacking caspase-3, were killed by this treatment. Therefore, our results indicate that two separate events, the loss of caspase-3 and a caffeine- or UCN-01–sensitive process that does not require p53 or the release of the G_2-M block, contribute to the apoptosis resistance of MCF-7 breast carcinoma cells to IR.

MATERIALS AND METHODS

Cells, Reagents, and Antibodies. MCF-7 and MCF-7/CASP-3 breast carcinoma cells (7) were cultured in RPMI 1640 supplemented with 10% heat-inactivated FCS, 10 mmol/L glutamine, and 50 μg/mL each of streptomycin and penicillin. The monoclonal actin antibody, caffeine, cycloheximide, propidium iodide, and the protease inhibitors phenylmethylsulfonyl fluoride, aprotinin, leupeptin, and pepstatin were from Sigma (St. Louis, MO). Pifithrin-α and the fluorogenic caspase-3 and -9 substrates *N*-acetyl-Asp-Glu-Val-Asp-aminomethyl-coumarin (DEVD-AMC) and *N*-acetyl-Leu-Glu-His-Asp-aminomethyl-coumarin (LEHD-AMC), respectively, were from BIOMOL International (Plymouth Meeting, PA). The monoclonal p53 antibody (Ab-6) was from Calbiochem (San Diego, CA); the monoclonal p21, cytochrome *c*, and poly(ADP-ribose) polymerase (PARP) antibodies were from PharMingen, Inc (San Diego, CA). The polyclonal goat and rabbit antibodies recognizing caspase-3 and Smac/Diablo, respectively, were from R&D Systems (Minneapolis, MN), and the polyclonal caspase-9 antibody was from New England BioLabs, Inc (Beverly, MA). UCN-01 was a kind gift from R. Schultz (National Cancer Institute, Bethesda, MD).

Treatment and Transfection of Cells. Cells were exposed to IR (usually 20 Gy) using a Philips gamma chamber (Philips Medical Systems, Andover, MA) with a cobalt-60 source (XK 5105–11) in the absence or presence of either caffeine (1 mmol/L), UCN-01 (100 nmol/L), pifithrin-α (15 μmol/L), or cycloheximide (Chx; 15 ng/mL). None of these compounds applied alone elicited an apoptotic response at the indicated concentrations.

MCF-7/CASP-3 cells were transfected using Lipofectamine 2000 (Invitrogen, Carlsbad, CA) with the pSilencer vector containing the specific p53 small interfering RNA (siRNA) sequence (29) according to the protocol supplied by the manufacturer (Ambion Inc., Austin, TX). After 48 hours, cells were trypsinized and reseeded in medium containing 400 μg/mL hygromycin (for selection of p53 siRNA-expressing clones) and 400 μg/mL G418 (for coselection of caspase-3–expressing clones).

Preparation of Cell Extracts, Western Blotting, and DNA Fragmentation Analysis. Cell extracts were prepared as described previously (8). Equal amounts of the proteins were separated by SDS-PAGE and transferred to a polyvinylidene difluoride membrane (Amersham Pharmacia, Piscataway, NJ). Proteins were visualized by enhanced chemiluminescence staining using ECL reagents (Amersham Pharmacia). For DNA fragmentation analysis, cellular DNA was prepared using the Blood and Cell Culture Mini DNA kit (Qiagen, Valencia, CA). Purified DNA was incubated for 2 hours at 37°C with 200 μg/mL RNase and analyzed on 1.6% agarose gels. DNA was visualized by ethidium bromide staining.

Measurement of Cytochrome *c* and Smac/Diablo Release. Approximately 4×10^6 cells were permeabilized for 5 minutes at 4°C in a buffer containing 50 μg/mL digitonin, 250 mmol/L sucrose, 20 mmol/L HEPES (pH 7.4), 1.5 mmol/L $MgCl_2$, 10 mmol/L KCl, 1 mmol/L EDTA, 1 mmol/L EGTA, 1 mmol/L DTT, 1 mmol/L phenylmethylsulfonyl fluoride, and 2 μg/mL of each of the protease inhibitors aprotinin, pepstatin, and leupeptin. Cells were centrifuged at $1000 \times g$ for 5 minutes at 4°C to remove cell nuclei. The supernatant was transferred to a fresh tube and centrifuged at $10,000 \times g$ for 15 minutes at 4°C. The resulting supernatants containing the cytosolic fractions were loaded onto a 0.1% SDS and 15% polyacrylamide gel. Cytochrome *c* and Smac/Diablo release were analyzed by immunoblot analysis.

Determination of the Mitochondrial Transmembrane Potential. The mitochondrial transmembrane potential ($\Delta\Psi_m$) was analyzed using the $\Delta\Psi_m$-specific stain TMRE (Molecular Probes, Eugene, OR). Briefly, 10^5 cells were stained in a solution containing 25 nmol/L TMRE for 30 minutes. Staining was quantified by FL2 and scatter characteristics using a flow cytometer.

Cell Death Assessment, Cell Cycle Analysis, and Fluorometric Determination of Caspase-3 and Caspase-9 Activities. Cell death was assessed by the uptake of propidium iodide (2 μg/mL) into nonfixed cells and subsequent flow cytometric analyses with the FSC/FL2 profile. For cell cycle analyses, nuclei were prepared by lysing cells in a hypotonic buffer (0.1% sodium citrate, 0.1% Triton X-100, and 50 μg/mL propidium iodide) and subsequently analyzed by flow cytometry with the FCS/FL2 profile. The proportion of cells in the G_2 *versus* G_1 phase is indicated. All of the flow cytometry analyses were performed on a FACScalibur (Becton Dickinson, Franklin Lakes, NJ) using CellQuest analysis software. For each determination, a minimum of 10,000 cells was analyzed. Caspase-3 and -9 activities were determined as described previously (8).

Clonogenic Survival Assay. Equal cell numbers were irradiated and seeded onto 96-well plates at 3000 cells per well. After 11 days, viable cells were stained for 20 minutes with 0.5% crystal violet in 20% methanol, washed extensively, and solubilized in 33% acetic acid followed by measurement of the A_{560}.

RESULTS

Caffeine Abrogates the Ionizing Radiation-Induced G_2-M Arrest in Both MCF-7 Lines but Induces Apoptosis only in MCF-7/CASP-3 Cells. MCF-7 cells are a widely used cellular system for breast cancer. We showed previously that MCF-7 cells have lost caspase-3 expression because of a 47-bp deletion within exon 3 of the *CASP-3* gene (7). Restoration of caspase-3 expression induced some hallmarks of apoptosis in response to tumor necrosis factor and anticancer drug treatment. However, regardless of the status of caspase-3 expression, MCF-7 cells remained resistant to apoptosis induction by IR. Instead, irradiated MCF-7 and MCF-7/CASP-3 cells displayed a persistent G_2-M arrest (8) that correlated with the induction of cellular senescence as measured by staining of the senescence-associated β-Galactosidase activity (data not shown).

To test our hypothesis that the IR-induced G_2-M arrest prevents the generation of an as yet unknown apoptotic signal, we exposed both cell lines to a single dose of 20 Gy in the absence or presence of the methylxanthine caffeine. Caffeine is a widely used radiosensitizing agent that was shown to override DNA damage-induced cell cycle arrest in a variety of cell lines (19, 20, 23–26). Despite the presence of wild-type p53, 1 mmol/L caffeine, a commonly used concentration, completely abrogated the IR-induced G_2-M arrest in both MCF-7 cell lines (Fig. 1*A, top*). Interestingly, induction of cell death as measured by the uptake of propidium iodide was only observed in caspase-3–expressing, but not in caspase-3–deficient, MCF-7 cells (Fig. 1*A, bottom*). MCF-7/CASP-3 cells exposed to IR and caffeine detached from the plastic surface and showed the morphologic changes typical of cells undergoing apoptosis, such as shrinkage and blebbing (data not shown). Consistent with the cell death data, cleavage of the caspase substrate PARP (Fig. 1*B*) and DNA fragmentation (Fig. 1*C*) also were predominantly evident in caspase-3–expressing MCF-7 cells exposed to IR and caffeine. These results indicated that in contrast to apoptosis induction by various death stimuli including anticancer drugs, caspase-3 is essential for IR- and caffeine-induced death of MCF-7 cells. Similar results were obtained when the experiments were performed with the staurosporine analog UCN-01 (data not shown), which, like caffeine, sensitizes cells to radiation-induced

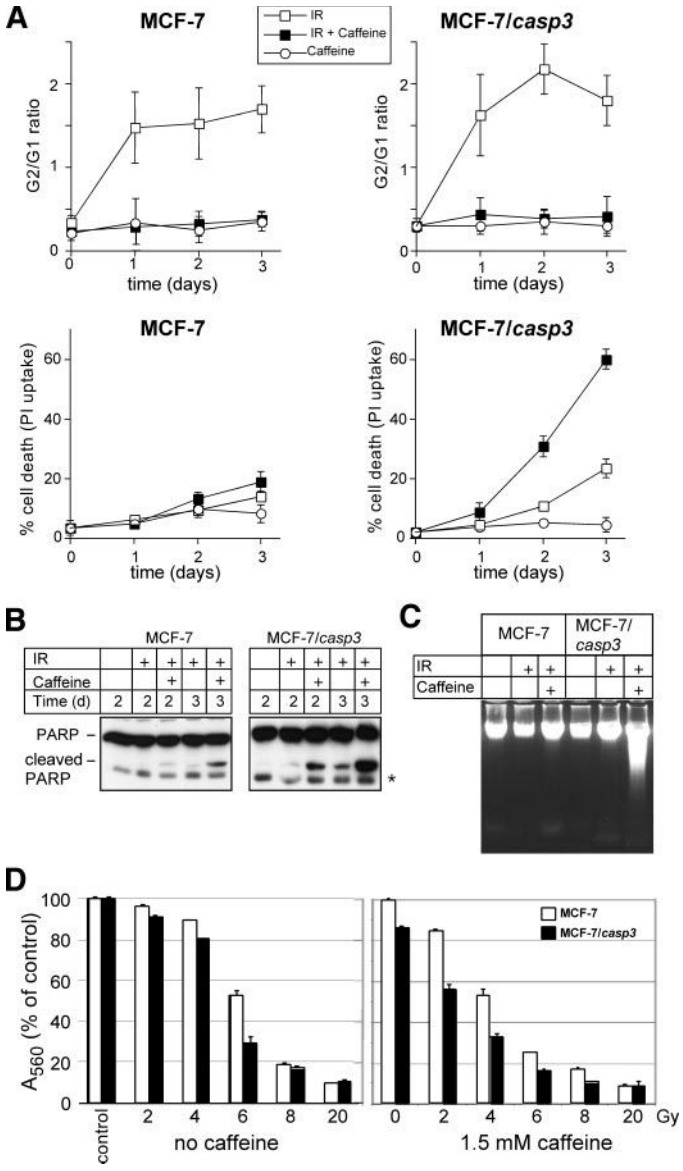

Fig. 1. Caffeine abrogates the radiation-induced G_2-M arrest in both MCF-7 lines but induces cell death only in MCF-7/CASP-3 cells. *A,* Cells were exposed to a single dose of either 20 Gy (□) or 1 mmol/L caffeine (○) alone, or to a combination of both (■). After the indicated times, the G_2 to G_1 ratio was determined by FACS analysis (*top*). The percentage of dead cells was measured in a flow cytometer by the uptake of propidium iodide (PI; *bottom*). Data represent the mean of three independent experiments ± SD. Similar results were obtained when cell death was assessed in crystal violet-stained cells (data not shown). *B,* Western blot analysis for the status of PARP in untreated MCF-7 and MCF-7/CASP-3 cells and in cells incubated for the indicated times following exposure to 20 Gy in the absence or presence of caffeine (1 mmol/L); ∗an unspecific band. *C,* DNA fragmentation in MCF-7 and MCF-7/CASP-3 cells exposed for 3 days to 20 Gy in the absence or presence of caffeine (1 mmol/L). *D,* clonogenic survival of cells that were exposed to the indicated radiation doses in the absence or presence of caffeine. Viable cells were stained with crystal violet 11 days following irradiation. Each bar represents the mean of duplicate absorbance values of control (nonirradiated cells).

apoptosis (22). Although MCF-7 cells do not undergo radiation-induced apoptosis even in the presence of caffeine, increasing radiation doses dramatically reduced their reproductive capacity as determined in a clonogenic survival assay (Fig. 1*D*). This effect was even more pronounced when MCF-7/CASP-3 cells were used, although the accelerated reproductive death rate was observed predominantly in the presence of caffeine, which is consistent with the apoptosis data. Collectively, these results indicate that caspase-3 radiosensitizes MCF-7 cells also in terms of their reproductive capacity in the presence of caffeine.

Caspase-9 Is Only Activated in MCF-7/CASP-3 Cells, Although Exposure to Caffeine and Ionizing Radiation Activates the Mitochondria in Both MCF-7 Cell Lines. These results suggested that the resistant phenotype of MCF-7 cells toward IR-induced apoptosis is caused by two independent events: one of them seems to be inhibitable by caffeine or UCN-01, and the other is most likely because of the absence of caspase-3. In an attempt to understand the latter, we analyzed characteristic apoptotic events that take place at the level or downstream of mitochondria. As expected, in contrast to either treatment alone, the combined treatment of MCF-7/CASP-3 cells with IR and caffeine resulted in the loss of the mitochondrial membrane potential (Fig. 2*A*), a process that is closely associated with the intrinsic death pathway (30). This treatment also induced the release of cytochrome *c* and Smac/Diablo, which represent two mitochondria-derived proapoptotic factors required for the activation of the intrinsic death pathway (Fig. 2*B*). Interestingly, all of these events also were induced to a similar extent by the combined treatment in MCF-7 cells, a cell line that does not undergo IR-induced apoptosis even in the presence of caffeine (Fig. 1).

Remarkably, despite our finding that IR, together with caffeine, induced cytochrome *c* and Smac/Diablo release in both cell lines, activation of the initiator caspase-9 was only observed in MCF-7/CASP-3 cells, in which this treatment resulted also in the activation of caspase-3 (Fig. 3). This could be readily shown by the specific fluorometric caspase substrate cleavage assays (Fig. 3*A*) and by Western blot analysis showing the processed and thereby activated caspases (Fig. 3*B*). Whereas neither treatment alone was able to activate these caspases above background levels, the combination of IR and caffeine resulted in an efficient activation of caspase-3 and -9 only in MCF-7/CASP-3 cells. Collectively, these results suggest that

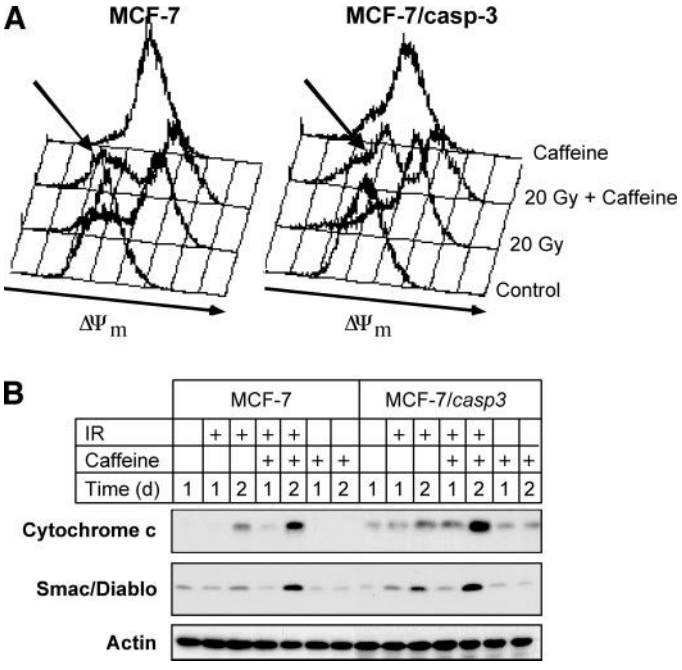

Fig. 2. IR and caffeine induce mitochondrial membrane depolarization and release of cytochrome *c* and Smac/Diablo in both MCF-7 cell lines. *A,* measurement of the mitochondrial membrane potential ($\Delta\Psi_m$) in untreated (control) MCF-7 and MCF-7/CASP-3 cells and in cells exposed to a single dose of 20 Gy, 1 mmol/L caffeine, or to a combination of both. Cells were analyzed after 3 days. The arrows indicate the decrease of the mitochondrial membrane potential induced by IR and caffeine. One representative experiment of four is shown. *B,* Western blot analysis for cytosolic cytochrome *c* (*top*), Smac/Diablo (*middle*), or as a control for actin (*bottom*) in untreated cells or in cells exposed either to a single dose of 20 Gy, 1 mmol/L caffeine, or to a combination of both. One representative experiment of three is shown.

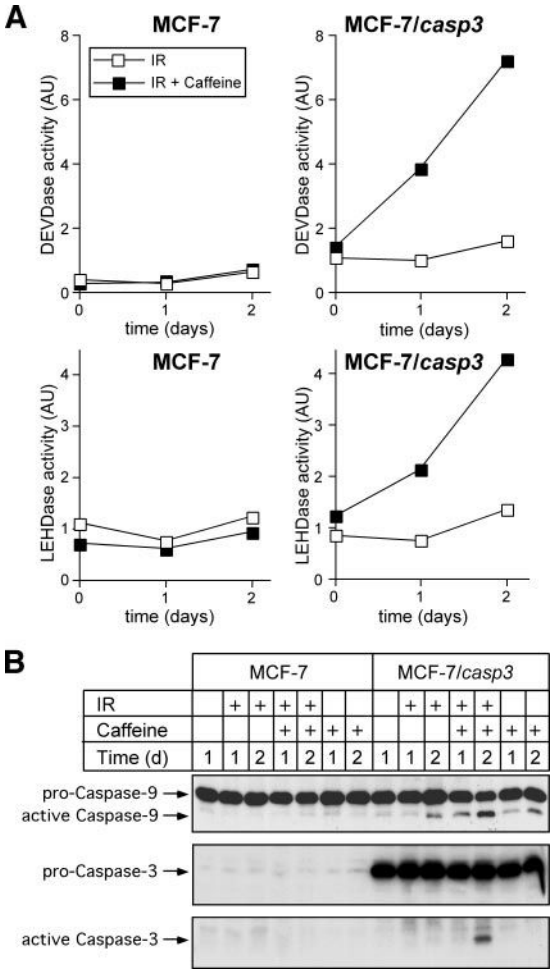

Fig. 3. IR and caffeine induce the activation of caspase-3 and -9 only in MCF-7/CASP-3 cells. *A,* caspase-3 (DEVDase; *top*) and caspase-9 (LEHDase; *bottom*) activities in cytoplasmic extracts of cells exposed to a single dose of 20 Gy in the absence (□) or presence of 1 mmol/L caffeine (■). Caffeine alone had no effect on caspase activities (data not shown). *B,* Western blot analysis showing that IR and caffeine induce caspase-9 (*top*) and caspase-3 (*middle* and *bottom*) activation only in MCF-7/CASP-3 cells. The caspase proforms and their active subunits are indicated. One representative experiment of five is shown.

caspase-3 is essential for the activation of caspase-9 and subsequently also for a fully functional mitochondrial death pathway induced by IR.

Caffeine Sensitizes MCF-7/CASP-3 Cells to Ionizing Radiation-Induced Apoptosis Independently of the Transcriptional Activity of p53 and Independently of Cell Cycle Control. Caffeine and UCN-01 specifically target and inhibit the ATM/ATR and the Chk1 kinases, respectively, which were both shown to phosphorylate p53 (11). To investigate a possible role of p53 in this process, we compared cell cycle progression and cell death induction in both MCF-7 cell lines exposed to a combination of IR and caffeine in the absence or presence of pifithrin-α, a potent inhibitor of the transcriptional activity of p53 (31). Similar to caffeine, treatment of MCF-7/CASP-3 and MCF-7 cells with pifithrin-α completely abrogated the IR-induced p53-dependent expression of p21 without affecting p53 levels (Fig. 4*B* and data not shown), showing that pifithrin-α efficiently blocked the transcriptional activity of p53. However, in contrast to caffeine that completely released the IR-induced G_2-M arrest in both cell lines, cotreatment of the cells with pifithrin-α resulted in an even more pronounced IR-induced cell cycle arrest that could not be overcome by caffeine (Fig. 4*A, top*). Treatment of the cells with pifithrin-α alone had no effect on cell cycle progression (data not shown).

However, although MCF-7/CASP-3 cells simultaneously exposed to the three treatments were arrested in the G_2-M phase to a similar extent as cells that were only irradiated, they were not protected from apoptosis (Fig. 4*A, bottom*). Pifithrin-α also had no effect on apoptosis of MCF-7 cells because they remained radiation resistant in the absence or presence of either compound. Similar results were obtained when the experiments were performed with UCN-01 (data not shown). Thus, these results clearly show that the radiosensitizing effect of caffeine is mediated independently of the transcriptional activity of p53. They also provide evidence that caffeine sensitizes MCF-7/CASP-3 cells to IR-induced apoptosis independent of its ability to release the irradiation-induced G_2-M arrest.

p53 Is Not Required for Caffeine-Mediated Radiosensitization of MCF-7/CASP-3 Cells. Next we asked whether p53 protein expression or new protein biosynthesis is required for the radiosensitizing effect of caffeine. To this end, we first performed similar experiments as described previously in the absence or presence of Chx. Although Chx almost completely blocked the IR-induced p21 expres-

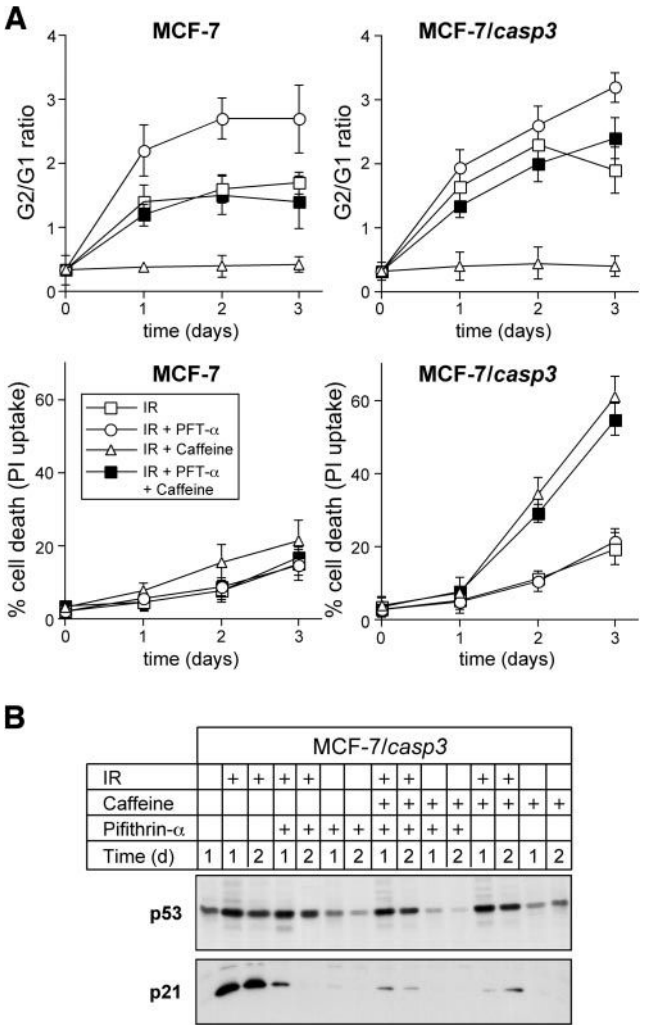

Fig. 4. Pifithrin-α reverses the caffeine-mediated release of the radiation-induced G_2-M arrest but has no effect on apoptosis induction. *A,* Cells were either left untreated or exposed to a single dose of 20 Gy in the absence (□) or presence of 1 mmol/L caffeine (△), 15 μmol/L pifithrin-α (○), or to a combination of both (■). After the indicated times, the G_2 to G_1 ratio and the percentage of apoptotic cells were determined by FACS analyses. Data represent the mean of three independent experiments. *B,* Pifithrin-α inhibits the transcriptional activity of p53. Western blot analysis of the status of p53 and p21 expression in untreated MCF-7/CASP-3 cells and in cells that were either exposed to a single dose of 20 Gy, 1 mmol/L caffeine, 15 μmol/L pifithrin-α alone, or to the indicated combinations. Cell extracts were harvested at the indicated times. One representative experiment of two is shown.

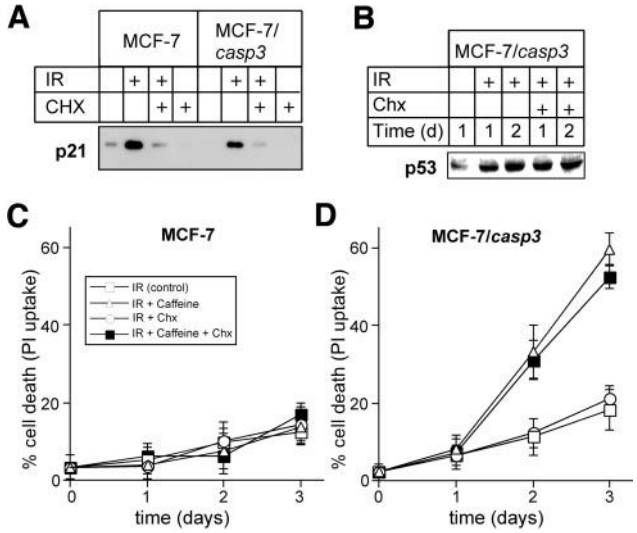

Fig. 5. Caffeine-mediated sensitization toward IR-induced apoptosis does not require new protein synthesis. *A,* Western blot analysis for the status of p21 in MCF-7 and MCF-7/CASP-3 cells that were either left untreated or exposed to a single dose of 20 Gy or 15 ng/mL Chx or to a combination of both. Cell extracts were harvested after 3 days. *B,* Western blot analysis for the status of p53 in MCF-7/CASP-3 cells that were either left untreated or exposed to a single dose of 20 Gy in the absence or presence of 15 ng/mL Chx. Cell extracts were harvested after the indicated days. *C* and *D,* Cell death determination of untreated MCF-7 and MCF-7/CASP-3 cells or cells that were exposed to a single dose of 20 Gy in the absence (□) or presence of 1 mmol/L caffeine (△), 15 ng/mL Chx (○), or to a combination of both (■). Data represent the mean of three independent experiments ± SD.

sion in both cell lines, verifying its inhibitory effect on translation (Fig. 5*A*), it did not influence IR- and caffeine-induced death of MCF-7/CASP-3 cells (Fig. 5*D*). Chx also did not affect the radiation-resistant phenotype of MCF-7 cells, ruling out the possible existence of an IR-induced apoptosis inhibitory factor such as nuclear factor κB (Fig. 5*C*). Therefore, the caffeine-mediated sensitization to IR-induced apoptosis does neither require p21 nor does it depend on *de novo* protein biosynthesis. Chx did not affect IR-induced p53 protein levels (Fig. 5*B*). This is most likely because p53 expression induced by DNA-damaging agents does not depend as much on new protein synthesis as it does on post-translational modifications that result in the stabilization of the existing p53 protein (32). Although these data cannot entirely rule out an involvement of p53 in radiosensitization by caffeine, they suggest that if p53 is involved in this process, it is not the inducible, but rather the preexisting, p53 population that may modulate apoptosis.

To further investigate the role of p53 in radiosensitization by caffeine, we analyzed an MCF-7 clone (MCF-7/p53si) in which p53 expression was efficiently suppressed because of stable transfection of a p53 siRNA (Fig. 6*A*; ref. 29). Because MCF-7 cells do not undergo IR- and caffeine-induced apoptosis because of the lack of caspase-3 (Fig. 1), we first examined whether this treatment requires p53 for the mitochondrial membrane depolarization, which we have shown to proceed also in the absence of caspase-3 (Fig. 2). We found that exposure of these cells to IR in the presence of caffeine substantially reduced the mitochondrial membrane potential, indicating that this event occurs independently of p53 expression (Fig. 6*B*). However, IR had an even more dramatic effect on the cell cycle distribution of MCF-7/p53si cells when compared with parental MCF-7 cells because almost the entire population of p53-deficient cells was arrested in the G_2-M phase (Fig. 6*C*). Furthermore, in contrast to p53-expressing MCF-7 cells, caffeine could not overcome this G_2-M arrest in MCF-7/p53si cells (Fig. 6*C*), although the activation of the mitochondria was achieved in both cell lines to a similar extent regardless of the p53 status. These data are consistent with our observation that suppression of the transcriptional activity of p53 by pifithrin-α resulted in an even more pronounced IR-induced G_2-M arrest that could not be overcome by caffeine (Fig. 4). Collectively, these results suggest that although p53 seems to be required for the caffeine-mediated release of the IR-induced G_2-M arrest, this event is not a prerequisite for sensitization achieved by caffeine.

Finally, we generated MCF-7/CASP-3 cells stably expressing the p53 siRNA described previously in which apoptosis induction could be more easily addressed than in caspase-3–deficient MCF-7 cells. Several clones were obtained that displayed reduced p53 levels following IR, and three clones with the highest suppression efficiencies were analyzed in more detail (Fig. 7*A*). As shown in Fig. 7*B*, the inability of these clones to up-regulate p53 expression following IR did not impair apoptosis susceptibility as judged by caspase-3 activity assays. Exposure to IR and caffeine induced comparable caspase-3 activities in the four cell lines regardless of the p53 status, indicating

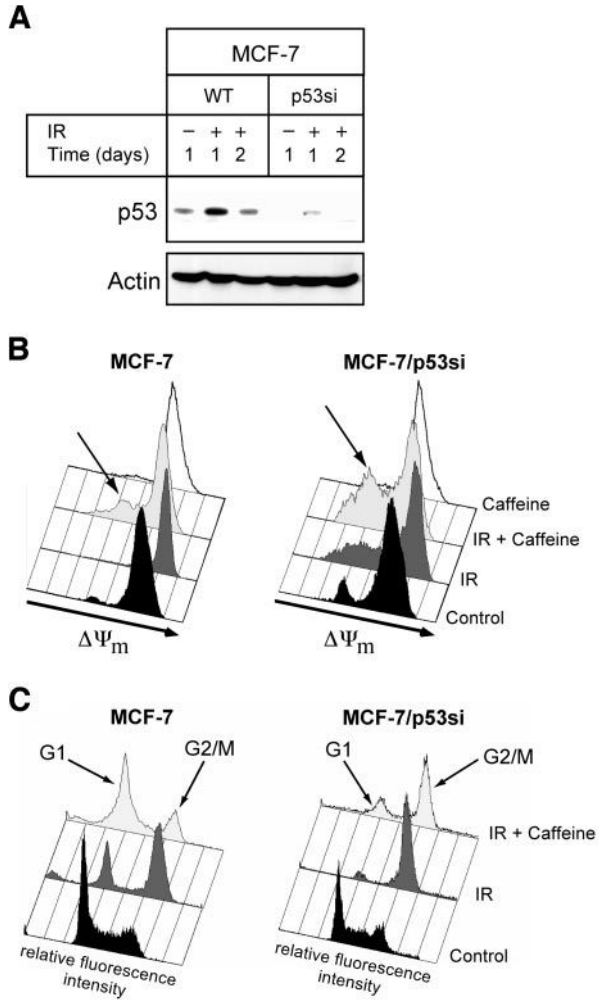

Fig. 6. Effect of the p53 siRNA on cell cycle progression and mitochondrial membrane depolarization in MCF-7 cells. *A,* Western blot analyses of the status of p53 in MCF-7 cells and cells stably expressing the p53 siRNA (29) that were either left untreated or exposed to 20 Gy. Cell extracts were prepared after the indicated times. Probing the membrane with actin served as loading control. One representative experiment of three is shown. *B,* measurement of the mitochondrial membrane potential ($\Delta\Psi_m$) in untreated (control) MCF-7 and MCF-7/siRNA cells and in cells exposed to a single dose of 20 Gy, 1 mmol/L caffeine, or to a combination of both. Cells were analyzed after 2 days. The arrows indicate the decrease of the mitochondrial membrane potential induced by IR and caffeine. One representative experiment of three is shown. *C,* cell cycle analyses of untreated MCF-7 and MCF-7/siRNA cells (control) or cells exposed for 1 day to 20 Gy in the absence or presence of caffeine. The arrows indicate cells in the G_1 and G_2-M phase, respectively. One representative experiment of three is shown.

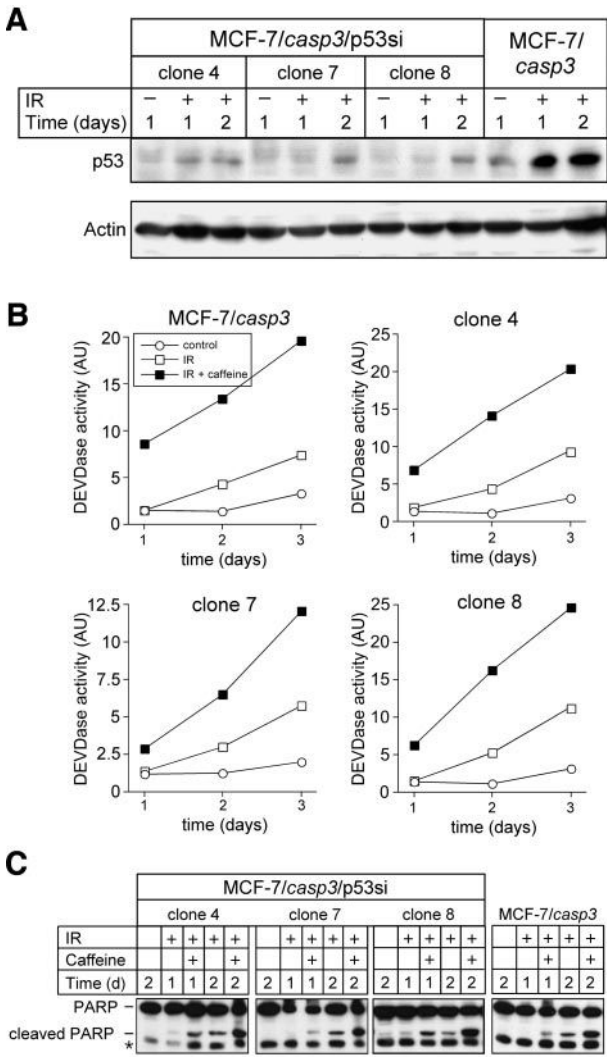

Fig. 7. Suppression of p53 levels by stable expression of the p53 siRNA has no effect on IR- and caffeine-induced caspase-3 activation. *A,* Western blot analyses of the status of p53 in MCF-7/CASP-3 cells and cells stably expressing the p53 siRNA that were either left untreated or exposed to 20 Gy. Probing the membrane with actin served as loading control. One representative experiment of three is shown. *B,* caspase-3 (DEVDase) activity in cytoplasmic extracts of MCF-7/CASP-3 and MCF-7/CASP-3/siRNA cells that were either left untreated (○) or cells exposed to a single dose of 20 Gy in the absence (□) or presence of 1 mmol/L caffeine (■). Treatment of cells with caffeine alone had no effect (data not shown). One representative experiment of three is shown. *C,* Western blot analysis of the status of PARP in untreated MCF-7/CASP-3 and MCF-7/CASP-3/siRNA cells and in cells incubated for the indicated times following exposure to 20 Gy in the absence or presence of caffeine (1 mmol/L); ∗an unspecific band.

that p53 is dispensable for this event. This was further confirmed by analyzing the mitochondrial membrane potential, which also dramatically decreased in the three MCF-7/CASP-3/p53si clones following IR and caffeine treatment (data not shown). As expected and consistent with these data, PARP cleavage induced by IR and caffeine also was observed independently of p53 expression in these cell lines (Fig. 7*C*). Thus, these data provide further evidence that the caffeine-inhibitable event upstream of the mitochondria does not require p53.

DISCUSSION

Role of Caspase-3 in Resistance to Ionizing Radiation-Induced Apoptosis. Chemotherapy and radiotherapy are important treatment modalities for many cancers, but the frequent occurrence of drug- and radiation-resistant tumors is a common clinical problem. Many different mechanisms can account for poor patient prognosis and treatment failure, including the loss or mutation of proapoptotic genes that regulate the intrinsic death pathway, such as p53 or apoptotic protease-activating factor 1 (13, 32, 33). Caspase-3 also was proposed to play a crucial role in DNA damage-induced apoptosis because it is frequently activated during apoptosis induced by various death stimuli, including DNA-damaging agents. However, the mere activation of a caspase during apoptosis does not necessarily imply its requirement for this process. Although caspase-3 is known to cleave a multitude of cellular substrates and is absolutely required for some classical alterations associated with apoptosis, it was shown to be dispensable for cell death induced by various death stimuli, including anticancer drugs (6–8, 34).

In the present study, we show that caspase-3 is required for IR- and caffeine-induced apoptosis of MCF-7 breast carcinoma cells and postulate that one reason for the radioresistant phenotype of these cells is the functional deletion of the *CASP-3* gene. Although IR did not evoke an apoptotic response even in MCF-7/CASP-3 cells, cotreatment with the methylxanthine caffeine or the staurosporine analog UCN-01 resulted in massive apoptosis in a caspase-3–dependent manner. Interestingly, exposure to IR in combination with caffeine triggered mitochondrial activation in both MCF-7 cell lines as judged by the loss of the mitochondrial membrane potential and the release of cytochrome *c* and Smac/Diablo. However, consistent with an obligatory role for caspase-9 in IR-induced apoptosis (5), activation of caspase-9 was only achieved in IR- and caffeine-treated MCF-7/CASP-3 cells, showing that caspase-3 also is required for this event. Because caspase-9 is believed to act upstream of caspase-3 in the mitochondrial death pathway, this scenario seems paradoxical. Nevertheless, similar observations also were reported previously in tumor necrosis factor- and cisplatin-induced apoptosis of MCF-7 cells in which caspase-9 was only activated in MCF-7/CASP-3 cells (35, 36). This is because a complete processing of caspase-9 requires two cleavage events in its proform, one of which is mediated at Asp-315 by the autoproteolytic activity of caspase-9 itself and the other by caspase-3 at Asp-330 (37, 38). However, caspase-9 activation differs greatly from that of other caspases because it does not necessarily require proteolytic processing. In this respect, it was shown that procaspase-9 contains only 10% of the activity of cleaved caspase-9, which increased 2000-fold following its integration into the apoptosome (39, 40). In our study, caspase-9 activity and processing as assessed by the cleavage of the fluorogenic substrate LEHD-AMC and by immunoblot analyses, respectively, were only detected in MCF-7/CASP-3 cells exposed to IR and caffeine but not in similarly treated MCF-7 cells lacking caspase-3. Therefore, our results suggest that caspase-3 is required for the activation of caspase-9 in IR- and caffeine-induced apoptosis of MCF-7 cells. These data also give rise to the speculation that caspase-3 may be an essential component of a fully active apoptosome. This is consistent with the finding that apoptosis induction by microinjected cytochrome *c* also requires caspase-3 in MCF-7 cells (41). Because the presence of caspase-3 in the apoptosome was documented in some reports (42, 43), but not in others (39), a possible obligatory role for caspase-3 in the apoptosome might be stimulus- and cell type-specific and remains to be further elucidated.

As mentioned, we have shown previously that the anticancer drugs etoposide and doxorubicin, but not IR, elicit a caspase-dependent apoptosis pathway even in the absence of caspase-3 (PARP cleavage and death of MCF-7 cells were inhibitable by z-Val-Ala-Asp-fluoromethyl ketone; ref. 8). Furthermore, in contrast to IR, exposure of MCF-7/CASP-3 cells to these anticancer drugs resulted in the activation of the mitochondrial death pathway, including cytochrome *c* release and activation of caspase-9 and -3. Therefore, we postulated that anticancer drug-induced apoptosis, but not apoptosis induced by

IR, uses, in addition to the classical mitochondrial pathway, an alternative route leading to caspase activation and cell death. Our present results strengthen and further extend this hypothesis because they show that IR- and caffeine-induced apoptosis of MCF-7 cells largely depends on the mitochondrial death pathway that requires the presence of caspase-3. The possible requirement of caspase-3 for a fully functional mitochondrial pathway, at least in MCF-7 cells, further implies that the alternative caspase-3–independent apoptotic pathway used by anticancer drugs also may be independent of the apoptosome. Although the existence of such a pathway(s) was documented recently in several reports (44–46), further investigations, preferentially in the MCF-7 cell system, are required to decipher anticancer drug- and IR-induced apoptotic pathways.

Potential Mechanisms Involved in Caffeine-Mediated Sensitization to Ionizing Radiation-Induced Apoptosis. In addition to the lack of caspase-3, our study also shows that the resistant phenotype of MCF-7 cells toward IR-induced apoptosis is caused by a caffeine- or UCN-01–inhibitable event that takes place upstream of the mitochondria. Thus far, numerous reports showed that caffeine and UCN-01 sensitize various tumor cell lines to IR-induced apoptosis, and most of them attributed this effect to the ability of these compounds to override the IR-induced G_2-M arrest (19–22) preferentially in cells lacking functional p53 (14, 23–26). However, our data show that both agents sensitize MCF-7/CASP-3 cells to IR-induced apoptosis not only independently of checkpoint inhibition but also independently of the p53 status. We did not observe a significant difference with regard to the rate of apoptosis induced by IR and caffeine in MCF-7/CASP-3 cells expressing a functionally active p53 protein and cells in which p53 was rendered inactive by either pifithrin-α or expression of a p53 siRNA. Abrogation of p53 function and/or expression by pifithrin-α and the p53 siRNA, respectively, clearly had the opposite effect on cell cycle distribution. Exposing MCF-7 or MCF-7/CASP-3 cells to these compounds significantly increased the IR-induced G_2-M arrest, which can be explained by the fact that cells defective or deficient for p53 bypass the G_1 checkpoint to accumulate in the G_2-M phase (47). Interesting, however, was the observation that this profoundly increased G_2-M arrest could not be overcome by caffeine, although these cells were as efficiently killed by this treatment as p53-expressing MCF-7/CASP-3 cells. Even though a direct causal link between checkpoint abrogation and sensitization toward IR-induced apoptosis is difficult to prove because of the complexity of the system, our results show that caffeine also mediates its radiosensitizing effect in p53-expressing cells and independently of its ability to release the IR-induced G_2-M arrest. Therefore, our results are, at least partially, consistent with more recent studies describing that caffeine releases the IR-induced cell cycle block in a p53-independent manner (27, 28). However, the reason why caffeine did not induce apoptosis in these studies is unknown but could be because of the lack of relevant mitochondrial apoptosis components in the used cells, a possibility that was not explored.

What are the mechanisms involved in radiosensitization by caffeine and UCN-01? Caffeine inhibits the nucleotide exchange activity of RCC1, alkaline phosphatase activity, phosphodiesterase activity, and the ATM and ATR kinases at least *in vitro*. Because ATM controls a pathway leading to G_2-M arrest involving inhibition of Cdc2 and cyclin B1 and because ATM-deficient cells are hypersensitive to IR, it seemed logical to assume that especially inhibition of ATM and its downstream target Chk1 by caffeine and UCN-01, respectively, is responsible for the sensitizing activity of these compounds. However, whether caffeine also can inhibit ATM *in vivo* seems to be controversial (48). In this context, we did not detect any caffeine-mediated adverse changes in the expression levels of various ATM-controlled cell cycle regulators, including Cdc2 and cyclin B1 (data not shown), that could account for the radiosensitizing activity of caffeine as was reported previously (26). Caffeine also did neither inhibit p53 expression or ATM-mediated phosphorylation of p53 on serine 15, nor did it block the rate of DNA repair in irradiated MCF-7 or MCF-7/CASP-3 cells (data not shown).

Caffeine was shown previously to induce apoptosis via p53 and Bax (49, 50). Although transcriptionally independent activities of p53 are much less understood than its function as a transcription factor (13), recent evidence suggests that cytoplasmic or mitochondrial p53 may directly interact with proapoptotic and antiapoptotic members of the Bcl-2 family, respectively, thereby inducing apoptosis (51, 52). However, suppression of endogenous p53 using a p53 siRNA did affect neither apoptosis of IR- and caffeine-treated MCF-7/CASP-3 cells nor the loss of the mitochondrial membrane potential regardless of caspase-3 expression. Hence, we clearly favor a p53- and cell cycle-independent radiosensitization pathway mediated by caffeine.

The BH3-only proapoptotic Bid protein might be involved in such a pathway because it was shown recently that cleavage of Bid by an as yet unknown aspartase is required for apoptosis induced by DNA-damaging agents, including IR (53). With regard to this, we noticed that caffeine significantly reduced phosphorylation of Bid, whereas expression of other members of the Bcl-2 family, such as Bcl-2, Bcl-xL, Bad, Bax, and Bak, was not affected by this treatment.[1] Phosphorylated Bid is uncleavable by caspases and hence is unable to induce cytochrome *c* release from mitochondria (54). Thus, our observation suggests that caffeine may radiosensitize cells via interfering with the phosphorylation status of Bid perhaps by inhibiting casein kinases I and II, which were shown to phosphorylate Bid. Both kinases are efficiently inhibited *in vitro* by staurosporine (54), making it highly likely that the staurosporine analog UCN-01 also acts in a similar fashion. However, further, more detailed studies are required to verify this hypothesis.

In summary, we have shown that the resistant phenotype of MCF-7 cells toward IR-induced apoptosis is caused by two independent events. One is a caffeine- and UCN-01–inhibitable event that is independent of cell cycle progression and p53 status, and the other is the functional deletion of the *CASP-3* gene. Especially in view of our observation that reexpression of caspase-3 also accelerates IR-induced reproductive death, these results provide evidence that the inactivation of caspase-3 may promote tumorigenesis and may have contributed to the development of the breast cancer from which MCF-7 cells are derived. Therefore, it now will be of particular interest to study whether IR-induced apoptosis of other tumor cell lines also depends on a functional caspase-3 because such findings may help to develop improved therapies for the management of radioresistant tumors.

ACKNOWLEDGMENTS

We thank R. Schultz for the kind gift of UCN-01, R. Agami for MCF-7/p53siRNA cells, and A. Powiton for her assistance with the radiation treatments.

REFERENCES

1. Cryns V, Yuan J. Proteases to die for. Genes Dev 1998;12:1551–70.
2. Los M, Wesselborg S, Schulze-Osthoff K. The role of caspases in development, immunity, and apoptotic signal transduction: lessons from knockout mice. Immunity 1999;10:629–39.
3. Li H, Yuan J. Deciphering the pathways of life and death. Curr Opin Cell Biol 1999;11:261–6.
4. Slee EA, Harte MT, Kluck RM, et al. Ordering the cytochrome c-initiated caspase cascade: hierarchical activation of caspases-2, -3, -6, -7, -8, and -10 in a caspase-9-dependent manner. J Cell Biol 1999;144:281–92.

[1] Essmann and Jänicke, unpublished observation.

5. Hakem R, Hakem A, Duncan GS, et al. Differential requirement for caspase 9 in apoptotic pathways in vivo. Cell 1998;94:339–52.
6. Porter AG, Janicke RU. Emerging roles of caspase-3 in apoptosis. Cell Death Differ 1999;6:99–104.
7. Janicke RU, Sprengart ML, Wati MR, Porter AG. Caspase-3 is required for DNA fragmentation and morphological changes associated with apoptosis. J Biol Chem 1998;273:9357–60.
8. Janicke RU, Engels IH, Dunkern T, Kaina B, Schulze-Osthoff K, Porter AG. Ionizing radiation but not anticancer drugs causes cell cycle arrest and failure to activate the mitochondrial death pathway in MCF-7 breast carcinoma cells. Oncogene 2001;20: 5043–53.
9. Zheng TS, Hunot S, Kuida K, et al. Deficiency in caspase-9 or caspase-3 induces compensatory caspase activation. Nat Med 2000;6:1241–7.
10. Zhou BB, Elledge SJ. The DNA damage response: putting checkpoints in perspective. Nature 2000;408:433–9.
11. Abraham RT. Cell cycle checkpoint signaling through the ATM and ATR kinases. Genes Dev 2001;15:2177–96.
12. Sionov RV, Haupt Y. The cellular response to p53: the decision between life and death. Oncogene 1999;18:6145–57.
13. Vousden KH, Lu X. Live or let die: the cell's response to p53. Nat Rev Cancer 2002;2:594–604.
14. Fan S, Smith ML, Rivet DJ 2nd, et al. Disruption of p53 function sensitizes breast cancer MCF-7 cells to cisplatin and pentoxifylline. Cancer Res 1995;55:1649–54.
15. Hawkins DS, Demers GW, Galloway DA. Inactivation of p53 enhances sensitivity to multiple chemotherapeutic agents. Cancer Res 1996;56:892–8.
16. Wahl AF, Donaldson KL, Fairchild C, et al. Loss of normal p53 function confers sensitization to Taxol by increasing G2/M arrest and apoptosis. Nat Med 1996;2: 72–9.
17. Schlegel R, Pardee AB. Caffeine-induced uncoupling of mitosis from the completion of DNA replication in mammalian cells. Science 1986;232:1264–6.
18. Bunch RT, Eastman A. Enhancement of cisplatin-induced cytotoxicity by 7-hydroxystaurosporine (UCN-01), a new G2-checkpoint inhibitor. Clin Cancer Res 1996;2: 791–7.
19. Narayanan PK, Rudnick JM, Walthers EA, Crissman HA. Modulation in cell cycle and cyclin B1 expression in irradiated HeLa cells and normal human skin fibroblasts treated with staurosporine and caffeine. Exp Cell Res 1997;233:118–27.
20. Bache M, Pigorsch S, Dunst J, et al. Loss of G2/M arrest correlates with radiosensitization in two human sarcoma cell lines with mutant p53. Int J Cancer 2001; 96:110–7.
21. Sarkaria JN, Busby EC, Tibbetts RS, et al. Inhibition of ATM and ATR kinase activities by the radiosensitizing agent, caffeine. Cancer Res 1999;59:4375–82.
22. Busby EC, Leistritz DF, Abraham RT, Karnitz LM, Sarkaria JN. The radiosensitizing agent 7-hydroxystaurosporine (UCN-01) inhibits the DNA damage checkpoint kinase hChk1. Cancer Res 2000;60:2108–12.
23. Powell SN, DeFrank JS, Connell P, et al. Differential sensitivity of p53(−) and p53(+) cells to caffeine-induced radiosensitization and override of G2 delay. Cancer Res 1995;55:1643–8.
24. Russell KJ, Wiens LW, Demers GW, Galloway DA, Plon SE, Groudine M. Abrogation of the G2 checkpoint results in differential radiosensitization of G1 checkpoint-deficient and G1 checkpoint-competent cells. Cancer Res 1995;55:1639–42.
25. DeFrank JS, Tang W, Powell SN. p53-null cells are more sensitive to ultraviolet light only in the presence of caffeine. Cancer Res 1996;56:5365–8.
26. Yao SL, Akhtar AJ, McKenna KA, et al. Selective radiosensitization of p53-deficient cells by caffeine-mediated activation of p34cdc2 kinase. Nat Med 1996;2:1140–3.
27. Ribeiro JC, Barnetson AR, Jackson P, Ow K, Links M, Russell PJ. Caffeine-increased radiosensitivity is not dependent on a loss of G2/M arrest or apoptosis in bladder cancer cell lines. Int J Radiat Biol 1999;75:481–92.
28. Deplanque G, Ceraline J, Mah-Becherel MC, Cazenave JP, Bergerat JP, Klein-Soyer C. Caffeine and the G2/M block override: a concept resulting from a misleading cell kinetic delay, independent of functional p53. Int J Cancer 2001;94:363–9.
29. Brummelkamp TR, Bernards R, Agami R. A system for stable expression of short interfering RNAs in mammalian cells. Science 2002;296:550–3.
30. Ferri KF, Kroemer G. Organelle-specific initiation of cell death pathways. Nat Cell Biol 2001;3:E255–63.
31. Komarov PG, Komarova EA, Kondratov RV, et al. A chemical inhibitor of p53 that protects mice from the side effects of cancer therapy. Science 1999;285:1733–7.
32. Burns TF, El-Deiry WS. The p53 pathway and apoptosis. J Cell Physiol 1999;181: 231–9.
33. Soengas MS, Capodieci P, Polsky D, et al. Inactivation of the apoptosis effector Apaf-1 in malignant melanoma. Nature 2001;409:207–11.
34. Pirnia F, Schneider E, Betticher DC, Borner MM. Mitomycin C induces apoptosis and caspase-8 and -9 processing through a caspase-3 and Fas-independent pathway. Cell Death Differ 2002;9:905–14.
35. Stennicke HR, Jurgensmeier JM, Shin H, et al. Pro-caspase-3 is a major physiologic target of caspase-8. J Biol Chem 1998;273:27084–90.
36. Blanc C, Deveraux QL, Krajewski S, et al. Caspase-3 is essential for procaspase-9 processing and cisplatin-induced apoptosis of MCF-7 breast cancer cells. Cancer Res 2000;60:4386–90.
37. Srinivasula SM, Fernandes-Alnemri T, Zangrilli J, et al. The Ced-3/interleukin 1ā converting enzyme-like homolog Mch6 and the lamin-cleaving enzyme Mch2α are substrates for the apoptotic mediator CPP32. J Biol Chem 1996;271:27099–106.
38. Srinivasula SM, Ahmad M, Fernandes-Alnemri T, Alnemri ES. Autoactivation of procaspase-9 by Apaf-1-mediated oligomerization. Mol Cell 1998;1:949–57.
39. Rodriguez J, Lazebnik Y. Caspase-9 and APAF-1 form an active holoenzyme. Genes Dev 1999;13:3179–84.
40. Srinivasula SM, Hegde R, Saleh A, et al. A conserved XIAP-interaction motif in caspase-9 and Smac/DIABLO regulates caspase activity and apoptosis. Nature 2001; 410:112–6.
41. Li F, Srinivasan A, Wang Y, Armstrong RC, Tomaselli KJ, Fritz LC. Cell-specific induction of apoptosis by microinjection of cytochrome c. Bcl-xL has activity independent of cytochrome c release. J Biol Chem 1997;272:30299–305.
42. Cain K, Brown DG, Langlais C, Cohen GM. Caspase activation involves the formation of the aposome, a large (approximately 700 kDa) caspase-activating complex. J Biol Chem 1999;274:22686–92.
43. Hu Y, Benedict MA, Ding L, Nunez G. Role of cytochrome c and dATP/ATP hydrolysis in Apaf-1-mediated caspase-9 activation and apoptosis. EMBO J 1999; 18:3586–95.
44. Ferguson HA, Marietta PM, Van Den Berg CLU. V-induced apoptosis is mediated independent of caspase-9 in MCF-7 cells: a model for cytochrome c resistance. J Biol Chem 2003;278:45793–800.
45. Ofir R, Seidman R, Rabinski T, et al. Taxol-induced apoptosis in human SKOV3 ovarian and MCF7 breast carcinoma cells is caspase-3 and caspase-9 independent. Cell Death Differ 2002;9:636–42.
46. Rao RV, Castro-Obregon S, Frankowski H, et al. Coupling endoplasmic reticulum stress to the cell death program. An Apaf-1-independent intrinsic pathway. J Biol Chem 2002;277:21836–42.
47. Fei P, El-Deiry WS. P53 and radiation responses. Oncogene 2003;22:5774–83.
48. Cortez D. Caffeine inhibits checkpoint responses without inhibiting the ataxia-telangiectasia-mutated (ATM) and ATM- and Rad3-related (ATR) protein kinases. J Biol Chem 2003;278:37139–45.
49. Dubrez L, Coll JL, Hurbin A, Solary E, Favrot MC. Caffeine sensitizes human H358 cell line to p53-mediated apoptosis by inducing mitochondrial translocation and conformational change of BAX protein. J Biol Chem 2001;276:38980–7.
50. He Z, Ma WY, Hashimoto T, Bode AM, Yang CS, Dong Z. Induction of apoptosis by caffeine is mediated by the p53, Bax, and caspase 3 pathways. Cancer Res 2003;63:4396–401.
51. Mihara M, Erster S, Zaika A, et al. p53 has a direct apoptogenic role at the mitochondria. Mol Cell 2003;11:577–90.
52. Chipuk JE, Kuwana T, Bouchier-Hayes L, et al. Direct activation of Bax by p53 mediates mitochondrial membrane permeabilization and apoptosis. Science 2004; 303:1010–4.
53. Werner AB, Tait SW, De Vries E, Eldering E, Borst J. Requirement for aspartate-cleaved bid in apoptosis signaling by DNA damaging anti-cancer regimens. J Biol Chem 2004;279:28771–80.
54. Desagher S, Osen-Sand A, Montessuit S, et al. Phosphorylation of bid by casein kinases I and II regulates its cleavage by caspase 8. Mol Cell 2001;8:601–11.

THE JOURNAL OF BIOLOGICAL CHEMISTRY VOL. 280, NO. 44, pp. 37169–37177, November 4, 2005

Irradiation-induced Translocation of p53 to Mitochondria in the Absence of Apoptosis*

Received for publication, February 23, 2005, and in revised form, August 9, 2005 Published, JBC Papers in Press, September 7, 2005, DOI 10.1074/jbc.M502052200

Frank Essmann[‡], Stephan Pohlmann[‡], Bernhard Gillissen[§], Peter T. Daniel[§] Klaus Schulze-Osthoff[‡], and Reiner U. Jänicke[‡1]

From the [‡]Institute of Molecular Medicine, University of Düsseldorf, 40225 Düsseldorf, Germany and the [§]Department of Hematology, Oncology and Tumor Immunology, Charite, Humboldt University, 13125 Berlin, Germany

The tumor suppressor protein p53 promotes apoptosis in response to death stimuli by transactivation of target genes and by transcription-independent mechanisms. Recently, it was shown that during apoptosis p53 can specifically translocate to mitochondria, where it physically interacts with and inactivates prosurvival Bcl-2 proteins. In the present study, we therefore investigated the role of mitochondrial translocation of p53 for the stress response of tumor cells. In various cell lines, DNA damage induced by either ionizing irradiation or topoisomerase inhibitors triggered a robust translocation of a fraction of p53 to mitochondria to a similar extent. Nevertheless, the cells succumbed to apoptosis only in response to topoisomerase inhibitors, but remained resistant to apoptosis induced by ionizing radiation. Irradiated cells became senescent, although irradiation triggered a functional p53 response and induced expression of p21, Bax, and Puma. Interestingly, even the targeted expression of p53 to mitochondria was insufficient to launch apoptosis, whereas overexpression of wild-type p53 induced Bax activation and apoptotic alterations. Together, these results suggest that, in contrast to previous reports, mitochondrial translocation of p53 does not *per se* lead to cell death and that this might constitute a mechanism that contributes to the resistance of tumor cells to ionizing radiation-induced apoptosis.

The tumor suppressor protein p53 is an important cellular integrator of stresses that triggers cell cycle arrest, senescence, DNA repair, or apoptosis. Upon activation by DNA damage or other stress-induced signaling pathways, p53 promotes the expression of a huge number of genes that coordinate the cellular stress response (1–4). The importance of p53 for the maintenance of genomic integrity and prevention of tumorigenesis becomes evident by the fact that p53 is mutated and thereby inactivated in nearly 50% of all malignant human tumors (5, 6). These mutations are primarily point mutations, and more than 90% of them are located within the central DNA-binding domain, underscoring the crucial role of p53 as a nuclear transcription factor (7).

As various apoptosis-relevant genes are under the control of p53, induction of apoptosis by p53 was initially believed to be mainly because of its function as a transcription factor. Furthermore, especially in view of the fact that p53 controls expression of death receptors such as CD95/Fas/APO1 or tumor necrosis factor-related apoptosis-inducing ligand receptor 2 (TRAIL-R2/KILLER/DR5), apoptosis induced by p53 was attributed to the extrinsic death receptor pathway (8–10). Soon it became evident, however, that p53 mediates cell death predominantly via the intrinsic death pathway, because cells deficient for crucial components of this pathway such as Apaf-1 or caspase-9 were shown to be highly resistant to p53-dependent apoptosis (11). The intrinsic pathway is initiated through the release of pro-apoptotic factors from the mitochondria, including cytochrome *c* and Smac/DIABLO (12). Released cytochrome *c* then allows the formation of a high-molecular weight complex, the apoptosome, containing Apaf-1 and caspase-9, that initiates the activation of the caspase cascade. Apoptotic signaling events at the level of the mitochondria are tightly controlled by pro- and anti-apoptotic Bcl-2 proteins including Bax, Bak, Bcl-2, Bcl-x_L, and others. These Bcl-2 proteins interact with another group of pro-apoptotic proteins that share at least one common motif with Bcl-2, namely the BH3-domain. BH3-only proteins have been proposed to be allosteric regulators of the Bcl-2 proteins and serve as sensors of apoptotic signaling. Upon interaction of anti-apoptotic Bcl-2 proteins with BH3-only proteins, both Bax and Bak undergo a conformational change in response to apoptotic stimuli. This event, which mediates exposure of an occluded N terminus (13, 14), results in the oligomerization of Bax and Bak and in the formation of a mitochondrial outer membrane pore with the subsequent release of cytochrome *c*. Interestingly, many pro-apoptotic Bcl-2 members, including, for instance, Bax and the BH3-only proteins Puma, Noxa, and Bid, are under the transcriptional control of p53 (15–19).

In addition to the transcriptional role of p53, there is now accumulating evidence for transcription-independent, p53-mediated apoptotic pathways (20–23). In some cell types, for example, p53-dependent apoptosis occurs in the absence of any gene transcription or translation or even upon expression of transcriptionally inactive p53 mutants (24–26). The precise molecular mechanisms, however, of how p53 induces apoptosis independently of its transcriptional activity are largely unknown. Intriguingly, p53 has been reported to directly induce mitochondrial cytochrome *c* release in a Bax-dependent manner *in vivo* and *in vitro*, providing evidence for a direct signaling pathway from the p53 protein to the downstream caspase activation cascade (27). These observations were further supported by recent findings demonstrating the appearance of p53 in the cytoplasm or even its translocation to the mitochondria during DNA damage- and stress-induced apoptosis (28–30). Moll and co-workers also found that bypassing the nucleus by targeting p53 expression directly to the mitochondria was sufficient to induce cell death in p53-deficient tumor cells (30). As a mechanistic explanation, it was proposed that p53, like BH3-only proteins, directly induces the permeabilization of the outer mitochondrial membrane by forming inhibitory complexes with anti-apoptotic Bcl-2 and/or Bcl-x_L proteins. Green and colleagues (28) have recently shown that the pro-apoptotic Bcl-2 protein Bax is one of the principal cytoplasmic targets of p53 (28). In a comparable scenario, a direct interaction of p53 with mitochondria-localized Bak rather than Bax was proposed that results

* This work was supported by the Deutsche Krebshilfe and Deutsche Forschungsgemeinschaft Grants SFB 503 and SFB 575. The costs of publication of this article were defrayed in part by the payment of page charges. This article must therefore be hereby marked "*advertisement*" in accordance with 18 U.S.C. Section 1734 solely to indicate this fact.

[1] To whom correspondence should be addressed: Universitätsstrasse 1, 40225 Düsseldorf, Germany. Tel.: 49-211-811-5973; Fax: 49-211-811-5892; E-mail: janicke@uni-duesseldorf.de.

in the disruption of the cyto-protective Mcl-1·Bak complex and hence in the oligomerization and activation of Bak (31). Thus, compelling evidence suggests that p53 directly impacts on mitochondria, although it is still a matter of debate by which route the transcription-independent apoptosis is achieved.

We have previously reported that MCF-7 breast carcinoma cells are sensitive to anti-cancer drug-induced apoptosis, but are remarkably resistant to apoptosis induced by ionizing radiation (IR)[2] regardless of whether or not they express caspase-3 (32). This finding was especially paradox because MCF-7 cells express a transcriptionally active wild-type p53 protein. Thus, we wondered whether the radio-resistant phenotype of these cells might be caused by an improper transcription-independent function of p53. We found that, although IR induced an efficient translocation of p53 to the mitochondria, this process was insufficient to induce apoptosis in MCF-7 and HCT116 carcinoma cells. In addition, in several cell lines that display different apoptosis susceptibilities toward IR or chemotherapeutics, we did not find a correlation between the amount of mitochondrial p53 and apoptosis induction. Interestingly, Bax oligomerization and apoptotic alterations were only observed when cells were transfected with wild-type p53, whereas the expression of p53 targeted directly to the mitochondria did not evoke an apoptotic response. Our results therefore suggest that the resistance to apoptosis induction by mitochondrial p53 might contribute to the radio-resistant phenotype of tumor cells.

MATERIALS AND METHODS

Cells, Reagents, and Antibodies—MCF-7 breast carcinoma cells and its subclones MCF-7/casp-3 (33), MCF-7 cells stably expressing a GFP-Bax fusion protein, as well as MCF-7/p53siRNA (34) and MCF-7/casp-3/p53siRNA cells (35), were cultured in RPMI 1640. The human B-lymphoblastoid cell line SKW6.4 and RKO colon carcinoma cells were cultured in Iscove's modified Dulbecco's medium and Dulbecco's modified Eagle's medium, respectively. All media were supplemented with 10% heat-inactivated fetal calf serum, 10 mM glutamine, and 100 μg/ml of each streptomycin and 100 units/ml penicillin (PAA Laboratories GmbH, Cölbe, Germany). The HCT116 and HCT116/p53$^{-/-}$ cells were maintained in McCoy's 5A medium supplemented as above. The monoclonal Chk1 antibody was obtained from Transduction Laboratories (Heidelberg, Germany), and the monoclonal p53 antibody (Ab-6) from Calbiochem (Bad Soden, Germany). The p21 and poly(ADP-ribose) polymerase monoclonal antibodies were from BD Pharmingen, and the polyclonal antibody to high mobility group 1 (HMG1) and the monoclonal antibody to Tom20 from BD Bioscience. The monoclonal antibodies to Bak and Bcl-2 were purchased from Oncogene Research Products (San Diego, CA) and Novocastra Laboratories (Newcastle, UK), respectively. Bcl-x_L and Bax antibodies were from Trevigen (Gaithersburg, MD), the conformation-specific anti-Bax-NT antibody was from Upstate Biotechnology. The polyclonal rabbit antibody recognizing Puma as well as the monoclonal antibody against proliferating cell nuclear antigen (PCNA) were purchased from Santa Cruz (Heidelberg, Germany) and the antibodies directed against caspase-3 and actin were from R&D Systems (Wiesbaden, Germany) and Sigma, respectively. Secondary antibodies for the immunofluorescence studies including chicken anti-mouse and anti-rabbit antibodies coupled to Alexa Fluor 488 and Alexa Fluor 594, respectively, or goat anti-mouse antibody coupled to Alexa Fluor 350 as well as Mitotracker Red were from Molecular Probes (Leiden, The Netherlands). Peroxidase-labeled antibodies to rabbit and mouse IgG were from Promega GmbH (Mannheim, Germany). The nuclear stain 4′,6-diamidino-2-phenylindole was from Sigma (Deisenhofen, Germany). For protease inhibition, buffers were supplemented with a protease inhibitor mixture (Roche Diagnostics).

Treatment and Transfection of Cells—Cells were exposed to ionizing radiation at the indicated dose using a Gammacell 1000 Elite (Nordion International Inc., Fleurus, Belgium) in the presence or absence of caffeine (1 mM, Sigma). Alternatively, cells were treated with the topoisomerase inhibitors etoposide (10 μM) or camptothecin (5 μM; both Sigma). The term "radio-resistant" that is used throughout the entire manuscript refers to "resistant to IR-induced apoptosis." Transfections of MCF-7 cells were performed with FuGENE reagent according to the instructions of the manufacturer (Roche Diagnostics). Mammalian expression vectors encoding for wild-type p53 (p53wt) or a p53 fused to the transmembrane domain of Bcl-2 (p53-CTM) were published before (30) and kindly provided by U. Moll. Stably transfected MCF-7 cells expressing a GFP-tagged Bax construct (36) were selected in G418 (1 mg/ml).

Immunofluorescence Microscopy—For immunofluorescence staining, cells were seeded on coverslides. At the indicated time points, cells were fixed for 20 min in ice-cold PBS containing 2% formaldehyde. Blocking and all following procedures were performed in PBS supplemented with 4% BSA and 0.05% saponin. Primary antibodies were applied at 4 °C overnight at the appropriate concentration. Then, cells were washed three times for 20 min and incubated with the secondary antibody (1:500). Finally, samples were washed extensively and mounted in fluorescent mounting medium (Dako Corporation, Carpintera, CA) with or without 10 ng/ml 4′,6-diamidino-2-phenylindole. Pictures were taken on an Axiovert 135 Microscope (Zeiss, Germany) with an Apochromat ×63 oil immersion lens using OpenLab software (Improvision, Tübingen, Germany).

Flow Cytometric Analysis—For cell cycle analysis and detection of apoptosis, samples were prepared according to Nicoletti *et al.* (37). Briefly, cells were harvested by trypsinization, washed in cold PBS, and resuspended in lysis buffer containing 0.1% sodium citrate, 0.1% Triton X-100, and 50 μg/ml propidium iodide. All flow cytometric analyses were performed on a FACScalibur (BD Biosciences) by using CellQuest analysis software. For each determination a minimum of 10,000 cells was analyzed.

Senescence-associated β-Galactosidase Staining—Staining for β-galactosidase activity was performed as previously described (38). Briefly, after the indicated treatment cells were washed with PBS, fixed in 0.2% glutaraldehyde and 2% formaldehyde for 5 min, washed again with PBS, and finally stained in the absence of CO_2 in staining solution (150 mM NaCl, 2 mM $MgCl_2$, 5 mM $K_3Fe(CN)_6$, 5 mM $K_2Fe(CN_6)$, 40 mM citric acid, and 12 mM sodium phosphate, pH 6.0) containing 1 mg/ml 5-bromo-4-chloro-3-indolyl-β-D-galactoside.

Cell Extracts and Subcellular Fractionation—Total cell extracts were prepared in high-salt lysis buffer containing 1% Nonidet P-40, 20 mM HEPES (pH 7.9), 2 mM phenylmethylsulfonyl fluoride, 350 mM NaCl, 20% glycerol, 1 mM $MgCl_2$, 0.5 mM EDTA, 0.1 mM EGTA, 0.5 mM dithiothreitol and protease inhibitors. For isolation of mitochondria, cells were harvested by scraping, centrifuged, washed, and resuspended in ice-cold buffer MB (400 mM sucrose, 50 mM Tris/HCl, pH 7.6, 1 mM EGTA, 5 mM 2-mercaptoethanol, 10 mM potassium phosphate, pH 7.6, and 0.2% BSA). After incubation on ice for 20 min, cells were Dounce homogenized with 40 strokes, and unbroken cells and nuclei were

[2] The abbreviations used are: IR, ionizing radiation; siRNA, small interfering RNA; PCNA, proliferating cell nuclear antigen; GFP, green fluorescent protein; PBS, phosphate-buffered saline; BSA, bovine serum albumin; CAPS, 3-(cyclohexylamino)propanesulfonic acid; HMG1, high mobility group 1; wt, wild-type; FACS, fluorescence-activated cell sorter.

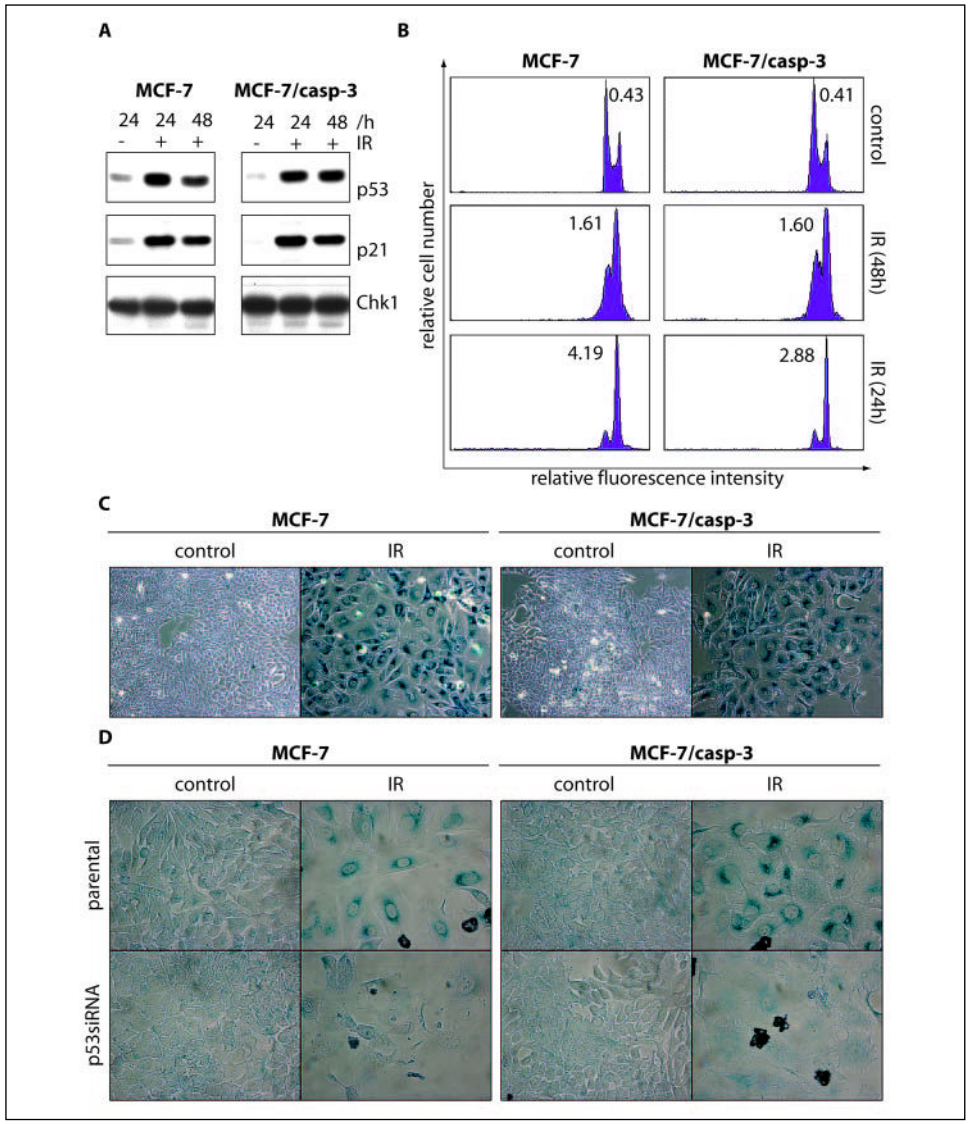

FIGURE 1. **Irradiation-induced cell cycle arrest correlates with the p53-dependent p21 expression and induction of cellular senescence in MCF-7 cell lines.** *A*, Western blot analysis of p53 and p21 protein levels in total cell extracts of MCF-7 and MCF-7/casp-3 cells in response to IR. The nuclear protein Chk1 was assessed for loading control. *B*, flow cytometric cell cycle analysis of MCF-7 and MCF-7/casp-3 cells 24 and 48 h after high dose IR (20 gray). The numbers given in the histograms indicate the G_2/G_1 ratio. *C*, MCF-7 and MCF-7/casp-3 cells were analyzed 5 days post-IR (20 gray) for the induction of cellular senescence using β-galactosidase staining. Note that the micrographs were all taken at the same magnification (see "Materials and Methods"). *D*, MCF-7, MCF-7/casp-3, and the corresponding p53 knock-down cell lines (see Ref. 35 and Fig. 5*A* for p53 suppression) were analyzed 6 days post-IR (20 gray) for the induction of cellular senescence. Senescence was induced in a p53-dependent manner irrespective of the caspase-3 status. One representative experiment out of three is shown.

removed by centrifugation at 4,000 × *g* for 1 min. The supernatant was centrifuged for 10 min at 15,000 × *g* to pellet mitochondria. The resulting supernatant was removed and designated the cytoplasmic fraction, whereas the pellet enriched for mitochondria was resuspended in buffer MSM (300 mM mannitol, 10 mM potassium phosphate, pH 7.2, 0.1% BSA) and was referred to as the M1 fraction. To obtain highly purified mitochondria, the M1 fraction was loaded onto a discontinuous 1.2–1.6 M sucrose gradient buffered with 10 mM Tris/HCl (pH 7.5) and 0.1% BSA. After centrifugation at 70,000 × *g* for 1 h, the interphase was harvested and diluted in MSM buffer at a ratio of 1:4. Mitochondria were centrifuged at 45,000 × *g* for 15 min, and the resulting pellet was designated M2.

Western Blot Analysis—Protein concentrations were determined using the BCA assay kit (Pierce Biotechnology), and 15 μg of protein per lane were loaded onto standard SDS-PAGE gels and separated at 200 V. The proteins were transferred onto a 0.2-μm pore size polyvinylidene difluoride membrane (Amersham Bioscience) by semi-dry blotting at a constant current of 40 mA for 90 min in a buffer containing 10 mM CAPS (pH 11) and 10% MeOH. The membranes were blocked in PBS containing 4% BSA and 0.05% Tween 20 for 1 h, followed by an overnight incubation with the primary antibody at 4 °C. After washing the membranes extensively, the appropriate secondary antibodies (1:5000) were applied for 1 h. Membranes were washed for an additional 2 h in PBS, 0.05% Tween 20, and proteins were visualized using ECL reagents (Amersham Biosciences).

RESULTS

Irradiation Induces a Functional p53 Response in the Absence of Apoptosis—The tumor suppressor p53 induces apoptosis in response to DNA damage in diverse cellular systems. Nevertheless, MCF-7 breast carcinoma cells are resistant to apoptosis induced by IR regardless of whether or not they express caspase-3, although they harbor a functional p53 gene (32, 35). Hence, we wondered whether the resistance of MCF-7 and MCF-7/casp-3 cells to IR-induced apoptosis could be caused by a mechanism rendering wild-type p53 unresponsive toward IR in these cells. However, exposure to IR induced significant p21 expression in both MCF-7 cell lines, a process that is most likely mediated via stabilization and transcriptional activation of p53 (Fig. 1*A*). In addition, irradiated MCF-7 and MCF-7/casp-3 cells displayed a persistent G_2/M arrest (Fig. 1*B*) that correlated with the induction of cellular senescence as evidenced by staining of the senescence-associated β-galactosidase activity and a dramatic increase in the cell volume (Fig. 1*C*). IR-induced senescence was substantially reduced in MCF-7 and MCF-7/casp-3 cells stably transfected with a p53siRNA construct (35), imply-

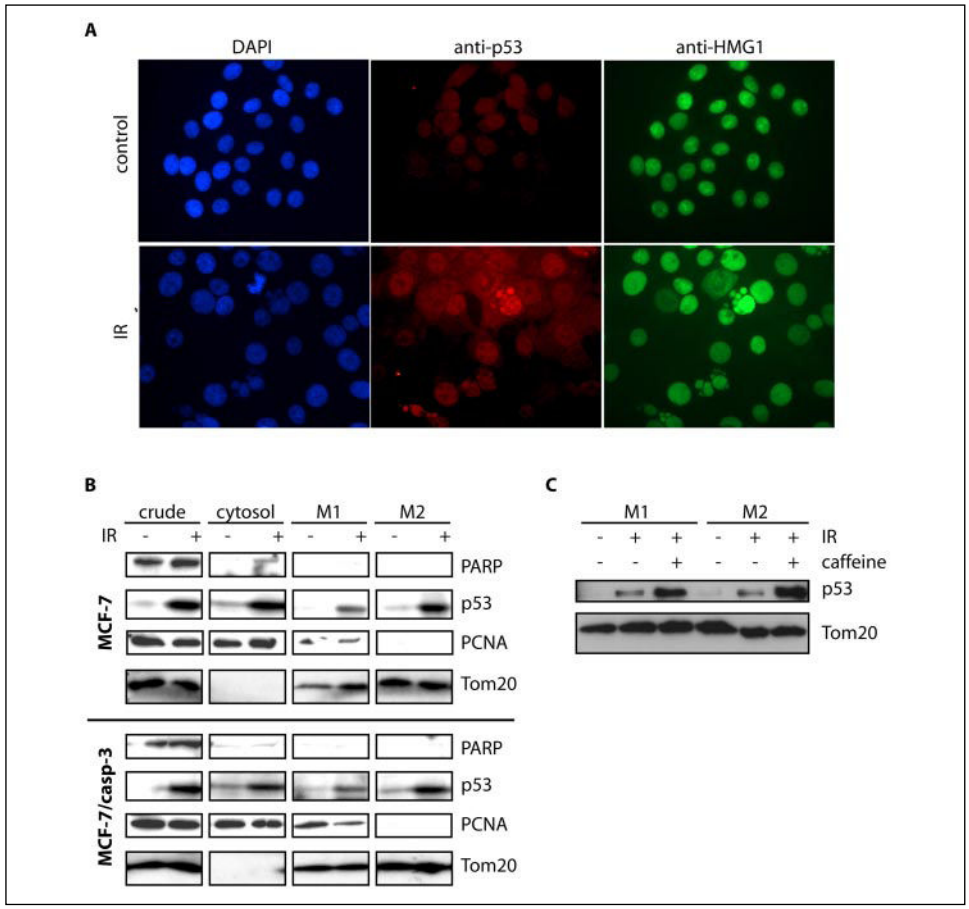

FIGURE 2. **Irradiation induces translocation of p53 to mitochondria in MCF-7 cells.** *A*, immunofluorescence staining of p53 and the nuclear protein HMG1 in untreated (control) MCF-7 cells and in cells 24 h post-IR treatment (20 gray) shows that p53 is predominantly localized in nuclei of irradiated cells. *B*, Western blot analyses for the status of the indicated proteins in various subcellular fractions of untreated and irradiated MCF-7 and MCF-7/casp-3 cells 24 h post-IR (20 gray). The specificity of the mitochondrial p53 localization in the M2 fraction was demonstrated by the absence of nuclear proteins such as poly(ADP-ribose) polymerase and PCNA and by the presence of the mitochondrial markers Tom20 and cytochrome *c* (data not shown). *C*, Western blot analysis for the status of p53 (*upper panel*) and Tom20 (*lower panel*) in mitochondrial M1 and M2 fractions of untreated MCF-7 cells and MCF-7 cells 24 h after they were exposed to IR (20 gray) in the absence or presence of 1 mM caffeine.

ing that senescence induction requires p53 expression in both cell lines (Fig. 1*D*). Together, these results demonstrate that the p53 protein expressed in MCF-7 cells is functionally active, at least with regard to its transcriptional activity.

Mitochondrial Translocation of p53 in Response to Irradiation—Accumulating evidence suggests that p53 can also induce apoptosis via transcription-independent events that are only poorly understood. One of these events might be the DNA damage-induced translocation of p53 to the mitochondria that was previously described (29, 30). To examine whether this process was a critical event for the apoptosis resistance of irradiated MCF-7 cells, we initially analyzed the subcellular localization of p53 by immunofluorescence microscopy. Compared with untreated cells, irradiation triggered an increase in nuclear size associated with the formation of micronuclei (Fig. 2*A*). Unlike expression of the nuclear HMG1 that remained unaffected by IR, p53 expression was barely detectable in untreated MCF-7 cells, but was highly induced in irradiated cells (Fig. 2*A*). However, IR-induced p53 was predominantly found in the nucleus, and no mitochondrial-associated p53 could be detected with this technique. Also the use of different antibodies recognizing either N- or C-terminal p53 epitopes did not result in the detection of endogenous mitochondria-associated p53 following IR (data not shown). Although this result would support our initial hypothesis that the radio-resistant phenotype of MCF-7 cells might be caused by an improper p53 function, our failure to detect mitochondrial translocation of endogenous p53 following exposure of the cells to IR might simply reflect the sensitivity restrictions of the immunofluorescence technique applied.

Therefore, we investigated the possible IR-induced p53 translocation by Western blot analyses of mitochondria-enriched fractions. Using this technique, we found indeed a significant amount of p53 protein that was associated with mitochondria (M1 fraction) only in irradiated, but not in untreated MCF-7 or MCF-7/casp-3 cells (Fig. 2*B*). However, the mitochondria-enriched M1 fractions prepared by such a method might be contaminated with diverse membrane particles and organelles including endoplasmic reticulum and other subcellular compartments. In addition, we had to rule out the possibility that the M1 fractions contained also nuclear or cytoplasmic p53 that was not specifically translocated to mitochondria during IR treatment *in vivo*, but was simply co-sedimented during the purification procedure. Western blot analyses revealed that the mitochondrial M1 fractions of both cell lines were indeed contaminated with nuclear proteins such as the PCNA but, for unknown reasons, not with poly(ADP-ribose) polymerase (Fig. 2*B*). Thus, the observed p53 signals in the M1 fractions of irradiated cells might only reflect contaminations with nuclear p53. To avoid such nuclear contaminations, and to undoubtedly establish whether IR induces the mitochondrial translocation of p53, we further purified the mitochondria-enriched M1 fractions by discontinuous sucrose gradient centrifugation. Western blot analyses of samples obtained with such a purification procedure (M2 fractions) now clearly revealed an irradiation-induced translocation of p53 to the mitochondria in both MCF-7 lines (Fig. 2*B*). Only the mitochondrial marker proteins Tom20 and cytochrome *c* (data not shown), but not the nuclear poly(ADP-ribose) polymerase or PCNA proteins were detected together with p53 in the M2 fraction of irradiated cells, confirming the composition and purity of these samples. In addition, these data suggest that the mitochondrial p53 translocation must have occurred *in vivo* as a response of the cell to IR exposure, but not because of an *in vitro* co-sedimentation artifact caused by the preparation procedure.

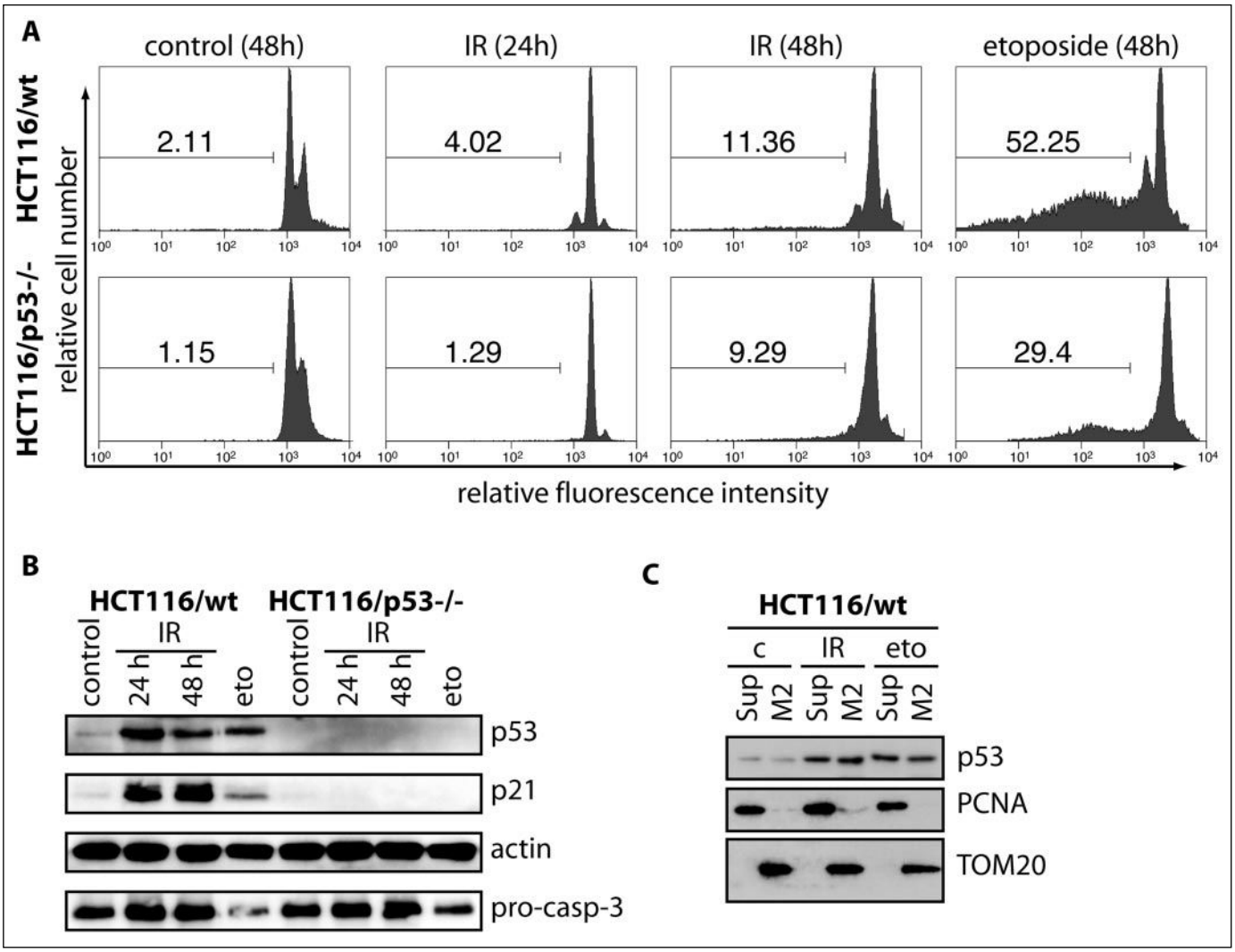

FIGURE 3. **Irradiation-induced translocation of p53 to mitochondria occurs also in radio-resistant HCT116 cells.** *A*, flow cytometric cell cycle analysis of untreated and irradiated (20 gray) HCT116/wt and HCT116/p53$^{-/-}$ cells 24 and 48 h post-IR. As a control, cells were also exposed to etoposide (10 μM) that induced the appearance of hypodiploid nuclei indicative of apoptotic cells. The *numbers* given in the histograms are the percentages of apoptotic cells. *B*, Western blot analyses for the status of the indicated proteins in total extracts of untreated and irradiated (20 gray) HCT116/wt and HCT116/p53$^{-/-}$ cells 24 and 48 h post-IR. As a control, cells were also treated for 24 h with etoposide (10 μM) and probed for the indicated proteins. *C*, Western blot analyses for the status of the indicated proteins in total cell extracts (*Sup*) and in the mitochondrial M2 fractions of HCT116/wt cells that were either left untreated (*c*) or analyzed 24 h following exposure to 20 gray (*IR*) or 10 μM etoposide (*eto*). The specificity of mitochondrial p53 localization in the M2 fraction of HCT116 cells was demonstrated by the absence of PCNA and HMG1 (data not shown) and by the presence of the mitochondrial marker Tom20.

It was reported previously that a fraction of p53 only localizes to mitochondria under conditions that provoke p53-dependent apoptosis, but not in apoptosis-resistant cells (28, 30). However, we now show that IR induces also the mitochondrial translocation of p53 in MCF-7 and MCF-7/casp-3 cells that are highly resistant to apoptosis induced by IR. In an attempt to explain this discrepancy, we prepared sucrose gradient fractions from MCF-7/casp-3 cells that were exposed to IR in combination with the methylxanthine and ATM inhibitor caffeine, a treatment that efficiently induces apoptosis in these cells (35). When compared with purified M2 fractions of cells that were only irradiated, co-treatment with caffeine resulted in even further increased p53 levels at the mitochondria (Fig. 2*C*). At first glance, this result would therefore support the idea that mitochondrial translocation of p53 correlates with apoptosis induction. However, IR-induced apoptosis in the presence of caffeine proceeds in a p53-independent manner in MCF-7/casp-3 cells (35).

Mitochondrial p53 Translocation in HCT116 Cells—In light of the surprising finding that IR induces the mitochondrial translocation of p53 in MCF-7 and MCF-7/casp-3 cells that are both resistant to irradiation-induced apoptosis, we extended our investigation to another experimental system. As demonstrated by FACS analyses, HCT116 colon carcinoma cells were also resistant to apoptosis induced by high dose IR regardless of whether or not they express p53 (Fig. 3*A*). Similar to MCF-7 cells (32), HCT116 cells displayed a persistent irradiation-induced G_2/M arrest, but were efficiently killed by the anti-cancer drug etoposide in a p53-dependent manner verifying their p53 status (Fig. 3*A*). Western blot analyses confirmed these observations and demonstrated the disappearance (and hence, activation) of the pro-caspase-3 protein predominantly in etoposide-treated HCT116 cells expressing wt-p53 (Fig. 3*B*, *lower panel*). Expression of p21 was clearly dependent on p53, as it was not observed in p53-deficient HCT116 cells (Fig. 3*B*). More importantly, p53 was found together with the mitochondrial marker protein Tom20 in the highly purified M2 fractions of both irradiated and etoposide-treated wild-type HCT116 cells, regardless of whether or not the cells were killed by this treatment (Fig. 3*C*). Again, the mitochondrial accumulation was specific for p53 because other nuclear proteins such as PCNA (Fig. 3*C*) and HMG1 (data not shown) were not detected in the M2 fraction. Thus, the specific mitochondrial

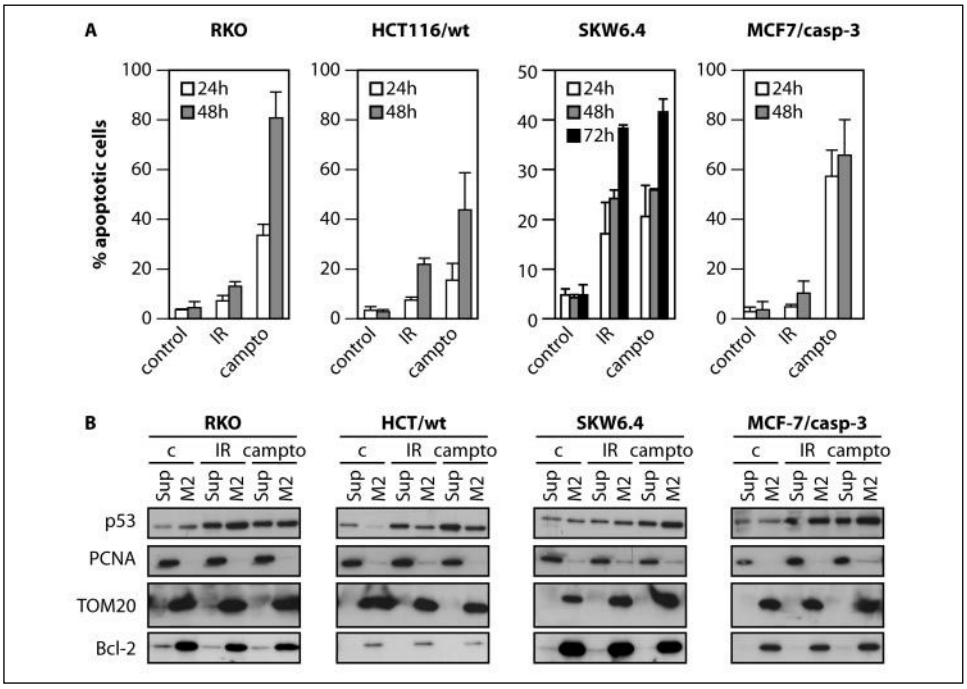

FIGURE 4. **No correlation between apoptosis induction and mitochondrial p53 accumulation.** *A*, the indicated cell lines were either left untreated or exposed to 20 gray (*IR*) or 5 μM camptothecin (*campto*) and apoptosis (percentage of sub-G_1 cells) was assessed by FACS analysis after the indicated times. *B*, Western blot analysis for the status of the indicated proteins in the cytosol (*Sup*) and in mitochondrial M2 fractions of the indicated cell lines that were either left untreated (*c*) or analyzed 6 (*RKO*) or 24 h (*HCT/wt*, *SKW6.4*, *MCF-7/casp-3*) following exposure to 20 gray (*IR*) or 5 μM camptothecin.

translocation of p53 in the absence of apoptosis is not only restricted to the MCF-7 cell system, but occurs also in HCT116 colon carcinoma cells that are largely resistant to IR-induced apoptosis.

Mitochondrial Translocation of p53 Does Not Correlate with Apoptosis Susceptibility—It was recently reported that mitochondrial translocation of p53 occurs specifically during p53-dependent apoptosis, but not during p53-mediated cell cycle arrest or in p53-independent apoptosis (20). Our data, however, demonstrate p53 accumulation at the mitochondria following a treatment (IR) that does not induce apoptosis in two different cell lines. To investigate this discrepancy in more detail, we compared apoptosis susceptibility and mitochondrial p53 translocation also in the RKO colon carcinoma cell line. In agreement with a previous report (29), we found that these two events correlated well when the cells were treated for 6 h with camptothecin, which efficiently induced apoptosis (Fig. 4*A*) and p53 accumulation at the mitochondria (Fig. 4*B*). We detected, however, comparable amounts of mitochondrial p53 when the cells were exposed to IR, a treatment that does not induce apoptosis in these cells (Fig. 4). Similar results were obtained when the effects of both treatments were compared in HCT116 and MCF-7/casp-3 cells (Fig. 4). In addition, we did not observe a correlation with regard to apoptosis sensitivity and mitochondrial p53 accumulation when we performed the experiments with the human B-lymphoblastoid cell line SKW6.4. Although these cells were equally susceptible to apoptosis induction by both treatments, a significantly larger portion of p53 accumulated at the mitochondria following incubation with camptothecin (Fig. 4). Interestingly, neither cell death nor p53 translocation appears to correlate with expression of the anti-apoptotic Bcl-2 protein at the mitochondria. Whereas the radio-resistant cell lines HCT116, MCF-7/casp-3, and RKO express extremely low and moderate levels of Bcl-2, respectively, we found very high Bcl-2 expression in IR-sensitive SKW6.4 cells (Fig. 4*B*).

Bax and Puma Expression Do Not Correlate with Apoptosis Susceptibility—Although we found in several cell lines no correlation between apoptosis susceptibility and mitochondrial p53 accumulation, we wondered whether the resistant phenotype of these cells to IR-induced apoptosis might be caused by defects in events downstream of mitochondrial p53. To address this possibility, we analyzed in MCF-7 cells expression of the p53-inducible pro-apoptotic proteins Bax and Puma that play key roles in apoptotic pathways mediated by mitochondria (17, 23). Western blot analyses of whole cell extracts of MCF-7/casp-3 and MCF-7/casp-3/p53siRNA cells showed that IR clearly induced up-regulation of Bax and Puma in a p53-dependent manner, whereas expression of other Bcl-2 family members such as Bak, Bcl-2, or Bcl-x_L was neither affected by this treatment nor by the p53 status of the cells (Fig. 5*A*). Interestingly, when we analyzed the mitochondrial M2 fractions of several cell lines exposed to either IR or the chemotherapeutic drugs etoposide or camptothecin, we did not observe a correlation between Puma expression and apoptosis susceptibility. Puma was induced in all cell lines by either treatment regardless of whether or not the cells succumbed to apoptosis (Fig. 4*B*). In fact, at both time points analyzed (6 h and 24 h), IR induced an even higher Puma expression in the mitochondrial M2 fraction of IR-resistant HCT116 cells than etoposide or in IR-sensitive SKW6.4 cells. Furthermore, we found similar Puma levels at the mitochondria of MCF-7/casp-3 and RKO cells exposed to either IR or to chemotherapeutic drugs although only the latter treatment induces efficient apoptosis in these cells. Thus, neither the mitochondrial translocation of p53 nor expression of Bcl-2 or Puma appear to correlate with apoptosis sensitivity in the cell lines investigated. Although these data do not rule out a possible contribution of these and other Bcl-2 proteins toward the apoptosis-resistant phenotype of the cell lines investigated, the observation that Bax and Puma can be induced by IR in these cells indicates the functionality of the p53 pathway.

Bax Activation in MCF-7 Cells—Next, we tested the functionality of Bax that is known to be located upstream of caspase activation in the apoptosis signaling pathway. Bax exerts pro-apoptotic activity upon its conformational change and the exposure of an occluded N terminus, resulting in Bax oligomerization and cytochrome *c* release. Using an antibody that specifically detects the N terminus of such a conformationally changed, *i.e.* active, Bax protein, we could demonstrate activation of Bax only in etoposide-treated MCF-7 cells, but not in cells that were exposed to IR (Fig. 5*C*). Analysis of an overexpressed GFP-Bax

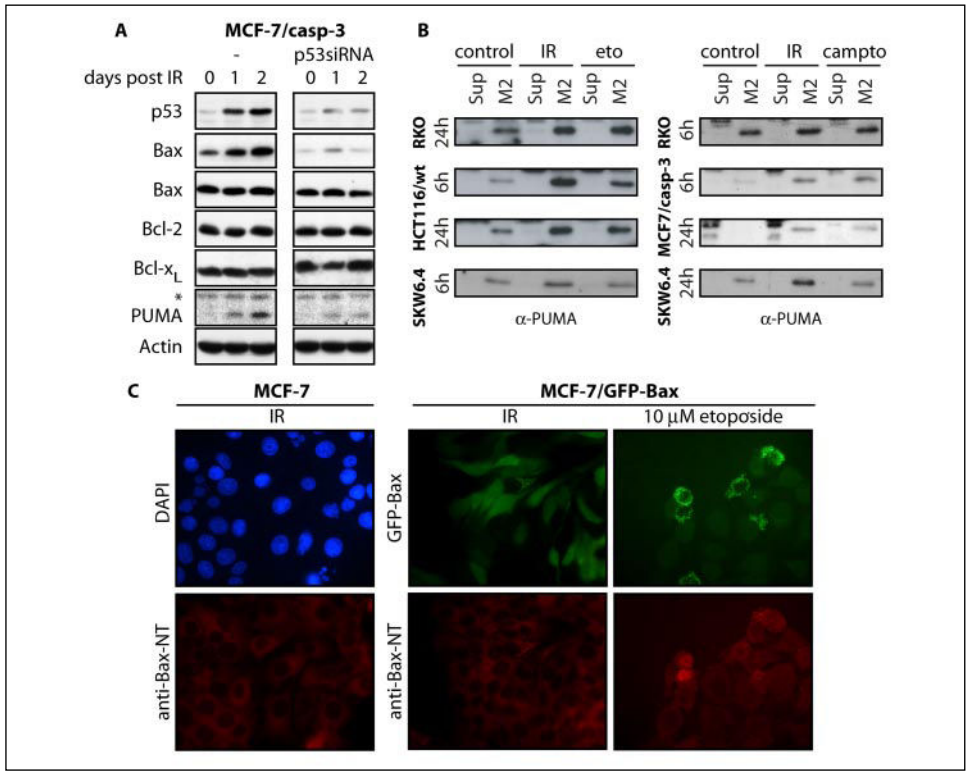

FIGURE 5. **Bax expression and activation only in etoposide-treated, but not in irradiated MCF-7 cells.** *A*, Western blot analyses for the status of Bax and other Bcl-2 and BH3-only proteins in total extracts of untreated and irradiated (20 gray) MCF-7/casp-3 and MCF-7/casp-3/p53siRNA cells 24 and 48 h post-IR. The *asterisk* indicates an unspecific band. *B*, Western blot analysis for the status of Puma in the cytosol (*Sup*) and in mitochondrial M2 fractions of the indicated cell lines that were either left untreated (*control*) or analyzed after the indicated times following exposure to 20 gray (*IR*), 10 μM etoposide, or 5 μM camptothecin. *C*, MCF-7 (*left panel*) and MCF7/GFP-Bax cells (*right panels*) were analyzed 24 h post-irradiation (20 gray) by immunofluorescence with either an antibody specific for conformationally changed (activated) Bax (Bax-NT) (*lower panels*), or by 4′,6-diamidino-2-phenylindole staining (*upper left panel*) and GFP expression (*upper right panel*). No clustering of Bax could be detected in irradiated cells (*left* and *middle panels*). Etoposide treatment (24 h), however, induced Bax oligomerization as indicated by the *dotted* GFP-Bax expression pattern (*upper right panel*), which is congruent with the Bax-NT-stained cells (*lower right panel*).

protein and N terminus-specific Bax staining in these cells confirmed Bax activation exclusively in etoposide-treated but not in irradiated MCF-7 cells (Fig. 5*C*). This is in agreement with our previous study (35) demonstrating that exposure of MCF-7 or MCF-7/casp-3 cells to IR does not result in a decrease of the mitochondrial membrane potential, which usually coincides with Bax clustering. Together with the observed p53-dependent expression of Bax and Puma, these results not only verify the functional wild-type status of p53 in these cells, but also suggest that Bax or Puma are not the limiting factors responsible for the apoptosis-resistant phenotype of MCF-7 cells toward IR.

Apoptosis Induction by Wild-type p53 but Not by Mitochondria-targeted p53—So far, we have shown that, although IR induces the translocation of p53 to the mitochondria, this event does not induce apoptosis of MCF-7 cells. This is most likely the case because IR does neither trigger Bax activation nor does it lead to a decrease of the mitochondrial membrane potential. We therefore hypothesized that the levels of endogenous p53 detected at the mitochondria following IR might simply not be sufficient to induce apoptotic events such as Bax oligomerization. To test this, we transiently transfected MCF-7 cells with either wild-type p53 or with a p53 construct fused to the Bcl-2 transmembrane domain (p53-CTM) that directly targets expression of the fusion protein to the mitochondria as shown previously (30). Targeted expression was verified using immunofluorescence analyses that clearly demonstrated an exclusive expression of the latter construct at the mitochondria (Fig. 6*A*). Interestingly, only cells expressing the wild-type p53 protein displayed the typical signs of apoptosis, such as shrinkage and rounding, and only those cells could be stained with the antibody recognizing conformationally changed, active Bax protein (Fig. 6, *B* and *C*). Importantly, during the whole course of these experiments, we could never detect wt-p53 localized at the mitochondria. In contrast, MCF-7 cells that were transfected with the mitochondria-targeted p53-CTM construct were still attached to the plastic surface and appeared healthy (Fig. 6, *B* and *C*). This finding was in contrast to the original reports

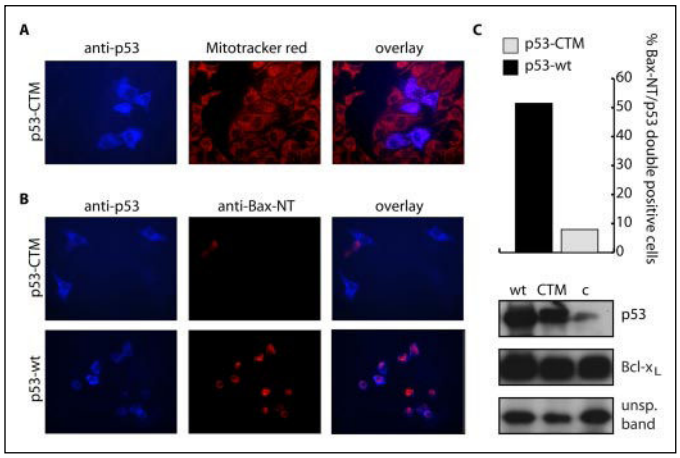

FIGURE 6. **Expression of wild-type p53 but not p53 targeted to mitochondria induces Bax clustering and apoptosis in MCF-7 cells.** MCF-7 cells transfected with p53-wt (*B*, *lower panel*) or with a mitochondria-targeted p53 construct (p53-CTM) (*A* and *B*, *upper panel*) were analyzed 36 h post-transfection by immunofluorescence for p53 expression and for Bax activation with the Bax-NT antibody. Mitochondrial expression of p53-CTM (*A*) was confirmed by staining the cells also with Mitotracker red. Transfection of MCF-7 cells with p53-wt (*B*, *lower panel*), but not with p53-CTM (*B*, *upper panel*) resulted in the appearance of double positive-stained cells indicating Bax oligomerization in p53-overexpressing cells. Note that the two cells stained positive for active Bax (*B*, *upper panel*) do not express the p53-CTM construct and hence represent apoptotic cells that have died spontaneously. The experiments were repeated at least four times yielding similar results. *C*, Western blot analysis (*lower panel*) of p53 expression in MCF-7 cells that were either untransfected (*c*), transfected with p53-wt (*wt*) or with the mitochondria-targeted p53 construct (*CTM*). Expression of an unrelated band serves as loading control. Pro-apoptotic effects were quantitated by counting cells that stained double positive for p53 and active Bax (*Bax-NT*) in 20 random microscopic fields (*upper panel*).

demonstrating that transfection of this construct resulted in efficient apoptosis induction even in p53-deficient cells (29, 30). In addition, and consistent with our results, we could not detect conformationally changed, active Bax protein in MCF-7 cells transfected with the p53-CTM construct (Fig. 6*B*). Although we cannot completely rule out the

possibility that the different apoptotic outcome upon transfection of these two constructs is caused by their differential expression, our results provide strong evidence that neither endogenous p53 upon IR treatment nor transiently expressed p53 targeted to mitochondria are able to induce Bax oligomerization and subsequent apoptotic events in MCF-7 cells.

DISCUSSION

For the last few years, substantial evidence has emerged suggesting the existence of p53-dependent apoptosis pathways that do not require its transcriptional activity. Recently, p53 was demonstrated to translocate into the cytoplasm and even onto mitochondria during DNA damage- and stress-induced apoptosis (28–30). Although it is still controversially discussed by which mechanism and interaction partners, in particular of the Bcl-2 family, p53 exerts an extranuclear, pro-apoptotic function, p53 may directly impact on mitochondria. p53 was shown to interact either with anti-apoptotic Bcl-2 proteins leading to the inhibition of their cytoprotective function (30), whereas in other studies a direct or indirect interaction with the pro-apoptotic Bcl-2 members Bak or Bax has been proposed (28, 31). A mitochondrial translocation of p53 was observed in a variety of human and mouse cell lines and occurred specifically only in p53-dependent apoptosis such as in drug-, hypoxia-, or radiation-induced apoptosis, but was not detected during p53-mediated cell cycle arrest or in p53-independent apoptosis (20). In addition, mitochondrial p53 appears to contribute also to the physiological p53 stress response *in vivo*, as it could be detected following IR or intravenous application of etoposide in several radio-sensitive murine organs including thymus, spleen, testis, and brain, but not in radio-resistant organs such as liver and kidney (40).

Based on these and other reports it was surprising to find that IR treatment induced the translocation of p53 to mitochondria also in MCF-7 and MCF-7/casp-3 cells that display a persistent G_2/M arrest following IR, but are resistant to apoptosis induction by this treatment (32). Although the IR-induced mitochondrial p53 levels were below the immunofluorescence detection limit, the presence of p53 at the mitochondria following IR could be readily demonstrated by Western blot analyses of subcellular fractions (M1 and M2). Only the M1 fractions were partially contaminated with nuclear proteins, whereas composition and purity of the M2 fractions could be confirmed by the absence and presence of nuclear and mitochondrial marker proteins such as HMG1, PCNA, and Tom20, respectively. Irradiation-induced translocation of p53 to mitochondria without any signs of apoptosis was not restricted to the MCF-7 cell line, but was also a prominent feature of similarly treated HCT116 and RKO cells. In addition, we did not observe a correlation between mitochondrial p53 and the extent of apoptosis as exposure of various cell lines to IR, etoposide, or camptothecin resulted in comparable levels of mitochondrial p53, whereas their apoptotic responses toward these stimuli differed dramatically. Hence, our data that are in line with a very recent report showing that a transcriptional inactive p53 mutant is completely unable to induce apoptosis *in vitro* and *in vivo* (41), demonstrate that the physical translocation of p53 to mitochondria is not necessarily associated with the induction of apoptosis as it was proposed previously (29, 30).

Although the exact reason for this discrepancy is presently unknown, one possible explanation might be that too little amounts of p53 protein are translocated to the mitochondria following IR treatment. Provided that the apoptotic machinery is only activated above a certain threshold level of mitochondrial p53, the IR-induced p53 levels at the mitochondria might simply be not sufficient to induce apoptosis. Several observations, however, argue against this explanation and clearly suggest that even elevated mitochondrial p53 levels do not trigger an apoptotic response at least in MCF-7 cells.

First, as quantitated by densitometry of the immunoblots, mitochondrial p53 comprised ~2% of the total induced p53 in MCF-7 or MCF-7/casp-3 cells. This amount is very similar to the mitochondrial fraction of p53 in other cell types in which mitochondrial p53 was originally proposed to provoke apoptosis (29). Second, although we found even further increased p53 levels associated with mitochondria in M2 fractions of MCF-7/casp-3 cells that were exposed to IR in the presence of caffeine than compared with cells exposed to IR alone, apoptosis induced by the combined treatment of IR and caffeine proceeds in a p53-independent manner (35). Hence, these results suggest that elevation of mitochondrial p53 levels induced by this treatment does not contribute to the rate of apoptosis in these cells. In addition, these data demonstrate that mitochondrial translocation of p53 can be also observed in p53-independent apoptosis systems, a finding that is in sharp contrast to previous studies (30, 40). Third, it is well accepted that the ratio of pro- and anti-apoptotic Bcl-2 proteins is an important factor determining the fate of a DNA-damaged cell. As p53 was shown to interact either with the pro-apoptotic Bcl-2 proteins Bax or Bak (28, 31) or with the anti-apoptotic proteins Bcl-2 and Bcl-x_L (30), it can be assumed that aberrant expression of either of these proteins would interfere with the pro-apoptotic activity of mitochondrial p53. However, MCF-7 cells do not express abnormal levels of either Bcl-2 or Bcl-x_L and Bax or Bak, respectively. In fact, IR treatment of MCF-7/casp-3 cells solely increased expression of the pro-apoptotic proteins Bax and Puma without affecting Bak, Bcl-2, or Bcl-x_L levels. Hence, also these results do not favor the above mentioned threshold hypothesis. This view is also supported by our findings that Bcl-2 and Puma levels neither correlate with apoptosis sensitivity nor with the amount of p53 translocated to the mitochondria following exposure of the cells to IR, camptothecin, or etoposide.

Finally, and most importantly, we have shown that even MCF-7 cells that are deficient for caspase-3 displayed oligomerized Bax (Fig. 6) and Bak (data not shown) and succumbed to apoptosis following overexpression of a wt-p53 construct. In contrast, when MCF-7 cells were transfected with a mitochondria-targeted expression construct of wt-p53 (p53-CTM) that was previously postulated to efficiently induce apoptosis (30), no activation of Bax or Bak (data not shown) or any other apoptotic sign was observed in these cells. Therefore, our data demonstrate that not only the IR-induced mitochondrial translocation of endogenous p53, but even the targeted overexpression of exogenous mitochondrial p53 is insufficient to induce apoptosis of MCF-7 cells. As chemotherapeutic drugs or overexpression of wt-p53 were sufficient to induce Bax activation and apoptosis, our data suggest that the radioresistant phenotype of these cells is not caused by a general resistance or unresponsiveness to p53-dependent cell death. Nevertheless, one has to keep in mind that apoptosis induction by overexpression of wt-p53 is most likely achieved via its transcriptional activity as overexpressed wt-p53 was mainly located in the nucleus, but was never detected at the mitochondria.

It is still possible that the inability of mitochondrial p53 to induce Bax oligomerization and apoptosis is caused by the absence or presence of certain inhibitory or stimulatory factors. In addition, it might well be the case that the interaction of mitochondrial p53 with Bcl-2 or Bcl-xL is for unknown reasons hampered in these cells, a scenario that would easily explain their unresponsiveness toward mitochondrial p53. Also the lack of post-translational modifications of p53 itself that might be required for its pro-apoptotic activity at the mitochondria might account for the observed resistance. With regard to phosphorylation and acetylation,

no major differences were observed in the modification patterns between the pro-apoptotic mitochondrial and nuclear p53 proteins (39). However, these data do not rule out that other post-translational events, such as ubiquitinylation or sumoylation, might play a role in apoptosis induction by mitochondrial p53. Finally, we cannot exclude the possibility that translocation of p53 to mitochondria is merely a consequence of DNA damage signaling without any implications for the fate of the cell.

In summary, we show that the IR-induced translocation of p53 to the mitochondria is not unequivocally associated with apoptosis and that mechanisms might exist that counteract the pro-apoptotic ability of mitochondrial p53. This could be convincingly demonstrated in several cell lines of different origin. The reason why most of these cell lines are resistant to apoptosis induction by mitochondrial p53 is completely unknown, but is especially intriguing as it might represent a potential mechanism that contributes to the occurrence of a radio-resistant tumor cell phenotype.

Acknowledgments—We thank Drs. U. Moll and B. Vogelstein for their kind gift of plasmids and cells.

REFERENCES

1. Vogelstein, B., Lane, D., and Levine, A. J. (2000) *Nature* **408,** 307–310
2. Vousden, K. H., and Lu, X. (2002) *Nat. Rev. Cancer* **2,** 594–604
3. Bargonetti, J., and Manfredi, J. J. (2002) *Curr. Opin. Oncol.* **14,** 86–91
4. Oren, M. (2003) *Cell Death Differ.* **10,** 431–442
5. Hollstein, M., Sidransky, D., Vogelstein, B., and Harris, C. C. (1991) *Science* **253,** 49–53
6. Vousden, K. H., and Prives, C. (2005) *Cell* **120,** 7–10
7. Olivier, M., Eeles, R., Hollstein, M., Khan, M. A., Harris, C. C., and Hainaut, P. (2002) *Hum. Mutat.* **19,** 607–614
8. Owen-Schaub, L. B., Zhang, W., Cusack, J. C., Angelo, L. S., Santee, S. M., Fujiwara, T., Roth, J. A., Deisseroth, A. B., Zhang, W. W., Kruzel, E., and Radinsky, R. (1995) *Mol. Cell. Biol.* **15,** 3032–3040
9. Wu, G. S., Burns, T., McDonald, E. R., 3rd, Jiang, W., Meng, R., Krantz, I. D., Kao, G., Gan, D. D., Zhou, J. Y., Muschel, R., Hamilton, S. R., Spinner, N. B., Markowitz, S., Wu, G., and El-Deiry, W. S. (1997) *Nat. Genet.* **17,** 141–143
10. Bennett, M., Macdonald, K., Chan, S. W., Luzio, J. P., Simari, R., and Weissberg, P. (1998) *Science* **282,** 290–293
11. Soengas, M. S., Alarcon, R. M., Yoshida, H., Giaccia, A. J., Hakem, R., Mak, T. W., and Lowe, S. W. (1999) *Science* **284,** 156–159
12. Johnstone, R. W., Ruefli, A. A., and Lowe, S. W. (2002) *Cell* **108,** 153–164
13. Nechushtan, A., Smith, C. L., Hsu, Y. T., and Youle, R. J. (1999) *EMBO J.* **18,** 2330–2341
14. Desagher, S., Osen-Sand, A., Nichols, A., Eskes, R., Montessuit, S., Lauper, S., Maundrell, K., Antonsson, B., and Martinou, J. C. (1999) *J. Cell Biol.* **144,** 891–901
15. Miyashita, T., Kitada, S., Krajewski, S., Horne, W. A., Delia, D., and Reed, J. C. (1995) *J. Biol. Chem.* **270,** 26049–26052
16. Oda, E., Ohki, R., Murasawa, H., Nemoto, J., Shibue, T., Yamashita, T., Tokino, T., Taniguchi, T., and Tanaka, N. (2000) *Science* **288,** 1053–1058
17. Nakano, K., and Vousden, K. H. (2001) *Mol. Cell* **7,** 683–694
18. Kannan, K., Amariglio, N., Rechavi, G., Jakob-Hirsch, J., Kela, I., Kaminski, N., Getz, G., Domany, E., and Givol, D. (2001) *Oncogene* **20,** 2225–2234
19. Sax, J. K., and El-Deiry, W. S. (2003) *Cell Death Differ.* **10,** 413–417
20. Moll, U. M., and Zaika, A. (2001) *FEBS Lett.* **493,** 65–69
21. Chipuk, J. E., and Green, D. R. (2003) *J. Clin. Immunol.* **23,** 355–361
22. Erster, S., and Moll, U. M. (2005) *Biochem. Biophys. Res. Commun.* **331,** 843–850
23. Yee, K. S., and Vousden, K. H. (2005) *Carcinogenesis* **23,** 1317–1322
24. Caelles, C., Helmberg, A., and Karin, M. (1994) *Nature* **370,** 220–223
25. Haupt, Y., Rowan, S., Shaulian, E., Kazaz, A., Vousden, K., and Oren, M. (1997) *Leukemia* **11,** Suppl. 3, 337–339
26. Haupt, Y., Rowan, S., Shaulian, E., Vousden, K. H., and Oren, M. (1995) *Genes Dev.* **9,** 2170–2183
27. Schuler, M., Bossy-Wetzel, E., Goldstein, J. C., Fitzgerald, P., and Green, D. R. (2000) *J. Biol. Chem.* **275,** 7337–7342
28. Chipuk, J. E., Kuwana, T., Bouchier-Hayes, L., Droin, N. M., Newmeyer, D. D., Schuler, M., and Green, D. R. (2004) *Science* **303,** 1010–1014
29. Marchenko, N. D., Zaika, A., and Moll, U. M. (2000) *J. Biol. Chem.* **275,** 16202–16212
30. Mihara, M., Erster, S., Zaika, A., Petrenko, O., Chittenden, T., Pancoska, P., and Moll, U. M. (2003) *Mol. Cell* **11,** 577–590
31. Leu, J. I., Dumont, P., Hafey, M., Murphy, M. E., and George, D. L. (2004) *Nat. Cell Biol.* **6,** 443–450
32. Jänicke, R. U., Engels, I. H., Dunkern, T., Kaina, B., Schulze-Osthoff, K., and Porter, A. G. (2001) *Oncogene* **20,** 5043–5053
33. Jänicke, R. U., Sprengart, M. L., Wati, M. R., and Porter, A. G. (1998) *J. Biol. Chem.* **273,** 9357–9360
34. Brummelkamp, T. R., Bernards, R., and Agami, R. (2002) *Science* **296,** 550–553
35. Essmann, F., Engels, I. H., Totzke, G., Schulze-Osthoff, K., and Jänicke, R. U. (2004) *Cancer Res.* **64,** 7065–7072
36. von Haefen, C., Gillissen, B., Hemmati, P. G., Wendt, J., Guner, D., Mrozek, A., Belka, C., Dörken, B., and Daniel, P. T. (2004) *Oncogene* **23,** 8320–8332
37. Nicoletti, I., Migliorati, G., Pagliacci, M. C., Grignani, F., and Riccardi, C. (1991) *J. Immunol. Methods* **139,** 271–279
38. Dimri, G. P., Lee, X., Basile, G., Acosta, M., Scott, G., Roskelley, C., Medrano, E. E., Linskens, M., Rubelj, I., Pereira-Smith, O., Peacocke, M., and Campisi, J. (1995) *Proc. Natl. Acad. Sci. U. S. A.* **92,** 9363–9367
39. Nemajerova, A., Erster, S., and Moll, U. M. (2005) *Cell Death Differ.* **12,** 197–200
40. Erster, S., Mihara, M., Kim, R. H., Petrenko, O., and Moll, U. M. (2004) *Mol. Cell. Biol.* **24,** 6728–6741
41. Nister, M., Tang, M., Zhang, X.-Q., Yin, C., Beeche, M., Hu, X., Enblad, G., van Dyke, T., and Wahl, G. M. (2005) *Oncogene* **24,** 3536–3573